



SAPIENZA
UNIVERSITÀ DI ROMA

Dipartimento di Chimica e Tecnologie del Farmaco
Dottorato di Ricerca in Scienze Farmaceutiche – XXXI Ciclo

Application of Nuclear Magnetic Resonance Spectroscopy in the study of complex matrices

PhD STUDENT
Simone Circi

TUTOR
Prof.ssa Luisa Mannina

COTUTOR
Dr. Anatoly P. Sobolev

LIST OF PUBLICATIONS

1. Sobolev, A.P., Thomas, F., Donarski, J., Ingallina, C., **Circi, S.**, Marincola, F.C., Capitani, D., Mannina, L. (2018). Use of NMR applications to tackle future food fraud issues. ACCEPTED in *Trends in Food Science & Technology*.
2. **Circi, S.**, Ingallina C., Vista S., Capitani D., Di Vecchia A., Leonardi G., D'Achille G., Centauri L., Camin F., Mannina L. (2018). A Multi-Methodological Protocol to Characterize PDO Olive Oils. *Metabolites* 8(43), 1-10.
3. Iebba, V., Guerrieri, F., Di Gregorio, V., Levrero, M., Gagliardi, A., Santangelo, F., Sobolev, A.P., **Circi, S.**, Giannelli, V., Mannina, L., Schippa, S., Merli, M. (2018). Combining amplicon sequencing and metabolomics in cirrhotic patients highlights distinctive microbiota features involved in bacterial translocation, systemic inflammation and hepatic encephalopathy. *Scientific Reports* 8(8210), 1-14.
4. Frascchetti, C., Guarcini, L., Zazza, C., Mannina, L., **Circi, S.**, Piccirillo, S., Chiavarino, B., Filippi, A (2017). A real time evolution of unprotected protonated galactosamine probed by IRMPD spectroscopy. *Physical Chemistry Chemical Physics* 20(2), 8737-8743.
5. **Circi, S.**, Capitani, D., Randazzo, A., Ingallina, C., Mannina, L., Sobolev, A.P. (2017). Panel test and chemical analyses of commercial olive oils: a comparative study. *Chemical and Biological Technologies in Agriculture* 4(18), 1-10.
6. Sobolev, A.P., **Circi, S.**, Capitani, D., Ingallina, C., Mannina, L. (2017). Molecular fingerprinting of food authenticity. *Current Opinion in Food Science* 16, 59-66.
7. Sobolev, A.P., **Circi, S.**, Mannina, L. (2016). Advances in Nuclear Magnetic Resonance Spectroscopy for Food Authenticity Testing. In book: *Advances in Food Authenticity Testing* (6), 147-170.

LIST OF POSTER

1. **Circi, S.**, Ingallina, C., Capitani, D., Sobolev, A.P., Mannina, L. NMR-based approach to characterize tomatoes from Lazio region. XLVII National Congress on Magnetic Resonance - Torino, 19-21 September **2018**.
2. **Circi, S.**, Ingallina, C., Sobolev, A.P., Capitani, D., Mannina, L. Applications of Metabolomics in food science and medical research: “teas” and “hepatic cirrhosis” as case studies. Secondo Workshop sulla Ricerca 2018 - Roma, 12 July **2018**.
3. **Circi, S.**, Ingallina, C., Botta, B., Capitani, D., Sobolev, A.P., Ghirga, F., Mannina, L. e-ALIERB Project: NMR characterization of typical products from Lazio region. International Conference on FoodOmics 2018 (5th Edition) - Cesena, 10-12 January **2018**.
4. **Circi, S.**, Quaglio, D., Sobolev, A.P., Capitani, D., Miccheli, A., Giusti, A.M., Donini, L.M., Mannina, L. 1H NMR-based metabolomic approach to characterize urine samples of female obese patients. Advances in NMR and MS-based Metabolomics - Padova, 14-16 November **2017**.
5. **Circi, S.**, Ingallina, C., Botta, B., Capitani, D., Sobolev, A.P., Ghirga, F., Mannina, L. NMR characterization of hemp products. XLVI National Congress on Magnetic Resonance - Fisciano, 27-29 September **2017**.
6. **Circi, S.**, Marini, F., Capitani, D., Sobolev, A.P., Mannina, L. Combined approach of NMR and Chemometrics for comparing European and non-European olive oils. Food Integrity Conference 2017 - Parma, 10-11 May **2017**.
7. **Circi, S.**, Capitani, D., Sobolev, A.P., Iebba, V., Schippa, S., Merli, M., Mannina, L. NMR-based metabolic approach to characterize stool samples of patients with liver cirrhosis. XLV National Congress on Magnetic Resonance - Modena, 5-7 September **2016**.
8. **Circi, S.**, Marini, F., Sanzò, G., Capitani, D., Sobolev, A.P., Mannina, L. Impiego della spettroscopia 1H-NMR e di metodi chemiometrici per confrontare oli europei e non europei. V Workshop Applicazioni della Risonanza Magnetica nella Scienza degli Alimenti - Roma, 26-27 May **2016**.

LIST OF ORAL COMMUNICATIONS

1. **Circi, S.** Caratterizzazione di Pomodori del Basso Lazio attraverso un approccio multimetodologico. VI Workshop Applicazioni della Risonanza Magnetica nella Scienza degli Alimenti - Roma, 21-22 June **2018**.
2. **Circi, S.** Caratterizzazione della Canapa Industriale dell'Alto Lazio mediante Risonanza Magnetica Nucleare. La Sapienza per valorizzare gli alimenti del territorio laziale - Roma, 13 April **2018**.
3. **Circi, S.** L'olio di oliva e la Risonanza Magnetica. Workshop "DayOne presenta il progetto ReInVenture" - Roma, 5 May **2017**.
4. Mannina, L., Sobolev, A.P., **Circi, S.** Caratterizzazione dei prodotti della canapa con *e*-ALIERB. Workshop "La canapa industriale: sviluppo e valorizzazione di una nuova filiera agroalimentare ecosostenibile" - Roma, 17 March **2017**.

TABLE OF CONTENTS

| | |
|---|----|
| Chapter 1 – Introduction | |
| 1.1 Nuclear Magnetic Resonance Spectroscopy in Food Science | 1 |
| 1.2 References | 22 |
| Chapter 2 – Basics of Nuclear Magnetic Resonance | |
| 2.1 Introduction | 27 |
| 2.2 Classical description of Nuclear Magnetic Resonance | 28 |
| 2.2.1 Nuclear magnetic moment | 28 |
| 2.2.2 Nuclear Magnetic Resonance phenomenon | 31 |
| 2.3 Quantum description of Nuclear Magnetic Resonance | 34 |
| 2.3.1 Theoretical basics of quantum mechanics applied to NMR | 34 |
| 2.3.1.1 Time independent perturbations | 35 |
| 2.3.1.2 Tensor representation of the Hamiltonians | 36 |
| 2.3.1.3 Rotations in NMR | 37 |
| 2.3.1.4 Average Hamiltonian and calculation of the perturbation | 39 |
| 2.3.2 Nuclear magnetic interactions | 39 |
| 2.3.2.1 The Zeeman interaction | 40 |
| 2.3.2.2 The chemical shift interaction | 43 |
| 2.3.2.3 The dipolar interaction | 46 |
| 2.3.2.4 The scalar interaction | 48 |
| 2.3.2.5 The electric quadrupolar interaction | 49 |
| 2.4 References | 50 |
| Chapter 3 – Chemometrics | |
| 3.1 Introduction | 53 |
| 3.2 Explorative unsupervised analysis | 56 |
| 3.2.1 Principal Component Analysis (PCA) | 56 |
| 3.2.2 Tree Clustering Analysis (TCA) | 58 |
| 3.3 Supervised classification/regression methods | 60 |
| 3.3.1 Partial Least Square (PLS) | 62 |
| 3.3.2 Linear Discriminant Analysis (LDA) | 62 |
| 3.3.3 PLS-DA | 64 |
| 3.3.4 SIMCA | 64 |
| 3.3.5 Genetic Algorithms (GA) and Genetic Programming (GP) | 65 |
| 3.3.6 Artificial Neural Networks (ANNs) | 66 |
| 3.4 References | 67 |
| Chapter 4 – Typical Foods of Lazio Region | |
| 4.1 Project “e-ALIERB” | 69 |
| 4.2 Peperone Cornetto di Pontecorvo DOP | 79 |
| 4.2.1 Introduction | 79 |
| 4.2.2 Material and Methods | 80 |
| 4.2.3 Results and Discussion | 86 |
| 4.2.4 References | 93 |
| 4.3 Sedano Bianco di Sperlonga IGP | 95 |
| 4.3.1 Introduction | 95 |

| | | |
|--|--|-----|
| 4.3.2 | Material and Methods | 96 |
| 4.3.3 | Results and Discussion | 98 |
| 4.3.4 | References | 107 |
| 4.4 | Tomatoes from Fondi | 109 |
| 4.4.1 | Introduction | 109 |
| 4.4.2 | Material and Methods | 110 |
| 4.4.3 | Results and Discussion | 113 |
| 4.4.4 | References | 128 |
| 4.5 | Hemp and processing products | 129 |
| 4.5.1 | Inflorescences (1 st case study) | 132 |
| 4.5.1.1 | Material and Methods | 132 |
| 4.5.1.2 | Results and Discussion | 135 |
| 4.5.2 | Inflorescences (2 nd case study) | 155 |
| 4.5.2.1 | Material and Methods | 155 |
| 4.5.2.2 | Results and Discussion | 156 |
| 4.5.3 | Hempseed Oil | 162 |
| 4.5.3.1 | Material and Methods | 162 |
| 4.5.3.2 | Results and Discussion | 165 |
| 4.5.4 | Hempseed Flour | 172 |
| 4.5.4.1 | Material and Methods | 172 |
| 4.5.4.2 | Results and Discussion | 175 |
| 4.5.5 | References | 179 |
| | | |
| Chapter 5 – Olive Oil | | |
| 5.1 | Panel Test and Chemical Analyses of commercial Olive Oils | 181 |
| 5.1.1 | Introduction | 181 |
| 5.1.2 | Material and Methods | 182 |
| 5.1.3 | Results and Discussion | 184 |
| 5.1.4 | Conclusions | 198 |
| 5.1.5 | References | 199 |
| 5.2 | A Multi-Methodological Protocol to Characterize PDO Olive Oils | 201 |
| 5.2.1 | Introduction | 201 |
| 5.2.2 | Material and Methods | 203 |
| 5.2.3 | Results and Discussion | 209 |
| 5.2.4 | Conclusions | 215 |
| 5.2.5 | References | 216 |
| | | |
| Chapter 6 – Foods with High Biological Value | | |
| 6.1 | Blueberries | 219 |
| 6.1.1 | Introduction | 219 |
| 6.1.2 | Material and Methods | 222 |
| 6.1.3 | Results and Discussion | 225 |
| 6.1.4 | References | 241 |
| 6.2 | Teas | 244 |
| 6.2.1 | Introduction | 244 |
| 6.2.2 | Material e Methods | 245 |
| 6.2.3 | Results and Discussion | 248 |
| 6.2.4 | References | 251 |
| | | |
| Chapter 7 – Baobab | | |
| 7.1 | Introduction | 253 |

| | |
|---|-----|
| 7.2 Material e Methods | 255 |
| 7.3 Results e Discussion | 258 |
| 7.4 Conclusions | 275 |
| 7.5 References | 276 |
| Chapter 8 – NMR-based metabolic approach to characterize stool samples of patients with liver cirrhosis | |
| 8.1 Introduction | 279 |
| 8.2 Material and Methods | 281 |
| 8.3 Results and Discussion | 284 |
| 8.4 References | 289 |
| Acknowledgements | 295 |

Chapter 1: Introduction

1.1 Nuclear Magnetic Resonance Spectroscopy in Food Science

Any foodstuff is a complex matrix including many compounds, widely ranging in concentration, with different chemical structure and physicochemical properties, which originate from biological raw material and/or are produced during treatment, storage, etc. Therefore, a very exhaustive food characterization, important to assure its quality and authenticity, usually needs different complementary analytical techniques to be used.

Foodomics (Capozzi & Bordoni, 2013) embodies a comprehensive approach to food characterization and with its different branches such as food-genomics, -proteomics, -glycomics, -lipidomics, and -metabolomics is able to give an exhaustive picture of foodstuff at different levels of molecular organization. Metabolomics (Fiehn, 2002) is the most comprehensive approach aimed to identification and quantification of all metabolites present in a given sample. Food metabolome originates from biochemical reactions and carries information not only about the biological source of a given foodstuff but also about all treatments during food production. The identity of a foodstuff is the fruit of its history from the origin (genetic background) to the final step when it is ready to be consumed. During this history different factors in a different manner influence its metabolite composition leaving an imprint at the molecular level. The most important factors are reported in the Figure 1.1.

An exhaustive characterization of food metabolome is possible by complementary analytical methodologies such as Nuclear Magnetic Resonance (NMR) spectroscopy (Mannina et al., 2012), Mass spectrometry (MS) (Gika et al., 2014), and vibrational spectroscopy (Cozzolino, 2015).

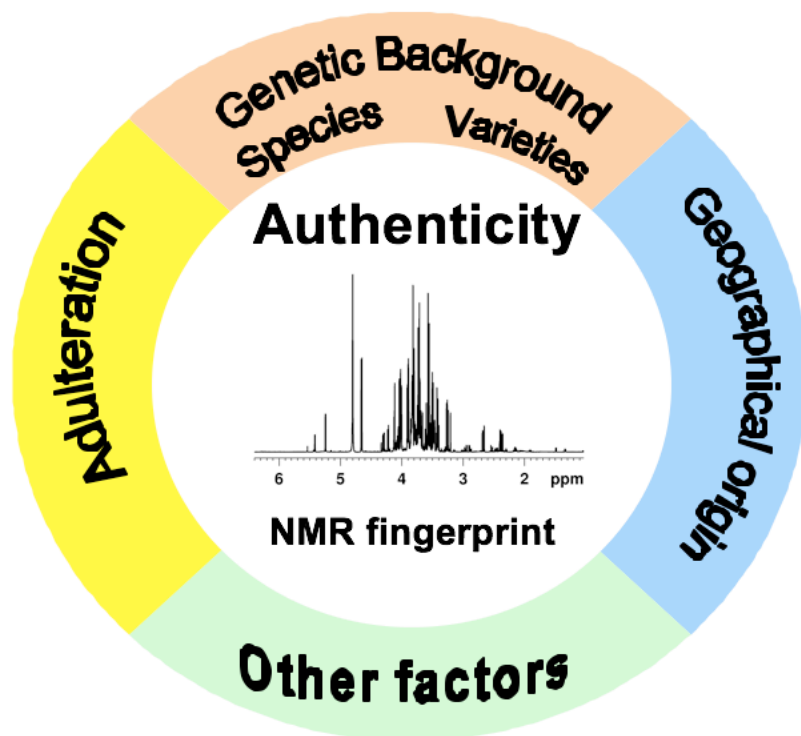


Figure 1.1. The most important factors influencing the metabolite composition of foodstuff.

High resolution Nuclear Magnetic Resonance (NMR) spectroscopy is known to be a robust quantitative analytical technique, but it also has proper tools for identification of compounds even in the absence of standards. One of the main advantages of NMR is that very different chemical species can be quantitatively determined altogether in a single NMR experiment. NMR simultaneously brings “high-throughput” spectroscopic/structural information on all metabolites present in food sample above the detection limit. Moreover, it does not require complicated sample preparation and separation of components prior to the analysis.

Liquid state high field NMR has been extensively used in foodstuffs analysis (Mannina et al., 2012). One of the most important characteristics of this technique is its high throughput due to the high resolution of NMR spectra that permits the direct qualitative and quantitative analysis of complex mixtures without physical separation of corresponding components. This characteristic makes liquid state NMR one of the most attractive and

suitable techniques for the direct analysis of liquid foods (beverages, oils etc.) and even for solid foods, although a minimal manipulation to extract metabolites is necessary.

NMR methodologies can be useful to characterize food matrices in terms of quality and authenticity, allowing also the identification of counterfeits (Sobolev, Circi & Mannina, 2016). Basically, this can be accomplished by using one of two approaches, either targeted or untargeted analysis according to specific application.

In the case of a specific component to be analyzed, a selective extraction can be also performed before the NMR analysis to concentrate the selected component and to avoid interference from other compounds. The targeted approach allows the identification of specific markers of identity/adulteration for a given foodstuff. For example, high resolution ^1H NMR analysis was successfully applied to detect the presence of 16-O-methylcafestol (16-OMC) in roasted coffee labeled as “100% Arabica”. 16-OMC is a chemical marker of less expensive Robusta coffee, therefore its presence in Arabica coffee confirms the adulteration (Monakhova et al., 2015). Another example is the control of sugar addition in honey: the characteristic minor sugar turanose present in honey can be easily observed and quantified by ^1H -NMR. The absence or extremely low levels of this molecule has been reported to indicate the dilution of honey with sugar syrup (Spiteri et al., 2015). Using specific markers, the NMR approach has been also used for the quantitation of sweeteners (sucralose or cyclamate, for instance) in non-alcoholic beverages (Ackermann et al., 2017), terpenols in coffee (Wei et al., 2012) or methylglyoxal or leptosperin in Manuka honey (Donarski, Roberts & Charlton, 2010a; Spiteri et al., 2017).

Unfortunately, the characterization of food authenticity or adulteration cannot always be simply restricted to the identification of a single or a few marker compounds. In some cases, an analysis based on the combination of several compounds or on the entire metabolite profile of the foodstuff, representing a unique pattern characteristic of the food identity, must be used to discriminate samples according to authenticity identifying fraudulent food. In this

case, the NMR based untargeted approach is used since it allows the characterization of the chemical composition of complex mixtures providing simultaneously information on a wide range of metabolites or a set of selected ones.

Several general untargeted approaches such as metabolic profiling, metabolic fingerprinting, and metabolomics developed for the analysis of metabolites in biological samples using liquid state NMR or diverse analytical methods have been successfully applied for food analysis. Metabolic profiling consists in identification and quantification of a number of selected metabolites, belonging to various classes of compounds, in a given sample often without a separation procedure. Metabolic fingerprinting is used when classification of samples without recognition of individual specific metabolites is sufficient: in this case, the NMR spectrum can be considered as a fingerprint of the foodstuff and all the NMR resonances are measured without any identification.

Figure 1.2 shows a typical workflow of a metabolomics study adaptable also to food quality, safety and authentication applications.

Each step is fundamental and critical with important consequences for obtaining reliable and meaningful biological results. The principles of experimental design are universal. In this phase, a number of aspect must be taken into consideration in order to maximize the possibilities of answering the research question of interest as clearly and efficiently as possible. This includes sampling size and collection, laboratory and data analysis, identification of variables (independent, dependent and controlled) and potential biases that could be introduced.

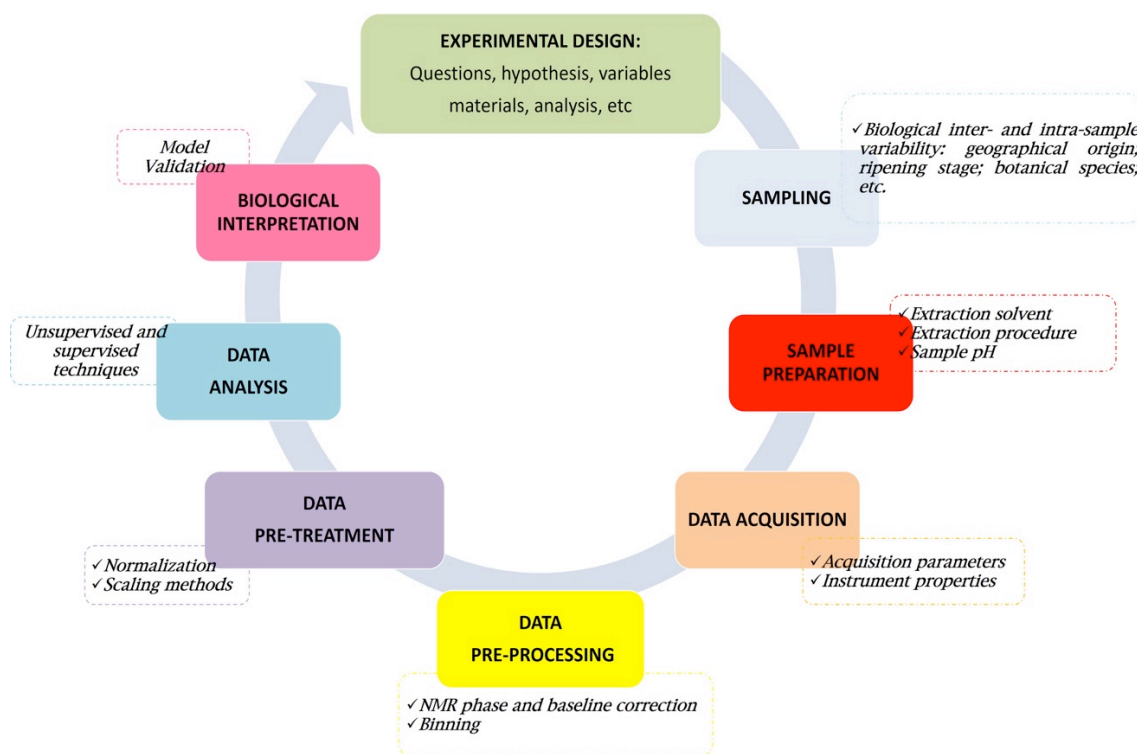


Figure 1.2. Typical metabolomics workflow and sources of variability (dashed box). Sources for data pre-processing and pre-treatment phases refer specifically to a NMR-based study.

Proper sampling is a crucial point of any analytical protocol. As previously underlined, foodstuff is a complex matrix where the distribution of metabolites can be not homogeneous. If it is necessary to analyze just a piece of sample since it is impossible to put in the instrument the foodstuff as a whole (which is the most common case) it is important to perform the sampling in a correct way. For instance, one can choose to take different parts of the foodstuff to have a “representative” sample to analyze. According to specific food, samples can be analyzed as it is (liquid foodstuffs) or after a pretreatments or a suitable extraction (liquid and solid samples). Olive oils, vinegars, wines, fruits juices are often analyzed without any treatment, whereas dilution for a viscous liquid such as honey is recommended. In the case of solid foodstuffs, after sample homogenization and/or disruption, an extraction with a suitable solvent has to be performed both for vegetal samples (Kaiser et al., 2009; Kim and Verpoorte, 2010), and for animal tissues (Lin et al., 2007; Wu et al., 2008). The combination of methanol/H₂O/chloroform in different proportions is often used since it

allows one to extract both hydrophobic and hydrophilic compounds. It has been used in the case of maize (Piccioni et al., 2009), lettuce (Sobolev et al., 2005), as well as in animal derived foodstuffs such as sea bass (Mannina et al., 2008), and meat (Jung et al., 2010).

Conservation occurring after sampling requires suitable care to preserve the quality and composition of foodstuffs. In fact, some operations such as harvesting for vegetables, and slaughter for animals can be followed by an enzymatic attack and other degradation processes. Freezing in liquid nitrogen followed by storing in the dark at low temperature are the most common procedures used to avoid chemical or enzymatic degradation.

In the case of targeted NMR analysis the choice of the solvent to extract selected metabolites is a crucial point. Acetic acid/H₂O is used for extracting specific target compounds, such as polyphenols (McDougall et al., 2008). Chloroform/ethyl acetate/2-butanol mixture is used to extract aromatic compounds (Khatib et al., 2006). Solid phase extraction (SPE) has also been suggested for isolation of the compounds of interest eliminating interference from high molecular weight compounds (Beretta et al., 2008). In the case of blueberry, the SPE has allowed to reduce the sugar content and to provide NMR characterization of anthocyanins not easily identifiable in aqueous solution (Capitani et al., 2014).

According to all said up to now, well-designed experiments together with appropriate analytical data and statistical analysis, enable researchers to increase the robustness and validity of their experimental results. The importance of these aspects on the quality of metabolomics output has been widely described in many papers and reviews (Scalbert et al., 2009; Wishart, 2008; Dunn & Ellis, 2005; Smolinskaa et al., 2012). Overall, each research group follows its own optimum protocol, often developed after a case-by-case evaluation of the best compromise between quality of data and throughput of analysis. In order to promote comparison of food data among different laboratories, it is recommended that any metabolomics study provides detailed information of the experimental design and the relative

experimental details. Indeed, at present, the lack of standardization in procedures is a serious drawback for inter-laboratory comparison.

The use of NMR as a methodology suitable for metabolomics is supported by its high resolution and robustness. Further considerations must be given on the source of variability when NMR-based metabolomics is used towards food authentication. Often in metabolomics projects all samples are analyzed simultaneously and no or minimal consideration is needed for factors that influence acquired data over time. These factors include instrumental drift, extraction solvents and NMR acquisition buffers. Instrumental drift (minor diminishing of the magnetic field strength of an NMR instrument), except in the most extreme of circumstances, will not impact comparability of data. A modern instrument can expect to have a magnetic field drift of less than 1 Hz per hour, corresponding to approximately 8000 Hz per annum. Using the minimal field strength of 400 MHz as an example, this impact equates to a change in field strength of 0.002 %. Furthermore, it is typical to bin NMR spectra to defined regions based on chemical shift. The universal nature of the chemical shift dictates that changes in magnetic field strength will not influence data. Extraction solvents and NMR acquisition buffers are considered together. These factors are controlled through the use of good laboratory practise, using precise and accurate volumes and masses. It is also recommended that where possible large batches of NMR acquisition buffers are prepared, and aliquots stored in suitable conditions (e.g. -20 °C). The incorporation of a known, previously analysed sample in all batches and checks to assure that these data are still comparable, is the recommended practice. This aspect is particularly important when the information is derived from the comparison between spectra as, for instance, in the case of fruit varieties, development, type of farming, etc. In order to have reproducible and comparable spectra it is extremely important to control pH and temperature which have to be maintained constant within a set of experiments. In particular, variation of pH cause changes in the chemical shift of NMR signals of compounds with acidic or basic

functional groups (organic acids, amino acids, etc). It is therefore often recommended the use of suitable buffered solution in proper concentration or the addition of small volumes of acid or basic solutions.

As with any other analytical method, each individual compound in a mixture can be identified by its characteristic signals in NMR spectrum after the comparison with the NMR spectrum of pure compound (database matching approach). One of the main limitations of this approach is that an exhaustive database should be available, otherwise it would require an enormous number of compounds to be synthesized or isolated from natural sources. Another limitation is the variation of NMR spectral parameters (chemical shifts, relaxation times, etc) that can occur when the compound is analyzed in a mixture, as opposed to alone in solution, due to interactions with other molecules or, more simply, to changes in experimental conditions (e.g. concentration, ionic strength, pH, temperature, solvent, etc.). In this case, it is clear that some chemical shift values can be different from the values found in the library database, thereby precluding unambiguous identification.

Along with database matching, another complementary approach for identification of metabolites present in food samples relies on specific NMR experiments that enable signal editing or reveal correlations between different signals present in NMR spectra (NMR elucidation approach).

Frequently used signal editing approaches consist in removing the NMR signals due to either low- (diffusion-filters) or high-molecular weight compounds (relaxation spin-spin or T_2 filters). The widely used correlation experiments give as a result 2D maps (or even nD maps, $n > 2$) with the cross correlations between the proton signals of the same molecule (^1H - ^1H COSY, ^1H - ^1H TOCSY, ^1H - ^1H NOESY) or between ^1H and ^{13}C NMR signals (2D HSQC for directly bound H-C or 2D HMBC for long-range correlations between protons and carbons generally two or three bonds away).

Finally, it is also useful to confirm assignments by directly adding to the investigated sample an appropriate amount of a pure chemical standard, once its presence has been inferred, or at least suspected. Overall, considering the high level of complexity of foodstuffs samples, the highest information content can only be revealed by combining all of these approaches.

Apart from qualitative and structural information, robust quantitative data can be obtained from NMR spectra. As a quantitative method, ^1H NMR is unbiased versus all classes of organic compounds owing to the proportionality of NMR signal integral only to the number of equivalent protons and molar concentration of the corresponding compound independently on its structure or physicochemical properties. Taking into account that each NMR spectrum is a sum of single scans repeated periodically, the recycling time (the time interval between consecutive scans) has to be sufficiently long (at least five times the longitudinal relaxation time (T_1) of the slowest relaxing nuclei) to assure the complete relaxation of all nuclei in mixture components and internal standard molecules.

The metabolomics workflow ends with the multivariate statistical analysis of the quantitative data and the subsequent biochemical or physiological interpretation of the experimental results, the last element of the workflow (van der Greef & Smilde, 2005; Wishart, 2008). Generally, explorative unsupervised techniques, such as Principal Component Analysis (PCA), are applied to evidence outliers or natural grouping of samples, while supervised multivariate techniques such as Partial Least Squares Discriminant Analysis (PLS-DA) are required to create classification or prediction models. Since different statistical methods use specific data treatment and a set of unique assumptions, it is recommended to verify metabolic difference by using a variety of tests.

It is therefore evident that the usefulness of metabolomics in obtaining reliable and biological meaningful results for food authentication largely depends on multiple factors and overall on the ability to set up appropriate quality control strategies to monitor the robustness

of the metabolomics workflow, thus minimizing the impact of error sources on the data interpretation.

The most foodstuffs are complex mixtures and their NMR analysis can be challenging because they are generally constituted of a myriad of distinct compounds (saccharides, polysaccharides, lipids, peptides, amino acids, etc.), which are present in a large range of concentrations. The corresponding ^1H NMR spectra of foodstuffs are highly crowded due to the presence of numerous, often multiplet, resonances. Excellent reviews relevant to the NMR based structural assignment of compounds present in mixtures are available in the literature (Novoa-Carballal et al., 2011; McKenzie et al., 2011).

A prominent example of the unique information available from the application of NMR and metabolomics regards honey. Verifying the geographical origin of honey samples from the French island of Corsica by applying a ^1H NMR statistical protocol has been demonstrated in a study performed on 118 samples collected from a range of European countries and regions (Donarski, Jones & Charlton, 2008). The subsequent statistical model, built using a combination of PLS-DA and genetic algorithm, was able to correctly identify honey samples as originating from Corsica (overall, correct classification rates, from a cross validated model, were 96.2%). A follow-up study which combined data from a second year of study investigated the variables used in a new classification algorithm and identified several biomarkers that were present in specific honey floral types (e.g. kynurenic acid was identified by a genetic algorithm as an indirect marker of geographical origin) (Donarski et al., 2010b). Spiteri et al. (2015) reported a bulk screening ^1H NMR study of 205 commercial honey samples against 518-reference honeys by using Independent Components Analysis. As a result, a significant number of the commercial samples were found to fall outside the classification model created with authentic samples, suggesting a possible addition of exogenous sugars.

NMR spectroscopy has proven to be an extraordinary tool also for the characterization of olive oils in terms of quality, authenticity and geographical origin (Mannina & Sobolev, 2011). A geographical classification of Mediterranean virgin olive oils produced in three consecutive years was performed on 896 authentic samples by ^1H NMR spectroscopy and different statistical models (Mannina et al., 2010). The potential influence of the historical meteorological parameter averages was investigated by the ^1H NMR-metabolomics approach on more than 200 samples of extravirgin olive oils collected over a four-year period in Italy, European and non-European countries. Besides suggesting the possible use of this approach for olive oils geographical origin prediction, the results of this study indicated also a possible application to the assessment of correlation between the profile of olive oils and climate data (Rongai et al., 2017). Blending of virgin olive oil with low-quality hazelnut oil can be unmasked by the statistical elaboration of ^1H NMR signals from fatty acid chains, squalene, and β -sitosterol (Mannina et al., 2009). Finally, it is worth reminding that, since NMR does not require prior knowledge about the compounds present in the sample, it is ideally suited to detect unexpected changes in the metabolite profile of food, such as the addition of new adulterants, without the need of an *a priori* hypothesis.

^1H NMR spectroscopy in combination with multivariate data analysis can be successfully used also to achieve information on various aspect of wine quality such as the authenticity, grape variety, geographical origin, and the year of vintage (Godelmann et al., 2013).

NMR method is becoming more and more popular within the food testing community, proving to be also a well suited technique for quality control (QC) applications, both as targeted or non-targeted approach. Indeed, a single NMR sample measurement can answer many authenticity issues that could not be resolved by conventional methods. The high throughput of NMR spectroscopy enables the analyst to quickly measure the large number of samples required to populate a comprehensive database. The whole spectrum is

measurable with a high reproducibility, even between laboratories. This is possible thanks to precise standard operating procedures for sample preparation and new technological developments that have minimised variability between laboratories. These include: precise monitoring of the sample temperature; automation of settings such as tuning and matching of the probe; gradient shimming to ensure magnetic field homogeneity. The whole spectrum can be considered as a reproducible fingerprint, without sophisticated pre-processing before statistical evaluation. To finalise the recognition of non-targeted NMR methods, standardisation is the final goal. Normalisation bodies are currently considering the potential of these methods including the wider requirements relating to data accessibility and database maintenance.

Therefore, the potential of NMR is not only to measure the major signals from the main metabolites but also to do so without the influence of spectral artefacts and inconsistencies such as electrical noise, peak width differences and chemical shift modification. Spectra can then be compared to each other, and by comparing an unknown spectrum with a series of reference spectra from a well-defined population, defaults are detected, without any *a priori* selection of variables. Such models of classification or verification are not performed as “black-box” since the user can move back to the spectral fingerprint and identify which signal is responsible for the deviation.

Through the integration of the NMR methodology inside a Quality Management System and with the use of periodic QC, the laboratory can even obtain Third Party accreditation for its NMR techniques. On the technical level, it should periodically evaluate its performance of tests. The performance validation of the analytical method must encompass all stages of preparation, extraction and analysis encountered by samples during routine analyses. Performance characteristics include: selectivity, measuring range, linearity, sensitivity, limit of detection, limit of quantitation, robustness, precision, and accuracy. Additionally, laboratories should start participating in collaborative trials and making use of

various International Proficiency Testing Schemes (PTS) for monitoring their analytical performance and compares the results to laboratories worldwide. They include the Pro-PTS organised by Eurofins laboratory and the Food Analysis Performance Assessment Scheme (FAPAS) from Fera.

A considerable number of literature reports have highlighted the use of NMR methodology for the study of food samples and its development of routine use in this field. This way of working is now adopted in different food control laboratories where NMR is in the portfolio of routine methods for control of products to protect producers and consumers. Applications include, for example, the control of honey (detection of added sugar, geographical and botanical origin confirmation), beverages (Lamanna et al., 2011; Li et al., 2016; Cuny et al., 2008; Spraul et al., 2009a; Spraul et al., 2009b), coffee, fats and oils (through the use of ^{13}C -NMR it is possible to observe the alpha or beta positional distribution of fatty acid chains in the glycerol moiety (Mannina & Sobolev, 2011), vinegars (Boffoet al., 2009; Consonni et al., 2008), spices (detection of added forbidden dyes or detection of other spices and herbs or natural adulterants (Petrakis et al., 2015; Yilmaz, 2010)) and many other applications (detection of non-authorized processes for dried fruits such as forbidden / non-declared cleaning or drying agents). Further details on how NMR could be use in food QC are provided in the following sections.

A NMR-based platform that uses targeted and untargeted analysis called FoodScreenerTM, has been developed. It allows the simultaneous evaluation of different quality and authenticity related-parameters. To date, two different modules of the FoodScreenerTM platform are available, namely: Spin Generated Fingerprint-Profiling (SGF-ProfilingTM) for fruit juice and Wine-ProfilingTM for wine. As demonstration of its commercial application and its increasing acceptance as routine use, it can be reported the recent decision of the Hungarian Ministry of Agriculture (August 2017) to start a program in order to authenticate and identify Hungarian wines using NMR FoodScreener-Wine-

Profiling™. The cost of single analysis can vary in relation to the possibility to buy and use the platform or to send the sample to a laboratory equipped with FoodScreener.

The SGF-Profiling™ module represents a heterogeneous collection of statistical models which can be applied consecutively to one single spectrum (Spraul et al., 2009a). Depending on the model used, the following are predictable: fruit and product type differentiation, adulteration by sugar or acid addition, geographical origin and fruit mixture. Furthermore, information on the quantification of substances can be carried out. In particular, targeted analysis provides information on the content of sugars (glucose, fructose and sucrose), the total acidity of the juice (citric, malic, isocitric and quinic acid), perishable indicators (ethanol, fumaric acid, lactate) and process control parameters (galacturonic acid, phlorin). The values are compared to reference standards. The screening is based on a database composed by thousands of NMR spectra from authentic juices. Finally, the combination of SGF-Profiling™ and the associated software JuiceScreener™ provides the analytical report in which the analytical answer and results are summarized. Regarding the untargeted analysis, both the assessment of concentration deviation of hundreds of compounds and unexpected ingredients are detectable to verify adulteration and unknown fraud (Spraul et al., 2013). The application of SGF-Profiling™ is well established for the routine use analysis of fruit products (juices, concentrates, nectars, purees...).

This technology has been extended to other types of food material such as wine (Spraul et al., 2009b; Monakhova et al., 2014a). Wine-Profiling™ is a method for wine analysis. The comparison of the spectroscopic fingerprint obtained for each individual sample with that of a large database of authentic wine samples allows to answer question on the composition, geographical origin, grape variety and vintage. Although this procedure had been already developed for fruit juice analysis, it was further optimized for wine and alcoholic beverages in general. In particular, to overcome the need to eliminate the major signals (water and ethanol), a methodology was developed which can suppress both signals from water and

ethanol during NMR experiment without losing signals outside those regions (Minoja & Napoli, 2014). In a similar way to SGF-Profiling™, Wine-Profiling™ provides both targeted and untargeted analysis. The former is performed through the quantification of 56 parameters per sample and their comparison with official reference values, while the latter is carried out through verification models able to detect any deviation from authentic reference data.

New NMR benchtop instrumentations, low field but high resolution, represent a new frontier in the food authentication field. Several manufacturers currently offer benchtop instruments that operate at a proton frequency between 45 - 90 MHz. These instruments have significantly lower purchase and maintenance costs than conventional NMR instruments, do not require liquid nitrogen and helium cryogenics and do not require specialised staff for their operation. Although some NMR phenomena are adversely affected at lower field strengths, e.g. sensitivity is lower and spectral overlap is greater, these instruments are still incredibly powerful for food authentication analysis.

The utilisation of low field instrumentation for food analysis was presented at the 7th International Symposium on Recent Advances in Food Analysis (RAFA 2015). The example of rapid analysis for spirit authentication was shown. Under Council Regulation (EEC) N° 110/2008 of the European Parliament and of the Council of 15 January 2008 “laying down general rules on the definition, description and presentation of spirit drinks”, minimum alcoholic strengths for spirit drinks are set. The alcohol content of a spirit drink can be altered by two common fraud types: extension (diluting a spirit drink with water) and counterfeiting (replacing a genuine product with a copy). Therefore, the ability to accurately assess the alcoholic strength of a spirit drink can assist in detection of these frauds. The quantitative nature of the NMR resonances can be theoretically exploited to determine the alcoholic strength of a sample without the requirement for an internal standard. In practise, the assumptions made are non-trivial and a correction coefficient must be calculated to routinely use ¹H NMR spectroscopy for alcohol content determination. A study (unpublished) using an

early generation low field spectrometer could accurately calculate ethanol content within 1.96% (CI 95%), whereas results from a high field 500 MHz NMR spectrometer were approximately 20-fold more accurate. It is expected that a significant increase on accuracy will be observed as further advances are made in instrumentation.

Benchtop NMR provides also a fast, direct, and user-friendly method to determine the fat and oil content in foodstuffs. The technique is based on measurement of the NMR response obtained from oil (fat) in the product, and quantification of its content by calibration. The study performed by Jakes et al. (2015) is a good demonstration on the ability of low field NMR spectroscopy to differentiate beef from horse meat. The lipid constituents of beef and horse samples analysed by low-field NMR were sufficiently different to enable the creation of classification models. When these models were challenged with blind samples (ones that had not been used in model creation) excellent classification results were obtained. Another successful example of food analysis by benchtop NMR is provided by Defernez et al. (2017). In this study, a methodology for distinguishing Arabica and Robusta coffee by using high field NMR spectroscopy (Monakhova et al., 2015) was transferred to a 60 MHz low field spectrometer. Arabica coffee beans command a higher price than Robusta beans, therefore an incentive exists for unscrupulous traders to substitute Robusta beans for Arabica. Although it is possible to differentiate whole Arabica and Robusta beans by eye due to morphological differences, this is not possible on roasted and ground coffee. Chemically, the beans can be distinguished through detection of the compound 16-O-methylcafestol (16-OMC), which is found exclusively in Robusta beans. Therefore, authentic samples of Arabica do not contain 16-OMC and this compound can be used to detect adulteration/substitution with Robusta. The developed low-field NMR methodology was rapid, with a total time for analysis, including extraction and data acquisition, of approximately 45 minutes. It could detect adulteration of Arabica with Robusta when the adulteration level was greater than 10-20%. The methodology was used to perform a small market survey, the results of which showed no adulteration.

Benchtop NMR instrumentation has the potential to be a breakthrough technology in the field of food authentication within the industry. It utilises the power of NMR spectroscopy but with significantly reduced infrastructure requirements and costs. It can be applied in either the targeted or the untargeted approach. In the targeted approach, it is possible to routinely quantify components within complex mixtures and to translate academic research into deployable solutions. In the untargeted approach, models of normality can be rapidly developed and used by industry to confirm their products are consistent with previous batches. This application of spectroscopic technology is not new, and has been implemented using profiling technologies such as near and Fourier Transform infra-red (NIR, FT-IR) spectroscopy. The unique advantage of routine profiling using low-field NMR spectroscopy though, is the interpretability of signals to specific chemicals. This is because NMR phenomenon is directly transferable from benchtop instrumentation to high field, laboratory based instrumentation and the advantages they provide. For example, in a theoretical case where a food sample is shown to be inconsistent by benchtop NMR, the same sample analysed on a high field instrument would show the same inconsistency, enabling rapid unknown identification. Once identified, intelligence can be applied to the inconsistent sample to determine what action, if any is required. Studies that apply both low of high field analysis are recommended to demonstrate the utility of this approach.

Liquid foods, such as beverages, vegetable oils and fully soluble foodstuffs like honey are very simple to analyse by ^1H NMR because they do not require specific preparation. Therefore, they can be analysed with no to minimal pre-treatment and high resolution spectra are usually obtained. Some experimental difficulties due to the presence of the signals of the most abundant components (water in fruit juices, ethanol and water in wine and beer, etc.) have been resolved using specific pulse sequences to suppress these signals (Mannina et al., 2016).

Non-homogeneous liquid foods usually do not show sufficiently resolved NMR spectra, and additional extraction procedures may be necessary to extract and study their components. Due to its nature, milk can be considered one of the most complicated foods to study. Milk is an emulsified colloid consisting of small globules of fat and protein suspended in water, the principal component of milk. Therefore, a well-resolved ^1H NMR spectrum is difficult to obtain. In literature, only one example of ^1H NMR analysis of milk without any pretreatment is reported (Hu et al., 2004). Other studies of milk have required sample pretreatment such as the use of spin filters with specific cut-off to remove residual lipids and protein (Sundekilde et al., 2013), the extraction of triacylglycerols, and/or adjustment of the pH before the acquisition of ^{13}C and ^{31}P NMR spectra (Belton & Lyster, 2009; Andreotti et al., 2002). The “traditional” frauds encountered in milk include: watering, lactoserum addition, species blend, old milk reuse, etc. More recently, other issues have involved the addition of nitrogen containing compounds (melamine, dicyandiamide, protein hydrolysates, etc.) to artificially increase the protein content (as determined from total nitrogen). The current approach offered by routine laboratories to control the authenticity of milk and milk powder consist of doing 2 extractions in parallel in order to cover all potential adulterations (unpublished):

- one extraction in water to monitor the sugar profile (with the possibility of identifying delactosed milk and to observe if sucrose or maltodextrin have been added), to detect protein hydrolysate and to control microbial degradation,
- one extraction in dimethyl sulfoxide to monitor the fat content (whole, semi-skimmed, skimmed), to detect addition of foreign fats, to identify the thermal treatment (pasteurized or sterilised) or to detect melamine or other N-enhancers.

Solid food samples require specific preparation, including sampling, conservation and homogenization for extraction, to be analyzed by liquid state ^1H NMR. The extraction procedure is a critical step contributing significantly to the final quali-quantitative profile

composition revealed by NMR. As an illustration of this extraction procedure, untargeted screening methods have been developed to authenticate caviar (Heude et al., 2016) as a tool to protect the PGI (Protected Geographical Indication) “caviar d’Aquitaine”. Using an untargeted approach, authentic caviar d’Aquitaine and foreign origin caviar were analysed using ^1H NMR spectroscopy. This method was validated and implemented in control laboratory.

Another problem source for NMR is the widespread presence of paramagnetic metals (i.e. Fe^{3+} , Mn^{2+}) in various foodstuffs, namely spices, cereals, dried fruits and meat. During the extraction procedure, these cations can be co-extracted and give rise to the broadening of ^1H signal of metabolites, leading to decreased resolution.

The direct application of the High Resolution Magic Angle Spinning (HR-MAS) for products without any pretreatment is possible for semisolid foodstuff (Ritota et al., 2010). Such technology has been used to control fish freshness (Heude et al., 2015) but because of the lack of automation, currently applications are limited to specific studies.

NMR methodologies have already shown a noticeable potential in food analysis to solve specific problems. The versatility of NMR and possibility to employ either targeted or untargeted approaches enable one to develop a suitable protocol ad hoc for a specific problem. Despite these prospectives, important challenges still remain. Due to high cost of equipment and its maintenance, as well as a necessity of high qualified personnel, high resolution NMR is still too expensive for day-to-day application. To reduce the cost per single measurement and make NMR more accessible, the complete automation of NMR analysis is in progress. The spectral processing, assignment and statistical analysis of NMR data are still too laborious and sometimes constitute a bottleneck of the entire analysis. Fortunately, the constant development of software suitable for assignment and quantification of metabolites in food matrices could significantly help and encourage the application of NMR. The creation and development of interactive databases with NMR data for foodstuffs and standardization

of successful protocols of analysis are also important to extend NMR application in the authenticity testing field.

An example of existing food databases is FooDB that aggregates data from different sources reporting food constituents and their chemical and biological properties, mostly for unprocessed foodstuffs. Unfortunately, the general classification of food types does not include some essential aspects relative to variety, processing, etc, that determine the food identity. For instance, tea (*Camellia sinensis*) is reported as a single type product without taking into consideration different fermentation types and varieties.

An attempt to create a comprehensive database including food NMR spectra and data on their origin, composition, variety etc. is being undertaken by the Italian Group of Magnetic Resonance in Food Science (e-ALIERB OpenLab, 2016 <http://www.e-alierb.it/>). Outputs and recommendations will be drawn from this research to provide implementation guidelines and it is recommended that these conclusions are published in a peer reviewed journal.

The creation of comprehensive NMR databases of foodstuffs is hindered by the fragmentation of experimental approaches used until to now. Different extraction procedures, solvents, quantification and statistical analysis have been applied for the same foodstuff that results in non-comparable NMR profiles. Therefore, an international collaboration between researchers is necessary to unify different approaches and can be a key element in the development of a food NMR database that is constantly, or at least periodically, updated.

The combination of data from different platforms (NMR and other analytical methods) is a powerful strategy to enrich the final information content regarding food identity and thus improve the identification of food frauds followed by routine applications. The benefit of combining two untargeted methods has been recently illustrated on honey by Spiteri et al. (2016). Using data from two analytical platforms, namely NMR and high resolution mass spectrometry (HRMS), and two separate HRMS technologies, honey samples were analysed with the aim of determining their botanical origins. No one of the PCA models built

with individual NMR or MS data set was able to discriminate samples in terms of botanical origin. Then, mid-level fusion of the data was explored in two ways to improve the discrimination: fusion of PCA scores from the combined data sets or after selection of variables by PLS-DA. In both cases, it was possible to improve the discrimination so that botanical origin could be assigned without the need for pollen analysis.

Another example of the benefit of fusing NMR data with alternative techniques has been provided by Monakhova et al. (2014b). The authors evaluated the combination of discrete isotopic data with untargeted NMR spectrum to have better control of wines. Both techniques are known to provide useful information to the characterization of wine: ^1H NMR spectroscopy can be used to build robust classification models for grape variety, year of vintage and geographical origin, while stable isotope ratio analysis is a good source of chemical information for the authenticity assessment of food products. By combining these two methodologies, improvement of classification rates of wine was achieved: 100% for the determination of geographical origin (60–70% correct prediction was obtained with stable isotope data alone and 82–89% with ^1H NMR spectroscopy) and 99% for the vintage of wine (from 88 to 97% with ^1H NMR).

1.2 References

- Ackermann, S.M., Dolsophon, K., Monakhova, Y.B., Kuballa, T., Reusch, H., Thongpanchang, T., ...Lachenmeier, D.W., 2017. Automated multicomponent analysis of soft drinks using 1D ¹H and 2D ¹H-¹H J-resolved NMR spectroscopy. *Food Anal. Methods* 3, 827-836.
- Andreotti, G., Lamanna, R., Trivellone, E., & Motta, A., 2002. ¹³C NMR spectra of TAG: An easy way to distinguish milks from different animal species. *J. Am. Oil Chem. Soc.* 79, 123-127.
- Belton, P.S., & Lyster, R.L.J. 2009., ³¹P nuclear magnetic resonance spectra of milk from various species. *J. Dairy Res.* 58, 443-451.
- Beretta, G., Caneva, E., Regazzoni, L., Bakhtyari, N.G., Facino, R.M., 2008. A solid-phase extraction procedure coupled to ¹H NMR, with chemometric analysis, to seek reliable markers of the botanical origin of honey. *Anal. Chim. Acta* 620, 176–182.
- Boffo, E.F., Tavares, L.A., Ferreira, M.M.C., Ferreira, A.G., 2009. Classification of Brazilian vinegars according to their ¹H NMR spectra by pattern recognition analysis. *LWT – Food Sci. Technol.* 42, 1455-1460.
- Capitani, D., Sobolev, A.P., Delfini, M., Vista, S., Antiochia, R., Proietti, N., Bubici, S., Ferrante, G., Carradori, S., De Salvador, F.R., Mannina, L., 2014. NMR methodologies in the analysis of blueberries. *Electrophoresis* 35, 1615-1626.
- Capozzi, F., Bordoni, A., 2013. Foodomics: a new comprehensive approach to food and nutrition. *Genes Nutr.* 8, 1–4.
- Consonni, R., Cagliani, L.R., Rinaldini, S., Incerti, A., 2008. Analytical method for authentication of Traditional Balsamic Vinegar of Modena. *Talanta* 75, 765-769.
- Cozzolino, D., 2015. Foodomics and infrared spectroscopy: from compounds to functionality. *Curr. Opin. Food Sci.* 4, 39-43.
- Cuny, M., Vigneau, E., Le Gall, G., Colquhoun, I., Lees, M., Rutledge, D.N., 2008. Fruit juice authentication by ¹H NMR spectroscopy in combination with different chemometrics tools. *Anal. Bioanal. Chem.* 390, 419-427.
- Defernez, M., Wren, E., Watson, A.D., Gunning, Y., Colquhoun, I.J., Le Gall, G., ...Kemsley, E.K., 2017. Low-field ¹H NMR spectroscopy for distinguishing between Arabica and Robusta ground roast coffees. *Food Chem.* 216, 106-113.
- Donarski, J.A., Jones, S.A., & Charlton, A.J., 2008. Application of cryoprobe ¹H nuclear magnetic resonance spectroscopy and multivariate analysis for the verification of Corsican honey. *J. Agric. Food Chem.* 56, 5451-5456.
- Donarski, J.A., Jones, S.A., Harrison, M., Driffield, M., & Charlton, A.J., 2010b. Identification of botanical biomarkers found in Corsican honey. *Food Chem.* 118, 987-994.

Donarski, J.A., Roberts, D.P.T., & Charlton, A.J., (2010a). Quantitative NMR spectroscopy for the rapid measurement of methylglyoxal in manuka honey. *Anal. Methods*. 10, 1479-1483.

Dunn, W.B., & Ellis, D.I., 2005. Metabolomics: Current analytical platforms and methodologies. *Trends Analyt Chem*. 24, 285-294.

Fiehn, O., 2002. Metabolomics – the link between genotypes and phenotypes. *Plant Mol. Biol*. 48, 155–171.

FoodDB., (2017). <http://foodb.ca/> Accessed 20.11.2017.

Godelmann, R., Fang, F., Humpfer, E., Schutz, B., Bansbach, M., Schafer, H., & Spraul, M., 2013. Targeted and nontargeted wine analysis by ¹H NMR spectroscopy combined with multivariate statistical analysis. Differentiation of important parameters: grape variety, geographical origin, year of vintage. *J. Agric. Food Chem*. 61, 5610-5619.

Heude, C., Lemasson, E., Elbayed, K., & Piotto, M., 2015. Rapid assessment of fish freshness and quality by ¹H HR-MAS NMR spectroscopy. *Food Anal. Methods*. 8, 907–915.

Heude, C., Elbayed, K., Jezequel, T., Fanuel, M., Lugan, R., Heintz, D., ...Piotto, M., 2016. Metabolic characterization of caviar specimens by ¹H NMR spectroscopy: Towards caviar authenticity and integrity. *Food Anal. Methods*. 9, 3428-3438.

Hu, F., Furihata, K., Ito-Ishida, M., Kaminogawa, S., & Tanokura, M., 2004. Nondestructive observation of bovine milk by NMR spectroscopy: analysis of existing states of compounds and detection of new compounds. *J. Agric. Food Chem*. 52, 4969–4974.

Jakes, W., Gerdova, A., Defernez, M., Watson, A. D., McCallum, C., Limer, E., ...Kemsley, E. K., 2015. Authentication of beef versus horse meat using 60 MHz ¹H NMR spectroscopy. *Food Chem*. 175, 1-9.

Gika, H.G., Wilson I.D., Theodoridis, G.A., 2014. Chapter 9 – The role of mass spectrometry in nontargeted metabolomics. In: *Comprehensive Analytical Chemistry. Fundamentals of advanced omics technologies: From genes to metabolites*. Edited by Simó, C., Cifuentes, A., García-Cañas, V., Elsevier, 63, 213-233.

Jung, Y., Lee, J., Kwon, J., Lee, K. S., Ryu, D. H., Hwang, G.S., 2010. Discrimination of the geographical origin of beef by ¹H NMR-based metabolomics. *J. Agric. Food Chem*. 58 (19), 10458–10466.

Kaiser, K.A., Barding Jr, G.A., Larive, C.K., 2009. A comparison of metabolite extraction strategies for ¹H NMR-based metabolic profiling using mature leaf tissue from the model plant *Arabidopsis thaliana*. *Magn. Reson. Chem*. 47, S147–S156.

Kim, H.K., Verpoorte, R., 2010. Sample preparation for plant metabolomics. *Phytochem. Anal*. 21, 4–13.

Khatib, A., Wilson, E.G., Kim, H.K., Lefeber, A.W.M., Erkelens, C., Choi, Y.H., Verpoorte, R., 2006. Application of two-dimensional J-resolved nuclear magnetic resonance spectroscopy to differentiation of beer. *Anal. Chim. Acta* 559, 264–270.

-
- Lamanna, R., Braca, A., Di Paolo, E., & Imparato, G., 2011. Identification of milk mixtures by ^1H NMR profiling. *Magn. Reson. Chem.* 49, S22-S26.
- Li, Q., Yu, Z., Zhu, D., Meng, X., Pang, X., Liu, Y., Frew, R., Chen, H., Chen, G., 2016. The application of NMR-based milk metabolite analysis in milk authenticity identification. *J. Sci. Food Agric.* 97, 2875-2882.
- Lin, C.Y., Wu, H., Tjeerdema, R.S., Viant, M.R., 2007. Evaluation of metabolite extraction strategies from tissue samples using NMR metabolomics. *Metabolomics* 3, 55–67.
- Mannina, L., Sobolev, A.P., Capitani, D., Iaffaldano, N., Rosato, M.P., Ragni, P., Reale, A., Sorrentino, E., D'Amico, I., Coppola, R., 2008. NMR metabolic profiling of organic and aqueous sea bass extracts: implications in the discrimination of wild and cultured sea bass. *Talanta* 77, 433–444.
- Mannina, L., Marini, F., Gobbino, M., Sobolev, A. P., & Capitani, D., 2010. NMR and chemometrics in tracing European olive oils: the case study of Ligurian samples. *Talanta* 80, 2141–2148.
- Mannina, L., & Sobolev, A. P., 2011. High resolution NMR characterization of olive oils in terms of quality, authenticity and geographical origin. *Magn. Reson. Chem.* 49, S3-S11.
- Mannina, L., Sobolev, A.P., Viel, S., 2012. Liquid state ^1H high field NMR in food analysis. *Prog. Nucl. Magn. Reson. Spectrosc.* 66, 1–39.
- Mannina, L., Marini, F., Antiochia, R., Cesa, S., Magrì, A., Capitani, D. & Sobolev, A.P., 2016. Tracing the origin of beer samples by NMR and chemometrics: Trappist beers as a case study. *Electrophoresis* 37, 2710-2719.
- McDougall, G., Martinussen, I., Stewart, D., 2008. Towards fruitful metabolomics: high throughput analyses of polyphenol composition in berries using direct infusion mass spectrometry. *J. Chromatogr. B* 871, 362–369.
- McKenzie, J.S., Donarski, J.A., Wilson, J.C., Charlton, A.J., 2011. Analysis of complex mixtures using high-resolution nuclear magnetic resonance spectroscopy and chemometrics. *Prog. Nucl. Magn. Reson. Spectrosc.* 59, 336–359.
- Minoja, A.P., & Napoli, C., 2014. NMR screening in the quality control and nutraceuticals. *Food Res. Int.* 63, 126-131.
- Monakhova, Y.B., Godelmann, R., Hermann, A., Kuballa, T., Cannet, C., Schäfer, H., Rutledge, D.N., 2014b. Synergistic effect of the simultaneous chemometric analysis of ^1H NMR spectroscopic and stable isotope (SNIF-NMR, ^{18}O , ^{13}C) data: application to wine analysis. *Anal. Chim. Acta.* 833, 29-39.
- Monakhova, Y.B., Ruge, W., Kuballa, T., Ilse, M., Winkelmann, O., Diehl, B., ...Lachenmeier, D.W., 2015. Rapid approach to identify the presence of Arabica and Robusta species in coffee using ^1H NMR spectroscopy. *Food Chem.* 182, 178-184.
- Monakhova, Y.B., Schutz, B., Schafer, H., Spraul, M., Kuballa, T., Hahan, H., & Lachenmeier, D.W., 2014a). Validation studies for multicomponent quantitative NMR analysis: the example of apple fruit juice. *Accredit. Qual. Assur.* 19, 17-29.

- Novoa-Carballal, R., Fernandez-Megia, E., Jimenez, C., Riguera, R., 2011. NMR methods for unravelling the spectra of complex mixtures. *Nat. Prod. Rep.* 28, 78–98.
- Petrakis, E.A., Cagliani, L.R., Polissiou, M.G., & Consonni, R., 2015. Evaluation of saffron (*Crocus sativus* L.) adulteration with plant adulterants by ¹H NMR metabolite fingerprinting. *Food Chem.* 173, 890-896.
- Piccioni, F., Capitani, D., Zolla, L., Mannina, L., 2009. NMR metabolic profiling of transgenic maize with the Cry1A(b) gene, *J. Agric. Food Chem.* 57, 6041–6049.
- Ritota, M., Marini, F., Sequi, P., & Valentini, M., 2010. Metabolomic characterization of Italian sweet pepper (*Capsicum annum* L.) by means of HRMAS-NMR spectroscopy. *J. Agric. Food Chem.* 58, 9675-9684.
- Rongai, D., Sabatini, N., Del Coco, L., Perri, E., Del Re, P., Simone, N., ...Fanizzi, F.P., 2017. ¹H NMR and multivariate analysis for geographic characterization of commercial extra virgin olive oil: A possible correlation with climate data. *Foods* 6, 96.
- Scalbert, A., Brennan, L., Fiehn, O., Hankemeier, T., Kristal, B.S., van Ommen, B., ...Wopereis, S., 2009. Mass-spectrometry-based metabolomics: limitations and recommendations for future progress with particular focus on nutrition research. *Metabolomics* 5, 435-458.
- Smolinskaa, A., Blancheta, L., Buydensa, L.M.C., & Wijmengaa, S.S., 2012. NMR and pattern recognition methods in metabolomics: From data acquisition to biomarker discovery: A review. *Anal. Chim. Acta.* 750, 82-97.
- Sobolev, A.P., Brosio, E., Gianferri, R., Segre, A.L., 2005. Metabolic profile of lettuce leaves by high-field NMR spectra. *Magn. Reson. Chem.* 43, 625–638.
- Sobolev, A.P., Circi, S., & Mannina, L., 2016. Advances in nuclear magnetic resonance spectroscopy for food authenticity testing. In: G. Downey (Ed.), *Advances in Food Authenticity Testing* (pp. 147-170). Elsevier Ltd. United Kingdom: Woodhead Publishing
- Spiteri, M., Dubin, E., Cotton, J., Poirel, M., Corman, B., Jamin, E., ...Rutledge, D.N., 2016. Data fusion between high resolution ¹H-NMR and mass spectrometry: A synergetic approach to honey botanical origin characterization. *Anal. Bioanal. Chem.* 408, 4389-4401.
- Spiteri, M., Jamin, E., Thomas, F., Rebours, A., Lees, M., Rogers, K.M., & Rutledge, D.N., 2015. Fast and global authenticity screening of honey using ¹H-NMR profiling. *Food Chem.* 189, 60-66.
- Spiteri, M., Rogers, K. M., Jamin, E., Thomas, F., Guyader, S., Lees, M., & Rutledge, D.N., 2017. Combination of ¹H NMR and chemometrics to discriminate Manuka honey from other floral honey types from Oceania. *Food Chem.* 217, 766–772.
- Spraul, M., Shutz, B., Humpfer, E., Mortter, M., Schafer, H., Koswig, S., & Rinke, P., 2009a. Mixture analysis by NMR as applied to fruit juice quality control. *Magn. Reson. Chem.* 47, S130-S137.

-
- Spraul, M., Schuz, B., Rinke, P., Koswig, S., Humpfer, E., Schafer, H., ...Minoja, A., 2009b. NMR-based multi parametric quality control of fruit juices: SGF profiling. *Nutrients* 1, 148-155.
- Spraul, M., Schafer, H., Shutz, B., Fang, F., & Link, M., 2013. Novel NMR-technology to assess food quality and safety. *IJABE* 7, 960-963.
- Sundekilde, U.K., Poulsen, N.A., Larsen, L.B., & Bertram, H.C., 2013. Nuclear magnetic resonance metabonomics reveals strong association between milk metabolites and somatic cell count in bovine milk. *J. Dairy Sci.* 96, 290–299.
- Wei, F., Furihata, K., Koda, M., Hu, F., Miyakawa, T., & Tanokura, M., 2012. Roasting process of coffee beans as studied by nuclear magnetic resonance: Time course of changes in composition. *J. Agric. Food Chem.* 60, 1005-1012.
- Wishart, D. S., 2008. Quantitative metabolomics using NMR. *Trends Analyt Chem.* 27, 228-237.
- Wu, H., Southam, A.D., Hines, A., Viant, M.R., 2008. High-throughput tissue extraction protocol for NMR and MS-based metabolomics. *Anal. Biochem.* 372, 204–212.
- van der Greef, J., & Smilde, A.K., 2005. Symbiosis of chemometrics and metabolomics: past, present, and future. *J. Chemom.* 19, 376-386.
- Yilmaz, A., 2010. ¹H NMR metabolic fingerprinting of saffron extracts. *Metabolomics* 6, 511-517.

Chapter 2: Basics of Nuclear Magnetic Resonance

2.1 Introduction

Nuclear Magnetic Resonance in the condensed phase was discovered in 1946 independently by two groups of scientists, Bloch, Hansen and Packard at the University of Stanford (California, USA) (Bloch, Hansen & Packard, 1946), and Purcell, Torrey and Pound at the University of Cambridge (Massachusetts, USA) (Purcell, Torrey & Pound, 1946).

Right from the beginning, NMR was approached from two distinct perspectives. Bloch and coworkers envisioned NMR in classical terms, considering the orientation of microscopic magnetic moments with respect to an external magnetic field, whereas Purcell and coworkers pictured NMR in terms of quantum transitions.

The first conception affords one a rather simple and efficient way to describe the NMR phenomenon, providing insight regarding fundamental issues such as magnetization precession and nuclear relaxation. However, the classical description becomes rapidly limited and the second approach, the so-called spectroscopic description, relying mainly on quantum mechanics, becomes indispensable as soon as a deeper understanding of the interactions that rule nuclear spins is sought.

Accordingly, this chapter is divided into two sections that reflect the views of Bloch and Purcell, respectively. In a first part, we present the Bloch formalism and show how it can be applied to describe the NMR phenomenon. In a second part, we address the NMR phenomenon more rigorously using quantum mechanics. Specifically, a quantum mechanical description of the main interactions controlling the behavior of the nuclear spins is given, both

for the liquid and the solid state. Because many excellent text books exist on these topics, only the main results will be exposed here and the reader is referred to the general references given at the end of this chapter for more rigorous treatments (Pople, Schneider & Bernstein, 1959; Abragam, 1961; Lynden-Bell & Harris, 1969; Ferrar & Becker, 1971; Shaw, 1976; Fukushima & Roeder, 1981; Mehring, 1983; Ernst, Bodenhausen & Wokaun, 1987; Neuhaus & Williamson, 1989; Callaghan, 1991; Sanders & Hunter, 1993; Schmidt-Rohr & Spiess, 1994; Stejskal & Memory, 1994; Cavanagh et al., 1996; Kimmich, 1997; Levitt, 2001; Canet, Boubel & Canet Soulas, 2002).

2.2 Classical description of Nuclear Magnetic Resonance

This section describes the theoretical bases of NMR focusing on the so-called classical approach due to Bloch. The notion of magnetic moment is explained and the NMR phenomenon is described.

2.2.1 Nuclear magnetic moment

The NMR phenomenon is related to the existence of nuclear paramagnetism caused by the orientation of the individual nuclear magnetic moments $\vec{\mu}$ in the presence of an external static magnetic field \vec{B}_0 . The magnetic moment of a nucleus $\vec{\mu}$ is proportional to the nuclear spin angular momentum \vec{I} according to

$$\vec{\mu} = \gamma \hbar \vec{I} \quad (1)$$

where γ is the magnetogyric ratio of the nucleus and \hbar is Planck's constant divided by 2π .

In contrast with the electron, whose spin number I always equals $\frac{1}{2}$, the nuclear spin number I of a nuclei ${}^A_Z X$ depends on the mass number A and the charge number Z such as:

- If A is odd, then I is an half integer (${}^1\text{H}$, ${}^{13}\text{C}$, ${}^{27}\text{Al}$, ${}^{23}\text{Na}$);
- If A is even and Z is odd, then I is an integer (${}^{14}\text{N}$, ${}^2\text{H}$);

- If both A and Z are even, then I is zero and the nucleus is not active in NMR (^{12}C , ^{16}O).

The application of an external magnetic field \vec{B}_0 , which we suppose in this thesis to be oriented along the z axis only, leads to a motion of precession of all nuclear magnetic moments around the z axis at the Larmor frequency (Figure 2.1) given by

$$\omega_0 = \gamma B_0 \text{ (rad s}^{-1}\text{) or } \nu_0 = \frac{\gamma B_0}{2\pi} \text{ (Hz)} \quad (2)$$

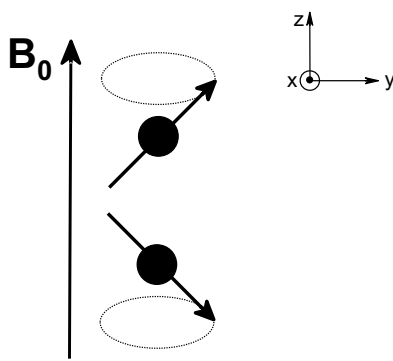


Figure 2.1 Motion of precession of the nuclear magnetic moments around the axis along which the external magnetic field is applied (by convention, the z axis).

In the classical description of NMR, the motion of precession does not affect the isotropic distribution of nuclear magnetic moments, and hence there is no net resulting magnetization. In contrast, the interaction of the nuclear magnetic moments with their environment (such as the thermal vibrations of the lattice) leads at equilibrium to an anisotropic distribution according to Boltzmann's law and hence gives a net longitudinal magnetization M_z (Figure 2.2).

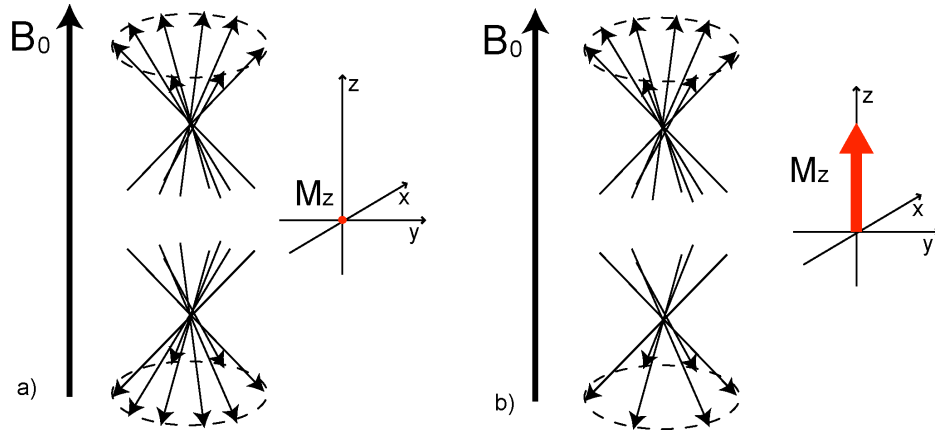


Figure 2.2 (a) Isotropic distribution of nuclear magnetic moments with no net resulting macroscopic magnetization; (b) Anisotropic distribution of nuclear magnetic moments with resulting net macroscopic magnetization, M_z , aligned the direction of the static magnetic field, \vec{B}_0 .

The longitudinal magnetization appears progressively with time according to the following law

$$M_z = M_0 \left(1 - e^{-\frac{t}{T_1}} \right) \quad (3)$$

where T_1 denotes the spin-lattice relaxation time or the longitudinal relaxation time. Eq (3) implies that

$$\frac{\partial M_z}{\partial t} = -\frac{M_z - M_0}{T_1} \quad (4)$$

with M_0 the longitudinal magnetization at equilibrium at the temperature T given by Langevin's law

$$M_0 = N_0 \frac{\gamma^2 \hbar^2 B_0}{kT} \frac{I(I+1)}{3} = \chi_0 B_0 \quad (5)$$

where N_0 is the number of magnetic moments per unit volume, and $\chi_0 = \frac{M_0}{B_0}$ is the static magnetic susceptibility. At room temperature, the difference in population for the two orientations of the nuclear magnetic moments is very weak (e.g., it is of the order of 1 in 10^5 for ^1H spin in a magnetic field of 11.7 T) (Cavanagh et al., 1996).

Time

2.2.2 Nuclear Magnetic Resonance phenomenon

The Nuclear Magnetic Resonance method consists in adding to the main static magnetic field \vec{B}_0 , a secondary magnetic field \vec{B}_1 , orthogonal to \vec{B}_0 and with $\|\vec{B}_1\| \ll \|\vec{B}_0\|$, which oscillates at the nuclear Larmor frequency. This second radio frequency field tips down the longitudinal magnetization to the xy plane, and hence generates a transverse magnetization M_{xy} . Then, the radiofrequency field is switched off and the magnetization progressively returns to its initial equilibrium position according to relaxation processes. The motion of precession of the magnetization while it returns to equilibrium induces a voltage in a coil placed perpendicularly to the main static field. This voltage constitutes the NMR signal and is called a Free Induction decay (FID): free of the influence of the radio frequency field, induced in the coil, and decaying back to equilibrium (Figure 2.3) (Sanders & Hunter, 1993).

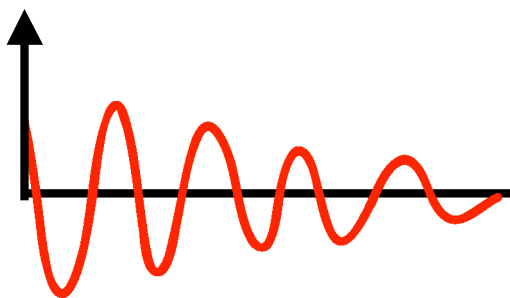


Figure 2.3 Schematic representation of a Free Induction Decay (off-resonance case).

Many relaxation mechanisms dictate the evolution of the transverse magnetization. To describe this evolution, a transverse relaxation time T_2 must be introduced. Transverse relaxation does not necessarily involve energy exchange but does however increase the entropy of the nuclear spin system. T_2 is defined by

$$\frac{\partial M_X}{\partial t} = -\frac{M_X}{T_2} \text{ and } \frac{\partial M_Y}{\partial t} = -\frac{M_Y}{T_2} \quad (6)$$

The system of nuclear magnetic moments can be associated with a macroscopic or bulk magnetization vector M . In turn, the bulk magnetization vector M is related to a bulk angular momentum \vec{J} through the nuclear magnetogyric ratio γ according to

$$\vec{M} = \gamma \cdot \vec{J} \quad (7)$$

Under certain conditions, the macroscopic behavior of the system of magnetic moments can be described by the laws of classical mechanics. The fundamental equation of motion is

$$\frac{\partial \vec{J}}{\partial t} = \vec{T} \quad (8)$$

where \vec{T} is a torque. In the presence of a magnetic field B , the torque exerted on the system of magnetic moments is given by

$$\vec{T} = \vec{M} \wedge \vec{B} \quad (9)$$

Thus, by combining eq (7), (8), and (9), we obtain

$$\frac{\partial M}{\partial t} = \gamma \cdot M \wedge B \quad (10)$$

In this NMR experiment, the total magnetic field B is composed of two distinct components: an intense, static magnetic field oriented along the z axis, \vec{B}_0 , and a weaker, oscillating field, \vec{B}_1 .

Formally, the oscillating field \vec{B}_1 is linearly polarized along an axis that belongs to the xy plane. In the following, we assume this axis to be the x axis without loss of generality (Cavanagh et al., 1996). As described elsewhere (Sanders & Hunter, 1993), a linearly polarized magnetic field of amplitude $2B_1$ is equivalent to two counter rotating magnetic fields of amplitude B_1 rotating along the z axis. To 1st order, only one of these two counter rotating components can affect the bulk magnetization vector M (Cavanagh et al., 1996), and hence the other component will not be further considered here. In other words, the linearly

polarized magnetic field \vec{B}_1 can be pictured as a magnetic field that rotates along the z axis with a frequency ω , an amplitude B_1 and an initial phase ϕ . By definition, ϕ is the angle formed between the x axis and the polarization axis of the \vec{B}_1 field, which, in our case, implies that ϕ is zero.

In these conditions, if we suppose $\gamma > 0$, the total effective field acting on the bulk magnetization M is given in the laboratory frame $(\vec{e}_x, \vec{e}_y, \vec{e}_z)$ by

$$(B_1 \cos \omega \cdot t) \vec{e}_x + (-B_1 \sin \omega \cdot t) \vec{e}_y + B_0 \vec{e}_z \quad (11)$$

Thus, in the laboratory frame, the Bloch equations are given by

$$\begin{aligned} M'_X &= \gamma \cdot [M_Y B_0 + M_Z B_1 \sin(\omega t)] - \frac{M_X}{T_2} \\ M'_Y &= \gamma \cdot [-M_X B_0 + M_Z B_1 \cos(\omega t)] - \frac{M_Y}{T_2} \\ M'_Z &= \gamma \cdot [-M_Y B_1 \cos(\omega t) - M_X B_1 \sin(\omega t)] - \frac{M_Z - M_0}{T_1} \end{aligned} \quad (12)$$

Additional simplification can be achieved by describing the NMR phenomenon in the so-called rotating frame, i.e. in an orthonormal frame that rotates along the z axis at the frequency of the radiofrequency field \vec{B}_1 . In this case, if we further suppose the frequency of the radiofrequency field to equal the Larmor frequency of the nucleus (on-resonance case), both M and \vec{B}_1 appear fixed in the rotating frame. In other words, we have mathematically (and artificially) removed their time dependence.

We now focus on pulsed NMR and do not consider continuous wave NMR (see reference 4 for a more complete presentation). In pulsed NMR, an intense radiofrequency field \vec{B}_1 is applied for a very short period of time, typically a few μs . Because the relaxation times T_1 and T_2 are much larger than the pulse duration τ (note that, rigorously, T_1 and T_2 are not mere times but time constants), relaxation processes can be safely neglected during the

pulse. Therefore, in the rotating frame, the effect of a radiofrequency pulse of duration τ and phase x (i.e. applied along the x axis) can be pictured as the rotation of the bulk magnetization vector M around the x axis through an angle θ of $\gamma B_1 \tau$ (Figure 2.4).

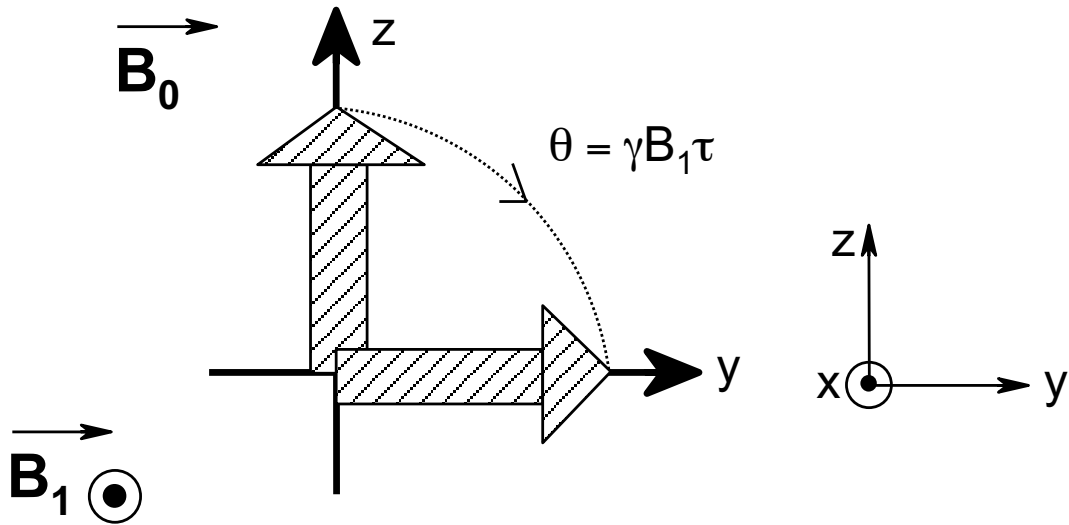


Figure 2.4 Schematic representation of the effect on the longitudinal magnetization vector M (represented by the large dashed arrow) of a radiofrequency pulse of duration τ applied with a x phase: M is rotated along the x axis of an angle θ that depends on the radiofrequency pulse amplitude B_1 and duration τ . Here γ is supposed to be positive.

One of the advantages of the pulsed method with respect to the continuous wave method, relies on the possibility to repeat each measurement in a faster way (typically every second). It then becomes possible to coherently add the results of n measurements, hereby increasing the signal-to-noise ratio by a factor of \sqrt{n} (Ernst, Bodenhausen & Wokaun, 1987).

2.3 Quantum description of Nuclear Magnetic Resonance

Nuclear magnetic resonance, such as any other spectroscopic technique involving electromagnetic waves, can only be fully explained in terms of a quantum mechanical framework.

2.3.1 Theoretical basics of quantum mechanics applied to NMR

2.3.1.1 Time independent perturbations

Many theoretical results regarding Nuclear Magnetic Resonance on the interactions of a spin system are based on the theory of stationary perturbations, i.e. time independent perturbations.

The aim of this theory is to determine the modifications of the energy levels of the Hamiltonian H_0 and of its stationary states by the adjunction of a perturbation described by the Hamiltonian H_p . The total Hamiltonian is hence given by:

$$H = H_0 + H_p \quad (13)$$

where the eigenstates of H_0 are known and H_p is an operator whose matrix elements are small compared with those of H_0 . In the presence of the perturbation, the energy of a given non degenerate eigenvalue associated with an eigenfunction $|\varphi_n\rangle$ of the Hamiltonian H_0 , ($H_0|\varphi_n\rangle = E_n^0|\varphi_n\rangle$) must be corrected according to

$$E_n = E_n^0 + \langle \varphi_n | H_p | \varphi_n \rangle + \sum_{p \neq n} \sum_i \frac{|\langle \varphi_n^i | H_p | \varphi_n \rangle|^2}{E_n^0 - E_p^0} + \varepsilon^3 \quad (14)$$

In eq (14), the first term represents the energy value associated with the non perturbed state, whereas the second and third terms are the first and second order corrections, respectively. Note that, in the case of a degenerate eigenvalue E_p^0 , the superscript i in eq (14) allows us to distinguish the diverse vectors of the orthonormal base associated with the corresponding eigen subspace.

In the case of time dependent perturbations, the energy corrections are more complex to determine. However, in certain experiments, especially when pulses must be considered, the results obtained for the case of time independent perturbations can still be applied by using the average Hamiltonian theory.

2.3.1.2 Tensor representation of the Hamiltonians

The total Hamiltonian of a quantum mechanical system can be decomposed into a sum of components according to

$$H_T = \sum_{\lambda=1}^N H_{\lambda} \quad (15)$$

where H_{λ} is the Hamiltonian associated with a specific interaction λ . For instance, in NMR, this Hamiltonian may describe the interaction of a spin I either with the external magnetic field \vec{B}_0 or with another spin S . Generally, H_{λ} can be written as

$$H_{\lambda} = V \cdot \overline{\overline{P}} \cdot W \quad (16)$$

where V and W are two vectorial operators, and $\overline{\overline{P}}$ is the tensor characterizing the interaction λ . $\overline{\overline{P}}$ is a rank 2 tensor which can be written in the Cartesian basis such as

$$\overline{\overline{P}} = \begin{pmatrix} P_{xx} & P_{xy} & P_{xz} \\ P_{yx} & P_{yy} & P_{yz} \\ P_{zx} & P_{zy} & P_{zz} \end{pmatrix} \quad (17)$$

A rank 2 Cartesian tensor can be decomposed in the sum of three tensors of rank 0, 1, and 2, respectively, such as

$$\overline{\overline{P}} = P^{(0)} + P^{(1)} + P^{(2)} \quad (18)$$

where

- $P^{(0)}$ is a rank 0 tensor, scalar invariant: $P_{\alpha\beta}^{(0)} = \frac{1}{3} \text{Tr}[P] \cdot \delta_{\alpha\beta}$
 - $P^{(1)}$ is a rank 1 tensor, antisymmetric and of trace null: $P_{\alpha\beta}^{(1)} = \frac{1}{2} (P_{\alpha\beta} - P_{\beta\alpha})$
 - $P^{(2)}$ is a rank 2 tensor, symmetric with a trace null: $P_{\alpha\beta}^{(2)} = \frac{1}{2} (P_{\alpha\beta} + P_{\beta\alpha}) - \frac{1}{3} \text{Tr}[P] \delta_{\alpha\beta}$
- (19)

The Hamiltonians can also be described in spherical coordinates by means of irreducible spherical tensors. This description eases the calculation of the resonance frequency characterizing the interactions, especially when changes in reference frames are required. The Hamiltonian that characterizes a given interaction is written by the product of two irreducible, rank 2 spherical tensors such as

$$H_\lambda = C_\lambda \sum_{k=0}^2 \sum_{q=-k}^k (-1)^q A_{k,-q} T_{kq} \quad (20)$$

where C_λ is a factor that depends only on the fundamental constants describing a given interaction, A_{kq} represents a component of the spherical space tensor (\overline{P}), and T_{kq} represents a component of the spherical spin tensor (V and W).

2.3.1.3 Rotations in NMR

In NMR, two distinct types of rotation can be considered, namely rotation in spin space and rotation in spatial space. Specifically, spin space rotation affects only the spin variables (e.g., radiofrequency pulses induce spin rotations), whereas spatial space rotations transform the spatial components of an interaction λ .

Generally the spatial components $A_{k,q}$ of an interaction λ are expressed in a reference frame directly linked to the molecule, the so-called Principal Axis System (PAS). In this reference frame, the tensor is diagonal. Usually a change of reference frame is then required to express $A_{k,q}$ in the laboratory frame (LAB), for which the z axis is chosen to be along the direction of the main static magnetic field. Using the matrix notation introduced by Wigner, $D_{pq}^{(k)}$, we can write that

$$PAS \xrightarrow{(\alpha, \beta, \gamma)} LAB$$

$$A_{kq}^{LAB} = \sum_{p=-k}^k A_{kp}^{PAS} D_{pq}^{(k)}(\alpha, \beta, \gamma) \quad (21)$$

where (α, β, γ) are the three Euler angles (Figure 2.5).

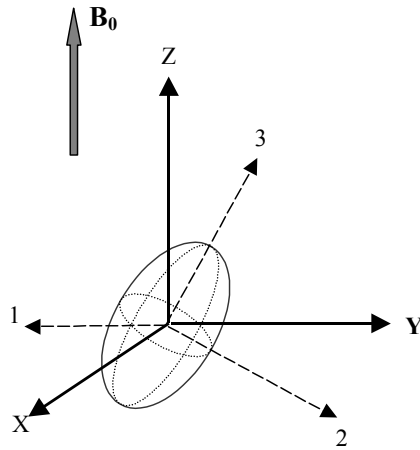


Figure 2.5 Schematic representation of the ellipsoid representing a rank 2 tensor.

Moreover, in most solid state NMR experiments, the sample to analyze is commonly placed inside a rotor that rotates around an axis which makes a specific angle with respect to the direction of the main static magnetic field. In this case, it may be useful to represent the tensors with respect to the corresponding rotation axis. Therefore, two changes of reference frames are required according to

$$PAS \xrightarrow{(\alpha, \beta, \gamma)} ROTOR \xrightarrow{(\omega_R t, \chi, 0)} LAB$$

where ω_R is the spinning rate. We can thus write the following relationship

$$A_{kq}^{LAB} = \sum_{l, p=-k}^k A_{kp}^{PAS} D_{pl}^{(k)}(\alpha, \beta, \gamma) D_{lq}^{(k)}(\omega_R t, \chi, 0) \quad (22)$$

Finally, if the Hamiltonian H_λ describing an internal interaction λ is expressed in a frame rotating at the Larmor frequency, i.e the so-called rotating frame, then H_λ becomes time dependent. To write the expression of H_λ in the rotating frame, the components of the spin tensor must be rotated by an angle of $-\omega_0 t$ around I_z . In other words, H_λ becomes

$$H_{\lambda}(t) = C_{\lambda} \sum_{k=0}^2 \sum_{q=-k}^k (-1)^q A_{k,-q} T_{kq} e^{iq\omega_0 t} \quad (23)$$

2.3.1.4 Average Hamiltonian and calculation of the perturbation

The Hamiltonian that describes an interaction in the laboratory frame is periodic and the Larmor period is given by $2\pi/\omega_0$. During this period, it becomes possible to transform $H_{\lambda}(t)$ into an average time independent Hamiltonian $\overline{H_{\lambda}}$. $\overline{H_{\lambda}}$ corresponds to a sum of terms of increasing order according to the so-called Magnus expansion, which is somehow equivalent to the calculation of a perturbation of order n. The first term of this series, otherwise called correction to first order, is given by

$$\overline{H_{\lambda}^{(1)}} = \frac{\omega_0}{2\pi} \int_0^{\frac{2\pi}{\omega_0}} H_{\lambda}(t_1) dt_1 \quad (24)$$

and the second order correction is

$$\overline{H_{\lambda}^{(2)}} = i \frac{\omega_0}{4\pi} \int_0^{\frac{2\pi}{\omega_0}} dt_2 \int_0^{t_2} dt_1 [H_{\lambda}(t_1), H_{\lambda}(t_2)] \quad (25)$$

2.3.2 Nuclear magnetic interactions

This section describes the nuclear magnetic interactions that are relevant in NMR. These interactions play different roles depending on the state of the matter, liquid or solid, that is considered. Although this thesis mainly focuses on liquid state NMR, all the nuclear magnetic interactions relevant to NMR are described.

In NMR, there are several mechanisms of interaction which can be distinguished according to whether they involve external or internal (local) magnetic fields. Accordingly, the complete Hamiltonian is given by

$$H = H_Z + H_1 + H_{\text{int}} \quad (26)$$

where the external interactions are described by the Hamiltonians H_Z and H_1 , due to the \vec{B}_0 and \vec{B}_1 fields, respectively, and the internal interactions are described by the Hamiltonian H_{int} . Precisely, the external interactions are due to the application of the static and radiofrequency fields, whereas the internal interactions are related to the influence of the local environment (local dipolar fields, neighboring electronic clouds) on the spin I . The Hamiltonian H_{int} is the sum of all the contributions due to the distinct internal interactions of the system

$$H_{\text{int.}} = H_{\sigma} + H_D + H_J + H_Q \quad (27)$$

where H_{σ} =electronic screening Hamiltonian; H_D =homonuclear and heteronuclear dipolar coupling Hamiltonian; H_J =scalar coupling Hamiltonian; H_Q =quadrupolar coupling Hamiltonian.

In the presence of the static magnetic field \vec{B}_0 , all internal interactions can be regarded as perturbations of the Zeeman interaction, and hence the theory of stationary perturbations can be applied.

2.3.2.1 The Zeeman interaction

As shown by eq (1), the nuclear magnetic moment $\vec{\mu}$ is proportional to the spin angular momentum \vec{I} . In the quantum description of NMR, the values of the spin angular momentum and, in turn, of the magnetic moment, are quantized. In particular, the projection along the z axis of the nuclear magnetic moment is given by

$$\mu_z = \gamma \cdot \hbar I_z = \gamma \cdot \hbar m \quad (28)$$

where m denotes the magnetic quantum number verifying

$$-I \leq m \leq +I \quad (29)$$

The Hamiltonian describing the interaction of the spin system with the magnetic field \vec{B}_0 is called the Zeeman Hamiltonian, and is written as

$$H_0 = -B_0\mu_z = -\gamma B_0 \hbar I_z = -\hbar\omega_0 I_z \quad (30)$$

The eigenvalues equation of the Hamiltonian giving the values of the energies of the spin system is then

$$H_0|m\rangle = E_m|m\rangle \Rightarrow -\hbar\omega_0 I_z|m\rangle = E_m|m\rangle \quad (31)$$

Thus we can write

$$E_m = -m\hbar\omega_0 \quad (32)$$

Eq (32) shows that the Zeeman interaction cancels the degeneracy leading to $2I+1$ energy levels. In the absence of any other interaction, these energy levels are equidistant. The transition frequency between two consecutive levels is hence independent of m (Figure 2.6).

$$\omega_{m,m+1} = \frac{1}{\hbar} [\langle m-1|H_0|m-1\rangle - \langle m|H_0|m\rangle] = \omega_0 = \gamma B_0 = 2\pi\nu_0 \quad (33)$$

where ν_0 is the Larmor frequency.

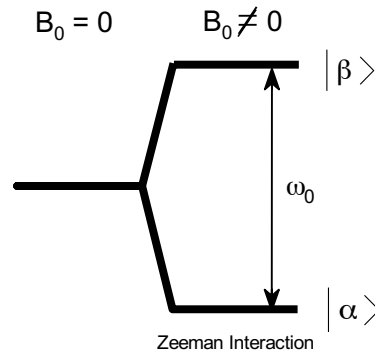


Figure 2.6 Schematic representation of the energy levels associated with a nucleus having a spin quantum number $I = \frac{1}{2}$ in the presence of an external magnetic field: the Zeeman interaction. The difference between the two energy levels, with which the two eigenfunctions $|\alpha\rangle$ and $|\beta\rangle$ are associated, equals the Larmor frequency ω_0 .

To induce an energy transition, a radiofrequency field \vec{B}_1 must be introduced perpendicularly to \vec{B}_0 . Here we consider only one of the two counter rotating components of \vec{B}_1 , rotating along the z axis at a frequency ω_1 and with an initial phase ϕ .

$$H_1(t) = -\gamma B_1 \hbar [I_x \cos(\omega_1 t + \phi) + I_y \sin(\omega_1 t + \phi)] \quad (34)$$

To avoid manipulating a time dependent Hamiltonian, it is easier to perform the calculations in a frame that rotates at ω_1 around the z axis. In fact, in this rotating frame, the Zeeman Hamiltonian reduces to

$$H_0 = -\hbar(\omega_0 - \omega_1)I_z \quad (35)$$

and the total effective Hamiltonian H_{eff} becomes time independent such as

$$H_{eff} = -\hbar\Omega_{RF}I_z - \hbar\omega_{RF}[I_x \cos(\phi) + I_y \sin(\phi)] \quad (36)$$

where $\Omega_{RF} = (\omega_0 - \omega_1)$ and $\omega_{RF} = \gamma B_1$ are an offset term and the intensity of the radiofrequency field, respectively; Ω_{RF} can be neglected if ω_{RF} verifies $\omega_{RF} \gg \Omega_{RF}$. The phase indicates the direction along which the radiofrequency field is applied; e.g., with our conventions, $\phi = 0$ means that the radiofrequency field is applied along x .

The transition probability between the eigenstates $|n\rangle$ and $|m\rangle$ is calculated according to

$$\langle m | H_{eff} | n \rangle = \langle m | -\hbar\Omega_{RF}I_z - \hbar\omega_{RF}[I_x \cos(\phi) + I_y \sin(\phi)] | n \rangle = -\frac{\hbar\omega_{RF}}{2} \langle m | I_+ e^{-i\phi} + I_- e^{i\phi} | n \rangle \quad (37)$$

The probability is different from zero if $(n-m) = \pm 1$. Note that only single-quantum (SQ) transitions, corresponding to $\Delta m = \pm 1$, are observable. This selection rule is valid only in the absence of other interactions such as the homonuclear dipolar interaction or the quadrupolar interaction. In these latter two cases, the presence of non secular terms in the effective Hamiltonian leads to the possibility to induce multiple-quantum (MQ) transitions. These transitions, however, cannot be detected directly and multidimensional NMR is required to observe them indirectly.

2.3.2.2 The chemical shift interaction

The electronic cloud surrounding a given nucleus may modify the effective magnetic field sensed by this nucleus in the presence of an external field \vec{B}_0 . This interaction is called the chemical shift and depends on the chemical and electronic environment of the nucleus. Because the electronic charge distribution at the nucleus is not necessarily spherical, the chemical shielding is anisotropic. The chemical shift Hamiltonian H_σ in the Cartesian basis is written as

$$H_\sigma = \gamma \hbar I \overline{\sigma} B_0 \quad (38)$$

The screening tensor $\overline{\sigma}$ can be represented by a symmetric matrix such as $\sigma_{ij} = \sigma_{ji}$. The diagonal components σ_{xx} , σ_{yy} and σ_{zz} allow the chemical shifts anisotropy to be simply described. The isotropic chemical shift, σ_{iso} , the amplitude of anisotropy, $\Delta\sigma$, and the asymmetry parameter, η_σ , are defined by

$$\left. \begin{aligned} \sigma_{iso} &= \frac{1}{3}(\sigma_{xx} + \sigma_{yy} + \sigma_{zz}) \\ \Delta\sigma &= (\sigma_{zz} - \sigma_{iso}) \\ \eta_\sigma &= \frac{1}{\Delta\sigma}(\sigma_{yy} - \sigma_{xx}) \end{aligned} \right\} \quad (39)$$

Then we can write

$$|\sigma_{zz} - \sigma_{iso}| \geq |\sigma_{xx} - \sigma_{iso}| \geq |\sigma_{yy} - \sigma_{iso}| \quad (40)$$

The Chemical shift Hamiltonian can be written as the product of irreducible spherical tensors expressed in the Laboratory frame according to

$$H_\sigma = \gamma \hbar B_0 \sum_{k=0}^2 \sum_{q=-k}^k (-1)^q A_{kq}^{LAB} T_{k-q} = \hbar \omega_0 \sum_{k=0}^2 \sum_{q=-k}^k (-1)^q A_{kq}^{LAB} T_{k-q} \quad (41)$$

where the non zero spatial components are, expressed in the PAS, given by

$$A_{00}^{PAS} = \sqrt{3\sigma_{iso}} \quad (42)$$

$$A_{20}^{PAS} = \sqrt{\frac{3}{2}} \Delta\sigma$$

$$A_{2,\pm 2}^{PAS} = \frac{1}{2} \eta_\sigma \Delta\sigma$$

and the spin components

$$\begin{aligned} T_{00} &= -\frac{1}{\sqrt{3}} I_z B_0 \\ T_{20} &= \frac{2}{\sqrt{6}} I_z B_0 \\ T_{2\pm 1} &= \frac{1}{2} I_\pm B_0 \end{aligned} \quad (43)$$

To render the Hamiltonian time independent, we must consider only the Hamiltonian averaged out over the Larmor period. This calculation is equivalent to a first order perturbation. We can show that only the T_{kq} terms that commute with the Zeeman Hamiltonian are to be considered. These terms, called secular terms, are proportional to I_z , i.e. T_{k0} .

We then obtain the average chemical shift Hamiltonian

$$\overline{H_\sigma^{(1)}} = \hbar\omega_0 (T_{00} A_{00}^{LAB} + T_{20} A_{20}^{LAB}) = \overline{H_{\sigma,iso}^{(1)}} + \overline{H_{\sigma,aniso}^{(1)}} \quad (44)$$

where $\overline{H_{\sigma,iso}^{(1)}} = \hbar\omega_0 T_{00} A_{00}^{LAB}$ and $\overline{H_{\sigma,aniso}^{(1)}} = \hbar\omega_0 T_{20} A_{20}^{LAB}$ are the isotropic and anisotropic parts of the Hamiltonian, respectively.

For a static sample, the average Chemical shift Hamiltonian takes the following form

$$\overline{H_\sigma^{(1)}} = \hbar\omega_0 \left[\sigma_{iso} + \frac{\Delta\sigma}{2} (3 \cos^2 \beta - 1 + \eta_\sigma \sin^2 \beta \cos 2\alpha) \right] I_z \quad (45)$$

Thus, the first order correction that must be brought to the frequency transition (m-1, m) is

$$\omega_\sigma^{(1)} = \frac{1}{\hbar} \left[\langle m-1 | \overline{H_\sigma^{(1)}} | m-1 \rangle - \langle m | \overline{H_\sigma^{(1)}} | m \rangle \right] \quad (46)$$

$$\omega_\sigma^{(1)} = -\omega_0 \left[\sigma_{iso} + \frac{\Delta\sigma}{2} (3 \cos^2 \beta - 1 + \eta_\sigma \sin^2 \beta \cos 2\alpha) \right] \quad (47)$$

For a sample spinning along an axis that makes an angle θ with \vec{B}_0 , the chemical shift becomes

$$\omega_{\sigma}^{(1)} = -\omega_0 \left[\sigma_{iso} + \frac{\Delta\sigma}{2} \left(\frac{3\cos^2\theta - 1}{2} \right) (3\cos^2\beta - 1 + \eta_{\sigma} \sin^2\beta \cos 2\alpha) \right] \quad (48)$$

where we have supposed to deal with an infinite spinning rate, i.e. we have considered only the time independent part of the Hamiltonian.

The isotropic part is not modified by the rotation around an axis and hence is usually included into the expression of the Larmor frequency together with the Zeeman interaction, such as

$$\omega_0' = (1 - \sigma_{iso})\omega_0 \quad (49)$$

$$\delta_{CS} = \frac{(\omega_0' - \omega_0)}{\omega_0} = -\sigma_{iso} \quad (50)$$

δ_{CS} is called the isotropic chemical shift. On the other hand, the anisotropic part is given by

$$\omega_{\sigma, aniso} = \frac{\omega_0 \Delta\sigma}{2} (3\cos^2\beta - 1 + \eta_{\sigma} \sin^2\beta \cos 2\alpha) P_2(\cos\theta) \quad (51)$$

with $P_2(\cos\theta) = \left(\frac{3\cos^2\theta - 1}{2} \right)$ the Legendre's polynomial function of order 2.

The broadening that characterizes a powder spectrum is due to the anisotropy of chemical shift which increases proportionally with the external magnetic field. The time dependent terms, which have been neglected, are responsible for the apparition in the NMR spectrum of spinning side bands at multiple integer of the spinning speed.

The angle θ at which the previously mentioned Legendre polynomial function, $P_2(\cos\theta)$, cancels out is called the magic angle ($\theta = 54.74^\circ$). When rotating the sample at this magic angle, because $P_2(\cos\theta)$ cancels out, only the isotropic part of the interaction is conserved.

2.3.2.3 The dipolar interaction

The dipolar interaction corresponds to the magnetic, through space coupling between two spins I and S . The amplitude of this interaction may vary from a few Hertz to a few thousands Hertz (for instance, in the case of the ^1H homonuclear interaction). The dipolar interaction allows the local environment of coupled nuclei to be characterized.

Similarly to the chemical shift interaction, the dipolar Hamiltonian between two spins I and S can be written in the Cartesian form as

$$H_D = -\gamma_I \gamma_S \hbar^2 \cdot I \cdot \overline{\overline{D}} \cdot S \quad (52)$$

where $\overline{\overline{D}}$ is the tensor describing the dipolar interaction. Using the notation of the irreducible spherical tensors, the representation of the dipolar Hamiltonian is such as

$$H_D = -\gamma_I \gamma_S \hbar^2 \sum_{q=-2}^{+2} (-1)^q A_{2-q}^{LAB} T_{2q} \quad (53)$$

According to the theory of the first order Hamiltonian, only the secular parts of the Hamiltonian are conserved over a Larmor period. In these conditions, only the component T_{20} of the tensor is conserved and we have

$$H_D^{(1)} = -\gamma_I \gamma_S \hbar^2 A_{20}^{LAB} T_{20} \quad (54)$$

with

$$T_{20} = \frac{1}{\sqrt{6}} (3I_z S_z - I S) \quad (55)$$

The only non zero component of A in the PAS reference frame is

$$A_{20}^{PAS} = \left(\frac{\mu_0}{4\pi} \right) \sqrt{6} r_{IS}^{-3} \quad (56)$$

Eq (56) indicates that the amplitude of A is inversely proportional to the cube of the distance between the two coupled nuclei. This means that, under certain conditions, internuclear distances can be calculated (Figure 2.7).

For a sample rotating around an axis that makes an angle θ with respect to the static magnetic field, and assuming that the sample spinning speed is infinite, we can write

$$A_{20}^{LAB} = \left(\frac{\mu_0}{4\pi}\right) \sqrt{6} r_{IS}^{-3} \left(\frac{3\cos^2\beta - 1}{2}\right) \left(\frac{3\cos^2\theta - 1}{2}\right) = \left(\frac{\mu_0}{4\pi}\right) \sqrt{6} r_{IS}^{-3} \left(\frac{3\cos^2\beta - 1}{2}\right) P_2(\cos\theta) \quad (57)$$

where β represents the angle between the internuclear vector \vec{r}_{IS} and the rotation axis.

For a static sample, the average dipolar Hamiltonian is obtained by taking $\theta = 0$, and is written as

$$\overline{H_D^{(1)}} = \left(\frac{\mu_0}{4\pi}\right) \gamma_I \gamma_S \hbar^2 r_{IS}^{-3} \left(\frac{3\cos^2\beta - 1}{2}\right) P_2(\cos\theta) (3I_Z S_Z - I S) \quad (58)$$

hence

$$\overline{H_D^{(1)}} = -2\pi\hbar D_{IS} \left(\frac{3\cos^2\beta - 1}{2}\right) P_2(\cos\theta) (3I_Z S_Z - I S) \quad (59)$$

where the quantity $D_{IS} = \frac{\hbar}{2\pi} \left(\frac{\mu_0}{4\pi}\right) \frac{\gamma_I \gamma_S}{r_{IS}^3}$, expressed in Hz, is generally called dipolar coupling constant.

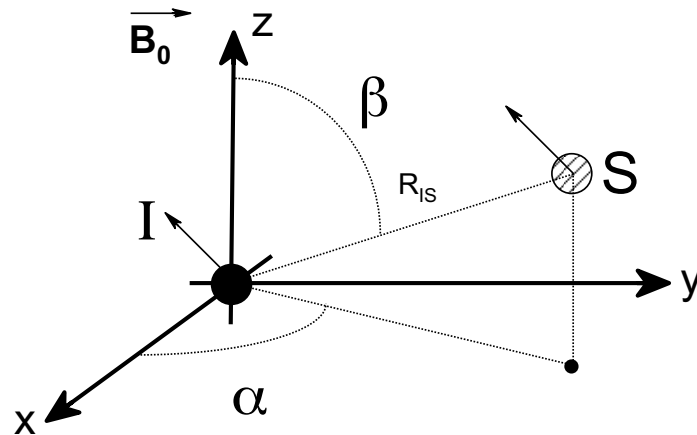


Figure 2.7 Schematic representation of the main parameters involved in the dipolar interaction.

By using the following relationship,

$$I \cdot S = I_z S_z + \frac{1}{2}(I_+ S_- + I_- S_+) \quad (60)$$

the Hamiltonian can be rewritten as

$$\overline{H_D^{(1)}} = -2\pi\hbar D_{IS} (3\cos^2 \beta - 1) P_2(\cos \theta) \left(I_z S_z - \frac{1}{4}(I_+ S_- + I_- S_+) \right) \quad (61)$$

In the case of an heteronuclear dipolar coupling, eq (61) simplifies to

$$\overline{H_{D,hetero}^{(1)}} = -2\pi\hbar D_{IS} (3\cos^2 \beta - 1) P_2(\cos \theta) I_z S_z \quad (62)$$

The correction factor that must be brought to the transition of spin I is then

$$\omega_D^{(1)} = 2\pi D_{IS} (3\cos^2 \beta - 1) P_2(\cos \theta) \quad (63)$$

Similarly to the chemical shift anisotropy, the rotation at the magic angle ($\theta = 54.74^\circ$) can cancel out the dipolar interaction if the spinning rate is large enough.

2.3.2.4 The scalar interaction

The scalar interaction is an indirect interaction that arises via the mediation of electrons in the molecular orbital. The nuclear spin causes a slight electron polarization which, because of electron delocalization, is transmitted to neighboring nuclei. The indirect nature of the spin-spin interaction leads to rotational invariance so that the scalar spin-spin Hamiltonian between two nuclei is given by

$$H_{scalar} = \pi J 2I_1 I_2 \quad (64)$$

where J is the scalar coupling constant whose magnitude is generally of the order of a few Hertz to a few hundreds Hertz. For ^1H homonuclear scalar coupling, J is usually between 0 and 18 Hz. It is important to note that, because the spin-spin interaction requires a molecular orbital, it acts only through the medium of covalent bonds. For this reason, the scalar coupling interaction is always intramolecular, which contrasts with the dipolar interaction.

In the solid state, the scalar coupling interaction is commonly discarded, whereas, in the liquid state, it allows fine structural and conformational information to be revealed.

2.3.2.5 The electric quadrupolar interaction

Nuclei bearing a spin quantum number I larger than $\frac{1}{2}$ possess an electric quadrupolar moment, eQ , because of the non spherical distribution of the electronic charge around the nucleus. This quadrupolar moment interacts with the electrical field gradient produced at the nucleus. The quadrupolar interaction is very sensitive to the orientation of the nucleus, and hence provides a lot of information on its local environment. However, because this thesis is only concerned with the study of non quadrupolar nuclei, we do not discuss the quadrupolar interaction any further.

2.4 References

- Abragam, A., 1961. The principles of nuclear magnetism. Oxford University Press: New York.
- Bloch, F., Hansen, W.W., Packard, M., 1946. Phys. Rev. 69, 127.
- Callaghan, P.T., 1991. Principles of Nuclear Magnetic Resonance Microscopy. Oxford University Press: New York.
- Canet, D., Boubel, J.C., Canet Soulas, E., 2002. La RMN: concepts, méthodes et applications. 2nd ed. Dunod.
- Cavanagh, J., Fairbrother, W.J., Palmer, A.G., Skelton, N.J., 1996. Protein NMR spectroscopy: Principles and practice. Academic Press: San Diego.
- Ernst, R.R., Bodenhausen, G., Wokaun, A., 1987. Principles of Nuclear Magnetic Resonance in one and two dimensions. Oxford University Press: New York.
- Farrar, T.C., Becker, E.D., 1971. Pulse and Fourier Transform NMR: introduction to theory and methods. Academic press: New York.
- Fukushima, E., Roeder, S.B.W., 1981. Experimental Pulse NMR: A nuts and bolts approach. Addison-Wesley Publishing: Reading (Massachusetts).
- Kimmich, R., 1997. NMR tomography, Diffusometry and Relaxometry. Springer: Berlin.
- Levitt, M.H., 2001. Spin dynamics. John Wiley & Sons, Ltd.: Chichester.
- Lynden-Bell, R.M., Harris, R.K., 1969. Nuclear magnetic resonance spectroscopy. Nelson.
- Mehring, M., 1983. Principles of high resolution NMR in solids. Springer-Verlag: Berlin.
- Neuhaus, D., Williamson, M., 1989. The Nuclear Overhauser Effect in structural and conformational analysis. VCH Publishers: New York.
- Purcell, E.M., Torrey, H.C., Pound, R.V., 1946. Phys. Rev. 69, 37-38.
- Pople, J.A., Schneider, W.G., Bernstein, H.J., 1959. High-resolution Nuclear Magnetic Resonance. McGraw-Hill: New York.
- Sanders, J.K.M., Hunter, B.K., 1993. Modern NMR spectroscopy: a guide for chemists. 2nd ed. Oxford University Press: New York.
- Schmidt-Rohr, K., Spiess, H.W., 1994. Multidimensional solid-state NMR of polymers. Academic press: London.
- Shaw, D., 1976. Fourier Transform NMR spectroscopy. Elsevier: Amsterdam.

Stejskal, E.O., Memory, J.D., 1994. High resolution NMR in the solid state. Oxford University Press: New York.

Chapter 3: Chemometrics

3.1 Introduction

The strength of the NMR metabolomic approach is its capacity to look at all the components of a mixture simultaneously: a ^1H NMR spectrum can contain thousands of proton signals originating from various metabolites. The NMR metabolic analysis generates a large amount of data from which it is necessary to extract the desired information using chemometric methods that can identify possible patterns among samples.

Data analysis in food metabolomics has been carried out using several chemometric tools that have been widely described in many papers and reviews (McKenzie et al., 2011; Izquierdo-Garcia et al., 2011; Ebbels & Cavill, 2009). Chemometrics represents the perfect solution to the challenge of extracting and identifying the relevant information out of the data, since it can reduce the dimension of the NMR spectral data and, at the same time, points out the existence of possible patterns among the analyzed sample (Giuliani et al., 1991; Giuliani et al., 1993; Giuliani et al., 2004; Khakimov et al., 2015).

But how can we define chemometrics? Scientific quantitative studies have historically been based on cause-effect one-to-one relationships, thoroughly exploiting and developing univariate data analysis methods coupled with randomized or structured design of experiments. This approach allowed understanding those phenomena that could be ascribed to uni- or low- variated causes and was very well suited for the relative low amount of information that univariate instruments provided, but represents nowadays a limitation for investigating the overwhelming amount of data that modern analytical platforms can collect in a short time and that can dig into the essence of more complex systems, such as those within

food metabolomics, which are characterized by latent many-to-many relationships. For unraveling these hidden relationships, multivariate methods, able to perform unsupervised data exploration, are required. Chemometric methods rely on the extraction of common latent factors (i.e., principal components) from underlying common or latent structures in the analyzed original data. Chemometric methods for data exploration and mining are designed to handle large multivariate data sets, exploiting the collinearity between variables and projecting the original multivariate data into a few dimensions (latent variables) that are much easier to be described by simple graphical representations.

The nature of quantitative data extracted from an NMR spectrum (all data points, buckets, integral or intensity of selected resonances) influences the choice of the statistical approach for their elaboration. To be properly applied, any statistical approach has to take into account several important aspects of data, such as number of variables, the data redundancy, and possible noise.

When a quantitative analysis is performed using all NMR spectral data points, the statistical elaboration has to face the problems of high data redundancy and noise introduction. The role of any single metabolite in statistical models is not easily deducible, but the data analysis is quick, and experimental data is not excluded a priori, thus avoiding the risk of losing any pertinent information.

Bucketing reduces the number of variables and hence data redundancy, but again the variables (buckets) are not necessarily associated with single metabolites thus hindering the interpretation of statistical results in terms of individual metabolic contributions.

Finally, the statistical analysis of integrals or intensities of selected resonances requires time consuming assignment and quantification procedures. The selection of signals, avoiding the data-redundancy problem, is an advantage with respect to other quantitative approaches, but pertinent information deriving from non-selected resonances could be lost.

Additionally, the interpretation of the statistical results in terms of individual metabolic contributions is straightforward.

Here, we report in brief the steps frequently used to perform a statistical analysis of NMR data in food analysis, see Figure 3.1.

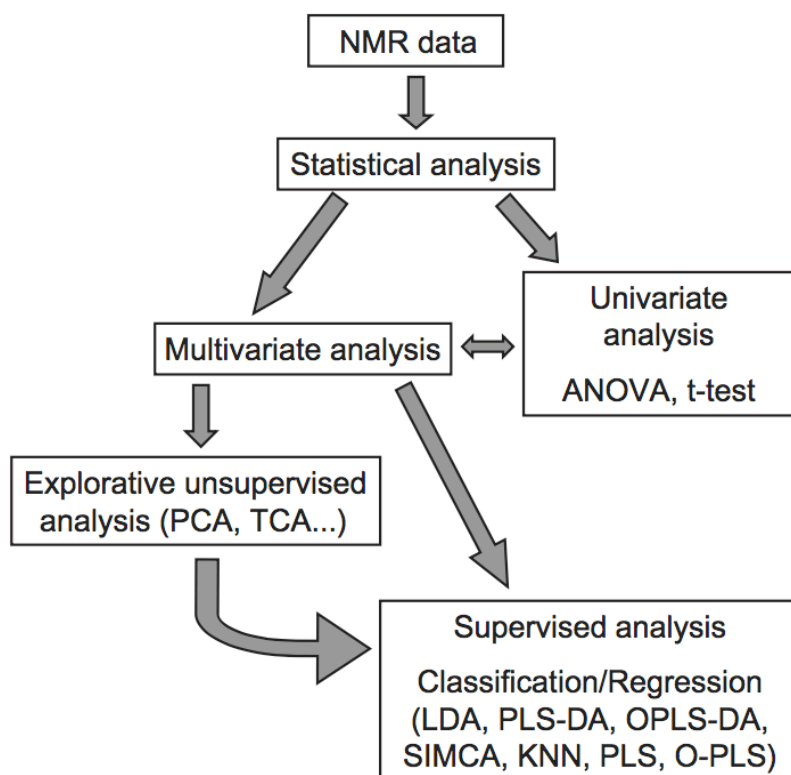


Figure 3.1. Statistical analysis applied to NMR data

Univariate analysis (ANOVA or Student's t-test) is usually applied to the metabolite resonances, rather than to spectral data points and buckets, to find the variables most discriminant for different groups of samples. It also can serve for variable selection/reduction before multivariate analysis.

The statistical approach common for all types of quantitative data consists in the application of multivariate statistical analysis to the total data. The selection of variables most pertinent to the problem is achieved within the multivariate analysis.

Explorative unsupervised analysis is often the first step of statistical treatment. Structure of data, presence of outliers and natural grouping of samples can be revealed at this

step. In many cases the results obtained at this stage are sufficient to distinguish different groups of samples according to metabolic differences. However, in the case of classification and prediction problems, the application of supervised multivariate techniques is necessary. Chemometrics have been widely used to cope with classification problems involving the authentication of the origins of foodstuffs and their variety, and quality discrimination. It should be emphasised that a single comprehensive statistical method suitable to describe all aspects of foodstuff analysis does not exist but rather an appropriate method has to be chosen for a specific problem.

3.2 Explorative unsupervised analysis

3.2.1 Principal Components Analysis (PCA)

When multiple spectra are collected on a set of samples, after the necessary preprocessing actions (alignment, bucketing or binning, when desired, or the extraction of relevant features, such as the concentration - or integrals - of selected metabolites) they are normally arranged into a rectangular matrix X , having as many rows as the number of samples and as many columns as the variables which have been chosen as descriptors for the system. This matrix represents the basis for the successive multivariate data analysis.

The first step of any multivariate data processing is the so-called exploratory data analysis (EDA) which, as the name suggests, consists in trying to summarize the main characteristics of the data in an easy-to-understand fashion, mainly through the use of graphical tools and without the formulation of any statistical model or a priori hypothesis (Marini, 2013). This approach is sometimes referred to as “let the data talk”. The main aims of EDA are to maximize insight into a data set, to uncover its underlying structure (e.g., spontaneous clustering, trends in data time series), to identify relevant variables, and to detect outliers and anomalies.

The variables (peak intensities, integrals, buckets or data points) extracted from NMR spectra define a multidimensional space where every spectrum and corresponding sample can be represented by a single point. Taking into account that the number of variables typically used in metabolomic studies is always higher than 3, the data space cannot be simply visualised, but, using the Principal Component Analysis (PCA) it is possible to transform the multidimensional space of experimental variables into a space with reduced dimensions which are linear combinations of variables, which are mutually orthogonal, called principal components. PCA is the main chemometric tool for exploratory data analysis since it allows the compression of the relevant information of a data set into a reduced set of abstract variables (the principal components), which constitute the best low dimensional approximation of the experimental matrix. In mathematical terms, such projection is expressed by the following bilinear decomposition: $X=TP^T+E$, where T is the matrix which collects the coordinates of the samples onto the new set of components (*scores*), which is used for visualizing the distribution of the samples, while P is the matrix containing the coefficients relating the principal components to the experimental variables (*loadings*), which provides the *trait d'union* for interpreting the samples' pattern in the scores space in terms of experimentally measured variables. Since PCA entails an approximation of the data matrix, the extent of such approximation is summarized by the matrix E, i.e., the residuals, which contain the difference between the true values of the data matrix X and its PCA estimate TP^T . Here, it must be stressed that, while in general PCA is the most appropriate tool for EDA, as it projects the data onto directions resulting in the best fit of the points in the multivariate space (i.e., which account for the maximum explained variance), for some specific problems other projection approaches could result more useful for the particular task. One of this is multivariate curve resolution (MCR), which, rather than aiming at extracting abstract directions, try to calculate components that can have a chemical interpretation, through the imposition of tailored constraints.

Summing up, PCA is commonly used as an explorative technique in multivariate analysis (Dunn, Bailey & Johnson, 2005; Ebbels & Cavill, 2009) and has proven to be a powerful and widely applicable technique. However, PCA may not be suitable if the effect of interest is not the main source of data variability, because this effect can be masked in PCA by other factors with higher variability. In this case other multivariate statistical methods should be used. For instance, in the case of pink and red tomatoes (Mattoo et al., 2006) the impact of transgene on metabolome is less important than ripening and the differences between pink transgenic and wild type tomatoes are scarcely visible in PCA, see Figure 2A.

3.2.2 Tree Clustering Analysis (TCA)

TCA, also called hierarchical clustering analysis (HCA), is another unsupervised exploration method used to discover the natural grouping (clustering) of samples. Tree clustering methods join together objects (samples) into successively larger clusters, using amalgamation rules for clusters and some measurements of the distance between single objects. The statistical results are reported as a dendrogram. All possible classifications in a prescribed number of groups can be obtained by cutting the tree at a suitable level. As an example, Figure 2B shows a TCA dendrogram of ^1H NMR data from aqueous extracts of tomatoes at red, breaker and green ripening stages.

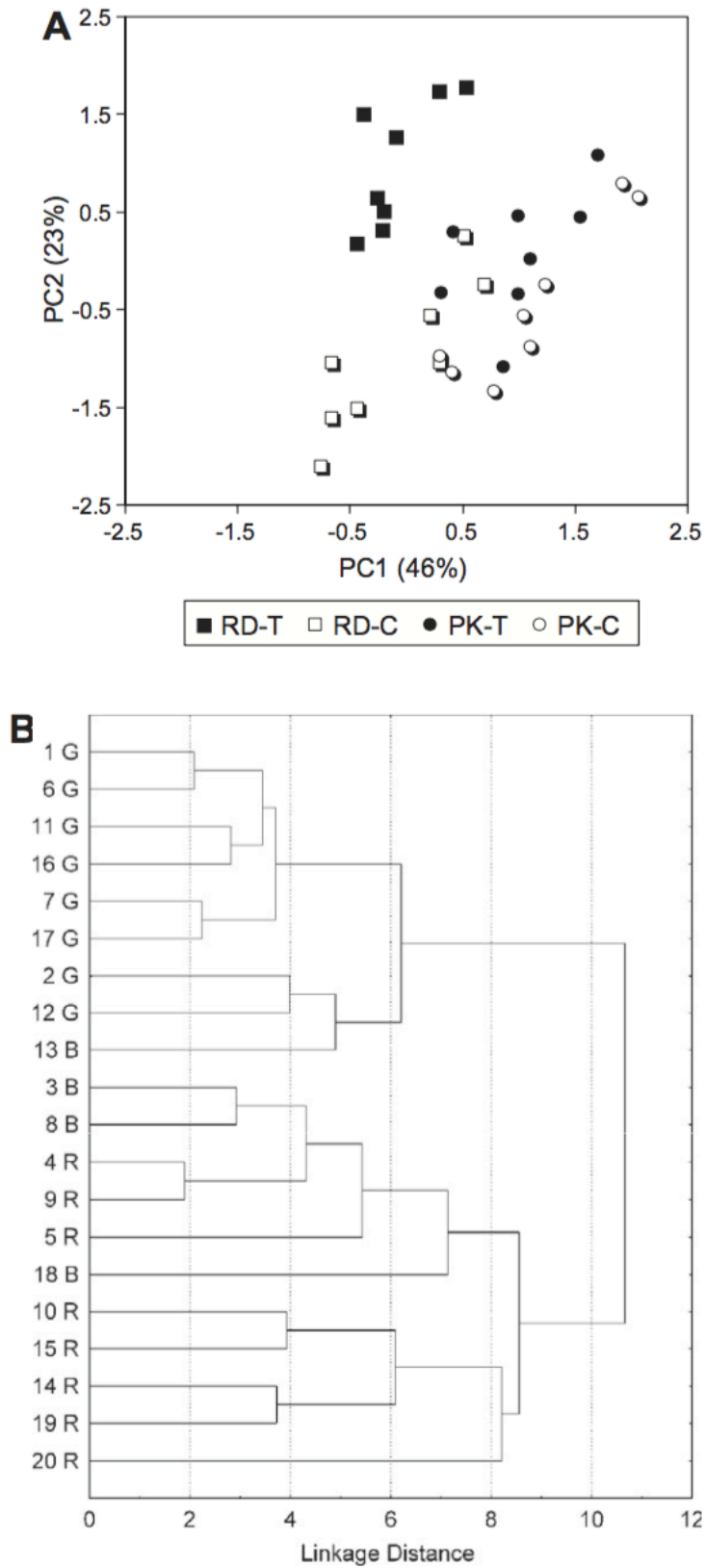


Figure 2. (A) PCA map of ^1H NMR data from aqueous extracts of tomatoes at red and pink ripening stages. RD-T, red transgenic line; RD-C, red control line; PK-T, pink transgenic line; PK-C, pink control line. (B) TCA dendrogram of ^1H NMR data from aqueous extracts of tomatoes at red (R), breaker (B) and green (G) ripening stages.

3.3 Supervised classification/regression methods

In some occasions, e.g., when the number of analysed samples is limited, or when reference measurements of some additional properties or characteristics of the samples are not available to be related with the experimental data from NMR, exploratory analysis represents not only the first but also the only data processing step that can be carried out. However, in any other situation, the spectral profiles recorded by NMR constitute the basis to build predictive models, i.e., models which allow not only the description of the main features of the samples under investigation, but also to accurately predict one or more characteristics of new samples. In particular, depending on the nature of the properties to be predicted, two families of methods can be distinguished: calibration methods, which are used to predict quantitative properties (e.g., peroxide number or iodine number for a lipid moiety, protein content in cereals and so on), and classification methods, which provide qualitative answers (as, for instance, in traceability studies, when one could be interested in verifying if the origin of the good is compliant with what declared in the label). Since the final aim of these methods is to be able to accurately predict the desired properties on new (unknown) samples, in order to be applicable to a particular problem, it is mandatory that (at least) the following two requirements are met: a sufficient number of training samples, for which the value of the property to be predicted is known beforehand and that span as much as possible the range of variability to be expected for future observations, and a careful validation step, to test the reliability of the approach providing also a quantitative estimate of the error. Validation (Westad & Marini, 2015) is indeed an unavoidable step for any predictive model, as it guarantees the applicability of the methods to any future sample: in its most essential form, it consists in applying the model to a new set of samples, which are treated as unknown by the model itself but for which the “true” values of the responses to be predicted are available to the experimenter. Accordingly, by comparing these reference values with the ones predicted by the model it is possible to have an estimate of how reliable is the proposed approach.

As anticipated above, one speaks of calibration problems when a predictive relation is sought between a matrix of experimentally measured variables (in our case, the NMR spectra or some features extracted from them) X and one or more quantitative variables to be predicted Y (Marini, 2013). In most cases, this relation is expected to be linear (or at least to be approximate by a linear function), so that one can express the calibration problem as: $Y=XB+E$, where B is the matrix collecting the coefficients of the model and E represents the residuals. The previous equation is a general form and there are various approaches to calibration which differ among one another in the way the coefficients B are calculated. The simplest linear regression approach (multiple linear regression) is an extension of ordinary univariate least squares but requires the data matrix X to have more observation (samples) than predictors (variables), and that the variables are as uncorrelated as possible (characteristics that are rarely met in the case of NMR data for which the variables are highly collinear). Indeed, when spectral data are concerned, the most commonly used approach is the so-called Partial Least Squares Regression (PLS-R). In PLS-R, data are first projected to a relevant lower dimensional subspace (in a way which is analogous to PCA, but that, instead of using maximum fit/explained variance to orient the components, identifies the new axes as the ones along which there is maximum covariance between X and Y), and then uses these scores as predictors for the responses.

When the answer to be predicted is of qualitative nature, then the corresponding approaches for predictive modelling are referred to as classification methods (Marini, 2013). Indeed, the aim of classification methods is to define a mathematical criterion to assign an individual (a sample) to one group (category or class) based on the measured variables. A class is then corresponding to any of the levels that the discrete property may assume: as an example, when one is interested of using NMR for predicting whether a wine sample comes from Spain, Italy, France or South Africa, this corresponds to a classification problem where there are 4 categories, each one identifiable with a different geographical origin.

Classification methods operate by defining boundaries (surfaces) in the multivariate space, to identify regions associated to the different categories. Depending on the complexity of the problem to be solved, these boundaries can be linear (as in Linear Discriminant Analysis, LDA, and its bilinear equivalent, Partial Least Squares Discriminant Analysis, PLS-DA, which is to be preferred, when dealing with many correlated variables) or not (as, for instance, in k-Nearest Neighbours, kNN).

3.3.1 Partial Least Square (PLS)

Partial Least Square (PLS) regression can be chosen to create a prediction model, in which the features from PCA and multiple regression are generalised and combined. Unlike PCA, PLS studies the relationship between two data matrices, X and Y. Matrix X contains the data extracted from NMR spectra for each sample, whereas matrix Y contains extra information on samples obtained using reference methodologies. PLS transforms the multidimensional space of variables from matrix X into a new coordinate system with axes corresponding to the highest covariance between measured NMR data (matrix X) and the response variables (matrix Y). In this way, the relationship between the NMR spectra and other properties of food samples can be used to predict these properties directly based on NMR data.

3.3.2 Linear Discriminant Analysis (LDA)

Linear Discriminant Analysis (LDA) is a rather simple method of classification, based on linear combinations of original variables, that maximises the difference between *a priori* defined classes. In LDA the hyperspace of the variables is divided in as many regions as the number of available categories or classes. An example of LDA is reported in Figure 3 (Mannina et al., 2009). In this case, LDA has been applied to the intensity of five ¹H NMR resonances to create a classification model for the detection of hazelnut oils in olive oils. LDA

is rather sensitive to data redundancy and a reliable model can be built only using a limited number of original non-correlated variables and a sufficient number of samples for each category, which is not always possible in practice. To overcome these serious limitations, LDA is frequently used in conjunction with other methods, mostly with PLS.

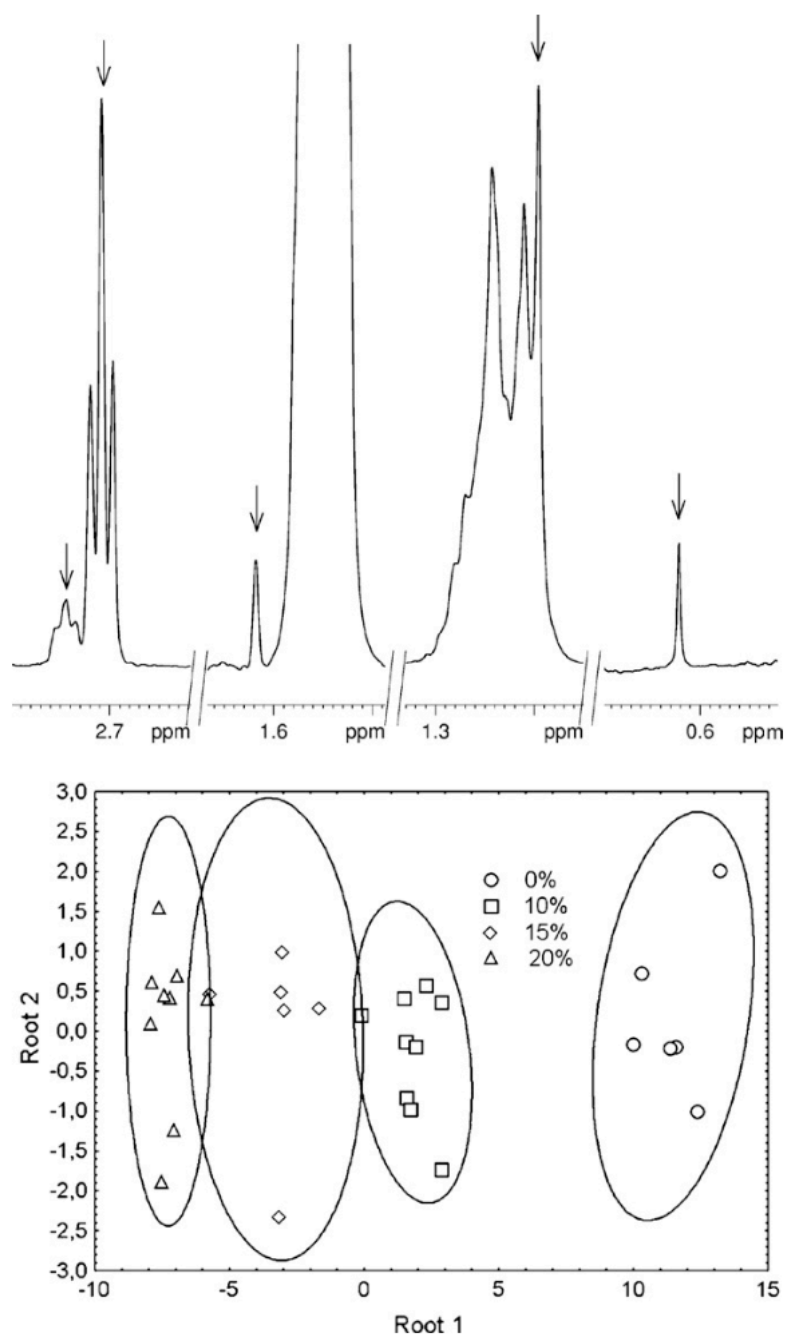


Figure 3. LDA applied to the intensity of five ^1H NMR resonances (labelled with arrows) in 600 MHz ^1H spectra of different samples of olive oils and hazelnut-olive oil mixtures. Percentages of hazelnut oil in olive oil: 0%, 10%, 15%, and 20%.

3.3.3 PLS-DA

Taking advantages of both statistical approaches (PLS and LDA) and avoiding their weaknesses, PLS-DA has found many applications in the analysis of NMR metabolomic data, especially in the cases when LDA cannot be used (low number of samples to number of variables ratio and high collinearity among the variables). In PLS-DA the information about the variables responsible for the classification of samples is obtained by examining VIP scores (Variable Importance in Projection) and the regression coefficients.

3.3.4 SIMCA

As a class-modelling technique, Soft Independent Modelling of Class Analogies (SIMCA) acts by defining the category space of one class at a time and is more focused on the similarities among samples of the same class than on the differences among the classes as in the case of discriminant analysis. Consequently, each sample can be assigned to one or more classes or to none of them. In SIMCA, each class model is defined on the basis of a principal component model of appropriate dimensionality. In Figure 4A and Figure 4B, PLS-DA and SIMCA models have been used both to discriminate between Ligurian and non-Ligurian olive oils and to define the Ligurian olive oil class (Mannina et al., 2010).

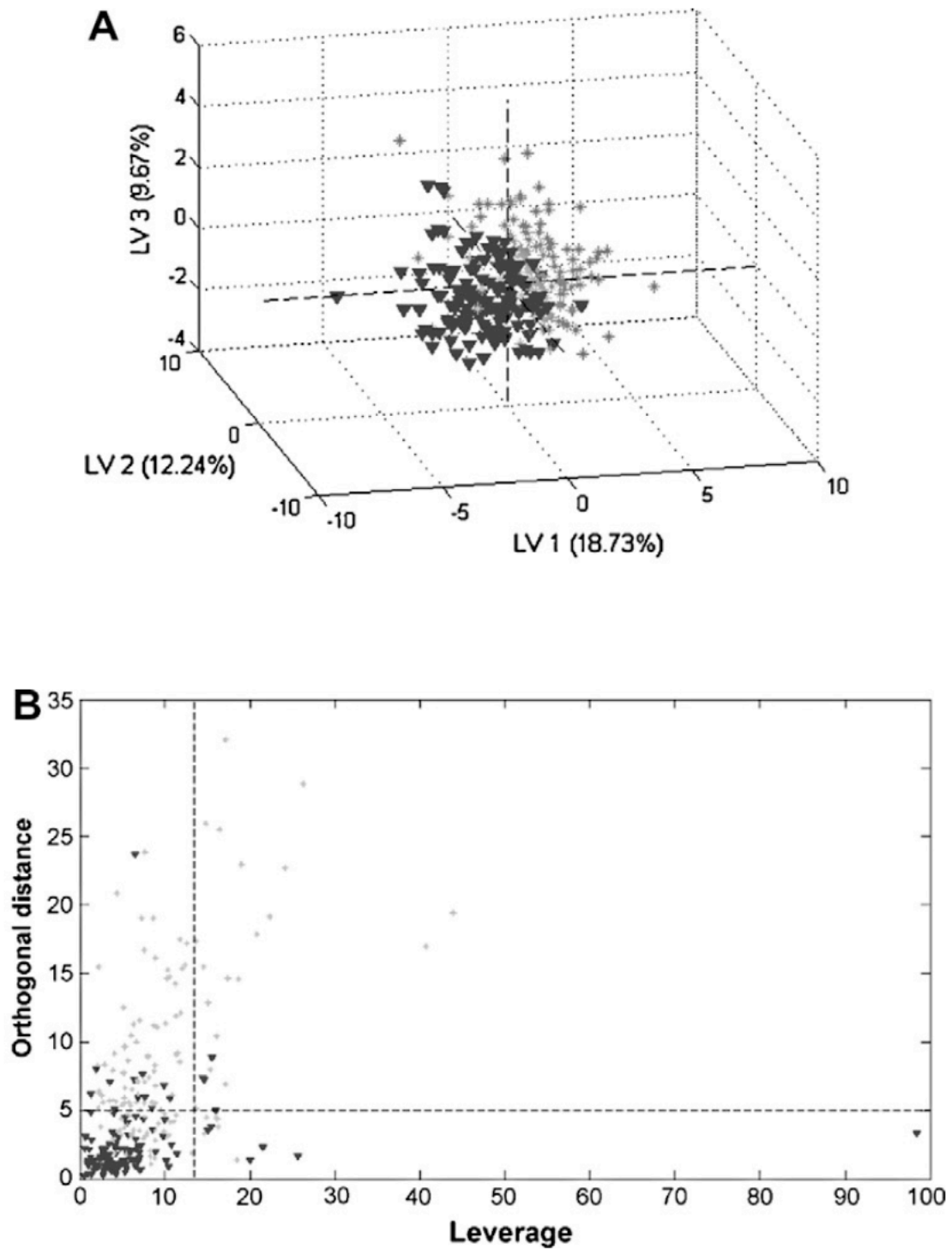


Figure 4. (A) PLS model and (B) SIMCA model relative to olive oils from Mediterranean areas analysed by ^1H NMR. Black triangle = Ligurian olive oils, Simple "+" = non-Ligurian olive oils.

3.3.5 Genetic Algorithms (GA) and Genetic Programming (GP)

Genetic algorithms (GA) and genetic programming (GP) are computer learning techniques based on an evolutionary processes simulation. They have been used for solving complex multidimensional optimisation problems. GA has also been applied to NMR- based metabolic profiling in order to select variables pertinent to desirable classification of food samples (Ebbels & Cavill, 2009). The importance of each variable has been determined by the frequency with which the variable appears in the best solutions across many runs and by comparing this frequency with the appropriate binomial distribution.

3.3.6 Artificial Neural Networks (ANNs)

Artificial Neural Networks (ANNs) are computational learning algorithms imitating the processes in the brain. A network of processing units, called neurons, is trained in an iterative updating procedure. Multidimensional data can be visualised in a two dimensional map using the most common unsupervised ANN, self-organising maps (SOMs). Moreover, SOMs are employed as supervised methods for classification. ANNs have been used in the classification of olive oils (Rezzi et al., 2005), differentiation of wines (Masoum et al., 2006), and classification of fish products (Martinez et al., 2005). Other examples and comprehensive review of ANN application in food analysis are reported elsewhere (Marini et al., 2009). However, the results of ANN are difficult to interpret in terms of the original variables, and the use of ANNs for the analysis of spectroscopic data is much less common than other techniques such as PCA and PLS-DA.

3.4 References

- Dunn, W.B., Bailey, N.J.C., Johnson, H.E., 2005. Measuring the metabolome: current analytical technologies. *The Analyst* 130, 606–625.
- Ebbels, T.M.D., Cavill, R., 2009. Bioinformatic methods in NMR-based metabolic profiling. *Prog. Nucl. Magn. Reson. Spectrosc.* 55, 361–374.
- Giuliani, A., Capuani, G., Miccheli, A., Aureli, T., Ramacc, M. T., Conti, F., 1991. Multivariate data analysis in biochemistry: a new integrative approach to metabolic control in brain aging. *Cell. Mol. Biol.* 37(6), 631-638.
- Giuliani, A., Capuani, G., Aureli, T., Miccheli, A., Manetti, C., Conti, F., 1993. Multivariate data analysis as applied to NMR results: a window on biological complexity. *J. Magn. Reson. Med. Biol.* 1, 5-12.
- Giuliani, A., Zbilut, J. P., Conti, F., Manetti, C., Miccheli, A., 2004. Invariant features of metabolic networks: a data analysis application on scaling properties of biochemical pathways. *Physica A* 337, 157-170.
- Izquierdo-García, J.L., Villa, P., Kyriazis, A., del Puerto-Nevado, L., Pérez-Rial, S., Rodriguez, I., Hernandez, N., Ruiz-Cabello, J., 2001. Descriptive review of current NMR-based metabolomic data analysis packages. *Prog. Nucl. Magn. Reson. Spectrosc.* 59, 263–270.
- Khakimov, B., Gurdeniz, G., & Engelsens, S. B, 2015. Trends in the application of chemometrics to foodomics studies. *Acta Aliment.* 44(1), 4-31.
- Mannina, L., D’Imperio, M., Capitani, D., Rezzi, S., Guillou, C., Mavromoustakos, T., Molero Vilchez, M.D., Fernández, A.H., Thomas, F., Aparicio, R., 2009. ¹H NMR-based protocol for the detection of adulterations of refined olive oil with refined hazelnut oil. *J. Agric. Food Chem.* 57, 11550–11556.
- Mannina, L., Marini, F., Gobbino, M., Sobolev, A.P., Capitani, D., 2010. NMR and chemometrics in tracing European olive oils: the case study of Ligurian samples. *Talanta* 80, 2141–2148.
- Marini, F., 2009. Artificial neural networks in foodstuff analyses: trends and perspectives. *Anal. Chim. Acta* 635, 121–131.
- Marini F., 2013. *Chemometrics in Food Chemistry* (1^oedition). Elsevier. UK: Oxford.
- Martinez, I., Bathen, T., Standal, I.B., Halvorsen, J., Aursand, M., Gribbestad, I.S., Axelson, D.E., 2005. Bioactive compounds in Cod (*Gadus morhua*) products and suitability of ¹H NMR metabolite profiling for classification of the products using multivariate data analyses. *J. Agric. Food Chem.* 53, 6889–6895.
- Masoum, S., Bouveresse, D.J.R., Vercauteren, J., Jalali-Heravi, M., Rutledge, D.N., 2006. Discrimination of wines based on 2D NMR spectra using learning vector quantization neural networks and partial least squares discriminant analysis. *Anal. Chim. Acta* 558, 144–149.

Mattoo, A.K., Sobolev, A.P., Neelam, A., Goyal, R.K., Handa, A.K., Segre, A.L., 2006. NMR spectroscopy based metabolite profiling of transgenic tomato fruit engineered to accumulate spermidine and spermine reveals enhanced anabolic and nitrogen–carbon interactions. *Plant Physiol.* 142, 1759–1770.

McKenzie, J.S., Donarski, J.A., Wilson, J.C., Charlton, A.J., 2011. Analysis of complex mixtures using high-resolution nuclear magnetic resonance spectroscopy and chemometrics. *Prog. Nucl. Magn. Reson. Spectrosc.* 59, 336–359.

Rezzi, S., Axelson, D.E., Héberger, K., Reniero, F., Mariani, C., Guillou, C., 2005. Classification of olive oils using high throughput flow ¹H NMR fingerprinting with principal component analysis, linear discriminant analysis and probabilistic neural networks. *Anal. Chim. Acta* 552, 13–24.

Westad, F., Marini, F., 2015. Validation of chemometric models - a tutorial. *Anal. Chim. Acta* 893, 14-24.

Chapter 4: Typical Foods of Lazio Region

4.1 Project “*e*-ALIERB: un OPEN LAB per caratterizzare e valorizzare i prodotti alimentari ed erboristici del territorio laziale”

Project “*e*-ALIERB” (FILAS-RU-2014-1157, Codice CUP B82I15003570002), started in December 2015 and ended the 30th of April 2018, was funded by “Regione Lazio”. The project aimed at setting up a multi-skilled “open laboratory” (we can call it as “*e*-ALIERB-OPENLAB”) made of different research facilities from several Departments of Sapienza University, Istituto di Metodologie Chimiche (CNR), and Policlinico Umberto I (Figure 4.1A and 4.1B), in order to characterize typical food and herbal products from Lazio region through a multi-methodological approach (Figure 4.2).

The valorisation of local productions will have a positive impact on the economic and social development of the areas of origin. The possibility of recognizing, characterizing and certifying these productions will allow, therefore, their distinction in the ambit of a wide range of similar products and the defence of their typicality and quality.

Although the quality of agro-food products is often defined taking as parameters of assessment above all the sensorial characteristics (colour, shape, aromas, etc.), the consumer's request is increasingly directed towards products with beneficial nutritional and health value and a low environmental impact. In this context, the analytical characterization provided by *e*-ALIERB-OPENLAB could give an added value to local productions, promoting also the functional properties deriving from bioactive compounds (nutraceuticals and phytochemicals). It is also known that a natural product is characterized by an extremely complex and variable composition depending on various factors, including the characteristics of the growing

environment and the preparation methods. Therefore, the standardization of the product and the definition of "metabolic fingerprinting" would allow to obtain a product with characteristics as constant and reproducible as possible, as a guarantee of quality and, consequently, of efficacy and safety of employment. This approach has also become a priority for companies which understand the importance of high quality and certified food to compete on the market.

In recent years, the liberalization of markets and the changing environmental and consumer life conditions have determined a very difficult competition environment on the global market. From this point of view, even the Lazio territory, despite the great traditional food and wine production heritage and the strong territorial vocations, is suffering a deep crisis. The valorisation of local and typical products could represent the great opportunity to project again the Lazio region in the national context and to win the challenge also with foreign markets.

In this context, *e*-ALIERB project starts from the consideration of the existence in the Lazio region of a vast patrimony of typical and traditional food and herbal productions. Typical products are distinguished from industrial ones because they have few substitutes, high market demand and relative low supply, low competition in relation to price. It is therefore necessary to protect the producers in order they do not suffer the competition of industrial products that try to imitate the typical ones. On the other hand, also the consumer must be protected, providing the guarantee that the product matches those characteristics that make it typical and specific.

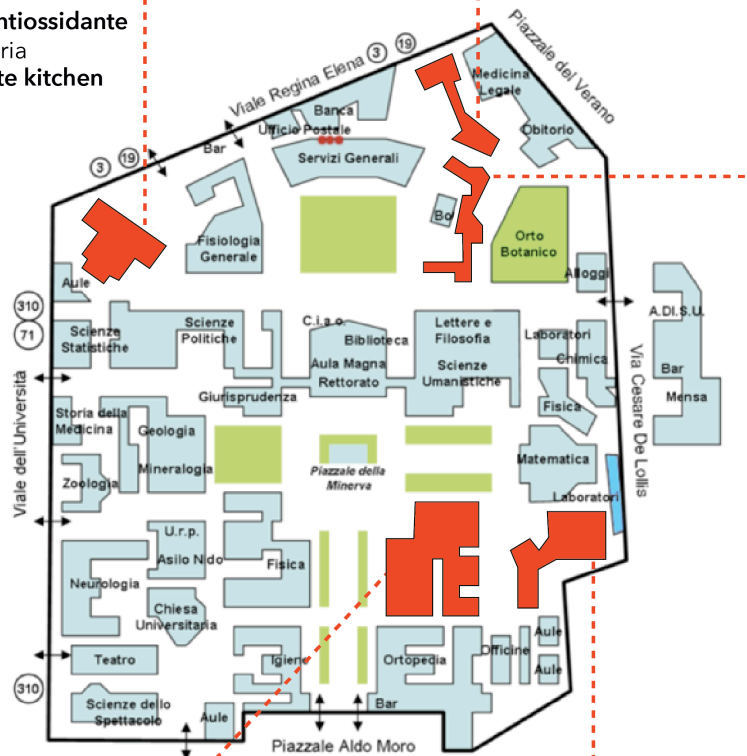


SAPIENZA
UNIVERSITÀ DI ROMA

Dip. di Medicina Sperimentale
Attività antiossidante
Fluorimetria
Metabolite kitchen

Dip. di Fisiologia e Farmacologia

Attività biologica - citotossicità, antimutagenesi, attività antiossidante ed ipoglicemizzante *in vitro*
Metodiche Estrattive - MW; ILs



Dip. di Chimica
Profilo Metabolico - NMR

Dip. di Chimica e Tecnologie del Farmaco

Profilo Metabolico - FT-ICR, Esquire 3000, HPLC-DAD, GS-MS
Metodiche Estrattive - MW; ILs
Proprietà reologiche
Sviluppo e Caratterizzazione di Sistemi di Veicolazione

Dip. di Biologia Ambientale

Analisi micotossine - HPLC/ESI-MS/MS; HPTLC
Metodiche Estrattive - MW; ILs

Dip. di Management

Spettrofotometria
Cromatografia
Metodiche estrattive



Figure 4.1A. Map of the facilities and methodologies involved in Project *e-ALIERB*



Istituto di Metodologie
Chimiche - CNR
Profilo Metabolico - NMR



UMBERTO I
POLICLINICO DI ROMA

Dip. di Sanità Pubblica e
Malattie Infettive
Attività antimicrobica *in vitro*



Figure 4.1B. Map of the facilities and methodologies involved in Project e-ALIERB

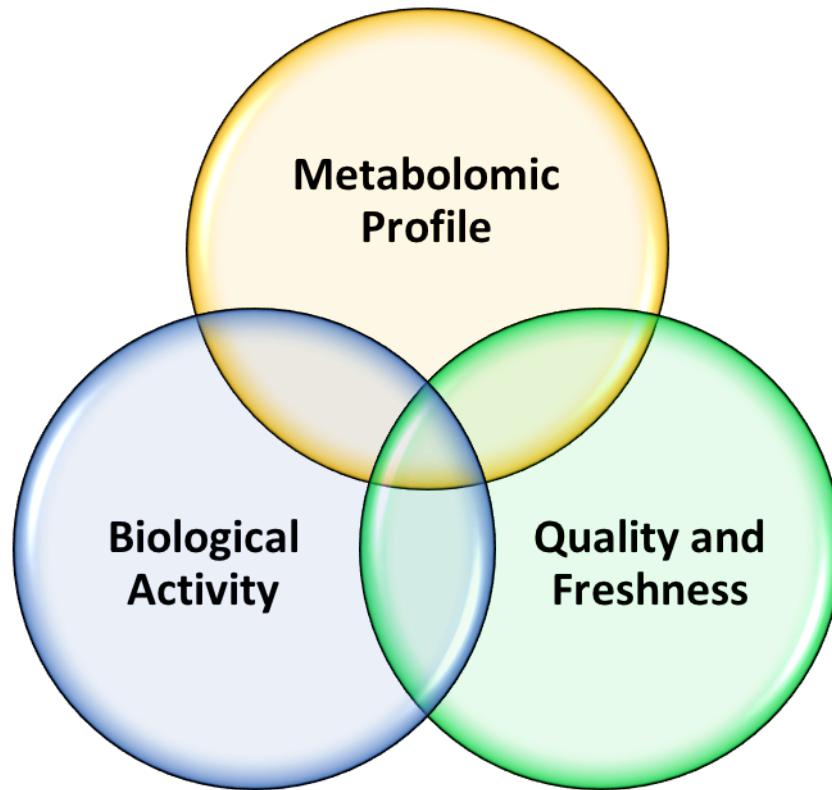


Figure 4.2. Multi-methodological approach of food analysis

Currently, Lazio has about 432 traditional products, among which are 16 products with Protected Designation of Origin (PDO), 10 with Protected Geographical Indication (PGI), 5 wines with a Typical Geographic Indication (IGT) and 27 wines with Controlled Denomination of Origin (DOC). Besides the typical products we must also consider the so-called "traditional" products, regulated by Decreto Legge (DL) 173/1998, which defines them as those "whose methods of processing, preservation and maturing are consolidated over time". The two main categories of typical and traditional products could then be placed side by side with other classes that, although not regulated, can represent a valid opportunity for the development of the economy of rural areas, such as local products (category of products that are characterized by the scarcity of production, by the lack of any specification or protocol and by the extreme variability of production techniques) or products promoted by

consumer associations. These productions respond to the Italian concept of “agri-food quality”. Within the European Union there is a rather marked difference between North and South Europe in this sense. In the first countries, quality is understood in a normative sense with respect for established production standards. On the contrary, in Mediterranean countries quality expressed by concepts such as typicality and origin prevails.

It is important to stress that quality is a strategic factor for the national agri-food economy. Therefore, there is great potential for development, both from an economic and environmental points of view, which very often, however, is not adequately exploited. There are many factors that can negatively affect the development of this potential: structural factors (consistency of surfaces, size of companies, etc.), technological factors (backwardness in production techniques and equipment), organizational factors (insufficient “associationism”) or even social factors (abandonment of rural areas, lack of generational changes). All these factors can be removed through specific improvement measures. In this regard it should be emphasized that cognitive studies of such productions are very limited. In fact, despite the recent publications dedicated to them (atlases, etc.), many of these are limited to providing little descriptive information. Knowledge of cultural, environmental, genetic, cultural, compositional, sensory, nutritional and technological factors that characterize the products are also very limited. If such knowledge exists, then, it has not been well studied in scientific terms; in other words, the chemical composition of the major and minor components, their genetic origin, etc. have not been adequately analysed by investigating all the factors that, combining tradition and innovation, can be the basis for the effective qualitative “typification” and commercial valorisation of the final product.

Some traditional products from the tradition of Lazio are excellent on the sensory level and have a remarkable quality from a nutritional point of view, which is related to the raw materials used and the production chains. A thorough characterization of these products is

pointed towards the definition of their quality. These characteristics can represent the added value of the products.

It should be remembered that the presence of a great variety of such typical products on the Lazio territory is largely due to the synergy between biological factors (germoplasm), environmental factors (crop and/or breeding environment), technical factors (traditional cultivation, breeding and processing techniques) and socio-economic factors.

Through the protection and valorisation of these products, therefore, we contribute to the integrated development of the territory. The importance of valorisation of those products that have a strong territorial link and/or are obtained in a "short supply chain", is also underlined by a recent document "Development of the first Food and Nutrition Plan for the WHO European region" promulgated by the World Health Organization, which highlights the multiple positive effects of this enhancement for the health of consumers, the protection of the environment and the protection of local production.

Summing up, in *e-ALIERB* project, an interactive structure that provides multidisciplinary skills to valorise and characterize food products of small-medium enterprises in the Lazio region is proposed. At the moment databases related to food and herbal products produced and marketed in the Lazio Region are absent. Through the valorisation of regional products from Lazio, the activity of the agri-food sector is complemented by new and different functions, including the protection of the environment and the territory. With the transition from the local market to the national one, the territory of origin will also be valorised attaining a touristic and gastronomic attraction. The agri-food development of the Lazio territory can thus represent the engine of a chain integrated with tourism, environment culture and services. Nowadays it is now recognized that typical local products, as a form of expression of the territory's culture, greatly influence the social and economic development of the local territory, in particular through the achievement of socio-economic benefits such as the increase in the income of agri-food companies, the emergence

of a qualified occupation, the development of food and wine tourism that can contribute to improve the economic sustainability of the territory.

In this context, the proposed project will have repercussions in particular in those areas in which the specificity, the local origin and the short supply chain of the product are elements of strong valorisation of the product itself. In the context in which biodiversity is considered a value to be preserved and promulgated, providing companies with potential tools to highlight the peculiar characteristics of their production is like giving a 'passport' of quality. Consumers, now more and more attentive to the need for a correct and appropriate diet, will have to take note of the commitment that a company assumes in guaranteeing optimal standards and of the "scientific" effort made in the direction of the origin and quality assessment. It is likely to believe that the effort made will be repaid by a recognition from the market, first of all by the most conscious portion, but the discourse will undoubtedly involve an ever-increasing use that can extend to the international level. It should not be forgotten that the Lazio region has the capital that is among the highest poles of tourist attraction in the world and that therefore can be an ideal showcase for experiencing the consequences of a valorisation of regional production.

The “ability” of typical products to valorise identity, quality and culture of the territory can lead to the establishment of new networks of social relations that can guide local development choices towards wider issues concerning the sustainability and quality of life of individuals.



Figure 4.3. e-ALIERB Logo

The pilot product of *e*-ALIERB has been the red sweet pepper (*Capsicum annuum* L.) ecotype “Cornetto di Pontecorvo” from which the logo takes inspiration (Figure 4.3). It represents a fusion between Latium region and the shape of a red pepper.

During the last two years and half, different typical Latium products were analysed by the OPENLAB, answering to the growing needs of supporting and valorising local and traditional products and farms. Some of these products (Figure 4.4) have been studied as part of my thesis work.



Figure 4.4. Any of typical and local Lazio products analysed by *e*-ALIERB-OPENLAB



4.2 Peperone Cornetto di Pontecorvo DOP

4.2.1 Introduction

The Italian “Cornetto di Pontecorvo” PDO (Protected Designation of Origin) red sweet pepper is a *C. annuum* ecotype, strictly cultivated at Pontecorvo town in the Ciociaria area (G.U. n. 285 del 52 6/12/2010 – Reg. UE 1021/2010) of the Lazio region (Central Italy). In this area, the volcanic nature of the soil confers to this pepper unique sensorial properties and an intensely sweet flavour.

The PDO production protocol requires the open-air cultivation of peppers. However, in recent years, the increased development of various soil-related fungal infections, including contaminations by *Phytophthora* spp., affected the growth and the yield of this peculiar fruit so leading to the development of new cultivation strategies. Among them, the greenhouse cultivation, which allows controlling different environmental parameters such as temperature, light intensity and humidity, enhances the plant growth (van Straten et al., 2011).

The development of accurate analytical protocols for the characterization of PDO products is an actual issue and an important challenge to grant consumers high quality products characterized not only by peculiar sensorial properties but also by assessed nutritional and healthy properties.

In the present work, a NMR based metabolomic approach to study PDO peppers, grown open field (OF) and greenhouse (GH), has been carried out within the Regional project “e-ALIERB” (FILAS-RU-2014-1157, Codice CUP B82I15003570002).

Untargeted Nuclear Magnetic Resonance (NMR) methodology was used to obtain a comprehensive metabolite profile of the samples. NMR is one of the most suitable techniques applied to identify and quantify simultaneously different classes of compounds (Mannina, Sobolev & Capitani, 2012; Mannina, Sobolev & Viel, 2012).

4.2.2 Materials and Methods

The fruits of red sweet pepper *C. annuum* ecotype “Cornetto di Pontecorvo”, carrying the PDO certification and grown both OF and GH, were collected at the end of August 2015, and provided by the Production Consortium located at Pontecorvo in the Lazio region (Central Italy).

Both open field and greenhouse crops were grown, in the space of three months, without the use of agrochemicals in the experimental sites, equipped with the necessary structures. The climate was humid subtropical, with an average monthly of 22.6 °C air temperature, 68% humidity and 50.6 mm precipitation during cultivation period (from May to September 2015). Climate data are revealed by the meteorological stations sited in Pontecorvo and Esperia (Lazio Region, Italy) and recorded by the Agricultural Information System of the Lazio Region (available at <http://www.arsial.it/portalearsial/agrometeo/>). The soil features for both OF and GH cultivations are shown in Table 4.1.

Table 4.1. Physical and chemical properties of the soil at the sites of open field and greenhouse cultivations of *C. annuum* var. Cornetto di Pontecorvo.

| SOIL FEATURES | Crop cultivation | |
|----------------------|------------------|--------|
| | OF | GH |
| Texture type | clayey | clayey |
| Clay (%) | 34 | 30 |
| Silt (%) | 28 | 29 |
| Sand (%) | 38 | 41 |
| Organic matter (%) | 1.9 | 2.9 |
| Organic carbon (%) | 1.7 | 1.7 |
| Organic nitrogen (%) | 0.17 | 0.09 |
| Limestone (%) | 5.0 | 5.0 |
| Phosphorus-free (%) | 0.014 | 0.06 |
| pH (soil to water) | 5.9 | 7.2 |

Each fruit was subjected to morphological analysis in order to verify the presence of the peculiar characteristics according to PDO certification. In addition, a careful separation of different components of the fruit, including peel, pulp, the edible part (i.e. fruit without seeds)

and seeds was performed. All components from fruits were examined and weighted, see Table 4.2 for mean \pm standard deviation. The components from 15 different fruits were pooled and then subjected to specific extraction processes.

Table 4.2. Morphological Analysis of fruit, edible part, peel, pulp and seeds of “Cornetto di Pontecorvo” pepper, grown in open field and greenhouse.

| | Fruit (g) | Edible part (g) | Peel (g) | Pulp (g) | Seeds | |
|------------|-------------|-----------------|-----------------|------------------|-------------|-----------|
| | | | | | N° | (g) |
| Open field | 107.9 \pm | 10.2 \pm | 1.84 \pm 0.01 | 6.12 \pm 0.09 | 237.4 \pm | 2.4 \pm |
| | 3.7 | 0.1 | | | 17.3 | 0.2 |
| Greenhouse | 91.7 \pm | 10.2 \pm | 1.60 \pm | 7.75 \pm 0.07* | 88.2 \pm | 0.9 \pm |
| | 4.4** | 0.1 | 0.02* | | 9.6*** | 0.1*** |

* $p < 0.05$, ** $p < 0.01$ and *** $p < 0.001$ t-Student test analysis of greenhouse vs. open field fruits.

Bligh-Dyer extraction was applied to each component of the pepper fruit. Bligh-Dyer protocol required the use of a mixture of methanol/chloroform (2:1 v/v) to optimize the quantification of the greater number of metabolites. For the extraction of peel, pulp and seeds this solvent mixture was added to the samples and the emulsion was preserved at 4 °C for 40 min. The sample was then centrifuged (800 g for 15 min at 4 °C). The upper (hydroalcoholic) and lower (organic) phases were carefully separated. The pellets were re-extracted using half of the solvent volumes (in the same conditions described above) and the separated fractions were pooled. Both fractions were dried under an N₂ flow at room temperature until the solvent was completely evaporated. The dried phases were stored at -20 °C until analysis (Capitani et al., 2014).

The dried organic fraction of each sample was dissolved in 0.7 mL of a CDCl₃/CD₃OD mixture (2:1 v/v) and then placed into a 5 mm NMR tube. Finally, the NMR tube was flame-sealed. Conversely, the dried hydroalcoholic phase of each sample was solubilized in 0.7 mL 600 mM phosphate buffer/D₂O, containing a 2 mM solution of TSP as

internal standard, and then transferred into a 5 mm NMR tube. Finally, the NMR tube was flame-sealed.

NMR spectra of all hydroalcoholic and organic extracts were recorded at 27 °C on a Bruker AVANCE 600 spectrometer operating at the proton frequency of 600.13 MHz and equipped with a Bruker multinuclear z-gradient 5 mm probe head. ¹H spectra were referenced to methyl group signals of TSP (δ = 0.00 ppm) in D₂O, and to the residual CHD₂ signal of methanol (set to 3.31 ppm) in CD₃OD/CDCl₃ mixture. ¹H spectra of hydroalcoholic extracts were acquired with 256 transients with a recycle delay of 5 s. The residual HDO signal was suppressed using a pre-saturation. The experiment was carried out by using 45° pulse of 6.68 μs, 32K data points. ¹H spectra of extracts in CD₃OD/CDCl₃ were acquired with 256 transients, recycle delay of 5 s and 90° pulse of 5 μs, 32K data points. The two-dimensional (2D) NMR experiments, such as ¹H-¹H TOCSY, ¹H-¹³C HSQC and ¹H-¹³C HMBC, were carried out under the same experimental conditions previously reported (Sobolev, Segre & Lamanna, 2003).

In order to evaluate the similarities or differences between samples the integrals of selected resonances in ¹H NMR spectra (Table 4.3 and Table 4.4) were measured. In the case of aqueous samples, the integral values were normalised with respect to the total sum of all integrals set to 1000.

Table 4.3. Summary of the metabolites identified in the 600.13 MHz ¹H spectra of the hydroalcoholic extracts of pulp, peel and seeds from “Cornetto di Pontecorvo” pepper, grown OF and GH. Asterisks indicate signals selected for integration.

| Compound | Assignment | ¹ H (ppm) | Multiplicity: <i>J</i> [Hz] | ¹³ C (ppm) |
|----------------------|-----------------------|----------------------|-----------------------------|-----------------------|
| <i>Carbohydrates</i> | | | | |
| α-Glucose | CH-1 | 5.25* | d [3.8] | 93.1 |
| | CH-2 | 3.55 | dd [9.8;3.8] | 72.5 |
| | CH-3 | 3.72 | | 73.7 |
| | CH-4 | 3.42 | | 70.6 |
| | CH-5 | 3.84 | | 72.5 |
| | CH ₂ -6,6' | 3.84;3.78 | | 61.6 |

| | | | | |
|----------------------------|---------------------------|------------|--------------|---------|
| β -Glucose | CH-1 | 4.66* | d [7.9] | 96.9 |
| | CH-2 | 3.26 | dd [9.3;8.0] | 75.1 |
| | CH-3 | 3.51 | t [9.1] | 76.7 |
| | CH-4 | 3.41 | | 70.6 |
| | CH-5 | 3.48 | | 76.9 |
| | CH ₂ -6,6' | 3.90;3.74 | | 61.7 |
| β -D-Fructofuranose | CH-1,1' | 3.60;3.57 | | 63.8 |
| | CH-2 | | | 102.6 |
| | CH-3 | 4.12 | | 76.4 |
| | CH-4 | 4.12 | | 75.4 |
| | CH-5 | 3.83 | | 81.7 |
| | CH ₂ -6,6' | 3.81;3.69 | | 63.3 |
| α -D-Fructofuranose | CH-3 | 4.13 | | 83.0 |
| | CH-5 | 4.07 | | 82.4 |
| β -D-Fructopyranose | CH-1,1' | 3.56;3.72 | | 64.8 |
| | CH-3 | 3.81 | | 68.6 |
| | CH-4 | 3.90 | | 70.6 |
| | CH-5 | 4.01* | | 70.2 |
| | CH ₂ -6,6' | 3.72;4.03* | | 64.4 |
| Sucrose | CH-1 (Glc) | 5.42* | d [3.8] | 93.2 |
| | CH-2 | 3.56 | | 72.5 |
| | CH-3 | 3.77 | | 73.6 |
| | CH-4 | 3.49 | | 70.6 |
| | CH-5 | 3.85 | | 73.5 |
| | CH ₂ -6 | 3.83 | | 60.9 |
| | CH ₂ -1' (Fru) | 3.70 | | 62.1 |
| | C-2' | | | 104.7 |
| | CH-3' | 4.23 | | 77.4 |
| | CH-4' | 4.05 | | 75.0 |
| | CH-5' | 3.90 | | 82.3 |
| | CH ₂ -6' | 3.81 | | 63.4 |
| | α -Xylose | CH-1 | 5.21 | d [3.7] |
| β -Xylose | CH-1 | 4.60 | d [7.9] | 97.5 |
| | CH-4 | 3.63 | | 70.2 |
| | CH-5,5' | 3.94;3.33 | | 66.2 |
| Myo-inositol | CH-1 | 4.08 | | |
| | CH-2,5 | 3.56 | | |
| | CH-3,6 | 3.62 | | |
| | CH-4 | 3.29* | t [9.4] | |
| <i>Organic acids</i> | | | | |
| Acetic acid | α -CH ₃ | 1.93 | s | |
| Ascorbic acid ^a | CH ₂ -6 | 3.74 | | |
| | CH-5 | 4.03 | | |

| | | | | |
|----------------------------|---------------------------------|------------|---------------|------|
| | CH-4 | 4.53* | d [1.8] | 79.4 |
| Citric acid | α,γ -CH | 2.55* | d [15.3] | 46.7 |
| | α',γ' -CH | 2.68 | d [15.3] | 46.7 |
| Formic acid | HCOOH | 8.46* | | |
| Quinic acid | CH ₂ -1,1' | 1.87; 2.08 | | 41.8 |
| | CH-2 | 4.01 | | 68.0 |
| | CH-3 | 3.56 | | |
| | CH-4 | 4.14 | | 71.6 |
| | CH ₂ -5,5' | 1.98; 2.05 | | 38.5 |
| Malic acid | α -CH | 4.30* | dd [9.9;3.2] | 71.4 |
| | β -CH | 2.68 | | 43.6 |
| | β' -CH | 2.39 | dd [9.9;15.4] | 43.6 |
| Succinic acid ^a | α,β -CH ₂ | 2.42 | s | 34.9 |
| <i>Amino acids</i> | | | | |
| Alanine | α -CH | 3.79 | | 51.5 |
| | β -CH ₃ | 1.49* | d [7.3] | 17.3 |
| Arginine | α -CH | 3.78 | | |
| | β -CH ₂ | 1.93 | m | 28.6 |
| | γ -CH ₂ | 1.74 | m | 24.9 |
| | δ -CH ₂ | 3.25 | | 41.5 |
| Asparagine | α -CH | 4.01 | | 52.2 |
| | β -CH | 2.89* | dd [16.9;7.2] | 35.6 |
| | β' -CH | 2.96 | dd [16.9;4.4] | 35.6 |
| Aspartate | α -CH | 3.90 | | 53.1 |
| | β -CH | 2.71 | | 37.6 |
| | β' -CH | 2.81* | dd [3.9;17.4] | 37.6 |
| Glycine ^a | α -CH | 3.57 | | 42.5 |
| Glutamate | α -CH | 3.79 | | 55.1 |
| | β -CH | 2.12 | | 28.0 |
| | β' -CH | 2.07 | | 28.0 |
| | γ -CH ₂ | 2.35* | m | 34.4 |
| Glutamine | α -CH | 3.78 | | 55.1 |
| | β -CH ₂ | 2.15 | m | 27.3 |
| | γ -CH | 2.46* | m | 31.9 |
| Isoleucine | α -CH | 3.69 | | 60.6 |
| | β -CH | 1.98 | | |
| | γ -CH | 1.26 | | 25.5 |
| | γ' -CH | 1.47 | | 25.5 |
| | γ -CH ₃ | 1.01 | d [7.0] | 15.8 |

| | | | | |
|-----------------------------------|----------------------------|-------|---------|-------|
| | δ -CH ₃ | 0.94* | t [7.4] | 12.2 |
| Leucine | α -CH | 3.74 | | 54.5 |
| | β -CH ₂ | 1.71 | | 40.8 |
| | δ -CH ₃ | 0.97* | d [6.1] | 23.1 |
| | δ' -CH ₃ | 0.96 | d [6.0] | 22.0 |
| γ -Aminobutyrate (GABA) | α -CH ₂ | 2.30 | t [7.4] | 35.4 |
| | β -CH ₂ | 1.91 | m | 24.7 |
| | γ -CH ₂ | 3.01* | t [7.5] | 40.2 |
| Proline | α -CH | 4.14 | | 62.2 |
| | β -CH | 2.36 | | 30.0 |
| | β' -CH | 2.07 | | 30.0 |
| | γ -CH ₂ | 2.01 | | 24.9 |
| | δ -CH | 3.41 | | 47.1 |
| | δ' -CH | 3.35 | | 47.1 |
| Phenylalanine | CH-2,6, ring | 7.34* | | 130.5 |
| | CH-3,5, ring | 7.43 | | 130.1 |
| | CH-4, ring | 7.39 | | 128.7 |
| | α -CH | 4.01 | | 56.9 |
| | β -CH | 3.28 | | 37.3 |
| | β' -CH | 3.16 | | 37.3 |
| Threonine | α -CH | 3.61 | | 61.4 |
| | β -CH | 4.27 | | 67.0 |
| | γ -CH ₃ | 1.34* | | 20.5 |
| Tyrosine | CH-2,6 | 7.20 | d[8.0] | 131.9 |
| | CH-3,5 | 6.92* | d[8.0] | 116.9 |
| Tryptophane | CH-4 | 7.74 | | |
| | CH-7 | 7.56* | | |
| | CH-6 | 7.29 | | |
| | CH-5 | 7.20 | | |
| Valine | α -CH | 3.62 | | 61.4 |
| | β -CH | 2.27 | | 30.2 |
| | γ -CH ₃ | 1.00 | d [7.1] | 17.8 |
| | γ' -CH ₃ | 1.05* | d [7.1] | 18.9 |
| <i>Other metabolites</i> | | | | |
| Choline | N-CH ₃ | 3.21* | s | 55.0 |
| | N-CH ₂ | 3.52 | | 68.4 |
| | CH ₂ -OH | 4.07 | | 56.6 |
| Ethanolamine | N-CH ₂ | 3.15 | | 42.3 |
| | OH-CH ₂ | 3.83 | | 58.7 |
| Uridine | CH-5 ring | 7.88 | d[8.0] | |

| | | |
|-----------|------|--------|
| CH-6 ring | 5.91 | d[8.0] |
| CH-1 | 5.93 | d[4.7] |
| CH-2 | 4.36 | |
| CH-3 | 4.24 | |
| CH-4 | 4.14 | |

^aNot identified in seeds extracts.

4.2.3 Results and Discussion

¹H spectra of hydroalcoholic extracts from pulp, peel and seeds solubilized in D₂O phosphate buffer, were assigned using 1D and 2D NMR experiments and literature data on vegetable food matrices (Table 4.3) (Sobolev et al., 2005; Ritota et al., 2010).

The ¹H spectra of pulp and peel extracts show the same signals suggesting the presence of the same metabolites. The ¹H spectra are dominated by the signals of glucose and fructose isomers, whereas in the high field 0.50-3.60 ppm spectral region minor signals belonging to the aliphatic groups of amino acids (alanine, arginine, asparagine, aspartate, γ -aminobutyrate, glutamine, glycine, glutamate, isoleucine, leucine, valine, proline, phenylalanine, threonine, tryptophan, and tyrosine) and organic acids (acetic, ascorbic, citric, malic, quinic and succinic acids) are observable (Figure 4.5).

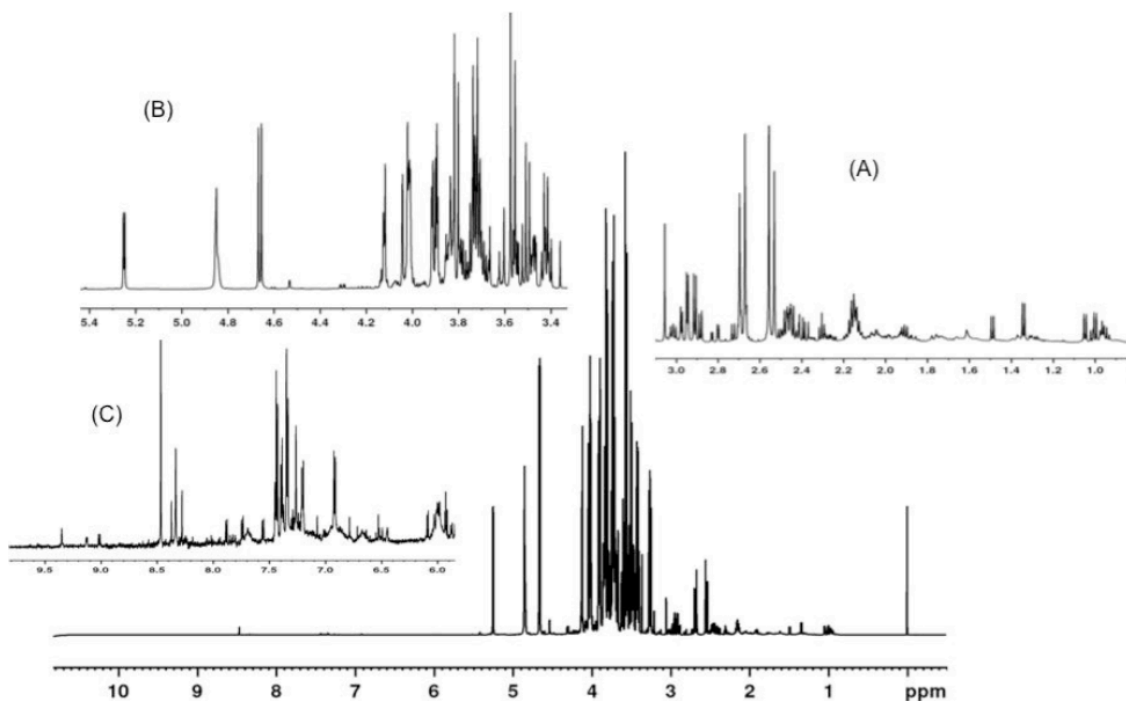


Figure 4.5. ^1H NMR spectrum of the hydroalcoholic Bligh-Dyer extract of the pulp from “Cornetto di Pontecorvo” pepper, grown open field, in 600 mM phosphate/D₂O buffer with 2 mM TSP: (A) high field region; (B) middle field region; (C) low field region.

In the low field region of ^1H spectrum, signals due to aromatic groups of amino acids (phenylalanine, tryptophan, and tyrosine), uridine and formic acid were assigned. Comparing the levels of specific metabolites in pulp and peel, see Table 4.4, it is worthy to note that a higher concentration of glucose and fructose is observed in pulp than in peel, whereas choline content is major in peel compared to pulp.

The extracts of pulp and peel from peppers grown OF and GH contain the same metabolites showing the higher levels of valine, alanine, glutamine, asparagine, aspartic acid, GABA and phenylalanine in OF fruits, whereas the level of glucose was higher in GH grown fruits.

In the case of seed extracts, the ^1H spectra (data not reported) show the presence of the same metabolites identified also in pulp and peel extracts, although succinic acid, ascorbic acid and glycine were not detectable. It is noteworthy that seeds contain sucrose as a prevalent sugar (Table 4.4).

Table 4.4. Molecular abundances (a.u.) of selected metabolites in extracts from *Capsicum annuum* ecotype “Cornetto di Pontecorvo” grown OF and GH.

| | Peel GH Bligh-Dyer | Peel OF Bligh-Dyer | Pulp GH Bligh-Dyer | Pulp OF Bligh-Dyer | Seeds GH Bligh-Dyer | Seeds OF Bligh-Dyer |
|-------------------|-----------------------|-----------------------|-----------------------|-----------------------|------------------------|------------------------|
| Alanine | 9.26 | 12.62 | 6.88 | 9.82 | 7.80 | 17.14 |
| Ascorbic acid | 11.69 | 4.53 | 10.58 | 13.47 | 0 | 0 |
| Asparagine | 32.07 | 47.51 | 29.82 | 44.21 | 20.47 | 31.45 |
| Aspartate | 6.38 | 10.83 | 6.83 | 10.29 | 7.08 | 11.88 |
| Choline | 18.65 | 22.20 | 10.47 | 14.58 | 133.47 | 164.83 |
| Citric acid | 108.55 | 111.63 | 121.50 | 118.28 | 23.05 | 38.68 |
| Formic acid | 6.27 | 2.46 | 6.10 | 3.80 | 0.42 | 1.01 |
| Fructose | 727.09 | 790.71 | 895.75 | 939.75 | 29.21 | 30.51 |
| GABA | 12.06 | 20.23 | 7.42 | 12.63 | 10.31 | 13.73 |
| α -Glucose | 166.50 | 148.14 | 194.36 | 177.96 | 14.17 | 14.04 |
| β -Glucose | 302.18 | 266.20 | 345.38 | 314.96 | 24.57 | 25.30 |
| Glutamate | 2.81 | 2.81 | 2.11 | 1.82 | 12.51 | 13.11 |
| Glutamine | 19.04 | 33.57 | 20.8 | 47.38 | 14.42 | 17.21 |
| Isoleucine | 1.49 | 1.77 | 1.27 | 1.82 | 2.53 | 2.92 |
| Leucine | 11.07 | 15.35 | 5.71 | 10.05 | n.d. ^a | n.d. ^a |
| Malic acid | 11.12 | 17.01 | 10.63 | 15.98 | 29.01 | 29.52 |
| Myo-Inositol | 2.59 | 2.78 | 1.78 | 2.54 | 1.12 | 1.19 |
| Phenylalanine | 2.78 | 3.92 | 2.34 | 3.40 | 6.13 | 8.54 |
| Sucrose | 2.82 | 5.36 | 3.71 | 3.77 | 132.38 | 124.28 |
| Threonine | 11.12 | 21.90 | 9.46 | 14.31 | 5.45 | 7.47 |
| Tryptophan | 0.34 | 0.41 | 0.22 | 0.34 | 1.66 | 1.58 |
| Tyrosine | 2.03 | 2.87 | 1.07 | 1.49 | 3.45 | 3.95 |
| Valine | 10.05 | 14.98 | 7.68 | 12.05 | 5.65 | 7.93 |

^a n.d., not determined

The ¹H spectra of organic extracts obtained from peel and pulp of peppers grown in OF and GH modalities show the same signals thus suggesting the presence of the same metabolites (Figure 4.6).

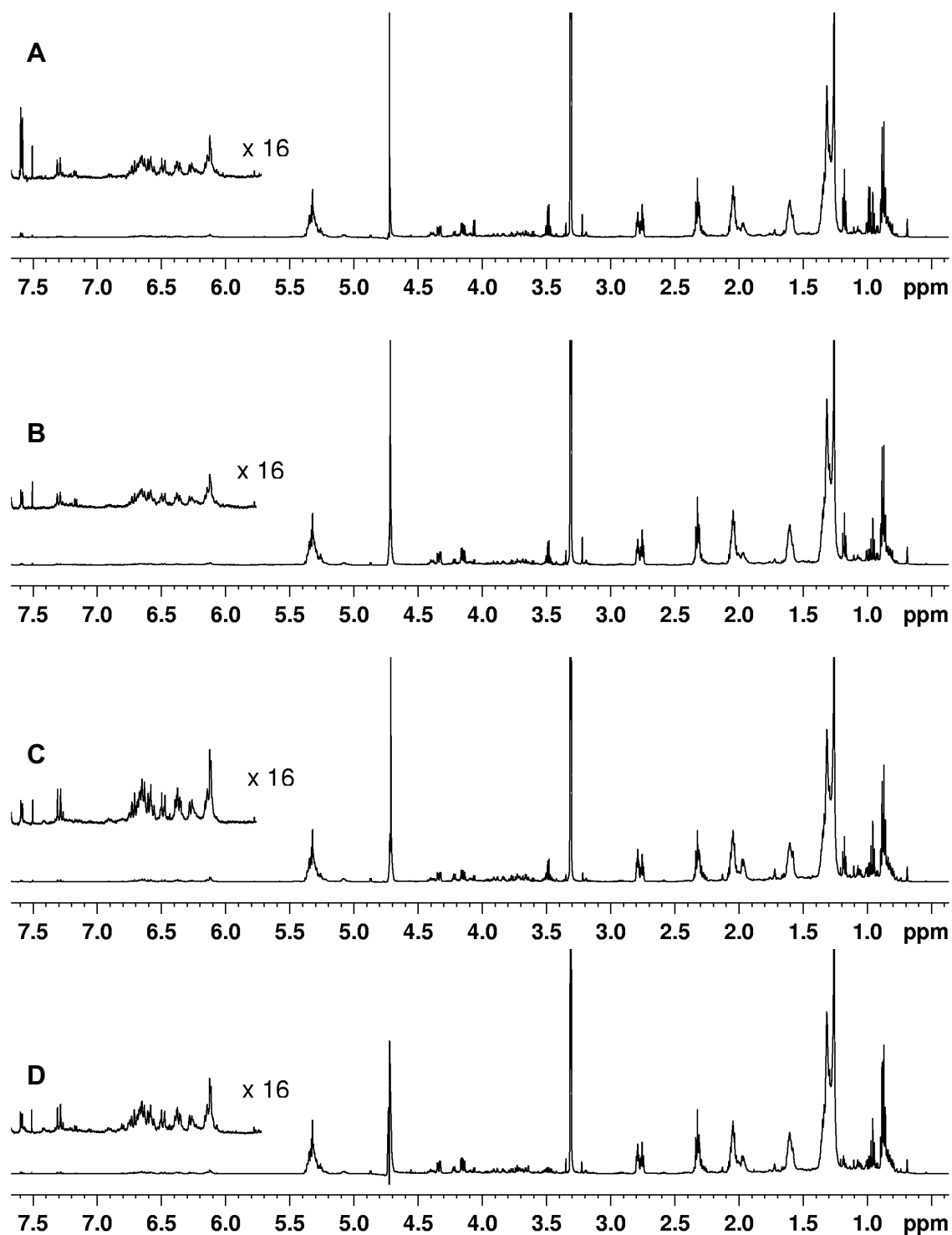


Figure 4.6. ^1H NMR spectra of organic fractions from pulp and peel of *Capsicum annuum* L. ecotype “Cornetto di Pontecorvo”. (A) Pulp, grown OF; (B) pulp, grown GH; (C) peel, grown OF; (D) peel, grown GH.

The spectral assignment of organic extracts (Table 4.5) was obtained using 2D experiments and literature data on vegetable food matrices (Capitani et al., 2014). Saturated, oleic, linoleic and linolenic fatty acid chains together with the glycerol moiety of triglycerides and β -sitosterol were identified. The molar ratio of linoleic/linolenic fatty acids varied depending on tissue and growing method. The highest ratio of linoleic/linolenic fatty chains was observed in pulp of both GH and OF fruits (2.2), followed by GH peel (1.8) and OF peel (1.4) extracts. A part from lipids (triacylglycerols, phosphatidylcholine, and digalactosyldiacylglycerols) and fatty acids, ^1H NMR spectra of organic extracts showed the presence of carotenoids owing to their characteristic signals in the range between 6.10 and 6.70 ppm due to conjugated trans double bonds. The doublet signal observed at 7.30 ppm ($J = 15$ Hz) and correlated in TOCSY map with another doublet at 6.49 ppm can be assigned to trans double bond $\text{CH}=\text{CH}-\text{C}(\text{R})=\text{O}$ characteristic of capsanthin and its derivatives reported in the literature as the major components of carotenoid fraction in red sweet pepper (Arimboor et al., 2015). The total carotenoid content estimated by the integration of 6.10-6.70 ppm spectral region was higher in peel with respect to pulp organic extracts.

Unlike peel and pulp, galactolipids, phospholipids and carotenoids signals were absent in ^1H NMR spectra of seed organic extracts. Moreover, linolenic acid identified in pulp and peel, was also absent (Figure 4.7).

Table 4.5. Summary of the metabolites identified in the 600.13 MHz ^1H spectra of organic extracts of pulp and peel from “Cornetto di Pontecorvo” pepper, grown OF and GH. The metabolites identified also in seed extracts are labelled with an asterisk.

| Compound | Assignment | ^1H (ppm) | Multiplicity: $J(\text{Hz})$ | ^{13}C (ppm) |
|---|--|--------------------|---------------------------------|-----------------------|
| Oleic fatty chain* | CH ₂ -2 | 2.32 | | 34.8 |
| | CH ₂ -3 | 1.60 | m | 25.5 |
| | CH ₂ -4,7 | 1.31 | | 29.9 |
| | CH ₂ -8,CH ₂ -11 | 2.07 | | 27.8 |
| | CH=CH 9,10 | 5.35 | | 130.8 |
| | CH ₂ -12,15 | 1.32 | | 30.4 |
| | CH ₂ -16 | 1.25 | | 32.6 |
| | CH ₂ -17 | 1.29 | | 23.4 |
| Linolenic fatty chain (C18:3 Δ 9,12,15) | CH ₂ -8 | 2.04 | m | 28.0 |
| | CH ₂ -2 | 2.32 | t [7.6] | 35.1 |
| | CH ₂ -3 | 1.60 | m | 25.8 |
| | CH-9 | 5.32 | m | 130.8 |
| | CH-10 | 5.31 | m | 128 |
| | CH-12 | 5.31 | m | 128 |
| | CH-13 | 5.31 | m | 128 |
| | CH-15 | 5.31 | m | 128 |
| | CH ₂ -11,14 | 2.78 | t [6.7] | 26.5 |
| | CH ₂ -17 | 2.06 | m | 21.3 |
| CH ₃ -18 | 0.95 | t [7.3] | 14.8 | |
| Linoleic fatty chain* (C18:2 Δ 9,12) | CH ₂ -8,14 | 2.04 | m | 28.0 |
| | CH-9,13 | 5.32 | m | 130.8 |
| | CH-10,12 | 5.31 | m | 128.9 |
| | CH ₂ -11 | 2.75 | t [6.0] | 26.6 |
| Triacylglycerol moiety* | CH ₂ sn 1,3 | 4.33;4.15 | dd [4.0;12.0]; dd [6.2;11.9] | 63.1 |
| | CH sn 2 | 5.26 | m | 70.2 |
| Saturated fatty acids* | CH ₂ -2 | 2.32 | | 34.8 |
| | CH ₂ -3 | 1.6 | m | 25.8 |
| | CH ₂ (n-3) | 1.31 | | 29.9 |
| | CH ₂ (n-2) | 1.29 | | 32.4 |
| | CH ₂ (n-1) | 1.29 | | 23.4 |
| | CH ₃ | 0.88 | t [6.92] | 14.6 |
| Free fatty acids* | CH ₂ -2 | 2.29 | m | 34.7 |
| | CH ₂ -3 | 1.61 | m | 25.5 |
| β -Sitosterol* | CH ₃ -18 | 0.68 | s | |
| | CH(OH)-3 | 3.51 | | 72.2 |
| Phosphatidylcholine | (CH ₃) ₃ N | 3.22 | s | 54.6 |
| | CH ₂ sn-3 | 4.09 | | 65.2 |
| | CH ₂ sn-1 | 4.39; 4.18 | | 63.0 |

| | | | | |
|----------------------------|------------------------|------------|--------------------|-------|
| | CH <i>sn</i> -2 | 5.22 | | 70.9 |
| Dygalactosyldiacylglycerol | CH-1' | 4.22 | | 105.0 |
| | CH-1'' | 4.87 | d [4.0] | 100.3 |
| | CH-2'' | 3.78 | | 69.9 |
| | CH-3'' | 3.72 | | |
| | CH-4'' | 3.91 | | 70.8 |
| Capsanthin and derivates | <i>t</i> -CH=CH-C(R)=O | 7.30; 6.49 | d [15.0]; d [15.0] | |

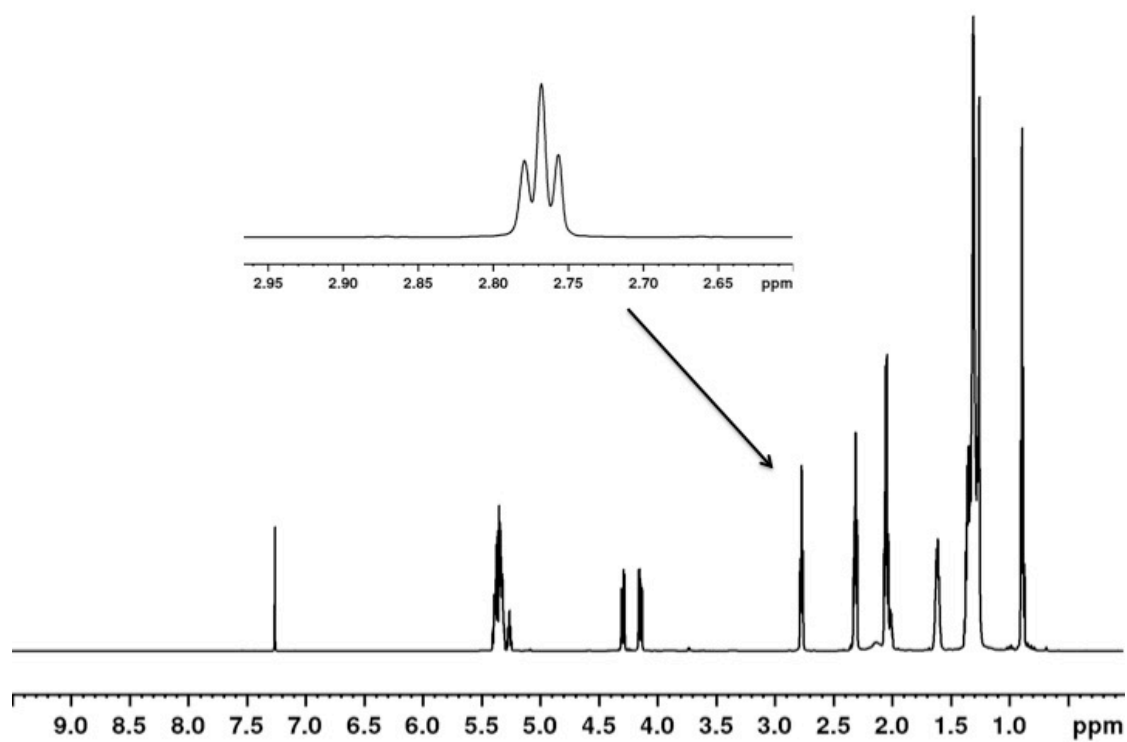


Figure 4.7. ¹H NMR spectrum of organic fraction in CDCl₃ from seeds grown open field. The arrow shows the signal of linoleic acid. The star indicates the position for the signal of linolenic acid absent in the sample.

4.2.4 References

- Arimboor, R., Natarajan, R.B, Menon, K.R., Chandrasekhar, L.P., & Moorkoth, V., 2015. Red pepper (*Capsicum annum*) carotenoids as a source of natural food colors: analysis and stability – a review. *J. Food Sci. Tech.* 52, 1258-1271.
- Capitani, D., Sobolev, A.P., Delfini, M., Vista, S., Antiochia, R., Proietti, N., Bubici, S., Ferrante, G., Carradori, S., De Salvador, F. R., & Mannina, L., 2014. NMR methodologies in the analysis of blueberries. *Electrophoresis* 35, 1615-1626.
- Mannina, L., Sobolev, A.P., & Capitani, D., 2012. Applications of NMR metabolomics to the study of foodstuffs: truffle, kiwifruit, lettuce, and sea bass. *Electrophoresis*, 33, 2290-2313.
- Mannina, L., Sobolev, A.P., & Viel, S., 2012. Liquid state ¹H high field NMR in food analysis. *Prog. Nucl. Magn. Reson. Spectrosc.* 66, 1-39.
- Ritota, M., Marini, F., Sequi, P., & Valentini, M., 2010. Metabolomic characterization of Italian sweet pepper (*Capsicum annum* L.) by means of HRMAS-NMR spectroscopy. *J. Agric. Food Chem.* 58, 9675-9684.
- Sobolev, A.P., Segre, A., & Lamanna, R., 2003. Proton high field NMR study of tomato juice. *Magn. Reson. Chem.* 41, 237-245.
- Sobolev, A.P., Brosio, E., Gianferri, R., & Segre, A.L., 2005. Metabolic profile of lettuce leaves by high-field NMR spectra. *Magn. Reson. in Chem.* 43, 625-638.
- Van Straten, G., van Willigenburg, G., van Henten, E., & van Ooteghem, R., 2011. *Optimal control of greenhouse cultivation*. New York: CRC Press.

4.3 Sedano Bianco di Sperlonga IGP

4.3.1 Introduction

White celery (*Apium graveolens* L.) is a daily consumption vegetable widely used in Italian traditional cuisine for its sensorial and nutritional properties. White celery is rich in biologically active compounds (Ovodova et al., 2009) which bring numerous health benefits in the human body. This vegetable shows antifungal, antibacterial, antioxidant, antidiabetic, antihypertensive and hepatoprotective activities (Kooti et al., 2014; Momin & Nair, 2001; Dianat et al., 2015). According to the literature data (Rupérez and Toledano, 2003) celery is a rich source of mannitol, thus a diet including celery consumption can be positive for preserving the intestinal health.

The Italian PGI (Protected Geographical Indication) “Bianco di Sperlonga” (*Apium graveolens* variety *dulce*) is strictly cultivated in the Lazio region of Central Italy, particularly at charming seaside of Sperlonga-Fondi in the Ciociaria area (G.U. L 68 del 18/3/2010 – Reg. UE 222/2010). Sperlonga and Fondi territories, the only areas of "Bianco di Sperlonga" celery production as well as specified by the PGI certification, are characterized by a very favourable soil and climate. The land on which the cultivation of celery has been developed is characterized by a sandy-loamy soil with a high degree of salinity which bestows “Bianco di Sperlonga” celery specific organoleptic qualities of flavour, sweet and moderately aromatic taste as well as a reduced breaking strength. The presence of high percentages of iron, manganese, zinc, copper, boron together with the peculiar pedoclimatic conditions of the maritime area of Sperlonga-Fondi provide unique nutritional properties of this celery among different varieties available on the market and contributed to develop a product with specific traits. For instance, “Bianco di Sperlonga” celery contains more than 135 mg/100 g of a total amount of organic acids and more than 13.00 mg/g of total sugars as reported in the product specification (G.U. L 93 del 31/3/2006 - Reg. CE 510/2006).

In the present work, a NMR based metabolomic approach to study local ecotype “Bianco di Sperlonga” celery, grown in greenhouse, has been carried out in the frame of the Regional project “*e*-ALIERB” (FILAS-RU-2014-1157, Codice CUP B82I15003570002). For this purpose, different parts of the plant, including petioles and leaves, were separated and studied.

Untargeted analysis, carried out by means of Nuclear Magnetic Resonance (NMR) methodology, enables to obtain the metabolomic profile of the samples. NMR is one of the most suitable techniques in metabolomics to identify and quantify simultaneously different classes of compounds (Capitani et al., 2013).

4.3.2 Materials and Methods

The plants of celery *Apium graveolens* variety dulce ecotype “Bianco di Sperlonga”, certificated PGI and grown in greenhouse were provided by a farm located at Sperlonga in the Lazio region (Central Italy). The consistency of samples with requirements of the PGI certification were confirmed by the morphological analysis. The whole heads of the celery were carefully divided in different edible parts (i.e. petioles and leaves) and analysed separately.

Fresh samples of leaves and different portions of petioles (distal, median and proximal portions with respect to the celery heart) coming from 4 different celeries were collected, frozen and ground in liquid nitrogen to obtain a homogeneous pool of each part. Each part of celery was subjected to the extraction according to the Bligh-Dyer method, which allows to optimize the quantification of a greater number of metabolites. In details, about 2.0 g of each part was added sequentially with 3 mL methanol/chloroform (2:1 v/v) mixture, 1 mL of chloroform and 1.2 mL of distilled water. After each addition the sample was carefully shaken. The emulsion was pre-served at 4 °C for 40 min. The sample was then centrifuged (800g for 15 min at 4 °C) and the upper (hydroalcoholic) and lower (organic)

phases were carefully separated. The pellets were re-extracted using half of the solvent volumes (in the same conditions described above) and the separated fractions were pooled. Both fractions were dried under a gentle N₂ flow at room temperature until the solvent was completely evaporated. The dried phases were stored at -20 °C until further analyses (Capitani et al., 2014).

The dried organic fraction of each sample was dissolved in 0.7 mL of a CDCl₃/CD₃OD mixture (2:1 v/v) and then placed into a 5 mm NMR tube. Finally, the NMR tube was flame-sealed. Conversely, the dried hydroalcoholic phase of each sample was solubilized in 0.7 mL 400 mM phosphate buffer/D₂O containing 1 mM solution of TSP as internal standard, and then transferred into a 5 mm NMR tube.

NMR spectra of all hydroalcoholic and organic extracts were recorded at 27 °C on a Bruker AVANCE 600 spectrometer operating at the proton frequency of 600.13 MHz and equipped with a Bruker multinuclear z-gradient 5 mm probe head. ¹H spectra were referenced to methyl group signals of TSP (δ = 0.00 ppm) in D₂O, and to the residual CHD₂ signal of methanol (set to 3.31 ppm) in CD₃OD/CDCl₃ mixture. ¹H spectra of hydroalcoholic extracts were acquired with 256 transients with a recycle delay of 5 s. The residual HDO signal was suppressed using a pre-saturation. The experiment was carried out by using 45° pulse of 6.5-7.5 μs, 32K data points. ¹H spectra of extracts in CD₃OD/CDCl₃ were acquired with 256 transients, recycle delay of 5 s and 90° pulse of 9-11 μs, 32K data points. The two-dimensional (2D) NMR experiments, such as ¹H-¹H TOCSY, ¹H-¹³C HSQC and ¹H-¹³C HMBC, were carried out under the same experimental conditions previously reported (Sobolev et al., 2018).

4.3.3 Results and Discussion

The assignment of ^1H spectra of hydroalcoholic extracts from petioles and leaves performed in D_2O phosphate buffer was obtained using 1D and 2D NMR experiments and literature data (Sobolev et al., 2005) and the results are reported in Table 4.6.

Table 4.6. Summary of the metabolites identified in the 600.13 MHz ^1H spectra (27 °C) of the hydroalcoholic extract from leaves from “Bianco di Sperlonga” celery. The metabolites identified also in the petiole extract were labelled with *.

| Compound | Assignment | ^1H (ppm) | Multiplicity: $J(\text{Hz})$ | ^{13}C (ppm) |
|-----------------------------|-----------------------|--------------------|------------------------------|-----------------------|
| <i>Carbohydrates</i> | | | | |
| α -Glucose* | CH-1 | 5.25 | d [3.80] | 93.13 |
| | CH-2 | 3.55 | | 72.52 |
| | CH-3 | 3.72 | | 73.72 |
| | CH-4 | 3.42 | dd | 70.68 |
| | CH-5 | 3.84 | | 72.46 |
| | CH ₂ -6,6' | 3.84; 3.74 | | 61.75 |
| β -Glucose* | CH-1 | 4.66 | d [7.98] | 96.92 |
| | CH-2 | 3.26 | dd [9.40; 8.06] | 75.14 |
| | CH-3 | 3.51 | t [9.15] | 76.90 |
| | CH-4 | 3.41 | dd [9.80; 9.20] | 70.65 |
| | CH-5 | 3.44 | | 77.07 |
| | CH ₂ -6,6' | 3.90; 3.74 | | 61.80 |
| β -D-Fructofuranose* | CH ₂ -1,1' | 3.60; 3.57 | | 63.80 |
| | CH-2 | | | 102.40 |
| | CH-3 | 4.12 | m | 76.40 |
| | CH-4 | 4.12 | m | 75.38 |
| | CH-5 | 3.84 | | 81.83 |
| | CH ₂ -6,6' | 3.81; 3.69 | | 63.40 |
| α -D-Fructofuranose* | CH-3 | 4.13 | | 83.02 |
| | CH-5 | 4.07 | | 82.44 |
| β -D-Fructopyranose* | CH ₂ -1,1' | 3.57; 3.72 | | 64.90 |
| | CH-3 | 3.81 | | 68.61 |
| | CH-4 | 3.90 | | 70.71 |
| | CH-5 | 4.01 | | 70.13 |
| | CH ₂ -6,6' | 3.72; 4.03 | | 64.44 |
| Sucrose* | CH-1 (Glc) | 5.42 | d [3.77] | 93.26 |
| | CH-2 | 3.57 | | 72.10 |
| | CH-3 | 3.78 | | 73.52 |
| | CH-4 | 3.48 | | 70.30 |

| | | | | |
|----------------------|---------------------------------|------------|------------------------|--------|
| | CH-5 | 3.85 | | 73.52 |
| | CH ₂ -6 | 3.83 | | 61.27 |
| | CH ₂ -1' (Fru) | 3.69 | | 62.34 |
| | CH-2' | | | 104.70 |
| | CH-3' | 4.22 | | 77.50 |
| | CH-4' | 4.06 | | 75.00 |
| | CH-5' | 3.89 | | 82.22 |
| | CH ₂ -6' | 3.83 | | 63.34 |
| <i>Polyalcohols</i> | | | | |
| Mannitol* | CH-1,6 | 3.87 | dd [11.78; 2.85] | 64.28 |
| | CH-1',6' | 3.68 | dd [11.80; 6.20] | 64.28 |
| | CH-2,5 | 3.75 | ddd [8.48; 6.20; 2.89] | 71.31 |
| | CH-3,4 | 3.80 | d [8.52] | 70.34 |
| Myo-inositol* | CH-1 | 4.08 | | 73.24 |
| | CH-2,5 | 3.63 | | |
| | CH-3,6 | 3.63 | | 73.45 |
| | CH-4 | 3.30 | | 75.38 |
| Scyllo-Inositol* | CH-1,6 | 3.36 | s | 74.6 |
| <i>Organic acids</i> | | | | |
| Acetic acid* | α -CH ₃ | 1.92 | s | 24.2 |
| Ascorbic acid* | CH ₂ | 3.69 | | 62.40 |
| | CH(OH) | 3.99 | | 69.70 |
| | CH(OCO) | 4.50 | d [4.30] | 76.98 |
| Citric acid* | α,γ -CH | 2.55 | d [16.08] | 46.06 |
| | α',γ' -CH | 2.69 | | 46.06 |
| | β -C | | | 75.80 |
| | 1,5-COOH | | | 179.3 |
| | 6-COOH | | | 181.9 |
| Formate* | HCOOC | 8.46 | s | |
| Malic acid* | α -CH | 4.31 | dd [9.70; 3.20] | 71.50 |
| | β -CH | 2.68 | dd [15.55; 3.30] | 43.40 |
| | β' -CH | 2.39 | dd [15.55; 9.70] | 43.40 |
| Quinic acid* | CH ₂ -1,1' | 1.87; 2.10 | dd [13.20; 10.80] | 41.77 |
| | CH-2 | 4.01 | | 69.76 |
| | CH-3 | 3.54 | | 76.29 |
| | CH-4 | 4.11 | | 71.43 |
| | CH ₂ -5,5' | 2.04; 2.12 | | 38.45 |
| Succinic acid* | α,β -CH ₂ | 2.40 | s | 34.90 |

| | | | | |
|--------------------|----------------------------------|-----------------|-------------------------|--------|
| Fumaric acid* | CH=CH | 6.52 | s | |
| <i>Polyphenols</i> | | | | |
| Chlorogenic acid | CH-2e | 2.19 | | 39.56 |
| | CH-2a | 2.02 | | 39.56 |
| | CH-3 | 5.31 | ddd [11.20; 9.92; 4.74] | 72.14 |
| | CH-4 | 3.88 | | |
| | CH-5 | 4.27 | | |
| | =CH-COO ⁻ | 6.35 | d [16.03] | 115.74 |
| | -CH= | 7.60 | d [16.17] | |
| | CH-2' | 7.16 | d [2.03] | 116.19 |
| | CH-5' | 6.93 | d [8.04] | 117.48 |
| CH-6' | 7.08 | dd [8.15; 2.08] | 123.70 | |
| <i>Amino acids</i> | | | | |
| Alanine* | α -CH | 3.80 | | 51.35 |
| | β -CH ₃ | 1.48 | d [7.33] | 17.03 |
| Asparagine* | α -CH | 4.02 | | 52.50 |
| | β -CH | 2.89 | dd [16.91; 7.24] | 35.70 |
| | β' -CH | 2.96 | dd [16.91; 4.38] | 35.70 |
| Aspartate* | α -CH | 3.90 | | 53.08 |
| | β -CH | 2.68 | | 37.20 |
| | β' -CH | 2.80 | dd [17.40; 3.84] | 37.20 |
| Glutamate* | α -CH | 3.75 | m | 54.66 |
| | β, β' -CH ₂ | 2.05; 2.11 | m | 27.70 |
| | γ -CH ₂ | 2.34 | m | 34.20 |
| Glutamine* | α -CH | 3.77 | | 55.35 |
| | β, β' -CH ₂ | 2.08; 2.14 | m | 26.97 |
| | γ -CH | 2.45 | dt [2.05; 8.61] | 31.68 |
| Isoleucine* | α -CH | 3.68 | | 60.50 |
| | γ -CH ₃ | 1.02 | d [7.10] | 25.40 |
| | γ -CH | 1.26 | | 25.40 |
| | γ' -CH | 1.46 | | 25.40 |
| | δ -CH ₃ | 0.94 | | |
| Phenylalanine* | α -CH | 3.96 | | 57.15 |
| | β, β' -CH ₂ | 3.15; 3.28 | | 37.62 |
| | CH-2,6, ring | 7.34 | | 130.56 |
| | CH-3,5, ring | 7.43 | | 130.28 |
| | CH-4, ring | 7.39 | | 129.10 |
| Threonine* | α -CH | 3.60 | m | 61.32 |
| | β -CH | 4.26 | | 66.87 |
| | γ -CH ₃ | 1.31 | d [6.40] | 20.85 |

| | | | | |
|--------------------------|---|------|----------|-------|
| Valine* | * α -CH | 3.62 | | |
| | β -CH | 2.27 | m | 29.86 |
| | γ -CH ₃ | 0.99 | d [7.02] | 17.35 |
| | γ' -CH ₃ | 1.04 | d [7.02] | 18.91 |
| <i>Other metabolites</i> | | | | |
| Choline* | N(CH ₃) ₃ ⁺ | 3.21 | s | 54.96 |
| | α -CH ₂ | | | 68.40 |

The ¹H spectra of all the extracts were dominated by the strong signals of sugars (glucose and fructose) in the range of 3.0-5.5 ppm, whereas in the high field 0.50-3.10 ppm spectral region minor signals belonging to the aliphatic groups of amino acids and organic acids were observable (Figure 4.8A). In the low field region of ¹H spectrum (Figure 4.8C), signals of aromatic groups of phenylalanine, formic acid, fumaric acid and chlorogenic acid were assigned.

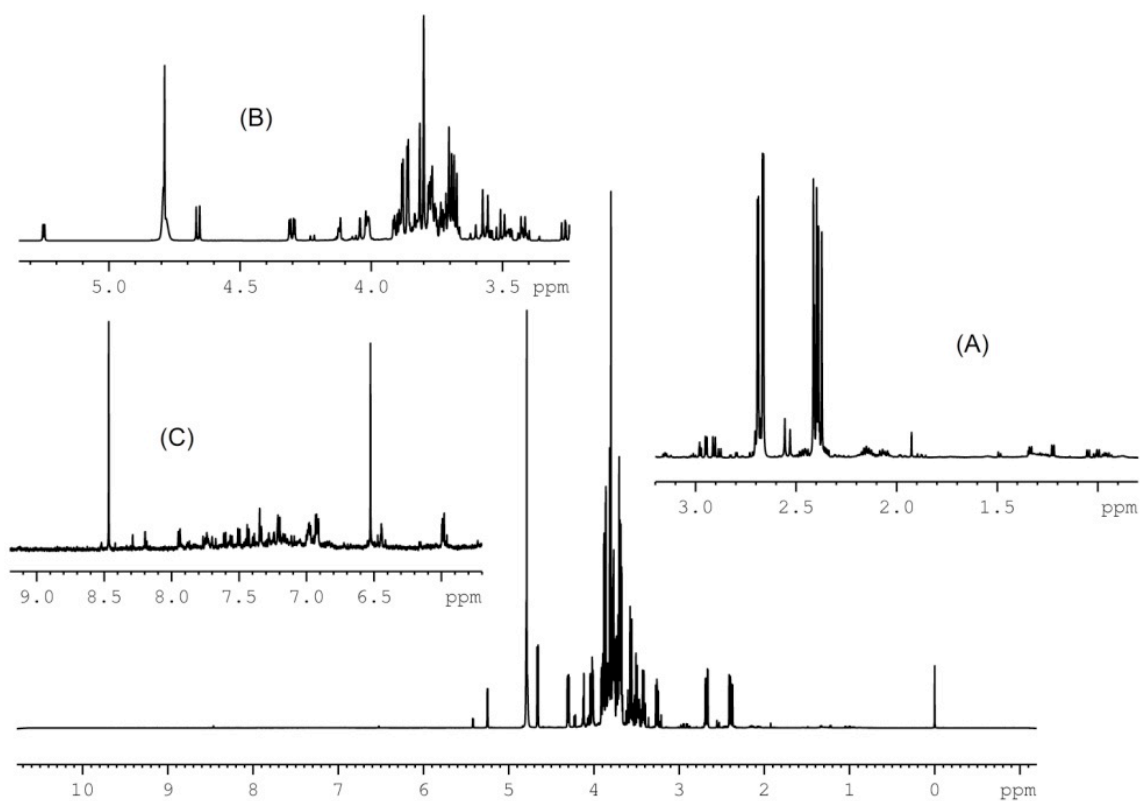


Figure 4.8. ¹H NMR spectrum of the hydroalcoholic Bligh-Dyer extract from the leaves of “Bianco di Sperlonga” celery, in 400 mM phosphate/D₂O buffer with 1 mM TSP: (A) high field region; (B) middle field region; (C) low field region.

In the case of the leaf extracts, the ^1H spectra showed the presence of carbohydrates (α -glucose, β -glucose, fructose and sucrose), amino acids (alanine, asparagine, aspartate, glutamate, isoleucine, leucine, lysine, phenylalanine, threonine, tyrosine and valine), organic acids (acetic, ascorbic, citric, formic, fumaric, malic, quinic and succinic), polyalcohols (mannitol, scyllo-inositol and myo-inositol) and other metabolites such as choline (Table 4.6). Chlorogenic acid and lysine assigned in these extracts were not identified in the samples from petioles, whereas glutamine was identified only in petioles.

Not only qualitative but also quantitative differences were evident by comparing the extracts from petioles and leaves. Leaves showed higher concentration of amino acids, organic acids and choline; only asparagine, acetic, lactic and formic acids resulted to be in higher concentration in petiole extract. In the case of carbohydrates, the extract from leaves contained higher concentration of sucrose, but minor concentration of glucose and fructose compared to the petiole extract (Figure 4.9).

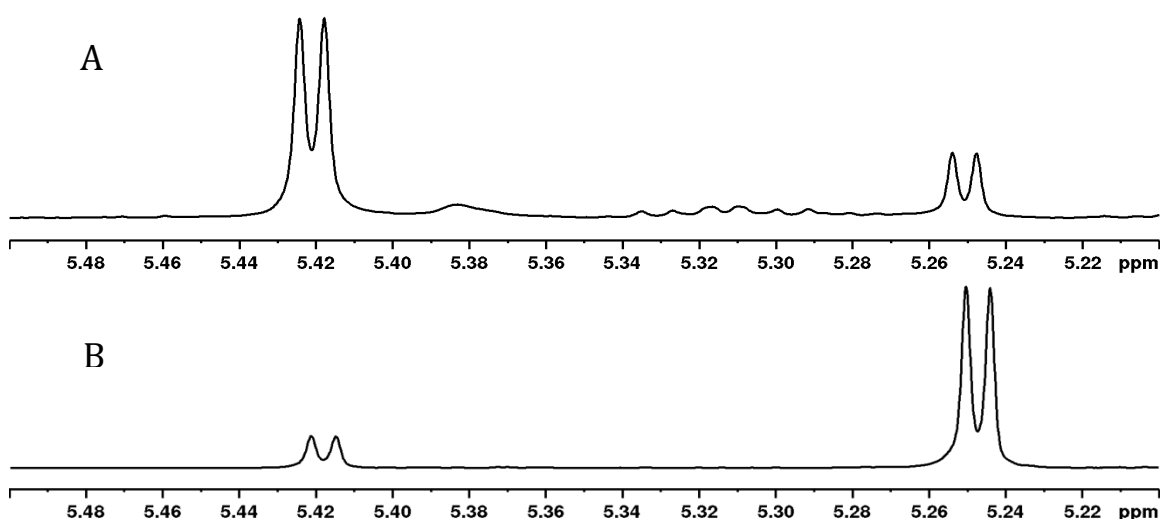


Figure 4.9. ^1H NMR spectra of the hydroalcoholic Bligh-Dyer extract from leaves (A) and petioles (B) of “Bianco di Sperlona” celery: doublet of α -glucose at 5.25 ppm and doublet of sucrose at 5.42 ppm.

Comparing the extracts obtained from three different parts of the celery petioles (distal, median and proximal parts with respect to the leaves), quantitative differences were

also observed. For instance, almost all amino acids were present in higher concentration in the median and distal portion than in proximal one, on the contrary, citric and formic acids were present in highest concentration in proximal part; conversely, the highest content of glucose and fructose was in the extract from the median portion.

The assignment of ^1H spectra of organic extracts from petioles and leaves performed in $\text{CDCl}_3/\text{CD}_3\text{OD}$ was obtained by 1D and 2D NMR experiments and literature data and the results are reported in Table 4.7. Saturated, oleic, linoleic and linolenic fatty chains together with pheophytins a and b (Katz et al., 1963; Sobolev et al., 2005), digalactosyldiacylglycerols, phosphatidylcholine, phosphatidylethanolamine and β -sitosterol were identified. Although the ^1H spectra of organic extracts were more conservative than the hydroalcoholic ones, some differences were observed. First, pheophytins (a and b) were present only in leaf extracts.

Table 4.7. Summary of the metabolites identified in the 600.13 MHz ^1H spectra (27 °C) of the organic extract from leaves from “Bianco di Sperlona” celery. The metabolites identified also in the petiole extract are labelled with *.

| Compound | Assignment | ^1H (ppm) | Multiplicity: $J(\text{Hz})$ | ^{13}C (ppm) |
|--------------------|----------------------------------|--------------------|------------------------------|-----------------------|
| Pheophytin a | CH-5 | 9.31 | s | 97.67 |
| | CH-10 | 9.49 | s | 104.87 |
| | CH-20 | 8.56 | s | 93.58 |
| | CH-3 ¹ | 7.96 | dd [17.80; 11.50] | 129.00 |
| | CH-3 ² | 6.18 | dd | 123.26 |
| | CH-3 ^{2'} | 6.25 | dd | 123.37 |
| | CH ₃ -2 ¹ | 3.38 | s | 12.10 |
| | CH ₃ -7 ¹ | 3.18 | s | 11.14 |
| | CH ₂ -8 ¹ | 3.73 | | 19.30 |
| | CH ₃ -8 ² | 1.67 | t [7.72] | 17.40 |
| | CH ₃ -12 ¹ | 3.64 | s | 12.01 |
| | CH-17 | 4.15 | | 51.34 |
| | CH-18 | 4.45 | | 50.31 |
| | CH-18 ¹ | 1.78 | d [7.29] | 23.06 |
| | CH ₃ -13 ⁴ | 3.87 | s | 53.10 |
| | CH ₂ -P1 | 4.34; 4.37 | | 61.78 |
| | CH-P2 | 4.99 | | 117.77 |
| CH-P3 ¹ | 1.49 | s | 16.20 | |
| Pheophytin b | CH-7 ¹ | 11.14 | s | |
| | CH-5 | 9.93 | s | |
| | CH-10 | 9.60 | s | 107.70 |

| | | | | |
|--|----------------------------------|------------------|----------|-------------|
| | CH-20 | | | |
| | CH-3 ¹ | 7.95 | | 129.21 |
| | CH-3 ² | | | |
| | CH-3 ^{2'} | | | |
| β -Sitosterol* | CH ₃ -18 | 0.67 | s | |
| | CH(OH)-3 | 3.50 | | 71.38 |
| | CH ₂ -4 | 2.24 | | |
| | CH ₂ -2,1 | 1.83; 1.49; 1.06 | | |
| Digalactosyldiacylglycerols* | CH <i>sn</i> 2 | 5.23 | | 70.57 |
| | CH ₂ <i>sn</i> 1 | 3.7; 3.94 | | 68.00 |
| | CH ₂ <i>sn</i> 3 | 4.20; 4.36 | | 63.02 |
| | CH-1' | 4.20 | | 104.17 |
| | CH-2' | 3.51 | | 71.76 |
| | CH-3' | 3.50 | | 73.91 |
| | CH-4' | 3.92 | | 69.83 |
| | CH-5' | 3.79 | | 70.91 |
| | CH ₂ -6' | 3.60; 3.68 | | 66.70 |
| | CH-1'' | 4.87 | d [3.80] | 99.55 |
| | CH-2'' | 3.84 | | 69.90 |
| | CH-3'' | 3.71 | | 70.40 |
| | CH-4'' | 3.93 | | 69.90 |
| | CH-5'' | 3.71 | | 70.40 |
| | CH ₂ -6'' | 3.73; 3.77 | | 61.54 |
| Phosphatidylcholine* | CH <i>sn</i> 2 | 5.25 | | 70.90 |
| | CH ₂ <i>sn</i> 1 | 4.42; 4.19 | | 63.18 |
| | CH ₂ <i>sn</i> 3 | 4.01 | | 63.59 |
| | CH ₂ OP | 4.26 | | 59.59 |
| | CH ₂ N | 3.61 | | 67.00 |
| | N(CH ₃) ₃ | 3.20 | s | 54.46 |
| Phosphatidylethanolamine* | CH <i>sn</i> 2 | 5.25 | | 70.90 |
| | CH ₂ <i>sn</i> 1 | 4.42; 4.19 | | 63.18 |
| | CH ₂ <i>sn</i> 3 | 4.01 | | 63.59 |
| | CH ₂ OP | 4.05 | | 62.10 |
| | CH ₂ N | 3.11 | | 40.60 |
| Oleic fatty chain (C18:1 Δ 9)* | CH ₂ -1 | | | 174.20 |
| | CH ₂ -2 | 2.30 | | 34.33 |
| | CH ₂ -3 | 1.59 | | 25.03 |
| | CH ₂ -4,7 | 1.29 | m | 29.34-30.2 |
| | CH ₂ -8 | 2.03 | m | 27.32 |
| | CH=CH 9-10 | 5.34 | | 130.25 |
| | CH ₂ -11 | 2.03 | | 27.32 |
| | CH ₂ -12,15 | 1.29 | m | 29.34-30.20 |
| | CH ₂ -16 | 1.28 | m | 31.68 |
| | CH ₂ -17 | 1.29 | m | 22.90 |
| | CH ₂ -18 | 0.84 | | 13.90 |

| | | | | | |
|--|--|--------------------|----------|--------------|--------|
| Linoleic fatty chain (C18:2 Δ 9,12)* | CH ₂ -1 | | | 174.20 | |
| | CH ₂ -2 | 2.30 | | 34.33 | |
| | CH ₂ -3 | 1.59 | | 25.03 | |
| | CH ₂ -4,7 | 1.29 | | 29.34; 30.20 | |
| | CH ₂ -8 | 2.03 | | 27.32 | |
| | CH-9 | 5.34 | | 130.25 | |
| | CH-10 | 5.34 | | 128.40 | |
| | CH ₂ -11 | 2.74 | t | 25.78 | |
| | CH-12 | 5.34 | m | 128.40 | |
| | CH-13 | 5.34 | m | 130.25 | |
| | CH ₂ -14 | 2.03 | q | 27.32 | |
| | CH ₂ -15 | 1.29 | | 29.34 | |
| | CH ₂ -16 | 1.29 | | 31.84 | |
| | CH ₂ -17 | 1.29 | | 22.90 | |
| | CH ₂ -18 | 0.93 | t | 14.09 | |
| | Linolenic fatty chain (C18:3 Δ 9,12,15)* | CH ₂ -1 | | | 174.20 |
| | | CH ₂ -2 | 2.30 | | 34.33 |
| | | CH ₂ -3 | 1.59 | | 25.03 |
| CH ₂ -4 | | 1.29 | | 29.34 | |
| CH ₂ -5,7 | | 1.29 | | 30.20 | |
| CH ₂ -8 | | 2.03 | | 27.32 | |
| CH-9 | | 5.34 | | 130.25 | |
| CH-10 | | 5.34 | | 128.40 | |
| CH ₂ -11 | | 2.74 | | 25.78 | |
| CH ₂ -13, CH-12 | | 5.34 | | 128.40 | |
| CH ₂ -14 | | 2.77 | | 25.73 | |
| CH-15 | | 5.28 | | 127.36 | |
| CH-16 | | 5.36 | | 132.00 | |
| CH ₂ -17 | | 2.05 | | 20.70 | |
| CH ₂ -18 | | 0.974 | | 14.18 | |
| Free fatty chains* | | CH ₂ -1 | | | 176.90 |
| | | CH ₂ -2 | 2.29 | t | 34.70 |
| | | CH ₂ -3 | 1.61 | | 25.21 |
| Saturated fatty chains* | CH ₂ -2 | 2.33 | | 34.66 | |
| | CH ₂ -3 | 1.61 | m | 25.36 | |
| | CH ₂ (n-3) | 1.29 | m | 29.21; 29.70 | |
| | CH ₂ (n-2) | 1.27 | m | 32.12 | |
| | CH ₂ (n-1) | 1.27 | | 23.20 | |
| | CH ₃ | 0.89 | t [7.20] | 14.08 | |

It was noteworthy that linolenic and linoleic acids ratio was different in leaves and petioles. Figure 4.10, showing the characteristic NMR signals of linolenic acid (2.77 ppm)

and linoleic acid (2.74 ppm) in the extracts from both leaves and petioles, evidences that in leaves extracts linolenic acid is present in higher concentration compared to linoleic acid; conversely, in petioles extract this ratio was inverted and linoleic acid was present in higher concentration with respect to the linolenic one.

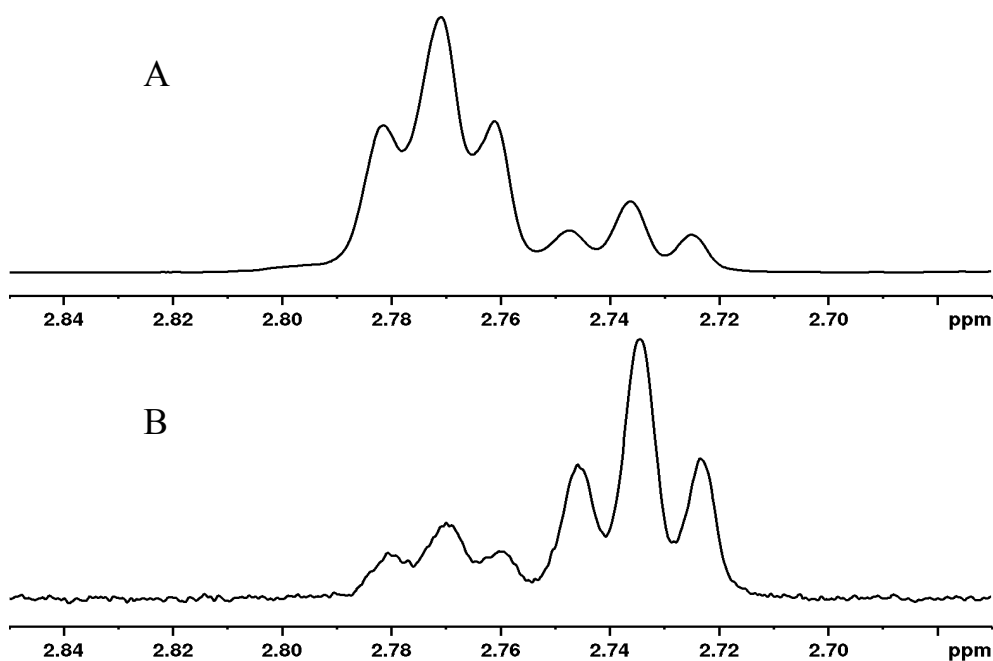


Figure 4.10. ^1H NMR spectra of the organic Bligh-Dyer extract from leaves (A) and petioles (B) of “Bianco di Sperlonga” celery: triplet of linolenic acid at 2.77 ppm and triplet of linoleic acid at 2.74 ppm.

4.3.4 References

- Capitani, D., Proietti, N., Sobolev, A., Antiochia, R., Delfini, M., Sciubba, F., ... & Mannina, L., 2013. Nuclear magnetic resonance-based approach to fruit characterization: the case studies of kiwifruits and peaches. *Spectroscopy Europe* 25, 6-13.
- Capitani, D., Sobolev, A.P., Delfini, M., Vista, S., Antiochia, R., Proietti, N., Bubici, S., Ferrante, G., Carradori, S., De Salvador, F. R., & Mannina, L., 2014. NMR methodologies in the analysis of blueberries. *Electrophoresis* 35, 1615-1626.
- Dianat, M., Veisi, A., Ahangarpour, A., & Moghaddam, H.F., 2015. The effect of hydro-alcoholic celery (*Apium graveolens*) leaf extract on cardiovascular parameters and lipid profile in animal model of hypertension induced by fructose. *Avicenna J. Phytomed.* 5, 203-209.
- Katz, J.J., Closs, G.L., Pennington, F.C., Thomas M.R., & Strain, H.H., 1963. Infrared spectra, molecular weights, and molecular association of chlorophyllides, and pheophytins in various solvents. *J. Am. Chem. Soc.* 85, 3801-3809.
- Kooti, W., Ali-Akbari, S., Asadi-Samani, M., Ghadery, H., & Ashtary-Larky, D., 2014. A review on medicinal plant of *Apium graveolens*. *Advanced Herbal Medicine* 1, 48-59.
- Mannina, L., Sobolev, A.P., & Capitani, D., 2012. Applications of NMR metabolomics to the study of foodstuffs: truffle, kiwifruit, lettuce, and sea bass. *Electrophoresis* 33, 2290-2313.
- Momin, R.A., & Nair, M.G., 2001. Mosquitocidal, nematicidal, and antifungal compounds from *Apium graveolens* L. seeds. *J. Agric. Food Chem.* 49, 142-145.
- Ovodova, R.G., Golovchenko, V.V., Popov, V.S., Popova, G.Y, Paderin, N.M., Shashkov, A.S., & Ovodov, Y.S., 2009. Chemical composition and anti-inflammatory activity of pectic polysaccharide isolated from celery stalks. *Food Chem.* 114, 610-615.
- Rupérez, P., & Toledano, G., 2003. Celery by-products as a source of mannitol. *Eur. Food Res. Technol.* 216, 224-226.
- Sobolev, A.P., Brosio, E., Gianferri R., & Segre, A.L., 2005. Metabolic profile of lettuce leaves by high-field NMR. *Magn. Reson. Chem.* 43, 625-638.
- Sobolev, A.P., Mannina, L., Capitani, D., Sanzò, G., Ingallina, C., Botta, B., ... & Di Sotto, A., 2018. A multi-methodological approach in the study of Italian PDO “Cornetto di Pontecorvo” red sweet pepper. *Food Chem.* 255, 120-131.



4.4 Tomatoes from Fondi

4.4.1 Introduction

The tomato ("Lycopersicum Esculentum") is an annual plant belonging to the "solanaceae" family. This plant, native from Latin America, was cultivated in Europe for centuries only for ornamental purposes because the fruits were not considered edible. In Italy, intensive cultivation and food processing of tomatoes began only in the sixteenth century. Today, country is ranked third in the world for tomatoes production and export.

Several studies on tomatoes carried out with NMR technique allowed to identify principal compounds, namely sugars, organic acids and amino acids, and minor components having a specific biological activity, for instance carotenoids like lycopene and β -carotene (Masetti et al., 2017; Hohmann et al., 2014; Sobolev, Segre & Lamanna, 2003). Previous NMR studies of tomatoes and tomato products were focused on carotenoid composition (Tiziani, Schwartz & Vodovotz, 2006), degree of ripeness (Sanchez et al., 2010; Mounet et al. 2007), quantitative NMR (Vallverdu-Queralt et al., 2011), MRI measurements (Musse et al., 2009), and differentiation between organic and conventional tomatoes (Hohmann et al., 2014).

In the present work, high field NMR methodology was used to study seven different varieties of tomato (San Marzano, Torpedino, Fiaschetta, Bamano, Dolce Miele, Confettino Rosso and King Creole). Some varieties, namely Torpedino, Bamano, Dolce Miele, Confettino Rosso and King Creole, have been introduced recently in the Lazio territory. The cultivation of these varieties, together with the already known San Marzano and Fiaschetta varieties, can be considered a challenge whose aim is to expand the regional agronomic market. This study, carried out in the frame of *e*-ALIERB OpenLab Project* funded by "Regione Lazio", aimed to characterize the chemical composition of these tomatoes and identify the best way to use them according to the variety.

4.4.2 Materials and Methods

Seven different cultivars of tomato cultivated in “Colline Pontine” area (Fondi, LT) were studied by using a NMR-based metabolomic approach. Both unripe and mature fruits of cultivars San Marzano, Torpedino and Fiaschetta were characterized; only mature fruits of cultivars Bamano, Dolce Miele, Confettino Rosso and King Creole were included in our study.

The plants of tomatoes were provided by 3 different farms located at Fondi (LT) in the Lazio region (Central Italy). Fifteen fresh whole fruits for each variety of tomato were frozen and ground in liquid nitrogen to obtain an homogeneous pool and then subjected to the Bligh-Dyer extraction method, which allows to extract in a quantitative manner of a greater number of metabolites. In details, about 1.0 g of each variety was added sequentially with 3 mL methanol/chloroform (2:1 v/v) mixture, 1 mL of chloroform and 1.2 mL of distilled water. After each addition the sample was carefully shaken. The emulsion was preserved at 4 °C for 40 min. The sample was then centrifuged (800g for 15 min at 4 °C) and the upper (hydroalcoholic) and lower (organic) phases were carefully separated. The pellets were re-extracted using half of the solvent volumes (in the same conditions described above) and the separated fractions were pooled. Both fractions were dried under a gentle N₂ flow at room temperature until the solvent was completely evaporated. The dried phases were stored at -20 °C until further analyses (Capitani et al., 2014).

The dried organic fraction of each sample was dissolved in 0.7 mL of a CDCl₃/CD₃OD mixture (2:1 v/v) and then placed into a 5 mm NMR tube. Finally, the NMR tube was flame-sealed. Conversely, the dried hydroalcoholic phase of each sample was solubilized in 0.7 mL 400 mM phosphate buffer / D₂O containing 1 mM solution of TSP as internal standard, and then transferred into a 5 mm NMR tube.

NMR spectra of all hydroalcoholic and organic extracts were recorded at 27 °C on a Bruker AVANCE 600 spectrometer operating at the proton frequency of 600.13 MHz and

equipped with a Bruker multinuclear z-gradient 5 mm probe head. ^1H spectra were referenced to methyl group signals of TSP ($\delta = 0.00$ ppm) in D_2O , and to the residual CHD_2 signal of methanol (set to 3.31 ppm) in $\text{CD}_3\text{OD}/\text{CDCl}_3$ mixture. ^1H spectra of hydroalcoholic extracts were acquired with 256 transients with a recycle delay of 5 s. The residual HDO signal was suppressed using a pre-saturation. The experiment was carried out by using 45° pulse of 6.5-7.5 μs , 32K data points. ^1H spectra of extracts in $\text{CD}_3\text{OD}/\text{CDCl}_3$ were acquired with 256 transients, recycle delay of 5 s and 90° pulse of 9-11 μs , 32K data points. The two-dimensional (2D) NMR experiments, such as ^1H - ^1H TOCSY, ^1H - ^{13}C HSQC and ^1H - ^{13}C HMBC, were carried out under the same experimental conditions previously reported (Sobolev et al., 2018).

The intensity of 25 selected signals in hydroalcoholic extract, see Table 4.8, was measured using the Bruker TOPSPIN software and normalized with respect to the resonance at 0.00 ppm, due to methyl group signals of TSP, normalized to 100. Results have been expressed in mg/100g.

The intensity of 6 selected signals in organic extract, see Table 4.9, was also measured using the Bruker TOPSPIN software and normalized with respect to the resonance at 2.23 ppm, due to signal of total fatty acids, normalized to 100. Results have been expressed in %.

The % values of monounsaturated and saturated fatty acids have been calculated using the following equation:

$$\%_{\text{MONO}} (I_{\text{MONO}}) = I_{\text{UNS}} - 2I_{\text{DI}} - 1.5I_{\text{TRI}} \quad (1)$$

$$\%_{\text{SAT}} = I_{\text{FA}} - I_{\text{DI}} - 0.5I_{\text{TRI}} - I_{\text{MONO}} \quad (2)$$

where I_{UNS} is the integral value of “unsaturated fatty acids” (signal at 5.27 ppm), I_{DI} is the integral value of “di-unsaturated fatty acids” (signal at 2.68), I_{TRI} is the integral value of “tri-unsaturated fatty acids” (signal at 2.72), I_{FA} is the integral value of “total fatty acids” (signal at 2.23). The integral value of total fatty acids has been fixed at 100.

Table 4.8. Compounds, and relative signals (ppm), selected for quantitative analysis in the hydroalcoholic extracts.

| ppm | Compounds | ppm | Compounds |
|------|-------------|------|-------------------|
| 0.96 | Leu | 3.25 | β -Glucose |
| 1.02 | Ile | 4.01 | Fructose |
| 1.05 | Val | 4.30 | Malic Acid |
| 1.33 | Thr | 5.24 | α -Glucose |
| 1.48 | Ala | 5.99 | Uridine |
| 2.29 | GABA | 6.91 | Tyr |
| 2.35 | Glu | 7.33 | Phe |
| 2.45 | Gln | 7.74 | Trp |
| 2.54 | Citric Acid | 8.15 | His |
| 2.81 | Asp | 8.46 | Formic Acid |
| 2.88 | Asn | 8.58 | Adenosine |
| 3.04 | Lys | 9.13 | Trigonelline |
| 3.20 | Choline | | |

Table 4.9. Compounds, and relative signals (ppm), selected for quantitative analysis in the organic extracts.

| ppm | Compounds |
|------|-----------------------------|
| 0.62 | β -Sitosterol |
| 0.70 | Stigmasterol |
| 2.68 | Di-unsaturated fatty acids |
| 2.72 | Tri-unsaturated fatty acids |
| 3.15 | Phosphatidylcholine |
| 5.27 | Unsaturated fatty acids |

4.4.3 Results and Discussion

Analysis of tomato hydroalcoholic extracts. Figure 4.11 shows the ^1H NMR spectrum (600 MHz) of the hydroalcoholic extract (in phosphate buffer / D_2O) of San Marzano mature fruits extract.

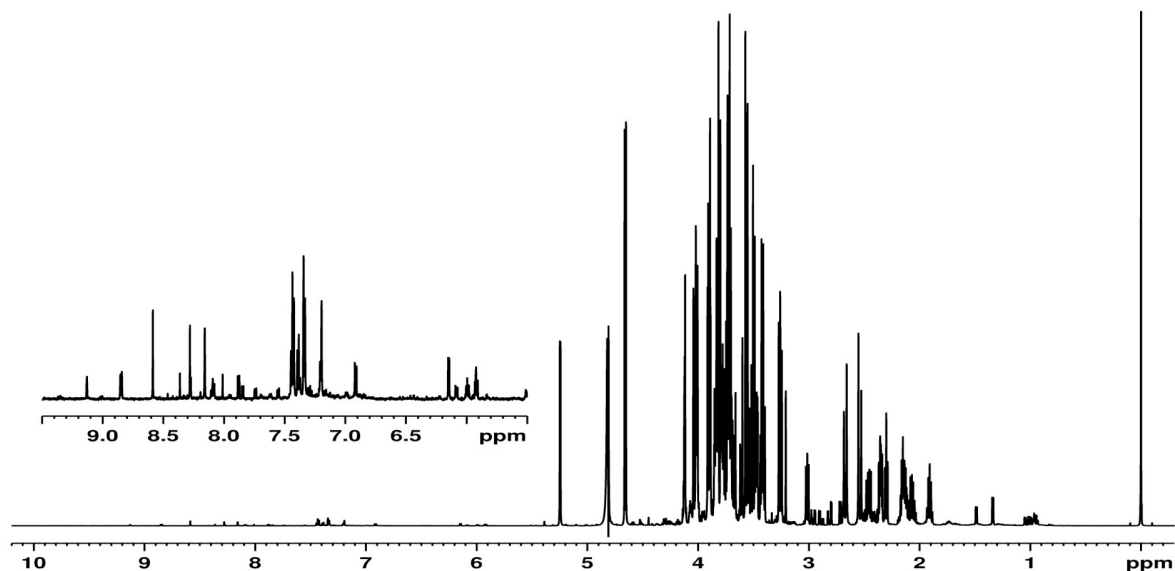
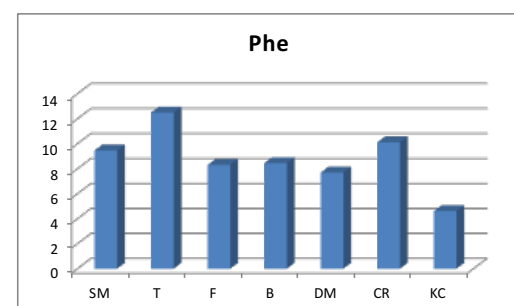
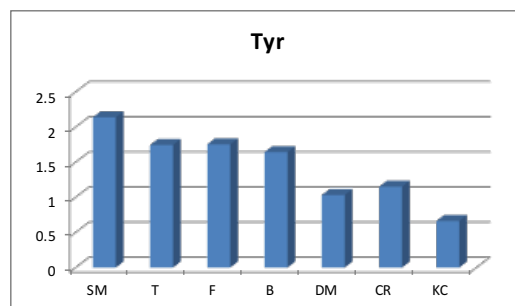
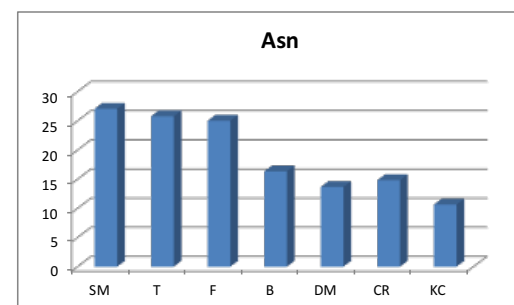
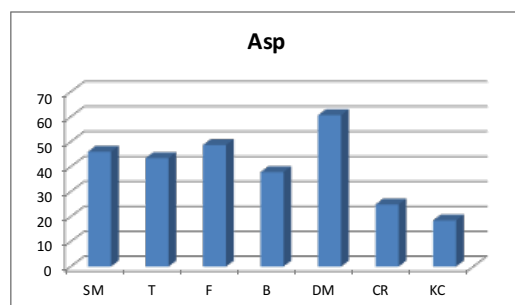
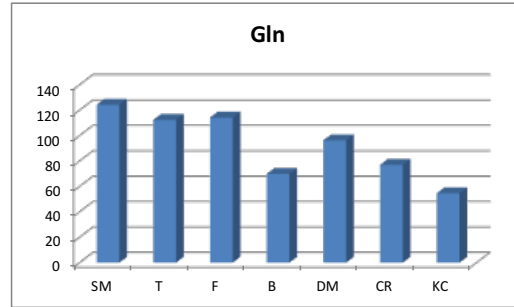
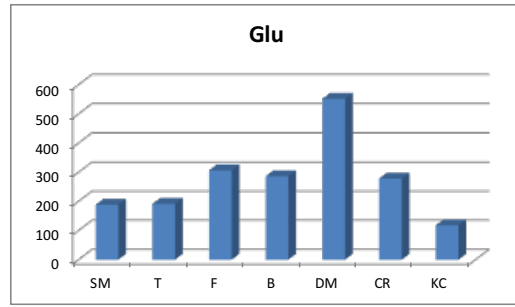
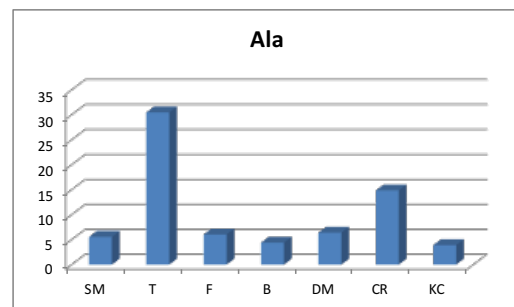
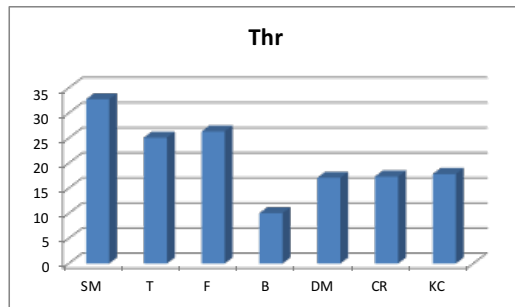
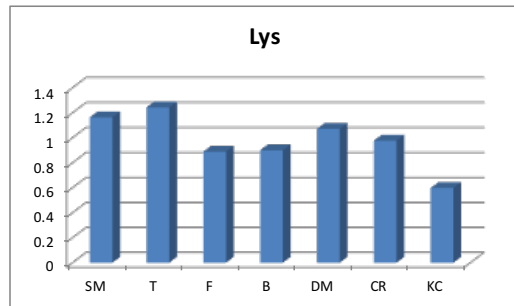
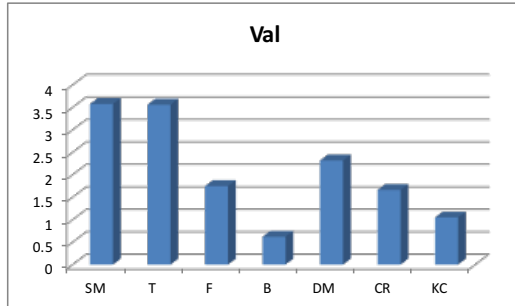
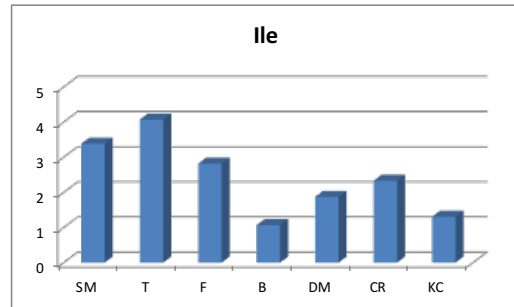
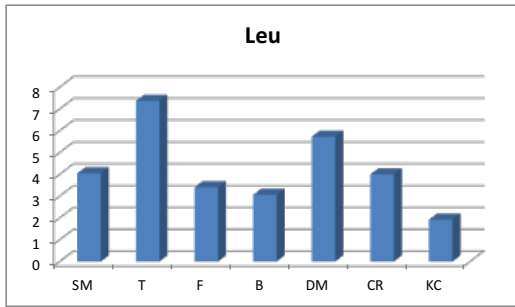


Figure 4.11. ^1H NMR spectrum (600 MHz, 300K) of the hydroalcoholic extract (phosphate buffer in D_2O) of San Marzano mature fruits extract.

1D and 2D NMR experiments confirmed the assignment of ^1H spectra from hydroalcoholic extracts solubilized in D_2O phosphate buffer (Sobolev, Segre & Lamanna, 2003; Sanchez Perez et al., 2010; Hohmann et al., 2014). In the high field 0.50-3.60 ppm spectral region minor signals belonging to the aliphatic groups of amino acids (alanine, asparagine, aspartate, γ -aminobutyrate, glutamine, glutamate, isoleucine, leucine, lysine, valine, threonine), malic acid and citric acid are observable. In the 3.15-6.95 ppm spectral region signals belonging to choline, malic acid, tyrosine, uridine and carbohydrates (glucose and fructose) are observable. In the low field 7.00-9.15 ppm signal belonging to aromatic and heteroaromatic amino acids (tryptophan, phenylalanine and histidine), adenosine, formic acid and trigonelline can be found.

The proton spectra of the hydroalcoholic extracts for each tomato variety appear to be conservative from a qualitative point of view since the same metabolites are present in all the samples examined. From a quantitative point of view, differences can be observed due to the different concentrations of the metabolites.

Figure 4.12 shows the histograms comparing the quantities of metabolites present in the seven varieties of tomatoes hydroalcoholic extracts (SM: San Marzano, T: Torpedino, F: Fiaschetta, B: Bamano, DM: Dolce Miele, CR: Confettino Rosso, KC: King Creole).



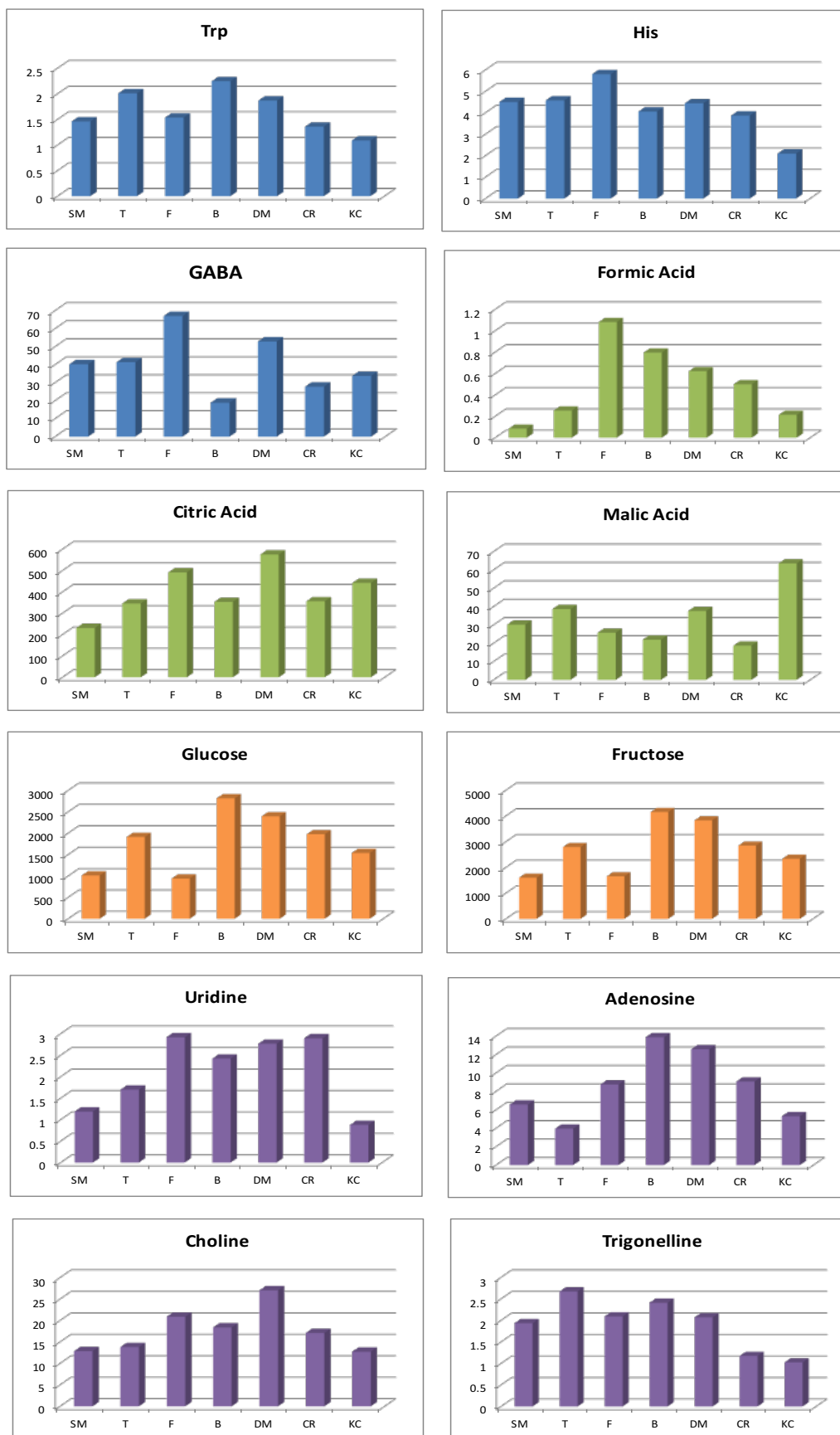


Figure 4.12. Histograms comparing the quantities of metabolites present in the seven varieties of tomatoes hydroalcoholic extracts (SM: San Marzano, T: Torpedino, F: Fiaschetta, B: Bamano, DM: Dolce Miele, CR: Confettino Rosso, KC: King Creole). Data shown are expressed as mg/100g.

San Marzano, Torpedino and Fiaschetta varieties showed a higher level of most of aminoacids (valine, isoleucine, glutamine, asparagine and tyrosine) than the others. Moreover, Torpedino resulted to be the variety richer of some essential amino acids (Leu, Ile, Lys, Val and Phe) than others. In particular, the content of Ala in Torpedino variety is about 30mg/100 g against its lower contents in other varieties (between 4mg/100g and 14mg/100g). San Marzano variety is rich in Asp (27.1mg/100g), Tyr (2.1mg/100g), Gln (124.3mg/100g), Val (3.6mg/100g) and of the essential amino acid Thr (32.7mg/100g). Dolce Miele is the richest variety in Glu (551.7mg/100g) and Asp (60.7mg/100g). Fiaschetta is the variety having the highest content of His (5.8mg/100g) and GABA (67.0mg/100g). Bamano is the variety having the highest Trp content (2.2mg/100g) and the lowest GABA content (18.9mg/100g). Confettino Rosso and King Creole are the varieties most deficient of amino acids.

Among organic acids, Dolce Miele variety showed the highest content of citric acid (575.0mg/100g) whereas Torpedino and King Creole varieties showed the highest content of malic acid (38.6mg/100g and 37.6mg/100g, respectively). Formic acid levels are low all over the varieties, being lower than 1.0mg/100g, except for Fiaschetta variety (1.1mg/100g).

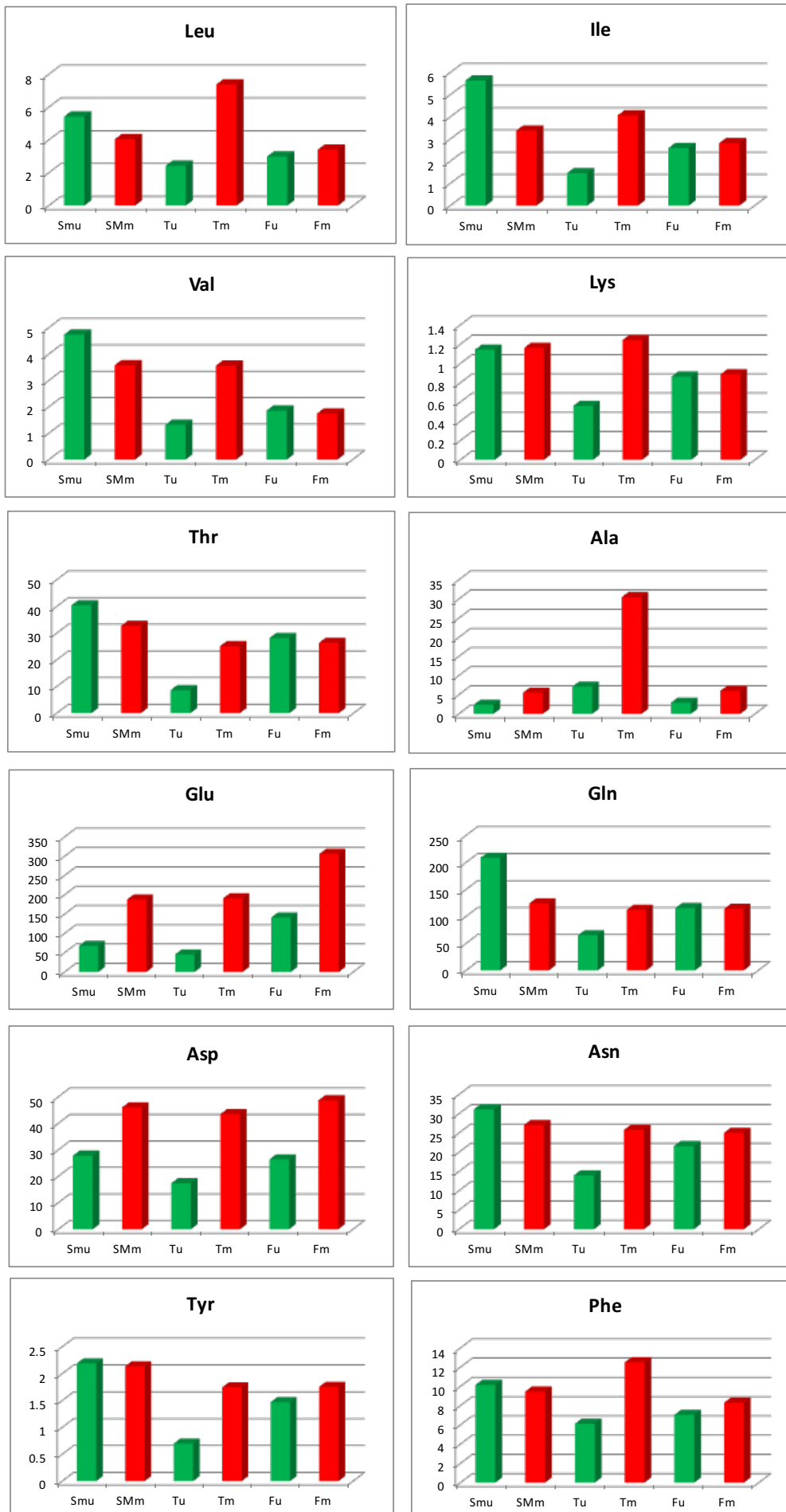
Dolce Miele and Bamano are the richest varieties in glucose (2.4g/100g and 2.8g/100g, respectively) and fructose (3.8g/100g and 4.2g/100g) whereas the Fiaschetta has the lowest quantity of glucose (940.8mg/100g) and fructose (1.7g/100g).

Regarding the content of the other metabolites, the concentration of choline results in a higher in Dolce Miele variety (27.0mg/100g). The uridine content ranges from 1mg/100g to 3mg/100mg in all the varieties, except for King Creole variety that has lower than 1mg/100 g of uridine. The amount of adenosine is the highest in Bamano variety (13.9mg/100g) whereas it is the lowest in Torpedino (3mg/100g). Trigonelline content ranges from 1.0mg/100g in King Creole to 2.7mg/100g in Torpedino.

In conclusion, San Marzano, Torpedino and Fiaschetta varieties have a higher amino acid content than other ones, but a lower content of carbohydrates, whereas in the other four

varieties there is an opposite trend. In particular, Bamano and Dolce Miele are the richest varieties in carbohydrates, followed by Confettino Rosso and King Creole. The tomato varieties having a higher content of organic acids are Dolce Miele, which is rich in citric acid, and King Creole, which is rich in malic acid.

Figure 4.13 shows the histograms comparing the quantities of metabolites present in hydroalcoholic extracts of three varieties of both unripe and mature tomatoes (SMu: San Marzano unripe, SMm: San Marzano mature, Tu: Torpedino unripe, Tm: Torpedino mature, Fu: Fiaschetta unripe, Fm: Fiaschetta mature).



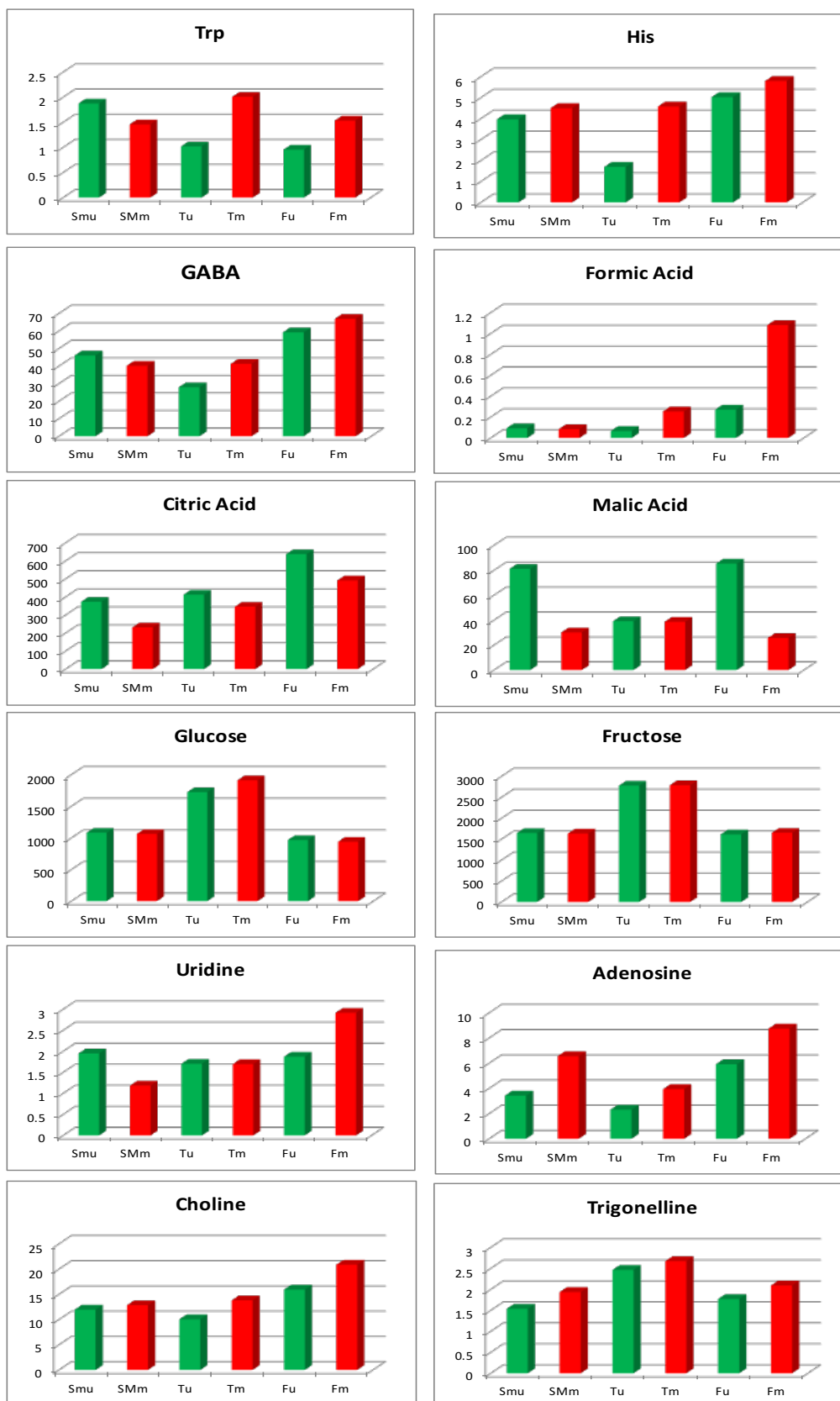


Figure 4.13. Histograms comparing the quantities of metabolites present in hydroalcoholic extracts of three varieties of both unripe and mature tomatoes (SMu: San Marzano unripe, SMm: San Marzano mature, Tu: Torpedino unripe, Tm: Torpedino mature, Fu: Fiaschetta unripe, Fm: Fiaschetta mature). Data shown are expressed in mg/100g.

By comparing unripe and mature fruits of Torpedino variety, it can be noted that the concentration of amino acids tends to increase according to maturation. A similar but less evident trend can be noticed also in Fiaschetta variety whereas only the concentration of some amino acids (Ala, Asp, Glu and His) increases according the maturation for San Marzano variety. The concentration of sugars (glucose and fructose) remains more or less constant during the maturation for each of the three varieties. As regards the acid content, the quantities of malic acid and citric acid decrease during the maturation, whereas the concentration of formic acid increases, especially for Fiaschetta variety. For other compounds, such as choline, uridine, adenosine and trigonelline, an increase of their concentration is observed during the maturation.

Analysis of tomato organic extracts. Figure 4.14 shows the ^1H NMR spectrum (600 MHz) of the organic extract ($\text{CDCl}_3/\text{CD}_3\text{OD}$ 2:1 v/v) of San Marzano mature fruits.

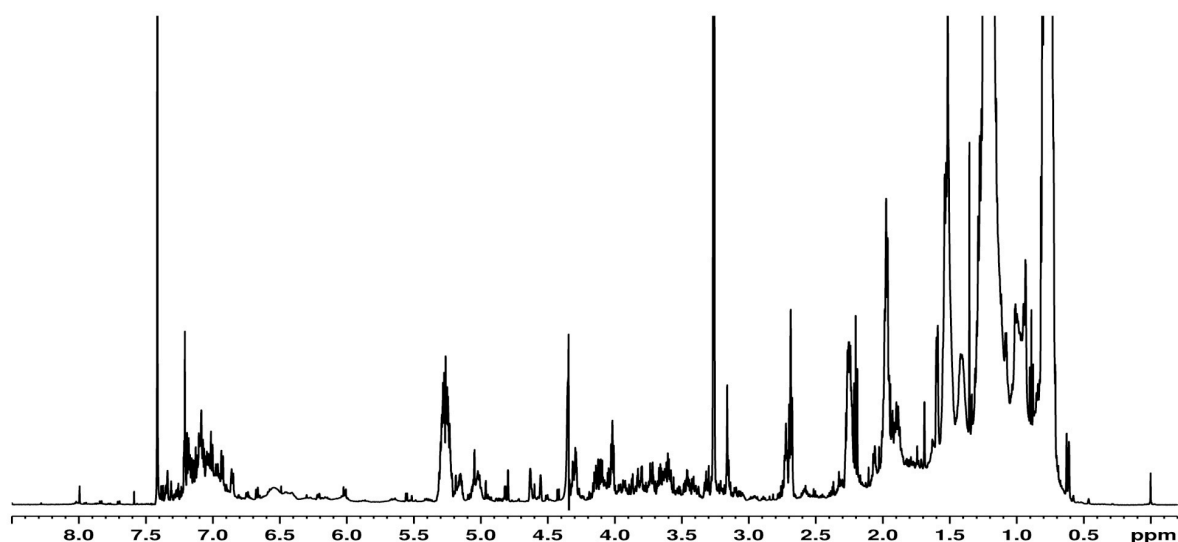


Figure 4.14. ^1H NMR spectrum (600 MHz, 300K) of the organic extract ($\text{CDCl}_3/\text{CD}_3\text{OD}$ 2:1 v/v) of San Marzano mature fruits.

By using literature data (Sobolev et al., 2005; Masetti et al., 2017), reference standards and two-dimensional NMR spectra (TOCSY, HSQC, HMBC), different metabolites

were assigned in the organic extracts of tomatoes. Table 4.10 shows the chemical shift values of the metabolites identified in spectra of organic fraction.

Table 4.10. Summary of the metabolites identified in the 600.13 MHz ^1H spectra (27 °C) of the organic extract from tomatoes.

| Compound | Assignment | ^1H (ppm) | Multiplicity: $J(\text{Hz})$ | ^{13}C (ppm) |
|--|--|---------------------|------------------------------|-----------------------|
| Oleic fatty chain (C18:1 $\Delta 9$) | CH ₂ -1 | | | 173.85 |
| | CH ₂ -2 | 2.27 | | 35.2 |
| | CH ₂ -3 | 1.53 | | 26.0 |
| | CH ₂ -4,7 | 1.35 | m | 29.4, 29.9 |
| | CH ₂ -8,CH ₂ -11 | 2.02 | m | 27.7, 27.8 |
| | CH=CH 9,10 | 5.28 | | 131.1 |
| | CH ₂ -12,15 | 1.30 | m | 30.2, 30.5 |
| | CH ₂ -16 | 1.28 | m | 30.4 |
| | CH ₂ -17 | 1.26 | m | 23.7 |
| | CH ₂ -18 | 0.79 | t [6.9] | 14.9 |
| Linoleic fatty chain (C18:3 $\Delta 9,12$) | CH ₂ -1 | | | 28.0 |
| | CH ₂ -2 | 2.25 | | |
| | CH ₂ -3 | 1.54 | | 35.1 |
| | CH ₂ -4,7 | 1.28 | | 25.8 |
| | CH ₂ -8 | 2.00 | q [6.7] | |
| | CH-9 | 5.29 | m | 130.8 |
| | CH-10 | 5.26 | m | 128 |
| | CH ₂ -11 | 2.72 | t [6.8] | |
| | CH-12 | 5.27 | m | 128 |
| | CH-13 | 5.29 | m | 128 |
| | CH ₂ -14 | 2.00 | q [6.7] | 128 |
| | CH ₂ -15 | 1.28 | m | 26.5 |
| | CH ₂ -16 | 1.29 | m | |
| | CH ₂ -17 | 1.23 | m | 21.3 |
| | | CH ₃ -18 | 0.80 | t [6.8] |
| Linolenic fatty chain (C18:2 $\Delta 9,12,15$) | CH ₂ -1 | | | 173.9 |
| | CH ₂ -2 | 2.25 | | 35.2 |
| | CH ₂ -3 | 1.54 | | 25.9 |
| | CH ₂ -4 | 1.29 | | 30.1 |
| | CH ₂ -5,7 | 1.33 | | 29.9 |
| | CH ₂ -8 | 2.00 | | 28.1 |
| | CH-9 | 5.30 | | 131.0 |
| | CH-10 | 5.27 | | 128.9 |
| | CH ₂ -11 | 2.73 | t [5.9] | 26.5 |
| | CH-12, CH ₂ -13 | 5.30 | | 131.1 |
| | CH ₂ -14 | 2.73 | t [5.9] | 25.6 |
| | CH-15 | 5.28 | | 129.2 |
| | CH-16 | 5.30 | | 131.2 |
| | CH ₂ -17 | 2.00 | pentet | 21.6 |

| | | | | |
|------------------------|----------------------------------|------------|---------------------------------|-------|
| | CH ₂ -18 | 0.81 | t [7.5] | 14.9 |
| Triacylglycerol moiety | CH ₂ sn 1,3 | 4.33;4.15 | dd [4.0;12.0]; dd [6.2;11.9] | 63.1 |
| | CH sn 2 | 5.26 | m | 70.2 |
| Saturated fatty acids | CH ₂ -1 | | | 173.9 |
| | CH ₂ -2 | 2.32 | | 34.8 |
| | CH ₂ -3 | 1.60 | m | 26.5 |
| | CH ₂ (n-3) | 1.30 | m | 30.2 |
| | CH ₂ (n-2) | 1.27 | m | 30.4 |
| | CH ₂ (n-1) | 1.25 | m | 23.6 |
| | CH ₃ | 0.81 | t [6.9] | 14.9 |
| Free fatty acids | CH ₂ -1 | | | 178.4 |
| | CH ₂ -2 | 2.29 | m | 34.9 |
| | CH ₂ -3 | 1.60 | m | 26.2 |
| β-Sitosterol | CH ₃ -18 | 0.68 | s | |
| Stigmasterol | CH ₃ -18 | 0.70 | s | |
| Squalene | CH ₃ -a | 1.68 | | |
| | CH ₃ -b | 1.53 | | 16.9 |
| | CH-c | 5.03 | | 125.4 |
| | CH ₂ -e | 2.00 | | 28.4 |
| | CH ₂ -f | 1.91 | | 40.7 |
| P-choline | CH sn2 | 5.16 | | 70.9 |
| | CH ₂ sn1 | 4.30, 4.10 | | 63.2 |
| | CH ₂ sn3 | 4.02 | | 65.3 |
| | N(CH ₃) ₃ | 3.17 | | 55.1 |

Figure 4.15 shows the histograms comparing the quantities of metabolites present in the seven varieties of tomatoes organic extracts (SM: San Marzano, T: Torpedino, F: Fiaschetta, B: Bamano, DM: Dolce Miele, CR: Confettino Rosso, KC: King Creole).

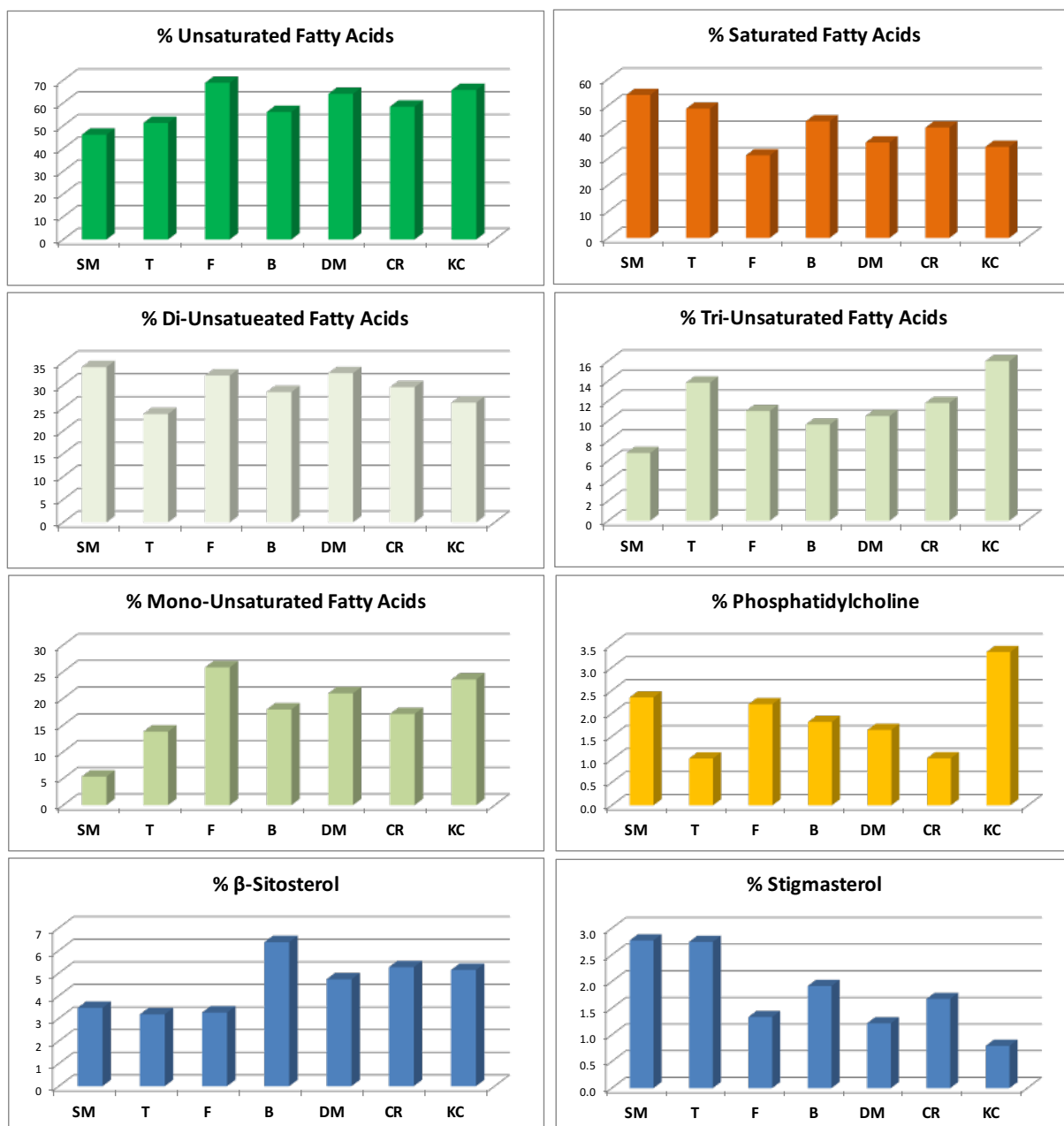


Figure 4.15. Histograms comparing the quantities of metabolites present in the seven varieties of tomatoes organic extracts (SM: San Marzano, T: Torpedino, F: Fiaschetta, B: Bamano, DM: Dolce Miele, CR: Confettino Rosso, KC: King Creole). Data shown are expressed in %.

According to the histograms, it can be noted that:

- I. the amount of β -sitosterol changes from 3.17% (Torpedino) to 6.36% (Bamano), while stigmasterol ranges from 0.79% in King Creole variety to 2.77% in San Marzano variety;
- II. the total concentration of unsaturated fatty acids varies from 46.03% in San Marzano variety to 68.83% in Fiaschetta variety;
- III. the content of mono-unsaturated fatty acids (oleic acid) changes from 5.34% in San Marzano variety to 25.79% in Fiaschetta variety;
- IV. the concentration of di-unsaturated fatty acids (linoleic acid) ranges from 23.66% (Torpedino) to 33.91% (San Marzano);
- V. the amount of tri-unsaturated fatty acids (linolenic acid) ranges from 6.77% in San Marzano variety to 15.96% in King Creole variety;
- VI. the amount of phosphatidylcholine varies from 1.021% (Fiaschetta) to 3.33% (King Creole).

Figure 4.16 shows the histograms comparing the quantities of metabolites present in organic extracts of three varieties of both unripe and mature tomatoes (SMu: San Marzano unripe, SMm: San Marzano mature, Tu: Torpedino unripe, Tm: Torpedino mature, Fu: Fiaschetta unripe, Fm: Fiaschetta mature).

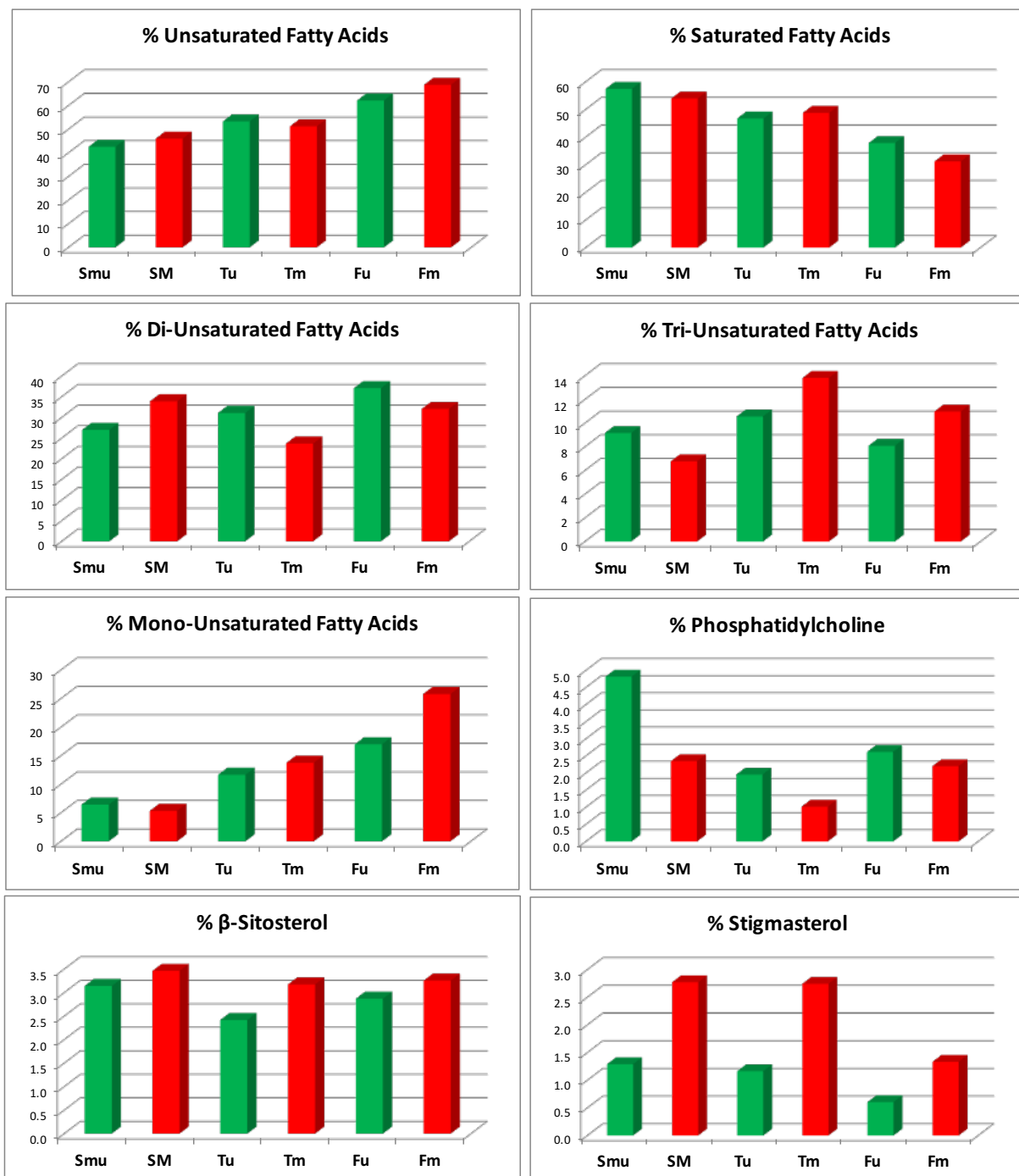


Figure 4.16. Histograms comparing the quantities of metabolites present in organic extracts of three varieties of both unripe and mature tomatoes (SMu: San Marzano unripe, SMm: San Marzano mature, Tu: Torpedino unripe, Tm: Torpedino mature, Fu: Fiaschetta unripe, Fm: Fiaschetta mature). Data shown are expressed in %.

From the interpretation of the histograms, it can be observed that:

- I. the level of sterols increases during maturation for each variety;
- II. the percentage of total unsaturated fatty acids increases slightly during the maturation only for San Marzano and Fiaschetta varieties;
- III. the percentage of mono-unsaturated and tri-unsaturated fatty acids (oleic acid and linolenic acid, respectively) decreases during the maturation of the San Marzano tomatoes whereas it increases for Torpedino and Fiaschetta varieties;
- IV. the percentage of di-unsaturated fatty acids (linoleic acid) decreases during the maturation only for Torpedino variety;
- V. the concentration of total saturated fatty acids (palmitic acid and stearic acid) increases only for Torpedino variety;
- VI. the levels of phosphatidylcholine always decrease from unripe to mature fruits independently of varieties.

4.4.4 References

- Hohmann, M., Christoph, N., Wachter, H., Holzgrabe U., 2014. ¹H-NMR Profiling as an approach to differentiate conventionally and organically grown tomatoes. *J. Agric. Food Chem.*, 62, 8530-8540.
- Masetti O., Ciampa A., Nisini L., Sequi P., Dell'Abate M.T., 2017. A multifactorial approach in characterizing geographical origin of Sicilian cherry tomatoes using ¹H-NMR profiling. *Food Res. Int.* 100, 623-630.
- Mounet, F., Lemaire-Chamley, M., Maucourt, M., Carbasson, C., Giraudel, J.L., Deborde, C., Lessire, R., Gallusci, P., Bertrand, W., Gaudillefé, M., Rothan, C., Rolin, D., Moing, A., 2007. Quantitative metabolic profiles of tomato flesh and seeds during fruit development: contemporary analysis with ANN and PCA. *Metabolomics* 3, 273-288.
- Musse, M., Quellec, S., Devaux, M. F., Cambert, M., Lahaye, M., Mariette, F., 2009. An investigation of the structural aspects of the tomato fruit by means of quantitative nuclear magnetic resonance imaging. *Magn. Reson. Imaging* 27, 709-719.
- Sánchez Perez, E.M., Iglesias, M.J., López Ortiz, F., Sánchez Perez, I., Martínez Galera, M., 2010. Study of the suitability of HRMAS NMR for metabolic profiling of tomatoes: application to tissue differentiation and fruit ripening. *Food Chem.* 122, 877-887.
- Sobolev, A.P., Segre, A.L., Lamanna R., 2003. Proton high-field NMR study of tomato juice. *Magn. Reson. Chem.* 41, 237-245.
- Sobolev, A.P., Brosio, E., Gianferri, R., Segre A.L., 2005. Metabolic profile of lettuce leaves by high-field NMR spectra. *Magn. Reson. Chem.* 43, 625-638.
- Sobolev, A.P., Mannina, L., Capitani, D., Sanzò, G., Ingallina, C., Botta, B., ... & Di Sotto, A., 2018. A multi-methodological approach in the study of Italian PDO "Cornetto di Pontecorvo" red sweet pepper. *Food Chem.* 255, 120-131.
- Tiziani, S., Schwartz, S.J., Vodovotz, Y., 2006. Profiling of carotenoids in tomato juice by one- and two-dimensional NMR. *J. Agric. Food Chem.* 54, 6094-6100.
- Vallverdu-Queralt, A., Medina-Remoñ, A., Casals-Ribes, I., Amat, M., Lamuela-Raventós, R.M., 2011. A metabolomic approach differentiates between conventional and organic ketchups. *J. Agric. Food Chem.* 59, 11703-11710.

4.5 Hemp and processing products

Cannabis sativa L., better known as “industrial hemp”, has been traditionally cultivated around the world, and in particular in Europe, for many decades, as source of textile fibre for the production of dresses, fishing nets, paper, canvas, etc. Italy was both the second world producer of hemp (just behind Russia) with an average annual world production of about 550000 tons, and the largest exporter, with about 47400 tons. However, during the '70s, *Cannabis sativa* L. cultivation disappeared due to the association with narcotic *Cannabis Indica* (marijuana), characterized by a high content of Δ^9 -tetrahydrocannabinol (THC), a psychotropic compound contained in the inflorescences. In Italy, according to a strict application of the “Legge Cossiga” (L. 22-12-1975 n. 685, “Disciplina degli stupefacenti e sostanze psicotrope. Prevenzione, cura e riabilitazione dei relativi stati di tossicodipendenza.”) by the judiciary and law enforcement agencies, hemp varieties could be cultivated only in enclosed fields under continuous surveillance and with night lighting. Those conditions were practically impossible to be respected according to the available funds and, consequently, all the hemp varieties including the traditional varieties of Italian origin celebrated all over the world disappeared from the territory.

After almost 30 years, the European Union published a Regulation (EC No 1251/99 and subsequent amendments), reintroducing the cultivation of some varieties of *Cannabis sativa* L. for fibre production. The varieties of *Cannabis sativa* allowed for cultivation within the European Union are listed in constantly update Annex XII art. 7bis par. 1 of the EC Reg. 2860/2000. These varieties are characterized by a THC content lower than 0.2% w/w in the inflorescences. Actually, it is absolutely necessary to use seeds certified by an Authorized Body: penal sanctions occur if this limit is exceeded.

The hemp rediscovery in Italy is closely related to the “Circolare del Ministero delle Politiche Agricole” (“Direzione Generale delle Politiche Agricole ed Agroindustriali

Nazionali”) of 2 December 1997, which defines the methods to be followed by the farmers in order to prevent confusion with the drug crops.

The introduction on the Italian market of seed belonging to varieties from foreign countries, selected in climatic conditions very different from the Mediterranean ones, needs a careful evaluation to avoid the spreading of poorly productive and unsuitable materials.

Beside the interest for textile uses, non-textile applications, related to the use of the other part of the plants, have been exploiting during the last fifteen years, discovering the versatile characteristic of this natural resource. Nowadays literature concerning hemp is exponentially growing and involves different aspects of scientific academia: from agronomical to pharmaceutical point of view (Campiglia, Radicetti & Mancinelli, 2017; Amaducci et al, 2015; Croxford et al., 2008; Appendino et al., 2008; Burstein, 2015; Nissen et al., 2010; Fishedick et al., 2010; Nalli et al., 2018), from bioenergetic to raw building material (Kreuger et al., 2011; Ingrao et al., 2015; Lühr et al., 2018), from cosmetics to food chemistry.

In this context the project entitled “La Canapa industrial: sviluppo e valorizzazione di una nuova filiera agroalimentare ecosostenibile” funded by Lazio region wants to fill the "gap" of knowledge created on the hemp chain in recent decade. The project proposes a research line to select high nutritional value varieties with a low THC content that can be reintroduced in Lazio territory. The project also aims to suggest correct cultivation techniques for the new requirements of environmental sustainability. The industrial hemp, in fact, is well suited to the pedo-climatic conditions present in the Lazio region and thanks to the characteristics of rusticity, easy cultivation, anti-erosion and repellent capacity, could be reintroduced as a renewal crop, with the aim of increase soil fertility, provide economically sustainable fibre and grain production and derivation products. Within the project, hemp raw material namely seeds and inflorescences have been analysed appropriately with both traditional and innovative analytical methods to lead to select hemp varieties that respond

positively to the pedo-climatic conditions of the areas providing a product with high nutritional value. The study wants to identify the varieties with an optimal metabolite profile, for instance with a considerable content of polyunsaturated fatty acids, in particular linoleic (omega-6) and α -linolenic (omega-3) fatty acids in a 3:1 ratio (optimal for human nutrition), and/or with a high protein content and/or a considerable fibre content that helps to preserve the natural regularity of the intestine as well as the sense of satiety. In addition, the study of the overall metabolic profile with advanced analytical techniques will increase and complete the degree of knowledge of hemp matrix. The return to the canapiculture have taken place on completely different bases than in the past, when the only salable product was the long fibre for the creation of fabrics and ropes. From the point of view of the possibilities of use, hemp is instead, thanks to its versatility, one of the most important herbaceous species among those cultivated. Therefore, despite being a traditional culture, hemp is helpful for a series of innovative uses that identify it as one of the most promising herbaceous crops in the national agricultural scenario. In this sense, the possibilities of economic integration are, potentially, innumerable and can involve companies operating in many sectors. In fact, in addition to the traditional use of fibre in the textile industry, nowadays new uses, namely in bio-building, in the chemical industry, in the food industry through the use of oil and flour obtained from hemp seeds (Korus et al., 2017; Frassinetti et al., 2018; Citti et al., 2018; Da Porto, Decorti & Tubaro, 2012; Aladic et al., 2015; Yu, Zhou & Parry, 2005; Oomah et al., 2002; Montserrat-delaPaz et al., 2014; Mikulcová et al., 2017) and in the production of clean energy, are emerging.

4.5.1 Inflorescences (1st case study)

4.5.1.1 Material and methods

Fresh flowering aerial parts from Ferimon, USO31 and Felina32 cultivars of *Cannabis sativa* L., belonging to CBD-rich chemotype (Chandra et al., 2017), were provided by the “Canapa Live” cultural association. These varieties were cultivated in some areas (Santa Severa Nord, Passo di Viterbo and Farnesiana, Allumiere) of Lazio region (Central Italy). The hemp inflorescences were harvested at four developmental stages: (1st stage) 13th June 2016, (2nd stage) 12th July 2016, (3rd stage) 28th July 2016 and (4th stage) 1st September 2016. Fresh hemp plant material was sampling and stored at -20°C.

Stems and seeds were removed from the freezed inflorescences (15 inflorescences for each sample). The crop flowering aerial parts were powdered under liquid nitrogen to obtain a fine powder and subjected to Bligh-Dyer extraction.

Bligh-Dyer extraction adapted for hemp inflorescences was performed according to literature (Capitani et al., 2014). Solvents (3mL of methanol/chloroform mixture 2:1 v/v, 1mL of chloroform and 1.2 mL of pure water) were added to the powdered flowering aerial parts of *Canabis sativa* var. Ferimon, USO31 and Felina32 samples (1g). Successively, samples were preserved at 4°C for 40 minutes and then centrifuged at 4500 rpm for 15 minutes at 4°C. The upper hydroalcoholic phase and the lower organic phase were carefully separated. The pellets were re-extracted using half of the solvent volumes and the same procedure reported above was followed. The fractions of the first and second extractions were pooled. Hydroalcoholic and organic fractions were dried under a nitrogen flow at room temperature. The hydroalcoholic phase was additionally freeze dried. The dried phases were then stored at -20°C until the NMR analysis.

The dried organic fraction of each sample was dissolved in 0.7 mL of a CDCl₃/CD₃OD mixture (2:1 v/v) and then placed into a 5 mm NMR tube. Finally, the NMR

tube was flame-sealed. Conversely, the dried hydroalcoholic phase of each sample was solubilized in 0.7 mL 400 mM phosphate buffer/D₂O, containing a 2 mM solution of TSP as internal standard, and then transferred into a 5 mm NMR tube.

NMR spectra of all hydroalcoholic and organic extracts were recorded at 27 °C on a Bruker AVANCE 600 spectrometer operating at the proton frequency of 600.13 MHz and equipped with a Bruker multinuclear z-gradient 5 mm probe head. ¹H spectra were referenced to methyl group signals of TSP (δ = 0.00 ppm) in D₂O, and to the residual CHD₂ signal of methanol (set to 3.31 ppm) in CD₃OD/CDCl₃ mixture. ¹H spectra of hydroalcoholic extracts were acquired with 256 transients with a recycle delay of 5 s. The residual HDO signal was suppressed using a pre-saturation. The experiment was carried out by using 45° pulse of 6.68 μs, 32K data points. ¹H spectra of extracts in CD₃OD/CDCl₃ were acquired with 256 transients, recycle delay of 5 s and 90° pulse of 10 μs, 32K data points. The two-dimensional (2D) NMR experiments, such as ¹H-¹H TOCSY, ¹H-¹³C HSQC and ¹H-¹³C HMBC, were carried out under the same experimental conditions previously reported (Sobolev, Segre & Lamanna, 2003).

In order to evaluate the similarities or differences between samples the integrals of selected resonances in ¹H NMR spectra were measured. The intensity of 14 selected signals in hydroalcoholic extract, see Table 4.11, was measured using the Bruker TOPSPIN software and normalized with respect to the total sum of all integrals.

The intensity of 5 selected signals in organic extract, see Table 4.12, was also measured and normalized with respect to the resonance at 0.89 ppm, due to signal of Total Fatty Acids, normalized to 100. Results have been expressed in %.

The % values of monounsaturated and saturated fatty acids have been calculated using the following equation:

$$\%_{\text{MONO}} (I_{\text{MONO}}) = I_{\text{UNS}} - 2I_{\text{DI}} - 1.5I_{\text{TRI}} \quad (1)$$

$$\%_{\text{SAT}} = I_{\text{FA}} - 1.5I_{\text{DI}} - 0.75I_{\text{TRI}} - I_{\text{MONO}} \quad (2)$$

where I_{UNS} is the integral value of “Unsaturated Fatty Acids” (signal at 5.33 ppm), I_{DI} is the integral value of “Di-Unsaturated Fatty Acids” (signal at 2.72 ppm), I_{TRI} is the integral value of “Tri-Unsaturated Fatty Acids” (signal at 2.77 ppm), I_{FA} is the integral value of “Total Fatty Acids” (signal at 0.89 ppm). The integral value of Total Fatty Acids has been fixed at 100.

Table 4.11. Compounds, and relative signals (ppm), selected for quantitative analysis in the hydroalcoholic extracts.

| Compounds | ppm |
|-------------------|------------|
| Ile | 1.02 |
| Val | 1.05 |
| Thr | 1.34 |
| Ala | 1.49 |
| Pro | 2.03 |
| GABA | 2.30 |
| Succinic Acid | 2.41 |
| Citric Acid | 2.56 |
| Asp | 2.81 |
| Asn | 2.89 |
| Choline | 3.20 |
| Malic Acid | 4.30 |
| α -Glucose | 5.25 |
| Sucrose | 5.42 |

Table 4.12. Compounds, and relative signals (ppm), selected for quantitative analysis in the organic extracts.

| Compounds | ppm |
|-----------------------------|------|
| β -Sitosterol | 0.65 |
| Di-Unsaturated fatty acids | 2.72 |
| Tri-Unsaturated fatty acids | 2.77 |
| Triglycerides | 4.12 |
| Unsaturated fatty acids | 5.33 |

4.5.1.2 Results and Discussion

NMR untargeted analysis of hydroalcoholic and organic extracts provided the metabolic fingerprint of each hemp cultivar (Table 4.13 and 4.14). Here, the metabolic profile of the hydroalcoholic and organic extracts from June to September period will be discussed separately for each cultivar.

Ferimon variety

Organic Acids. In the ^1H spectrum of Ferimon inflorescences hydroalcoholic extracts Acetic, Succinic, Citric, Malic, Formic and Fumaric acids were identified (Table 4.13). However, the quantification and, thus, the monitoring of the concentration over the season was possible only for three of them (Figure 4.16A), Succinic, Citric and Malic acids because of the bad resolution of others signals in the ^1H spectra. These three acids showed a complete different trend over the season. Succinic Acid reached the highest concentration in June, at the early flowering, then decreased over the season and reach the minimum value just before the threshing. Citric Acid showed the opposite trend: its concentration increased over

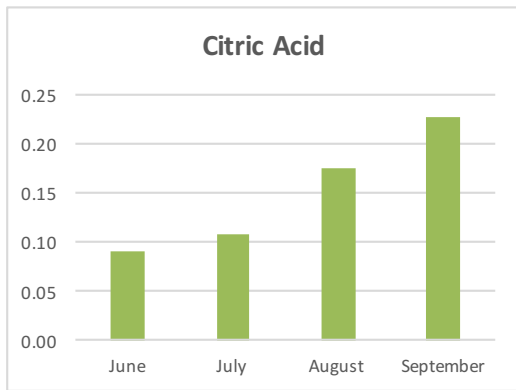
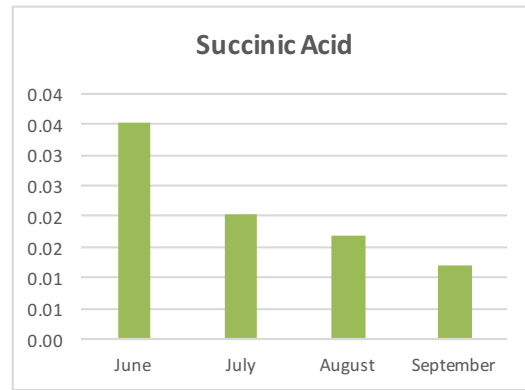
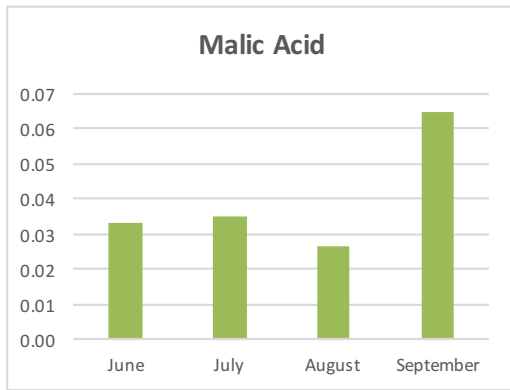
the season. Finally, Malic Acid content seemed to stay constant for the first two harvesting periods and then dropped down to drastically increase in September.

Sugars. Different sugars were identified in the hydroalcoholic fraction of Ferimon inflorescence extracts. The curve chart (Figure 4.16B) showed Glucose and Sucrose concentration increased in the first harvesting period (July), but while Glucose stayed constant until the threshing, Sucrose content decreased over the season.

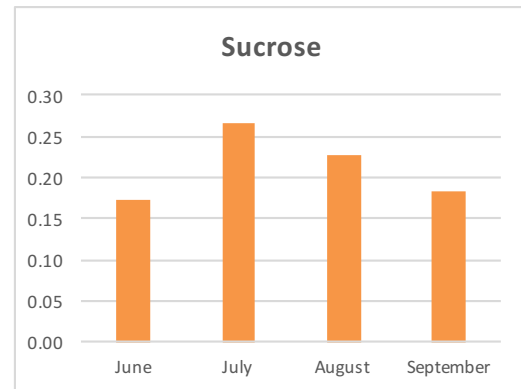
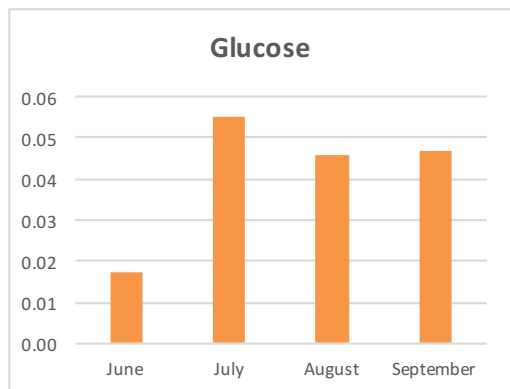
Free Amino Acids. Several amino acids have been identified, as showed in Table 4.13. Among all, 8 out of 15 were monitored through the season (Figure 4.16C). Ile, Val and Pro showed a similar trend, as their content is high at the first harvesting period (June), drastically dropped down at the second one and it was more or less constant over the rest of the season. Thr content slowly decreased during the harvesting time. GABA and Asn slowly increased during the season while Asp increased rapidly in July and slowly decreased over the rest of the period. Ala is the only amino acid showing a fluctuating behaviour.

Miscellaneous compounds. In the extracts of Ferimon inflorescence two nucleosides, Uridine and Adenosine, the alkaloid Trigonelline, and Choline (Table 4.13) were identified. It was possible to monitor the trend of concentration just for the last compound because of the good spectral resolution of Choline compared to other signals ones (Figure 4.16D). Choline showed a rapid increase in the first period (July) followed by a slowly decrease over the rest of the season.

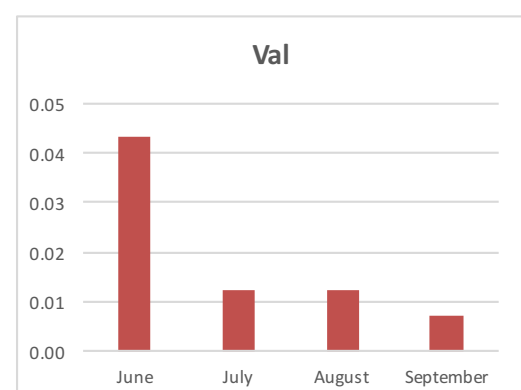
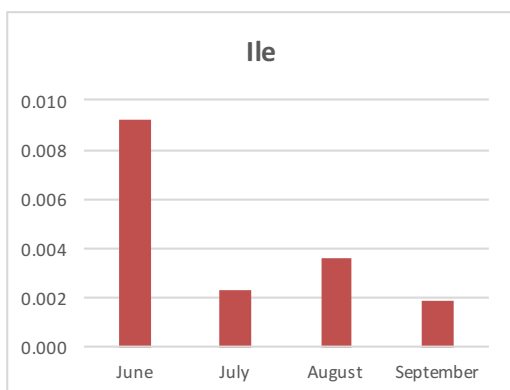
A



B



C



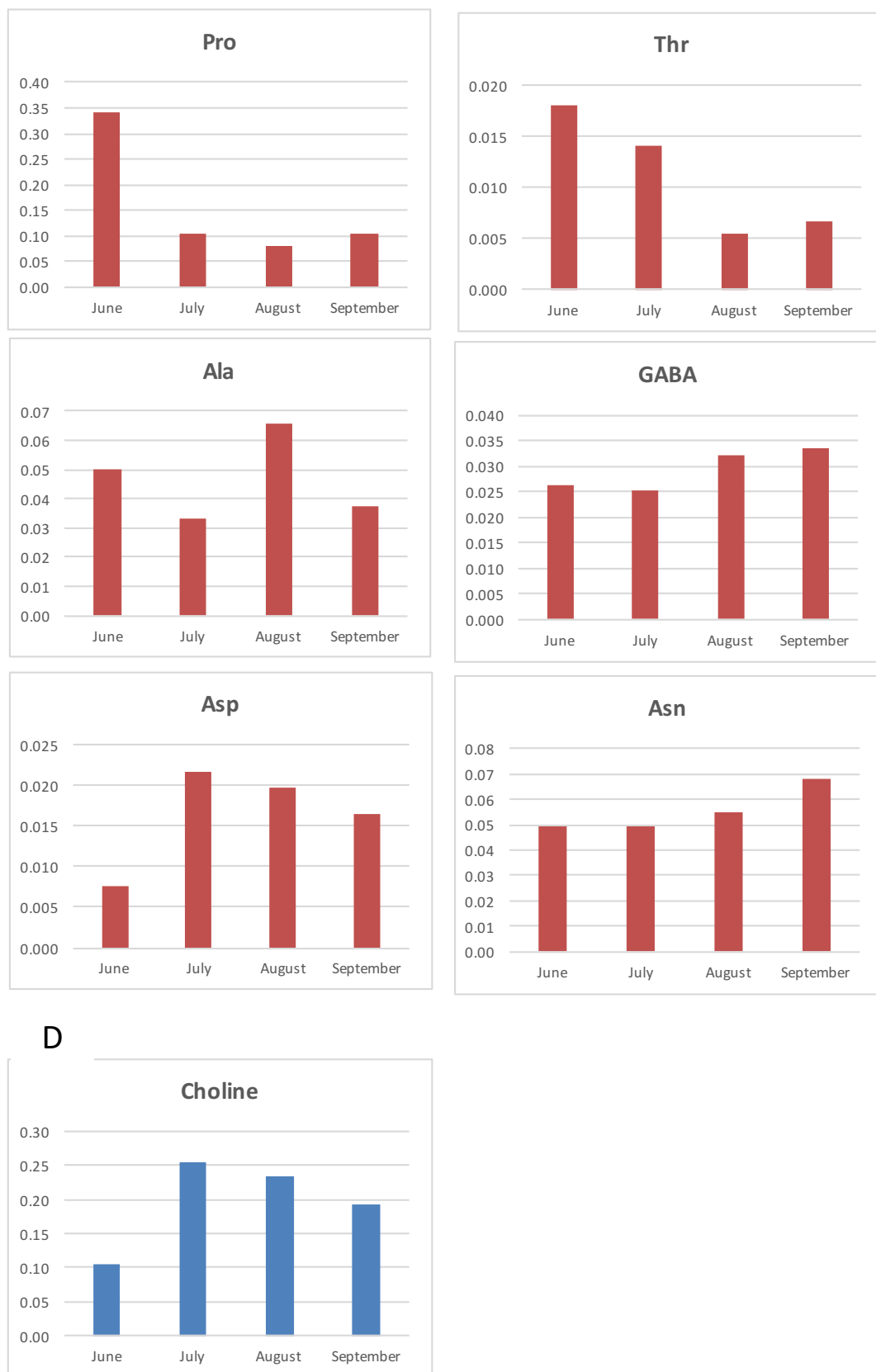


Figure 4.16. Histograms of main A) Organic acids, B) Sugars, C) Amino Acids, and D) Miscellaneous compounds identified in hydroalcoholic extracts of Femenon inflorescences over the season. Data shown are expressed as molecular abundance.

Organic fraction. In the organic extracts several lipids were identified (Table 4.14). Regarding the quantification and the evaluation of the trend of concentrations during the flowering period, as shown in Figure 4.17, Total Unsaturated and Saturated Fatty Acids showed the opposite trend: the first ones kept its content constant until July, then increased in August and stayed at the same level in September. The second ones showed higher levels at the beginning of flowering, which stayed constant until July, followed by a decrease in August. Analogously, β -Sitosterol and Triglycerides contents were characterized by opposite trends. β -Sitosterol level showed a slowly decrease over the season whereas the amount of triglycerides gradually increased to the maximum just at the end of flowering. Mono-Unsaturated Fatty Acids and, above all, Di-Unsaturated Fatty Acids concentrations were very low in June and July but then increased in August and September. Tri-Unsaturated Fatty Acids contents increased from June to July and then constantly dropped down until September.



Figure 4.17. Histograms of lipid fraction of Ferimon inflorescences organic extracts. Data shown are expressed in %.

Table 4.13. Summary of the metabolites identified in the 600.13 MHz ^1H spectra of the hydroalcoholic extracts of *Cannabis sativa* L. inflorescences (and hempseed flour samples).

| Compound | Assignment | ^1H (ppm) | Multiplicity [J(Hz)] | ^{13}C (ppm) |
|--|--|-----------------------|-------------------------|--------------------------|
| <i>Carbohydrates</i> | | | | |
| α -Glucose (α -Glc) | CH-1 | 5.27 | d [3.80] | 93.3 |
| | CH-2 | 3.56 | | 72.8 |
| | CH-3 | 3.73 | | 73.9 |
| | CH-4 | 3.42 | | 70.7 |
| | CH-5 | 3.84 | | 72.7 |
| | CH2-6,6' | 3.86; 3.78 | | 61.6 |
| β -Glucose (β -Glc) | CH-1 | 4.66 | d [8.0] | 96.9 |
| | CH-2 | 3.26 | dd [9.37; 7.99] | 75.2 |
| | CH-3 | 3.50 | | 76.8 |
| | CH-4 | 3.43 | dd [9.02; 9.68] | 70.7 |
| | CH-5 | 3.47 | | 76.9 |
| | CH2-6,6' | 3.90; 3.74 | | 61.8 |
| β -D-Fructofuranose (β -FF) | CH2-1,1' | 3.61; 3.57 | | 63.8 |
| | CH-3 | 4.12 | | 76.5 |
| | CH-4 | 4.12 | | 75.5 |
| | CH-5 | 3.84 | | 81.7 |
| | CH2-6,6' | 3.82; 3.66 | | 63.4 |
| | α -D-Fructofuranose (α -FF) | CH-3 | 4.13 | |
| CH-5 | | 4.07 | | 82.4 |
| β -D-Fructopyranose (β -FP) | CH2-1,1' | 3.57; 3.73 | | 64.9 |
| | CH-3 | 3.82 | | 68.6 |
| | CH-4 | 3.90 | | 70.7 |
| | CH-5 | 4.01 | | 70.2 |
| | CH2-6,6' | 3.72; 4.04 | | 64.4 |
| | Sucrose | CH-1 (Glc) | 5.42 | d [3.77] |
| CH-2 | | 3.56 | | 72.3 |
| CH-3 | | 3.77 | | 73.7 |
| CH-4 | | 3.49 | | 70.3 |
| CH-5 | | 3.85 | | 73.4 |
| CH2-6 | | 3.83 | | 61.2 |
| CH2-1' (Fru) | | 3.69 | d [3.32] | 62.4 |
| C-2' | | | | 104 |
| CH-3' | | 4.23 | d[8.7] | 77.5 |
| CH-4' | | 4.06 | t[8.7] | 75 |
| CH-5' | | 3.91 | | 82.5 |
| CH2-6' | | 3.82 | | 63.4 |
| <i>Myo-Inositol</i> | | CH-1 | 4.08 | |
| | CH-2,5 | 3.55 | | 72.5 |
| | CH-3,6 | 3.63 | | 73.6 |
| | CH-4 | 3.29 | | 75.3 |
| <i>Raffinose</i> | CH-1 (Gal) | 5.01 | d [3.8] | 99.4 |
| | CH-2 | 3.85 | | |
| | CH-3 | 3.91 | | |
| | CH-4 | 4.03 | | |
| | CH-1 (Glc) | 5.44 | d [3.9] | |
| | CH-2 | 3.59 | | |
| CH-3 | 3.78 | | | |
| CH-5 | 4.06 | | | |

| | | | | |
|----------------------------|-----------|-------------|---------------------|-------|
| <i>α-Galactose (α-Gal)</i> | CH-1 | 5.26 | d [4.0] | |
| | CH-2 | 3.78 | | |
| | CH-3 | 3.83 | | |
| | CH-4 | 3.88 | | |
| | CH-5 | 4.08 | | |
| <i>β-Galactose (β-Gal)</i> | CH-1 | 4.60 | d [8.0] | 97.4 |
| | CH-2 | 3.51 | | |
| | CH-3 | 3.67 | | |
| | CH-4 | 3.95 | | |
| | CH-5 | 4.01 | | |
| | CH-6 | 3.78 | | |
| <i>Organic acids</i> | | | | |
| <i>Acetic acid</i> | CH3 | 1.93 | s | 24.6 |
| <i>Citric acid</i> | α,γ-CH | 2.56 | d [15.92] | 46.3 |
| | α',γ'-CH | 2.69 | | 46.3 |
| | β-C | | | 75.8 |
| | 1,5-COOH | | | 179.3 |
| | 6-COOH | | | 181.9 |
| <i>Formic acid</i> | HCOOH | 8.47 | s | |
| <i>Fumaric Acid</i> | α,β-CH=CH | 6.53 | s | |
| <i>Malic acid</i> | α-CH | 4.31 | dd [9.84; 3.21] | 71.5 |
| | β-CH | 2.69 | dd [15.41; 3.21] | 43.8 |
| | β'-CH | 2.39 | dd [15.41; 9.84] | 43.8 |
| <i>Succinic acid</i> | α,β-CH2 | 2.41 | s | 35.3 |
| <i>Amino acids</i> | | | | |
| <i>Alanine (Ala)</i> | α-CH | 3.80 | | 51.7 |
| | β-CH3 | 1.49 | d [7.24] | 17.4 |
| | COOH | | | 176.3 |
| <i>Glutamine (Gln)</i> | α-CH | 3.78 | | 55.4 |
| | β,β'-CH2 | 2.16 | m | 27.4 |
| | γ-CH | 2.46 | m | 31.9 |
| <i>Threonine (Thr)</i> | α-CH | 3.62 | d(6.5) | 61.6 |
| | β-CH | 4.28 | | 68.3 |
| | γ-CH3 | 1.34 | | 20.7 |
| <i>Arginine (Arg)</i> | α-CH | 3.77 | | 55.6 |
| | β-CH2 | 1.93 | | 28.8 |
| | γ-CH2 | 1.73 (1.67) | | 25.1 |
| | δ-CH2 | 3.24 | | 41.6 |
| <i>Glutamate (Glu)</i> | α-CH | 3.77 | | 55.7 |
| | β,β'-CH2 | 2.13 2.08 | | 28.1 |
| | γ-CH2 | 2.36 | | 34.6 |
| <i>Proline (Pro)</i> | α-CH | 4.14 | | 62.4 |
| | β,β'-CH | 2.07; 2.35 | | 30.2 |
| | γ-CH2 | 2.01 | | 24.9 |
| | δ,δ'-CH | 3.41; 3.35 | | 47.2 |
| <i>Asparagine (Asn)</i> | α-CH | 4.02 | | 52.4 |
| | β,β'-CH2 | 2.91; 2.95 | | 35.8 |
| | γ-CONH2 | | | 174.9 |
| <i>Aspartate (Asp)</i> | α-CH | 3.91 | | 53.3 |
| | β,β'-CH2 | 2.72; 2.82 | dd [3.96; 17.46] | 37.7 |
| <i>Valine (Val)</i> | α-CH | 3.63 | | |

| | | | | |
|--|------------------------------------|-------|------------------|--------|
| | β -CH | 2.35 | | 30.2 |
| | γ -CH ₃ | 1.00 | d [7.03] | 17.9 |
| | γ' -CH ₃ | 1.05 | d [7.03] | 19.2 |
| <i>Leucine (Leu)</i> | α -CH | 3.74 | | 54.6 |
| | β -CH ₂ | 1.72 | | 41.0 |
| | γ -CH | 1.68 | | 27.7 |
| | δ -CH ₃ | 0.97 | | 23.3 |
| | δ' -CH ₃ | 0.96 | | 22.2 |
| <i>Isoleucine (Ile)</i> | α -CH | 3.69 | | |
| | β -CH | 1.99 | | 37.1 |
| | γ -CH | 1.28 | | 25.2 |
| | γ' -CH | 1.47 | | 21.9 |
| | γ -CH ₃ | 1.03 | | |
| | δ -CH ₃ | 0.95 | | |
| <i>Tryptophane (Trp)</i> | CH-4 | 7.70 | d[7.8] | 119.7 |
| | CH-7 | 7.52 | d[7.8] | 113.1 |
| | CH-6 | 7.26 | | 118.5 |
| | CH-5 | 7.19 | | |
| <i>γ-Aminobutyrate (GAB)</i> | α -CH ₂ | 2.31 | | 35.5 |
| | β -CH ₂ | 1.91 | | 24.9 |
| | γ -CH ₂ | 3.02 | | 40.3 |
| <i>Phenylalanine (Phe)</i> | CH-2,6 | 7.34 | d | 130.6 |
| | CH-4 | 7.38 | t(7.6) | 128.8 |
| | CH-3,5 | 7.43 | t(7.6) | 130.4 |
| <i>Tyrosine (Tyr)</i> | CH-3,5 | 7.19 | d(8.4) | 131.89 |
| | CH-2,6 | 6.9 | d(8.4) | 117.06 |
| | | 3.06 | dd(8.4, 14.3) | |
| <i>Miscellaneous metabolites</i> | | | | |
| <i>Choline</i> | | | | |
| | N(CH ₃) ₃ + | 3.21 | s | 54.9 |
| | α -CH ₂ | | | 67.5 |
| <i>Trigonelline</i> | | | | |
| | CH-1 | 9.12 | | |
| | CH-3,5 | 8.83 | | |
| | CH-4 | 8.08 | t(7) | |
| | CH ₃ -9 | 4.436 | | 49.4 |
| <i>Uridine</i> | CH-1 | 7.858 | | |
| | CH-2 | 5.897 | | |
| | CH-1' | 5.917 | | |
| | CH ₂ -2' | 4.348 | | |
| | CH ₂ -3' | 4.231 | | |
| | CH-4' | 4.132 | | |
| <i>Adenosine</i> | CH-1 | 8.3 | | |
| | CH-1' | 6.03 | | |
| | CH-2' | 4.74 | | |
| | CH-3' | 4.43 | | |
| | CH-4' | 4.29 | | |

Table 4.14. Summary of the metabolites identified in the 600.13 MHz ¹H spectra of the organic extracts of *Cannabis Sativa* L. inflorescences (and hempseed flour samples).

| <i>Compound</i> | <i>Assignment</i> | <i>1H (ppm)</i> | <i>Multiplicity [J(Hz)]</i> | <i>13C (ppm)</i> |
|---|------------------------|------------------|-----------------------------|------------------|
| <i>Pheophytins</i> | | | | |
| <i>Pheophytin a (Phe-a)</i> | | | | |
| | CH-5 | 9.33 | s | 97.6 |
| | CH-10 | 9.49 | s | 104.7 |
| | CH-20 | 8.55 | s | 93.4 |
| | CH-3 ¹ | 7.97 | | 128.9 |
| | CH-3 ² | 6.26 | dd | 123.1 |
| | CH-3 ^{2'} | 6.17 | dd | 123.1 |
| | CH3-2 ¹ | 3.37 | s | 11.9 |
| | CH3-7 ¹ | 3.19 | s | 11.0 |
| | CH2-8 ¹ | 3.64 | | 11.8 |
| | CH3-8 ² | 1.67 | | 17.3 |
| | CH3-12 ¹ | 3.65 | s | 19.4 |
| | CH-17 | 4.15 | | 51.2 |
| | CH-18 | 4.44 | | 50.2 |
| | CH3-18 ¹ | 1.79 | | 22.9 |
| | CH3-13 ⁴ | 3.86 | s | 52.9 |
| | CH2-P1 | 4.35; 4.20 | | 62.9 |
| | CH-P2 | 5.00 | | 117.6 |
| | CH-P3 ¹ | 1.48 | | 16.1 |
| <i>Sterols</i> | | | | |
| <i>β-Sitosterol</i> | | | | |
| | CH3-18 | 0.65 | s | |
| | CH(OH)-3 | 3.50 | | 71.3 |
| | CH2-4 | 2.20 | | |
| | CH2-2,1 | 1.03; 1.46; 1.78 | | |
| <i>Lipids: Galactosyldiacylglycerols</i> | | | | |
| <i>O-α-D-Galp-(1''->6')-O-β-Galp-(1'<->1)-2,3-diacyl-D-glycerol (DGDG)</i> | | | | |
| | CH <i>sn</i> 2 | 5.22 | | 70.4 |
| | CH2 <i>sn</i> 1 | 3.68; 3.91 | | 67.9 |
| | CH2 <i>sn</i> 3 | 4.20; 4.35 | | 62.9 |
| | CH-1' | 4.19 | | 104.0 |
| | CH-2' | 3.51 | | 71.3 |
| | CH-3' | 3.48 | | 73.4 |
| | CH-4' | 3.93 | | 69.9 |
| | CH-5' | 3.71 | | 70.3 |
| | CH2-6' | 3.67; 3.87 | | 66.3 |
| | CH-1'' | 4.87 | d [4.04] | 99.4 |
| | CH-2'' | 3.84 | | 69.9 |
| | CH-3'' | 3.79 | | 70.8 |
| | CH-4'' | 3.93 | | 69.9 |
| | CH-5'' | 3.79 | | 70.8 |
| | CH2-6'' | 3.79; 3.80 | | 61.7 |
| <i>Lipids: Fatty acid chain</i> | | | | |
| <i>Saturated fatty chain</i> | | | | |
| <i>p: palmitic acid (C16)</i> | | | | |
| <i>S: stearic acid (C18)</i> | | | | |
| | CH2-1 | | | 174.2 |
| | CH2-2 | 2.28 | | 34.2 |
| | CH2-3 | 1.64 | m | 25.5 |
| | CH2-4,13(p) or 4,15(s) | 1.3 | m | 29.3-29.7 |
| | CH2-14(p) or 16(s) | 1.28 | m | 32.1 |
| | CH2-15(p) or 17(s) | 1.28 | m | 22.5 |
| | CH2-16(p) or 18(s) | 0.84 | t [6.95] | 13.9 |
| <i>Oleic fatty chain (C18:1 Δ⁹)</i> | | | | |
| | CH2-1 | | | 174.2 |
| | CH2-2 | 2.38 | | 35.6 |
| | CH2-3 | 1.63 | | 25.3 |

| | | | | | |
|--|--|-----------|----------|-----------|-------|
| | CH2-4,7 | 1.32 | m | 29.6-30.5 | |
| | CH2-8 | 2.03 | m | 27.3 | |
| | CH=CH 9-10 | 5.35 | | 131.9 | |
| | CH2-11 | 2.03 | m | 27.3 | |
| | CH2-12,15 | 1.28 | m | 29.6-30.5 | |
| | CH2-16 | 1.28 | m | 32.7 | |
| | CH2-17 | 1.31 | m | 22.5 | |
| | CH2-18 | 0.84 | t [6.95] | 13.9 | |
| <i>Linoleic fatty chain (C18:2 $\Delta^{9,12}$)</i> | CH2-1 | | | 174.2 | |
| | CH2-2 | 2.28 | | 35.1 | |
| | CH2-3 | 1.62 | | 25.4 | |
| | CH2-4,7 | 1.33 | | 29.6-30.5 | |
| | CH2-8 | 2.03 | q [7.21] | 27.4 | |
| | CH-9 | 5.35 | m | 131.9 | |
| | CH-10 | 5.32 | m | 128.2 | |
| | CH2-11 | 2.77 | t [6.66] | 25.6 | |
| | CH-12 | 5.32 | m | 128.2 | |
| | CH-13 | 5.35 | m | 131.9 | |
| | CH2-14 | 2.03 | q [7.21] | 27.4 | |
| | CH2-15 | 1.33 | | 29.6 | |
| | CH2-16 | 1.33 | | 32.7 | |
| | CH2-17 | 1.31 | | 22.5 | |
| | CH2-18 | 0.94 | | 13.9 | |
| | <i>Linolenic fatty chain (C18:3 $\Delta^{9,12,15}$)</i> | CH2-1 | | | 174.2 |
| | | CH2-2 | 2.28 | | 35.1 |
| | | CH2-3 | 1.62 | | 25.4 |
| CH2-4 | | 1.33 | | 29.6 | |
| CH2-5,7 | | 1.33 | | 30.5 | |
| CH2-8 | | 2.03 | | 27.4 | |
| CH-9 | | 5.35 | | 131.8 | |
| CH-10 | | 5.32 | | 128.2 | |
| CH2-11 | | 2.78 | | 25.6 | |
| CH2-13, CH-12 | | 5.32 | | 128.2 | |
| CH2-14 | | 2.78 | | 25.6 | |
| CH-15 | | 5.28 | | 127.2 | |
| CH-16 | | 5.37 | | 132.3 | |
| CH2-17 | | 2.05 | | 20.6 | |
| CH2-18 | | 0.97 | | 14.0 | |
| <i>Free fatty chains</i> | | CH2-1 | | | 176.9 |
| | | CH2-2 | 2.29 | | 34.2 |
| | | CH2-3 | 1.64 | | 35.4 |
| <i>Lipids: Diacylglycerophospholipids Phosphatidylcholine (PC)</i> | CH2 sn2 | 5.22 | | 70.5 | |
| | CH2 sn1 | 4.21;4.36 | | 62.9 | |
| | CH2 sn3 | 4.03 | | 64.8 | |
| | CH2OP | 4.29 | | 61.5 | |
| | CH2N | 3.66 | | 66.4 | |
| | N(CH3)3 | 3.2 | | 54.2 | |
| <i>Hydrocarbons Squalene</i> | CH3-a | 1.64 | | | |
| | CH3-b | 1.57 | | 15.9 | |
| | CH-c | 5.1 | | 125.1 | |
| | CH2-e | 2.01 | | 30.5 | |
| | CH2-f | 1.95 | | 39.7 | |

USO31 variety

Organic Acids. Succinic Acid content decreased drastically after the first sampling and slowly increased at the last period (Figure 4.18A). Citric Acid concentrations stayed constant over three samplings and increased just before the last harvesting. Last, Malic Acid showed a fluctuating behaviour, reaching the maximum content during the end of the flowering.

Sugars. In USO31 inflorescence, Glucose increased its content until August and then decreased at the end of the flowering, whereas Sucrose showed a fluctuating behaviour (Figure 4.18B).

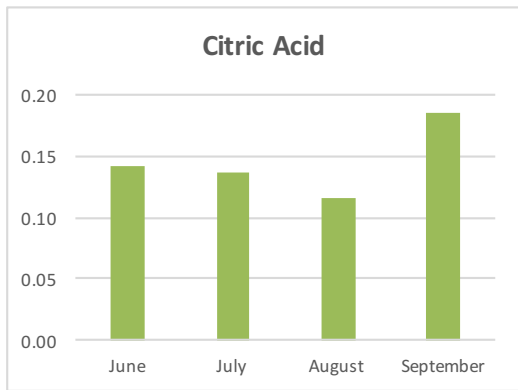
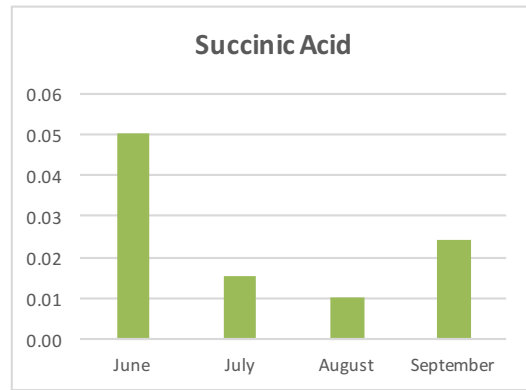
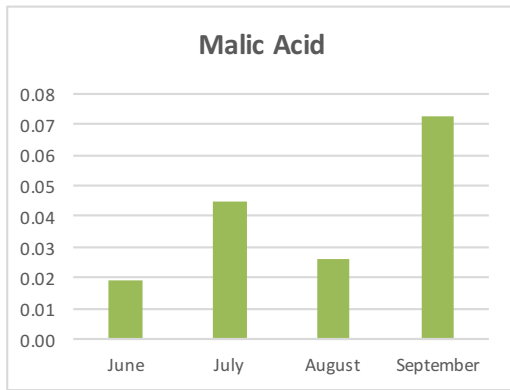
Free Amino Acids. The amino acid profile of free amino acid content in USO31 inflorescences is reported in Figure 4.18C. Ile, Val and Ala showed a gradual decrease over the season, similar to Pro but in September its content increased. Both Thr and Asn rapidly increased their content from June to July, stayed constant over two months and then dropped down. Asp reached the maximum concentration in July but slowly decreased over the season. GABA content showed a gradual increase until August but decrease at the end of flowering.

Miscellaneous compounds. USO31 inflorescences showed an increase of the Choline content over season, see Figure 4.18D.

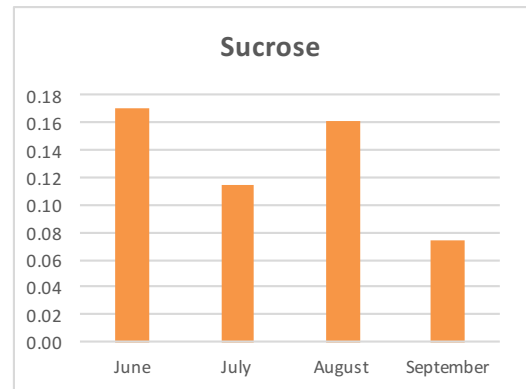
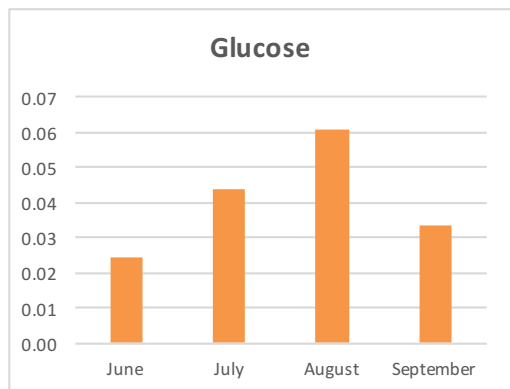
Organic fraction. Regarding the quantification and the evaluation of the trend of concentrations during the flowering period, as shown in Figure 4.19, the Unsaturated Fatty Acids fraction content showed a generally decrease trend over the season. In particular, Mono-Unsaturated Fatty Acids concentrations increased until August and decreased in September, whereas Di-Unsaturated Fatty Acids and Tri-Unsaturated Fatty Acids contents

dropped down in July reaching the minimum just before the harvesting. Total Saturated Fatty Acids showed an opposite trend compared to Total Unsaturated Fatty Acids, a gradually increase over the season to the maximum in September. Triglycerides content drastically decreased in July and continued to slowly decrease to the minimum just before the harvesting. Last, β -Sitosterol content showed a fluctuating trend: it was detected a minimum content in June, it reached a maximum in July decreased in August and finally increased in September.

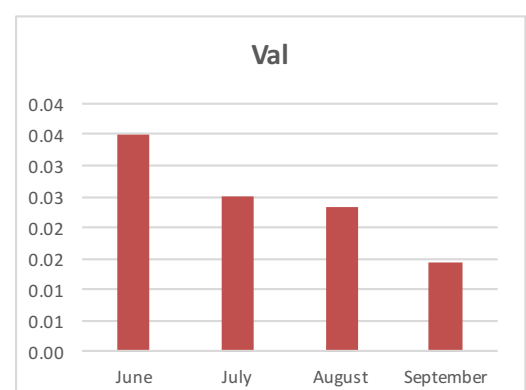
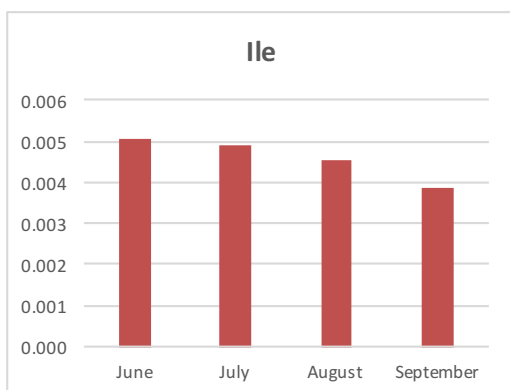
A



B



C



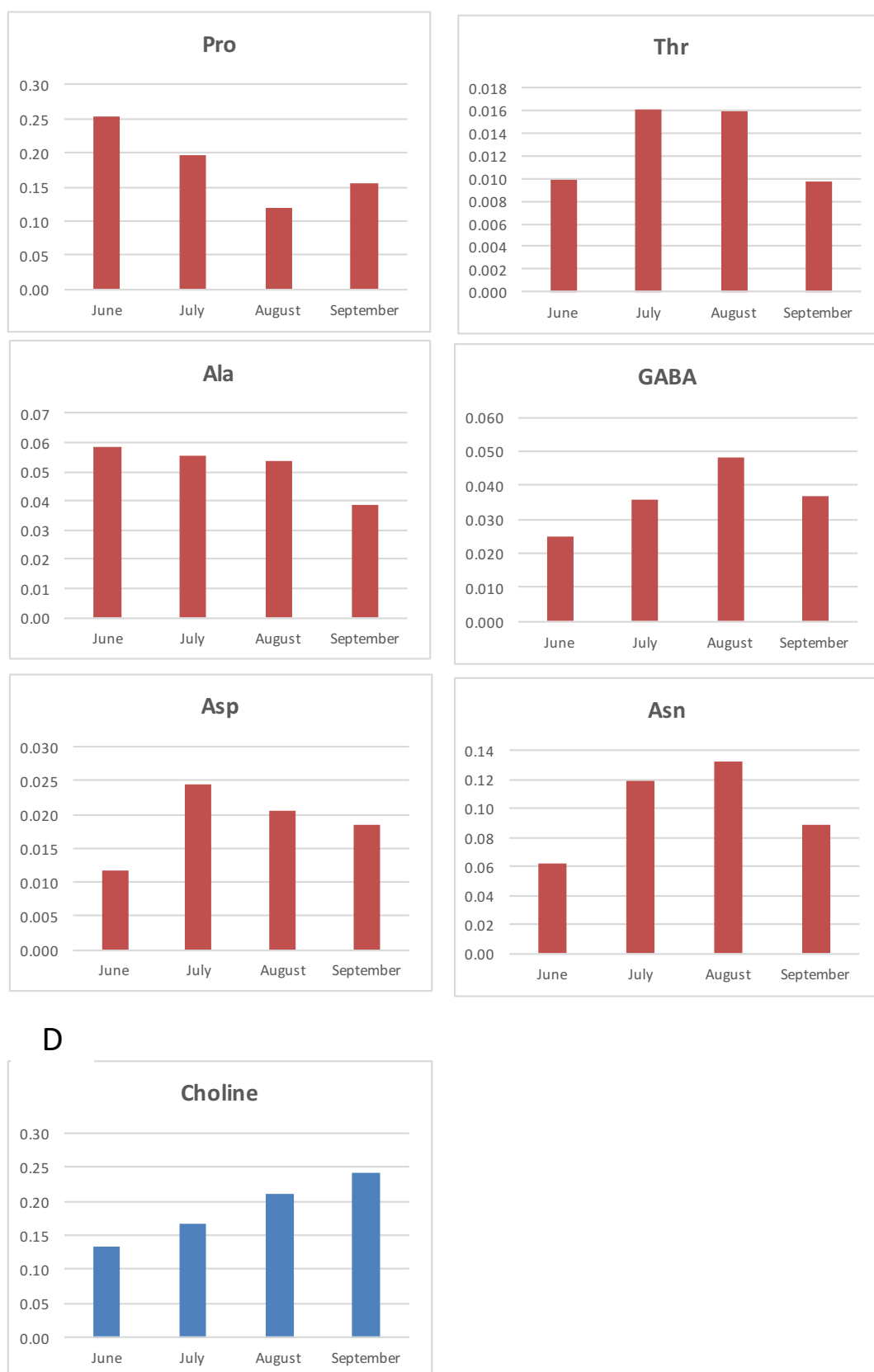


Figure 4.18. Histograms of main A) Organic acids, B) Sugars, C) Amino Acids, D) Miscellaneous compounds identified in hydroalcoholic extracts of Uso31 inflorescences over the season. Data shown are expressed as molecular abundance.



Figure 4.19. Histograms of lipid fraction of USO31 inflorescences organic extracts. Data shown are expressed in %.

Felina32 variety

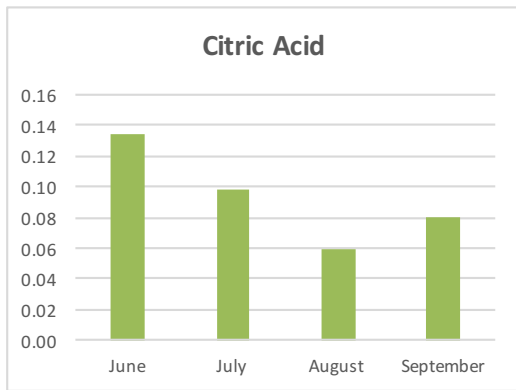
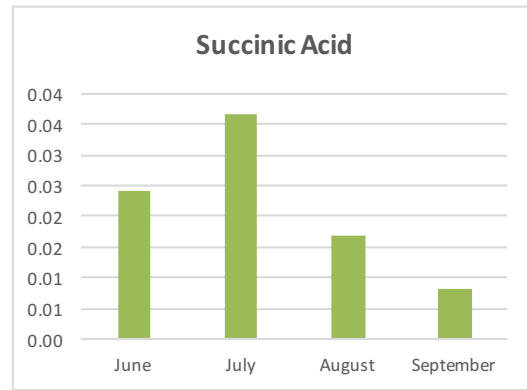
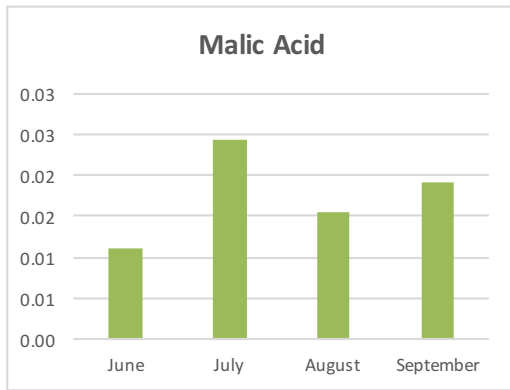
Organic Acids. The organic acids concentrations were different from each other over the season (Figure 4.20A). Succinic Acid content increased from June to July and slowly decreased at the last period. Citric Acid showed a fluctuating behaviour with the maximum content during the first sampling, Last, Malic Acid stayed constant over the first three months and then drastically increased reaching the maximum content during the end of the flowering.

Sugars. In Felina32 inflorescence, the content of Glucose increased until August and then decreased at the end of the flowering, whereas Sucrose showed a fluctuating behaviour with the highest concentration in the months of July and August with respect to the June and September ones (Figure 4.20B).

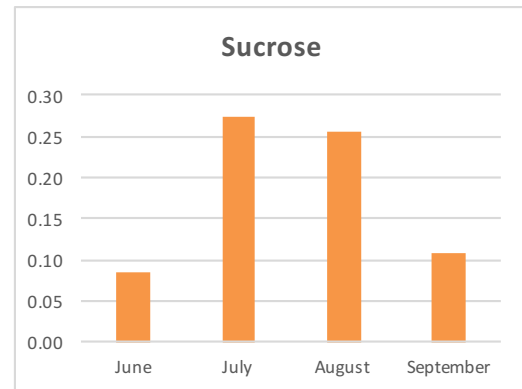
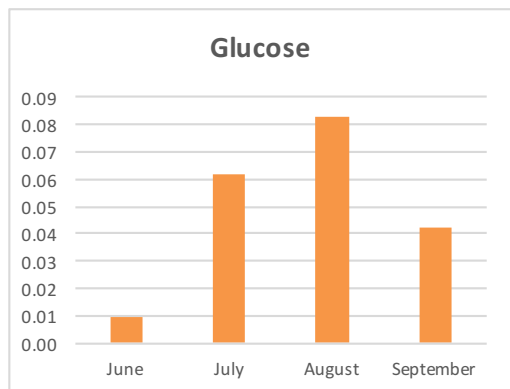
Free Amino Acids. The amino acid profile of free amino acid content in Felina32 inflorescences is reported in Figure 4.20C. Ile and Val showed a similar trend, as their content is high at the first harvesting period (June), drastically dropped down at the second one and it was more or less constant over the rest of the season. Pro and Asn contents dropped down from June to July but then constantly increased over the season. GABA, Asp and Ala showed their maximum content in July with respect to the other months. Thr slowly decreased over the season from June to August, then increased at the end of flowering.

Miscellaneous compounds. Felina32 inflorescences showed that Choline increased their content from June to July, stayed constant over two months and then dropped down, see Figure 4.20D.

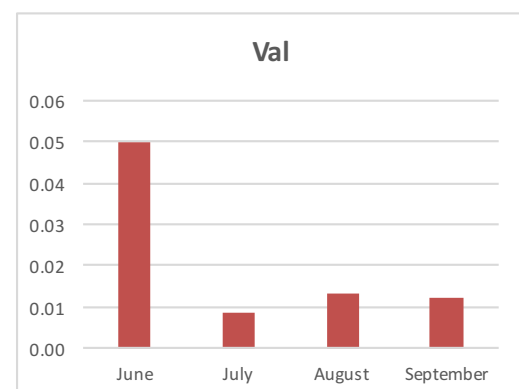
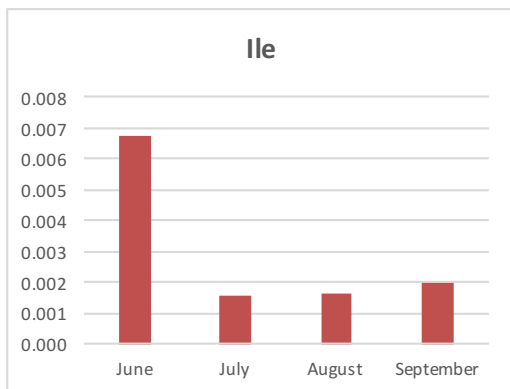
A



B



C



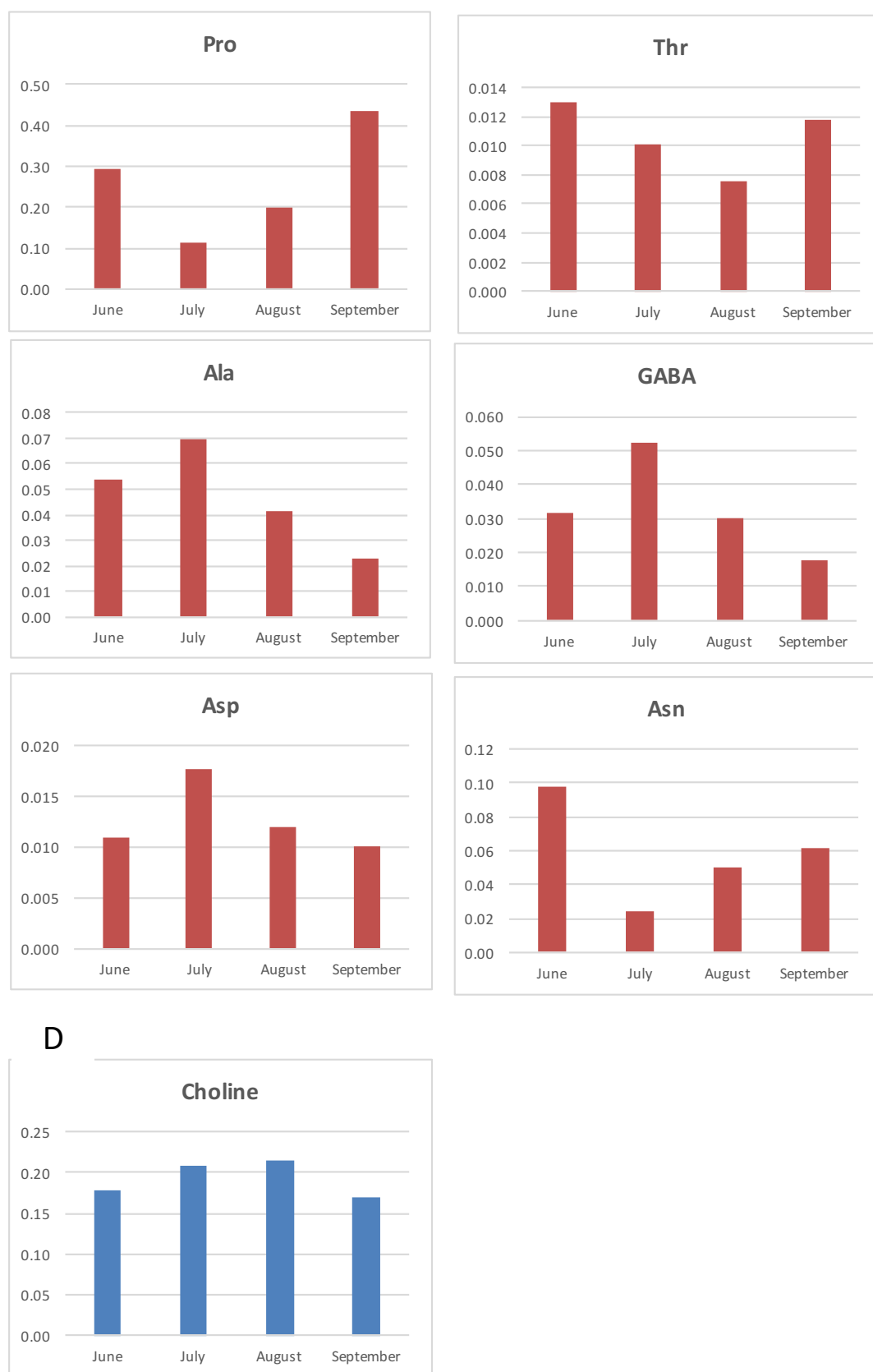


Figure 4.20. Histograms of main A) Organic acids, B) Sugars, C) Amino Acids, D) Miscellaneous compounds identified in hydroalcoholic extracts of Felina32 inflorescences over the season. Data shown are expressed as molecular abundance.

Organic fraction. During the flowering period Total Unsaturated Fatty Acids and Triglycerides showed a fluctuating behaviour, staying more or less constant over three sampling and then drastically dropped down before the last harvesting, see Figure 4.21. Total Saturated Fatty Acids showed an opposite trend compared to Total Unsaturated Fatty Acids, with a maximum content in September. Last, β -Sitosterol content decrease gradually from June to August and then drastically increased in September.



Figure 4.21. Histograms of lipid fraction of Felina32 inflorescences organic extracts. Data shown are expressed in %.

4.5.2 Inflorescences (2nd case study)

4.5.2.1 Material and methods

Field experiments were carried out in the 2017 growing season at the “Nello Lupori” Experimental Farm of the University of Tuscia in Viterbo (latitude 42°25'N, longitude 12°04'E and altitude 310 m a.s.l.). The climate of the experimental site located in Central Italy is typically Mediterranean with a mean annual temperature of 14.5°C, minimum and maximum temperatures observed in February and July respectively, and approximately 750 mm total annual rainfall which falls mainly in the period October-May. The soil is volcanic, classified as Typic Xerofluvent with the following average characteristics in the 0–30 cm soil layer: 10.4% clay, 13.3% silt, 76.3% sand; pH 6.9 (water, 1:2.5); organic matter 1.3% (Lotti methods); total N 0.94 g kg⁻¹ of dry soil (Kjeldahl); available P₂O₅ 33 mg kg⁻¹; and exchangeable K₂O 575 mg kg⁻¹.

Fresh flowering aerial parts from Ferimon cultivar of *Cannabis sativa* L. were harvested at three developmental stages (June, August and September). The experimental field test is a two-level factorial combination (two N fertilizations for two P fertilizations) for a total of four samples for each month (see Table 4.15).

Nitrogen fertilization was applied at a ratio of 0 and 100 or 150 kg N ha⁻¹ (hereafter called N₀ and N₁₀₀ or N₁₅₀, respectively), as ammonium nitrate, divided into two doses applied at 15 and 30 days after crop emergence (50% of the total amount for each application). On the other side, phosphate fertilization was applied at a ratio of 0 and 90 kg P ha⁻¹ (hereafter called P₀ and P₉₀, respectively), as phosphorus salts, in a single dose insufflated in the soil before sowing.

Sampling was carried out in order to ensure that the sample is representative of the field. The fresh hemp plant material was stored at -80°C.

Sample preparation as well as NMR spectra acquisition and processing were carried out as reported above for the 1st case study of hemp inflorescences. Differently, the results relative to the metabolites quantified in hydroalcoholic extracts are here expressed in mg/100g.

Table 4.15. Two-level factorial combination (two N fertilizations for two P fertilizations) in a three-months harvesting period, for a total of 12 samples. The dates of inflorescences collection are reported above.

| | 26-6-2017 | 10-8-2017 | 10-9-2017 |
|--------------------------------------|-----------|-----------|-----------|
| N₀P₀ | ✓ | ✓ | ✓ |
| N₀P₉₀ | ✓ | ✓ | ✓ |
| N₁₀₀P₀ | ✓ | ✓ | |
| N₁₀₀P₉₀ | ✓ | ✓ | |
| N₁₅₀P₀ | | | ✓ |
| N₁₅₀P₉₀ | | | ✓ |

4.5.2.2 Results and Discussion

NMR untargeted analysis provided the metabolic fingerprint of each sample and the quantification of specific metabolites whose signal are well resolute in protonic spectra. The analysis of the metabolic profile of the extracts in the three-months harvesting period will be discussed for each class of compounds.

Hydroalcoholic fraction. In Figure 4.22, graphs of main organic acids, sugars, amino acids, and miscellaneous compounds identified in hydroalcoholic inflorescences extracts over the season are reported.

It can be observed that the metabolites belonging to the same chemical class (organic acids, sugars, amino acids) do not show a common trend, but each metabolite shows a trend that is influenced in some cases by the harvesting month and in other cases by the type of

fertilization carried out (nitrogen or phosphate fertilizations). In other words, the fertilization type shows a different effect on different metabolites.

Basically, by observing the graphs of hydrosoluble metabolites, it can be seen that the phosphate fertilization (N_0P_{90}) determines in June a higher concentration of most of them; this can be related to the fact that the phosphate fertilizer, unlike the nitrogenous fertilizer, is distributed all before sowing.

Organic Acids. The phosphate fertilization (N_0P_{90}) always decreases a decrement of each organic acid from June to September. Only in the case of Succinic Acid there is a common decreasing trend from June to September independently by the use of single fertilizers ($N_{100}P_0$ and N_0P_{90}) or by their combined use ($N_{100}P_{90}$). Instead, there is an opposite trend of Succinic Acid between June and August without the use of fertilizers (N_0P_0). Citric Acid drops down of 60mg/100g from June to September in the case of phosphate fertilization (N_0P_{90}). The same situation happens for the Malic Acid that drops down of 100mg/100g from June to September in the case of phosphate fertilization (N_0P_{90}).

Sugars. Nitrogen fertilizations ($N_{100}P_0$ and $N_{100}P_{90}$) determine a constant increase of Glucose quantity from June to September. Instead, the use of the phosphate fertilization (N_0P_{90}) determines a strong decrease in the amount of Glucose, from 200mg/100g to 75mg/100g, between August and September. In contrast, without the use of fertilizers, there is a strong increase in the amount of Glucose, from 75mg/100g to 200mg/100g, between June and August.

Nitrogen fertilizations ($N_{100}P_0$ and $N_{100}P_{90}$) determine the same decreasing trend of Sucrose content from June to August (from 531.9mg/100g to 132.4mg/100g). The phosphate fertilization, regardless of the combination or not with the nitrogen fertilization (N_0P_{90} and $N_{100}P_{90}$), decreases a decrease in the sucrose concentration over time (from June to September)

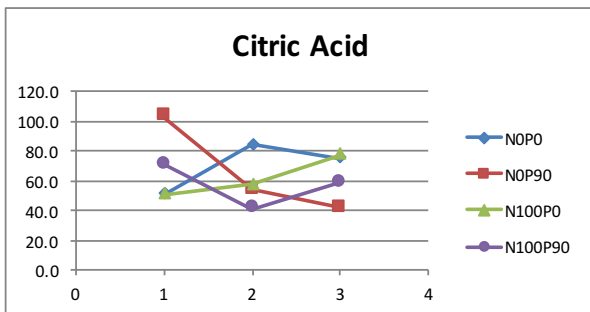
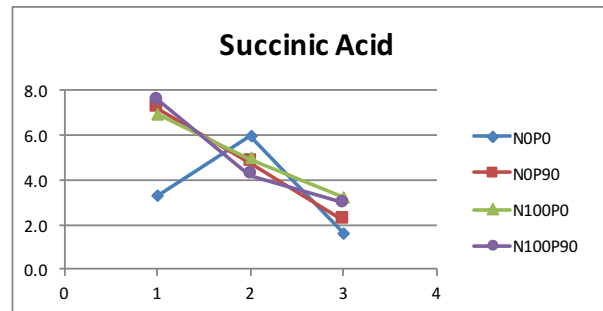
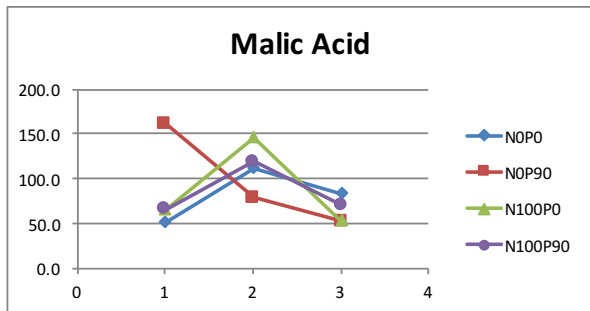
up to about 80mg/100g. The decrease is more significant in the case of the N_0P_{90} phosphate fertilization since the amount present in the June (745.1mg/100g) is higher than one (512.8 mg/100g) present in the same month for “ $N_{100}P_{90}$ sample”. Even without fertilizers (N_0P_0), a decrease in the amount of sucrose occurs over time; the decrease in this case is less significant between June and September. In other words, the lack of fertilizer determines a lower concentration of sucrose in June, but its decrease over time is lower than that of samples that have received fertilization treatments.

Free Amino Acids. It can be observed that with a phosphate and nitrogen combined fertilization ($N_{100}P_{90}$), the trend over time of the concentrations of all the amino acids (with the exception of Proline) tends to increase. For instance, Val content shows a drastically increase between August and September in the case of the $N_{100}P_{90}$ fertilization. Thr and Asn show a progressive increase during the growth of the plant, from June to September, both considering the combined use of them ($N_{100}P_{90}$) and without fertilizers (N_0P_0). Asn content also has a similar trend, showing an increases up to about 200mg/100g both with the combined fertilization ($N_{100}P_{90}$) and without fertilizers (N_0P_0). Pro shows a completely different trend with respect the other amino acids. Its content increases considerably in the month of August, especially with the nitrogen fertilization ($N_{100}P_0$) where the amount of Pro rises from 20mg/100g to 70mg/100g.

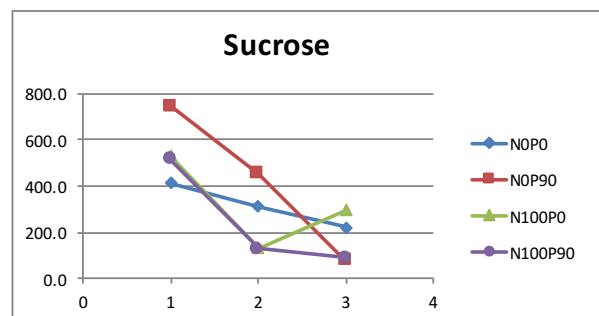
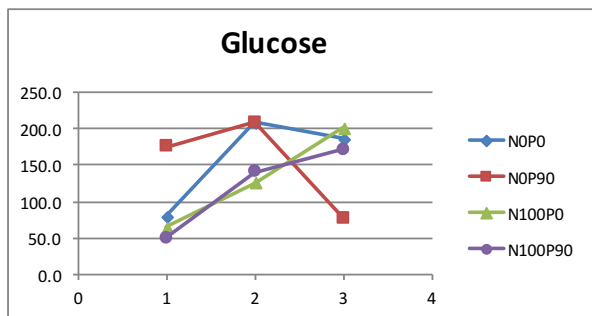
Organic fraction. In Figure 4.23, graphs of liposoluble compounds identified in organic inflorescences extracts over the season are reported. The phosphate fertilization (N_0P_{90}) determines a significant increase of unsaturated fatty acids content, especially of Di-Unsaturated Fatty Acids, from June to August. The content of Tri-unsaturated Fatty Acids is not influenced from by the use or not of the fertilizers, showing a similar trend over the time for each sample. Last, β -Sitosterol content gradually decreases from June to September

without the use of fertilizers (N_0P_0) whereas it decreases from June to August with the use of fertilizers ($N_{100}P_0$, N_0P_{90} , $N_{100}P_{90}$) and then increased in September returning to the the same levels present at the beginning in June.

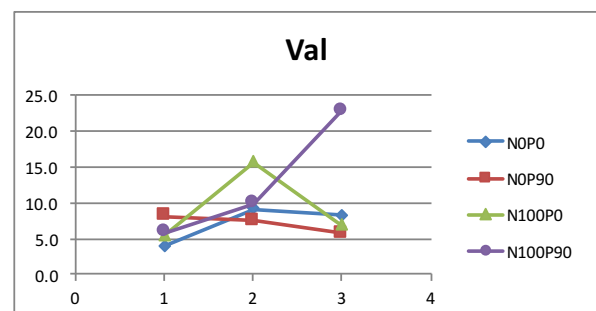
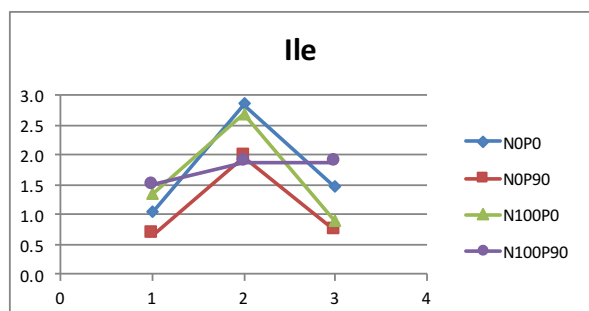
A



B



C



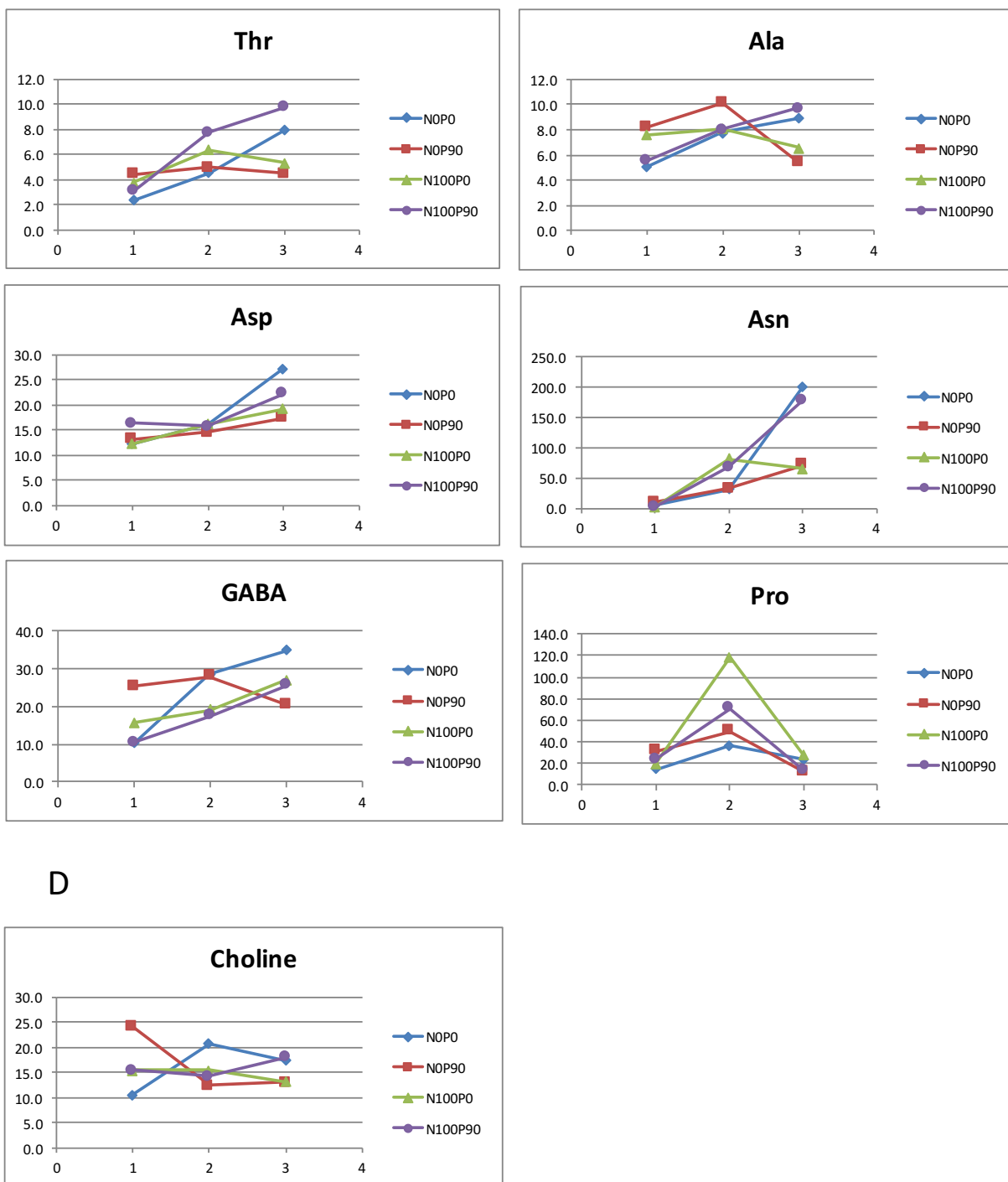


Figure 4.22. Graphs of main Organic acids (A), Sugars (B), Amino Acids (C), and Miscellaneous compounds (C) identified in hydroalcoholic inflorescences extracts over the season. Data shown are expressed in mg/100g. Nitrogen fertilization was applied at a ratio of 0 and 100 kg N ha⁻¹ (hereafter called N₀ and N₁₀₀ or N₁₅₀, respectively) whereas phosphate fertilization was applied at a ratio of 0 and 90 kg P ha⁻¹ (hereafter called P₀ and P₉₀, respectively). 1=June; 2=August; 3=September.

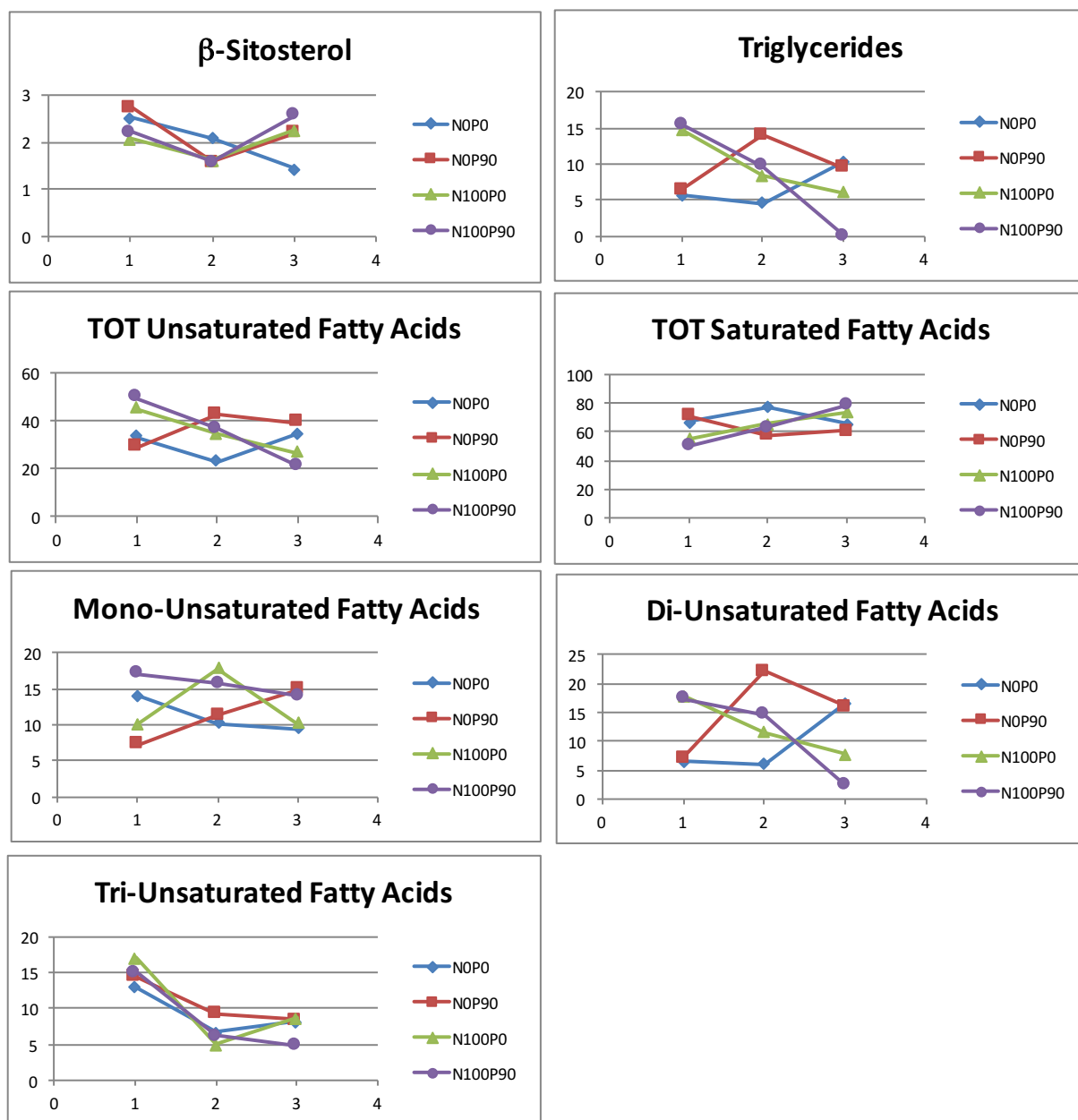


Figure 4.23. Graphs of lipid fraction inflorescences organic extracts. Data shown are expressed in %. Nitrogen fertilization was applied at a ratio of 0 and 100 kg N ha⁻¹ (hereafter called N₀ and N₁₀₀ or N₁₅₀, respectively) whereas phosphate fertilization was applied at a ratio of 0 and 90 kg P ha⁻¹ (hereafter called P₀ and P₉₀, respectively). 1=June; 2=August; 3=September.

4.5.3 Hempseed oil

4.5.3.1 Material and methods

Nine commercial hempseed oil were purchased in biological foods stores. Brand names and their prices are reported in Table 4.16. As reported, the price per litre ranges from 20€/L to 80€/L. Hempseed oil are sold in a 25 mL bottles. Only one of these samples – Baule Volante branded - was stored at 4°C when it was purchased. Before carrying NMR analysis, samples, given their high degree of unsaturation, have been stored in a cool and dry place, away from sources of light and heat, to prevent oxidation reactions.

Each hempseed oil sample (20 μ L) was dissolved in DMSO (20 μ L) and CDCl_3 containing 0.03% TMS (700 μ L) directly in the 5 mm NMR tube. The NMR spectra were recorded at 27 °C on a Bruker AVANCE 600 spectrometer operating at the proton frequency of 600.13 MHz and equipped with a Bruker multinuclear z-gradient 5 mm probe head. The ^1H spectra were acquired using the following conditions: number of scans 1024, 90° pulse 9.5 μ s, time domain 64 K data points, relaxation delay plus acquisition time 3.5 s and spectral width 18 ppm. ^1H NMR spectra were obtained by the FT of the Free Induction Decay applying an exponential multiplication with a line-broadening factor of 0.3 Hz and a zero filling (size 64 K) procedure. ^1H NMR spectra were manually phased. Chemical shifts were reported with respect to the residual CHCl_3 signal set at 7.26 ppm. The baseline was corrected using the Cubic Spline Baseline Correction routine in the Bruker Topspin software.



In order to compare the spectra of different samples, the integrals of 7 selected signals were measured. The selected proton resonances were due to hexanal (CH) at 9.699 ppm, trans 2-hexenal (CH) at 9.448 ppm, diallylic protons of linolenic fatty chains (CH_2) at 2.778 ppm, diallylic protons of linoleic fatty chains (CH_2) at 2.729 ppm, α -methylene protons of all acyl chains (CH_2) at 2.251 ppm, allylic protons of all fatty chains (CH_2) at 1.999 ppm, β -sitosterol (CH_3) at 0.622 ppm. The integrals of the selected resonances were normalized by

setting the integral of the resonance at 2.251 ppm to 100. This kind of normalization procedure gives an index proportional to the molar ratio between each compound and the total amount of fatty chains. Since the integral of the resonance at 2.251 ppm refers to 2 protons, each integral has been normalized by referring to 2 protons too. For instance, to calculate the percentage of linolenic fatty chains the integral of diallylic protons has been divided by two. The percentage of saturated fatty acids was calculated by subtracting the half integral value of all fatty chains allylic protons from the integral of all acyl chains α -methylene protons. The percentage of monounsaturated fatty chains was calculated by subtracting the integral value of diallylic protons of linoleic fatty chains and the half integral value of diallylic protons of linolenic fatty chains from the half integral value of all fatty chains allylic protons.

Table 4.16. Brand names, prices and pictures of the nine commercial hempseed oils analysed.

| Brand Name | Price (€/L) | Picture |
|---------------|-------------|---|
| Erbology | 20 |  |
| Fiori di Loto | 24 |  |

| | | |
|----------------------|-----------|---|
| <p>Crudolio</p> | <p>25</p> |  |
| <p>Baule Volante</p> | <p>26</p> |  |
| <p>Germinal Bio</p> | <p>30</p> |  |
| <p>Hemp Farm</p> | <p>44</p> |  |
| <p>Hanfol nu3</p> | <p>52</p> |  |

| | | |
|--------|----|---|
| Pipkin | 64 |  |
| Sabo | 80 |  |

4.5.3.2 Result and discussions

A typical NMR analysis on a food matrix is highly informative because lets us to have information about quali-quantitative composition of different classes of compounds quickly and in a single experiment (Circi et al., 2018; Camin et al., 2016).

Both majority and minority compounds have been identified in the ^1H NMR spectra of the nine hempseed oils. Hempseed oils spectra, similarly to other vegetable oils spectra, are dominated by strong signals of fatty acids and triglycerides. Smaller signals belonging to monoglycerides and aldehydes also have been detectable. In Figure 4.24, spectrum of a hempseed oil sample, showing the expansions of seven selected resonances (labelled from A to G), is reported.

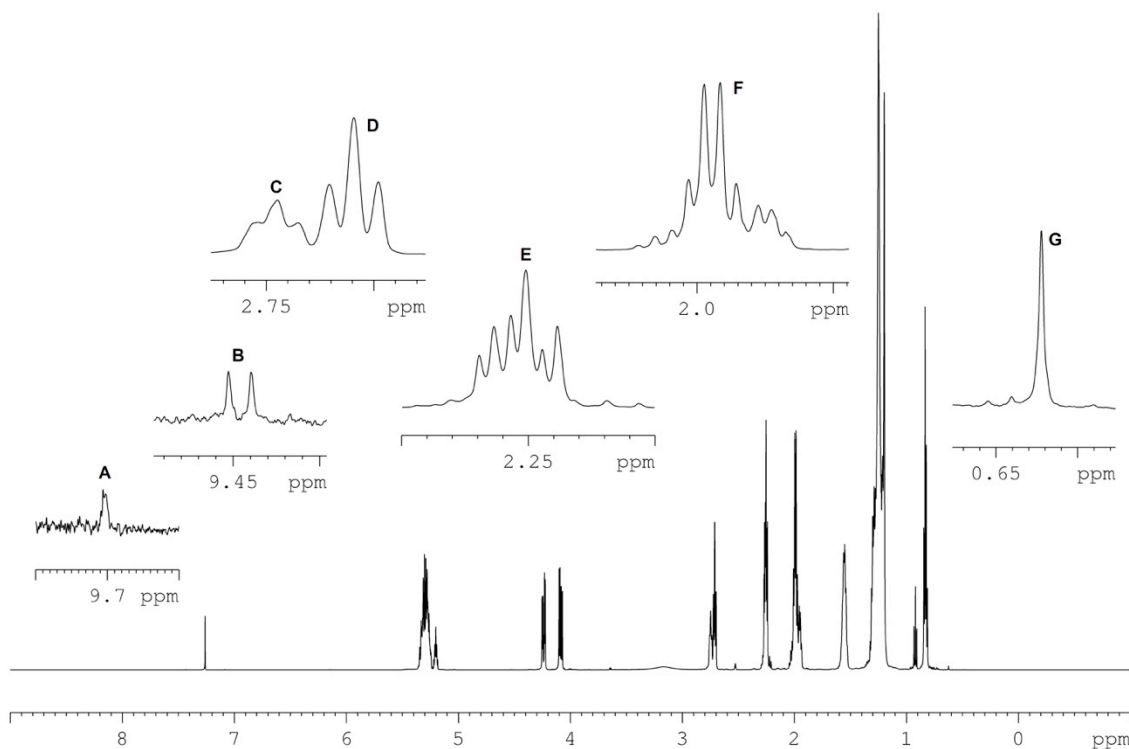


Figure 4.24. 600.13 MHz ¹H NMR spectrum of a hempseed oil sample. The selected NMR signals used to make a comparison between different samples are reported in expanded scale and labelled. A: hexanal (9.699 ppm); B: trans 2-hexenal (9.448 ppm); C: diallylic protons of linolenic fatty chains (2.749 ppm); D: diallylic protons of linoleic fatty chains (2.741 ppm); E: α -methylene protons of all acyl chains (2.251 ppm); F: allylic protons of all fatty chains (1.999 ppm); G: β -sitosterol (0.622 ppm).

Spectra show that fatty acids profile of all nine hempseed oils are characterized by a higher content of unsaturated fatty acids with respect to saturated fatty acids.

The signals belonging to the methyl groups of oleic acid, linoleic acid and linolenic acid, respectively at 0.820 ppm, 0.831 ppm and 0.916 ppm, can be exploited to evaluate differences about unsaturated fatty acids content. Spectra show a similar content of fatty acids in each of hempseed oils, with a linoleic acid signal more intense than oleic acid and linolenic acid ones. On the contrary, in each sample linolenic acid peaks result the least intense with respect to oleic acid and linoleic acid signals. Intensities differences of polyunsaturated fatty acids signals are also maintained considering the peaks of diallylic protons at 2.749 ppm and 2.741 ppm respectively for linolenic acid and linoleic acid.

Integrals of resonances reported in Figure 4.24 have been used to obtain histograms in order to compare easily the nine hempseed oils. Histograms of fatty acids relative content for hempseed oils are reported in Figure 4.25A, whereas histograms with relative content of β -sitosterol and aldehydes are reported in Figure 4.25B.

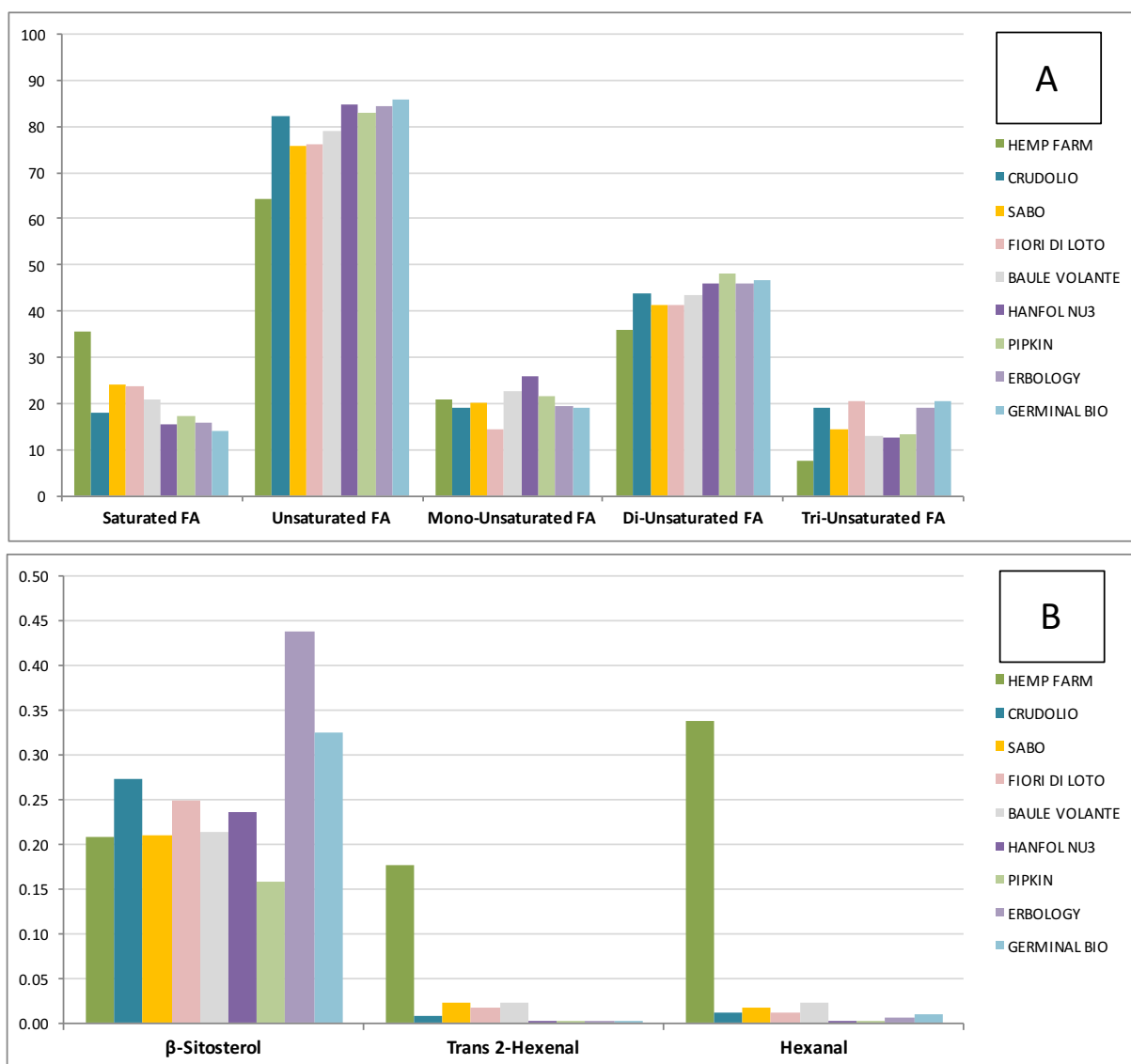


Figure 4.25. Histograms resulting from the quantitative NMR spectroscopic analysis of (A) Fatty Acids (FA), (B) β -Sitosterol and aldehydes. The relative molecular abundance (mol%) are reported.

The content of mono-unsaturated, di-unsaturated and tri-unsaturated fatty acids ranges between 15-28%, 35-48% and 8-20%, respectively.

Considering β -sitosterol, its content ranges from 0.15% of sample PIPKIN to 0.33% and 0.45% of samples GERMINAL BIO and ERBOLOGY, respectively. Other samples have an intermediate concentration of β -sitosterol.

The aldehydic content of trans 2-hexenal and hexanal is on average low in all samples (between 0 and 0.5%). On the contrary, sample HEMP FARM shows a drastically higher content of hexanal and trans 2-hexenal with respect to other ones. In particular, hexanal is about thirty times more abundant with respect to others hempseed oils, reaching even the 0.34%, whereas trans 2-hexenal reach the 0.17%. Since aldehydes are partially responsible for the flavour, we can deduce that sample HEMP FARM is a very tasty hempseed oil. However, such a high concentration of aldehydes is also a degradation index of polyunsaturated fatty acids and it does not necessarily have to represent a positive aspect. Looking at the fatty acids profile content, sample HEMP FARM results to be the one with the lower tri-unsaturated fatty acids content.

Generally, hempseed olive oils are renowned for having an optimal $\omega 6:\omega 3$ ratio, between 3:1 and 4:1. However, a lower value of this ratio for three hempseed oils analysed can be extrapolated by reading their labels. In other words, not all the nine hempseed oils show an optimal ratio of 3/4:1. In Table 4.17, $\omega 6:\omega 3$ ratios labelled on the nine commercial hempseed oils bottles are compared with ratios resulting from NMR analysis.

Table 4.17. $\omega 6:\omega 3$ ratios reported on the label and resulted by NMR analysis of the nine commercial hempseed oils analysed.

| Samples | $\omega 6:\omega 3$ ratios labelled | NMR results |
|---------------|-------------------------------------|-------------|
| Erbology | 2.80 | 2.40 |
| Fiori di Loto | 3.37 | 1.99 |
| Crudolio | 3.17 | 2.30 |
| Baule Volante | 3.21 | 3.36 |
| Germinal Bio | 2.39 | 2.27 |
| Hemp Farm | 4.20 | 4.71 |
| Hanfol nu3 | 3.11 | 3.64 |
| Pipkin | 3.37 | 3.61 |
| Sabo | 2.57 | 2.86 |

In some cases, NMR results do not coincide with the values reported on the labels. For instance, four hempseed oils (Erbology, Fiori di Loto, Crudolio, Germinal Bio) have a lower $\omega 6:\omega 3$ ratio with respect to that declared in the labels. From NMR results only Hanfol nu3, Pipkin, Baule Volante and, especially, Hemp Farm hempseed oils, with values of 3.6, 3.6, 3.3 and 4.7 respectively, can be considered “good” hempseed oils. As evidenced, Hemp Farm hempseed oil presents a particularly high ratio compared to other ones.

There are four hempseed oils (Crudolio, Herbology, Sabo and Germinal Bio) that do not reach the value of 3 whereas Fiori di Loto hempseed oil does not reach even the value of 2.

It is interesting to note that Sabo hempseed oil is sold at the price of 80€/L but it has not the best $\omega 6:\omega 3$ ratio whereas Baule Volante one, with a good ratio value of 3.36, is sold at a much more affordable price (26€/L).

According to the high market prices of these hempseed oils, we have decided to compare the metabolite profile of one of them (Hemp Farm, having the best $\omega 6:\omega 3$ ratio among hempseed oils analysed) with a good Extra Virgin Olive Oil (Lametia DOP, sold at about 10€/L) in order to find out what could justify the big difference of price. A classical olive oil, such as Lametia DOP, is characterized by very different levels of fatty acids with respect to hempseed oils because it is a source naturally rich in oleic acid whereas polyunsaturated fatty acids such as linoleic acid and linolenic acid represent only a small percentage of the fatty acids content (Figure 4.26). The relevant content of unsaturated fatty acids with respect to a classical olive oil makes the hempseed oils more susceptible to oxidation reactions. Moreover, the signal of squalene, an important antioxidant normally present in the olive oil matrix, has not been identified in hempseed oils spectra. These two aspects – the lack of squalene and the higher content of unsaturated fatty acids - suggest that these hempseed oils have a shelf-life not very high and storage conditions become fundamental to guarantee a good quality product.

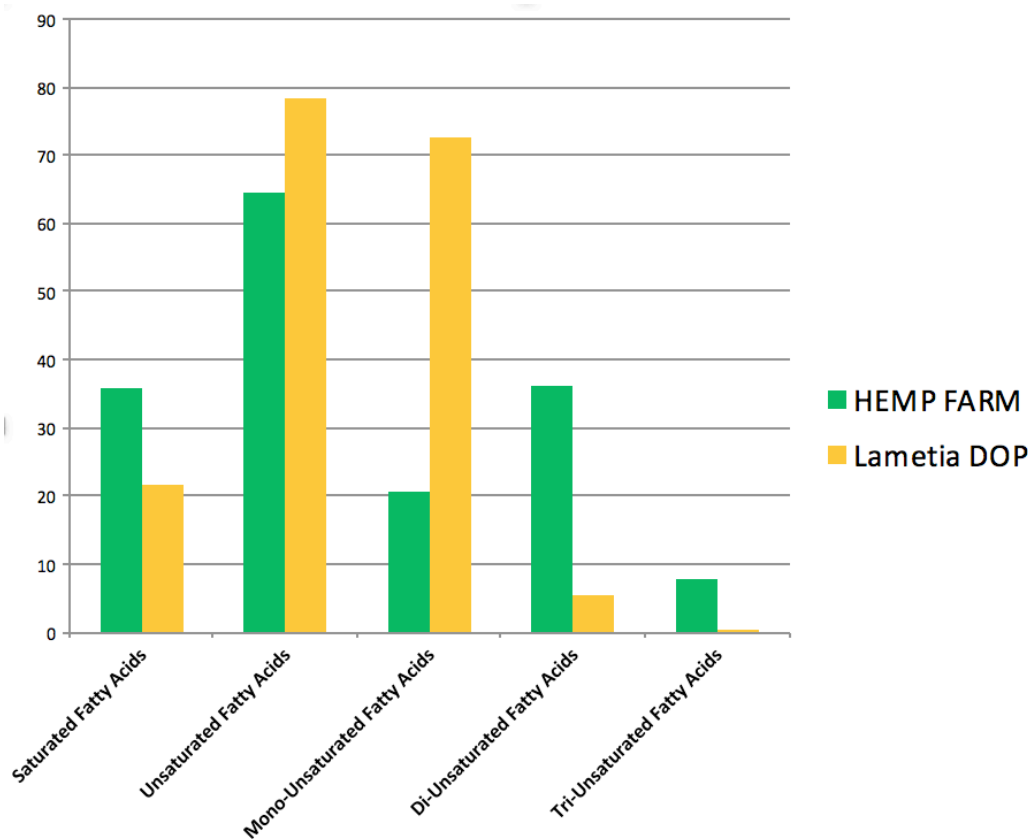


Figure 4.26. Histograms resulting from the quantitative NMR spectroscopic analysis of the Hemp Farm hempseed oil (in green) and the Extra Virgin Olive Oil “Lametia DOP” (in orange). The relative molecular abundance (mol%) are reported.

By comparing the DOP Extra Virgin Olive Oil and Hemp Farm hempseed oil in relation to the ratio of unsaturated fatty acids (omega 6/omega 3), the first one results to have a higher ratio (16.98) compared to the value of 4.71 of the Hemp Farm hempseed oil.

Our critical analysis highlights that a hempseed oil has many quali-quantitative differences with respect to a classical olive oil in terms of metabolic profile and results to be similar to a seed oil. The most significant difference regards the contents of monounsaturated fatty acids and polyunsaturated fatty acids. Hempseed oils are richer in Poly-Unsaturated Fatty Acids (PUFAs) whereas a classical olive oil is richer in Mono-Unsaturated Fatty Acids (MUFAs). Moreover, spectra of hempseed oils don't contain any particular molecule with respect to spectra of an olive oil. The only exception is represented by squalene, not identified in hempseed oils. Can all this justify the high difference of price per liter between a hempseed oil and an extra virgin olive oil?

4.5.4 Hempseed flour

4.5.4.1 Material and methods

Five different samples of hempseed flours were analysed: three samples (Flour 1, Flour 1.1 and Flour 3), provided by the Cultural Association “Canapa Live”, are part of the same flour but differ in granulometry, whereas the other two samples (branded as Lara Hemp and Hemp Farm) were purchased in biological food stores.

Each hempseed flour sample (0.5 g) was subjected to the Bligh-Dyer extraction following the same identical procedure reported above for the inflorescences samples.

The dried organic fraction of each sample was dissolved in 0.7 mL of a CDCl_3 and then placed into a 5 mm NMR tube. Conversely, the dried hydroalcoholic phase of each sample was solubilized in 0.75 mL 400 mM phosphate buffer/ D_2O , containing a 1 mM solution of TSP as internal standard and EDTA, and then transferred into a 5 mm NMR tube.

NMR spectra of all hydroalcoholic and organic extracts were recorded at 27 °C on a Bruker AVANCE 600 spectrometer operating at the proton frequency of 600.13 MHz and equipped with a Bruker multinuclear z-gradient 5 mm probe head. ^1H spectra were referenced to methyl group signals of TSP ($\delta = 0.00$ ppm) in D_2O , and to the signal of chloroform (set to 7.26 ppm) in CDCl_3 mixture. ^1H spectra of hydroalcoholic extracts were acquired with 256 transients with a recycle delay of 5 s. The residual HDO signal was suppressed using a pre-saturation. The experiment was carried out by using 45° pulse of 7.5 μs , 32K data points. ^1H spectra of extracts in CDCl_3 were acquired with 256 transients, recycle delay of 5 s and 90° pulse of 9.7 μs , 32K data points. The two-dimensional (2D) NMR experiments, such as ^1H - ^1H TOCSY, ^1H - ^{13}C HSQC and ^1H - ^{13}C HMBC, were carried out under the same experimental conditions previously reported (Sobolev, Segre & Lamanna, 2003).

In order to evaluate the similarities or differences between samples the integrals of selected resonances in ^1H NMR spectra were measured. The intensity of 16 selected signals in

hydroalcoholic extract, see Table 4.18, was measured using the Bruker TOPSPIN software and normalized with respect to the total sum of all integrals. Results have been expressed in mg/100g.

The intensity of 4 selected signals in organic extract, see Table 4.19, was also measured and normalized with respect to the resonance at 0.89 ppm, due to signal of total fatty acids, normalized to 100. Results have been expressed in %.

The % values of monounsaturated and saturated fatty acids have been calculated using the following equation:

$$\%_{\text{MONO}} (=2 \cdot I_{\text{MONO}}) = 2 \cdot (0.25I_{\text{UNS}} - 0.5I_{\text{DI}} - 0.25I_{\text{TRI}}) \quad (1)$$

$$\%_{\text{SAT}} = I_{\text{FA}} - 0.5I_{\text{UNS}} \quad (2)$$

where I_{UNS} is the integral value of “unsaturated fatty acids” (signal at 1.99 ppm), I_{DI} is the integral value of “di-unsaturated fatty acids” (signal at 2.72 ppm), I_{TRI} is the integral value of “tri-unsaturated fatty acids” (signal at 2.77 ppm), I_{FA} is the integral value of “total fatty acids” (signal at 2.29 ppm). The integral value of total fatty acids has been fixed at 100.

Table 4.18. Compounds, and relative signals (ppm), selected for quantitative analysis in the hydroalcoholic extracts.

| Compounds | ppm |
|-------------------|------------|
| Ile | 1.02 |
| Val | 1.05 |
| Thr | 1.34 |
| Ala | 1.49 |
| Pro | 2.03 |
| GABA | 2.30 |
| Glutammate | 2.35 |
| Succinic Acid | 2.41 |
| Citric Acid | 2.56 |
| Asp | 2.81 |
| Asn | 2.89 |
| Choline | 3.20 |
| Myo-inositol | 3.31 |
| Malic Acid | 4.30 |
| α -Glucose | 5.25 |
| Sucrose | 5.42 |

Table 4.19. Compounds, and relative signals (ppm), selected for quantitative analysis in the organic extracts.

| Compounds | ppm |
|-----------------------------|------------|
| β -Sitosterol | 0.65 |
| Di-unsaturated fatty acids | 2.72 |
| Tri-unsaturated fatty acids | 2.77 |
| Unsaturated fatty acids | 5.33 |

4.5.4.2 Results and Discussion

NMR analysis provided the metabolic fingerprint of each sample and, on the other hand, the quantification of each metabolite identified. ^1H spectra of hempseed flour samples are superimposable for metabolites content with ^1H spectra of inflorescences samples (see Table 4.13 and Table 4.14). Figure 4.27 and Figure 4.28 summarize the metabolites identified in hempseed flour hydroalcoholic and organic extracts samples. Histograms relative to the metabolites quantified in hempseed flour hydroalcoholic and organic samples are reported in Figure 4.29 and Figure 4.30, respectively.

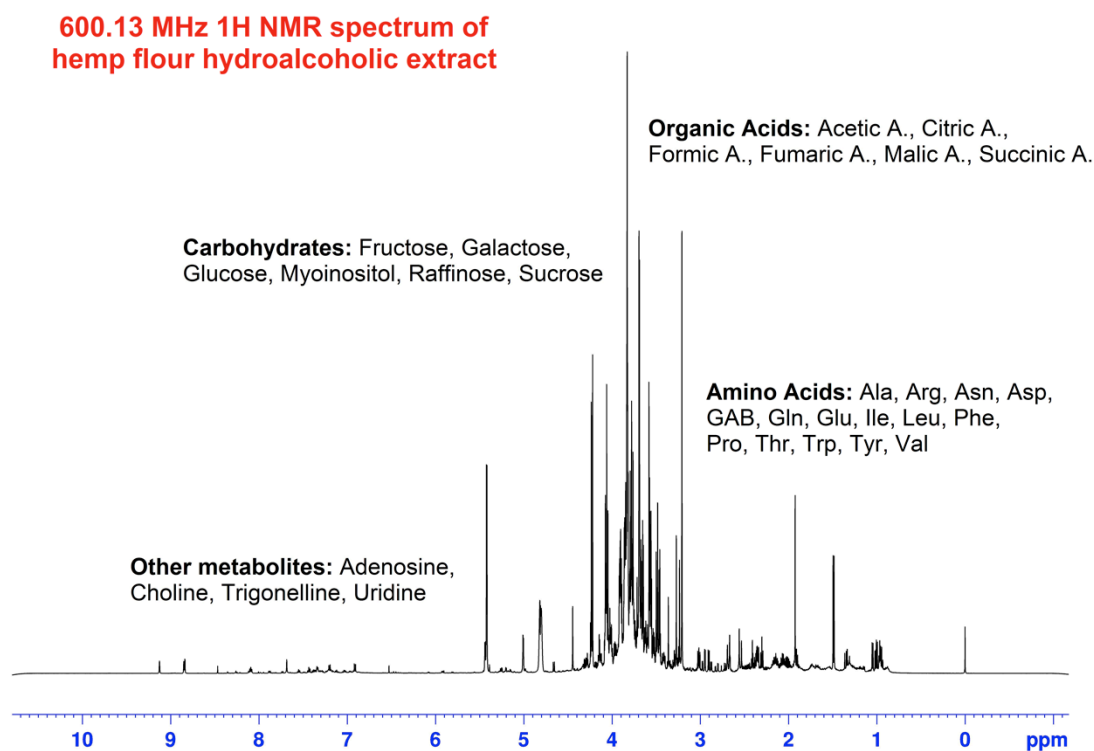


Figure 4.27. ^1H spectrum of a hempseed flour hydroalcoholic extract sample, reporting the metabolites identified.

600.13 MHz ¹H spectrum of hemp flour organic extract

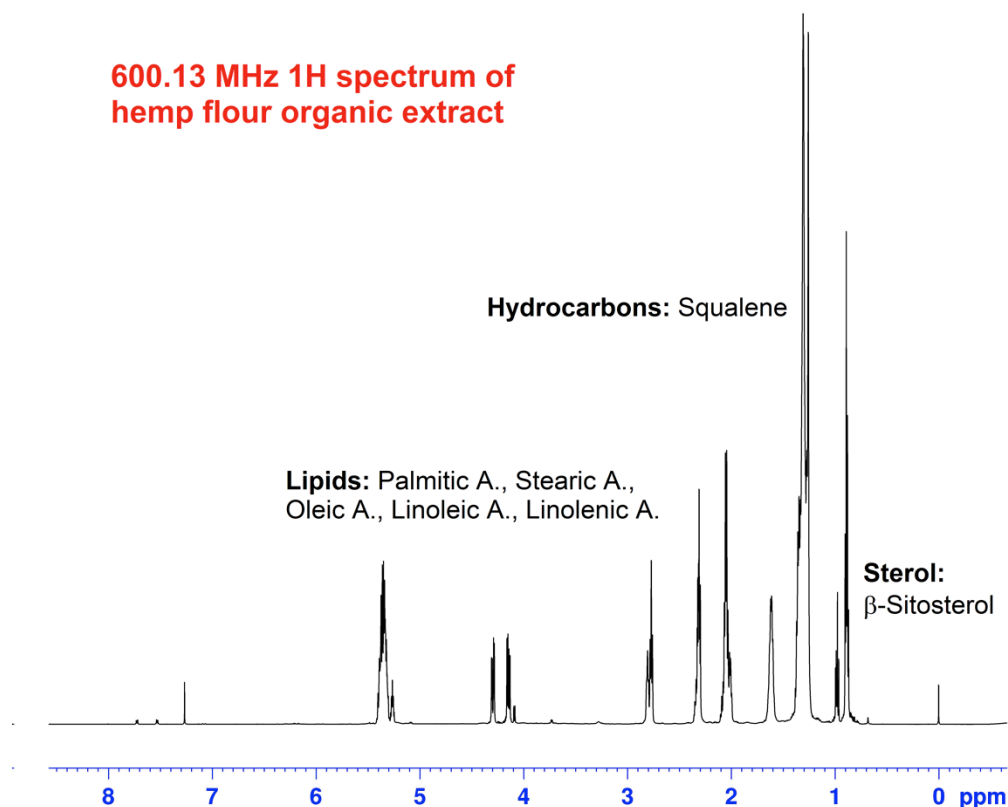


Figure 4.28. ¹H spectrum of a hempseed flour organic extract sample, reporting the metabolites identified.

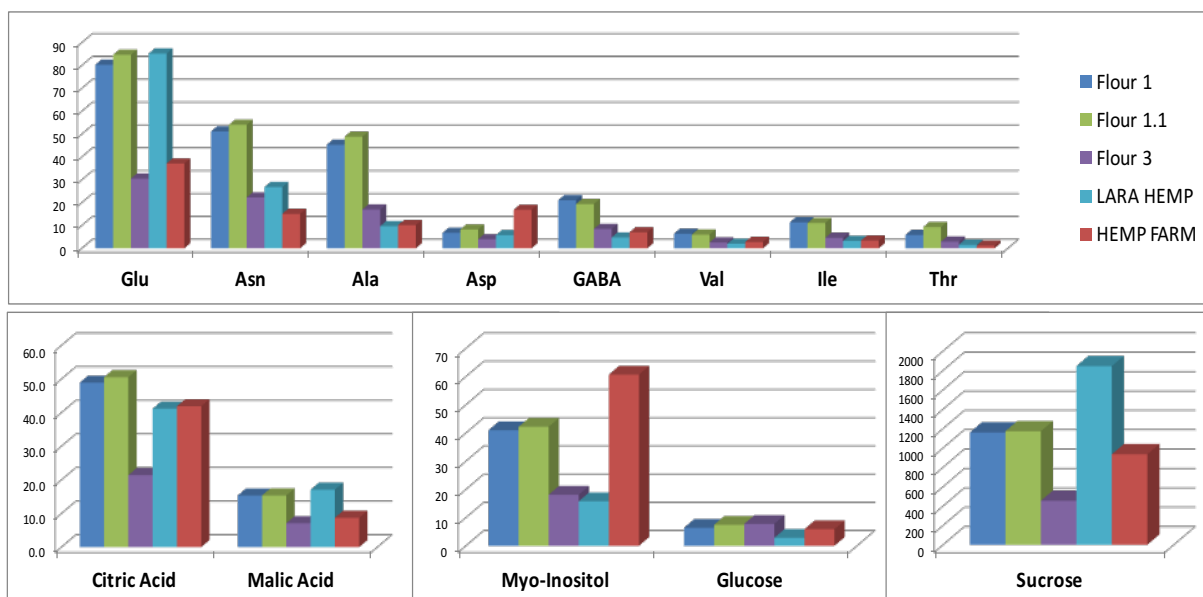


Figure 4.29. Histograms resulting from the quantitative NMR spectroscopic analysis of hydroalcoholic extracts of five hempseed flour samples. Data shown are expressed in mg/100g.

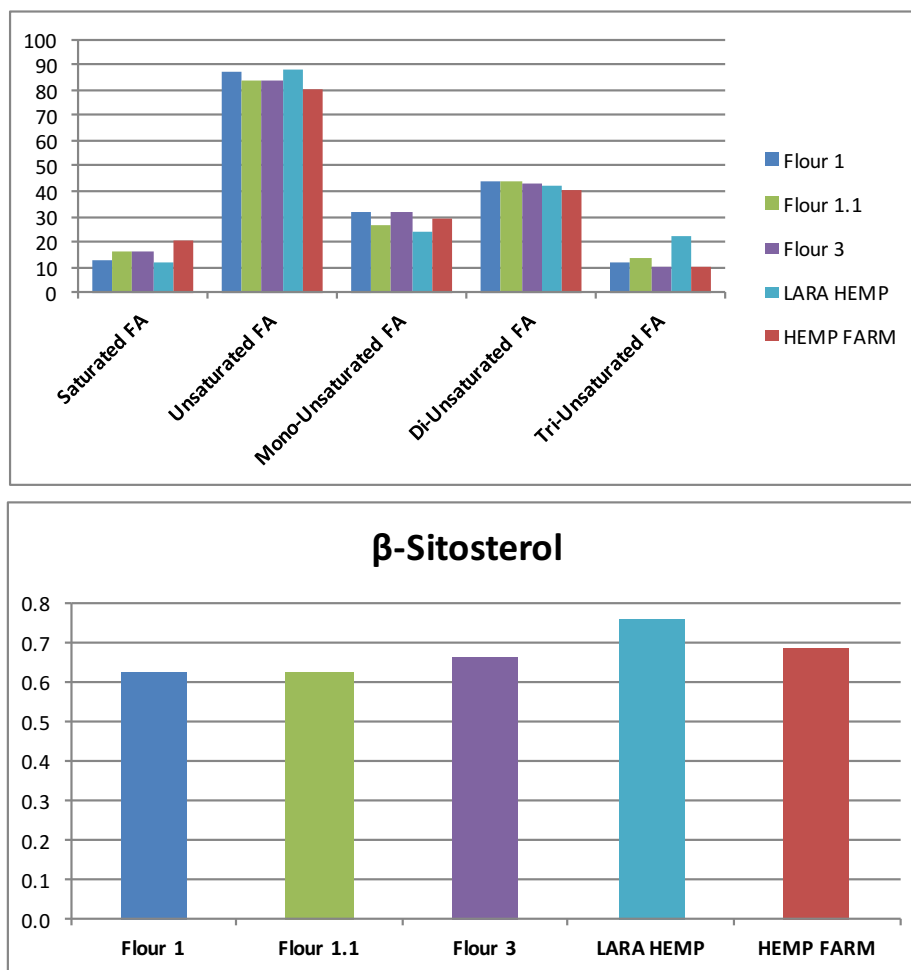


Figure 4.30. Histograms resulting from the quantitative NMR spectroscopic analysis of organic extracts of five hempseed flour samples. Data shown are expressed in %.

Observing the results of the hydroalcoholic extracts, it can be easily noticed that amino acids and choline contents in Flour 1 and Flour 1.1 samples are similar and higher with respect to the other flours. Flour 3, the one with finer granulometry compared to Flour 1 and Flour 1.1, shows a trend more similar to the two commercial flours (Lara Hemp and Hemp Farm) relative to the quantity of the most of the metabolites. However, there are some exceptions considering some metabolite. For example, Lara Hemp flour has an extremely high concentration of glutamate and malic acid that is comparable to that of flours with greater granulometry (Flour 1 and Flour 1.1). Aspartate and myo-inositol contents, instead, are particularly high in Hemp Farm flour with respect the other samples. Lara Hemp flour is

characterized by the highest content of sucrose (1.8g/100g) whereas Flour 3 has the lowest content of this sugar (453mg/100g).

In fatty acids profile, the percentage of di-unsaturated fatty acids is higher than the percentages of mono- and tri-unsaturated ones. Lara Hemp flour results to be the sample with the highest content of tri-unsaturated fatty acids, that is about twice compared to the content in the other flour sample.

4.5.5 References

- Aladic, K., Jarni, K., Barbir, T., Vidovic, S., Vladic, J., Bilic, M., Jokic, S., 2015. Supercritical CO₂ extraction of hemp (*Cannabis sativa* L.) seed oil. *Ind. Crops Prod.* 76, 472-478.
- Amaducci, S., Scordia, D., Liuc, F.H., Zhang, Q., Guo, H., Testa, G., Cosentino, S.L., 2015. Key cultivation techniques for hemp in Europe and China. *Ind. Crops Prod.* 68, 2–16.
- Appendino, G., Gibbons, S., Giana, A., Pagani, A., Grassi, G., Stavri, M., Smith, E., (...), Rahman, M.M., 2008. Antibacterial cannabinoids from *Cannabis sativa*: A structure-activity study. *J. Nat. Prod.* 71(8), 1427-1430.
- Burstein, S., 2015. Cannabidiol (CBD) and its analogs: A review of their effects on inflammation. *Bioorg. Med. Chem.* 23(7), 1377-1385.
- Capitani, D., Sobolev, A.P., Delfini, M., Vista, S., Antiochia, R., Proietti, N., Bubici, S., Ferrante, G., Carradori, S., De Salvador, F. R., Mannina, L., 2014. NMR methodologies in the analysis of blueberries. *Electrophoresis* 35, 1615-1626.
- Camin, F., Pavone, A., Bontempo, L., Wehrens, R., Paolini, M., Faberi, A., Marianella, R.M., Capitani, D., Vista, S., Mannina, L., 2016. The use of IRMS, (1)H NMR and chemical analysis to characterise Italian and imported Tunisian olive oils. *Food Chem.* 196, 98-105.
- Campiglia, E., Radicetti, E., Mancinelli, R., 2017. Plant density and nitrogen fertilization affect agronomic performance of industrial hemp (*Cannabis sativa* L.) in Mediterranean environment. *Ind. Crops Prod.* 100, 246-254.
- Chandra, S., Lata, H., ElSohly, M. A., Walker, L. A., Potter, D., 2017. Cannabis cultivation: Methodological issues for obtaining medical-grade product. *Epilepsy Behav.* 70(Pt B), 302-312.
- Circi, S., Ingallina, C., Vista, S., Capitani, D., Di Vecchia, A., Leonardi, G., D'Achille, G., Centauri, L., Camin, F., Mannina, L., 2018. A Multi-Methodological Protocol to Characterize PDO Olive Oils. *Metabolites* 8(3).
- Citti, C., Pacchetti, B., Vandellic, M.A., Fornic, F., Cannazzab, G., 2018. Analysis of cannabinoids in commercial hemp seed oil and decarboxylation kinetics studies of cannabidiolic acid (CBDA). *J. Pharm. Biomed. Anal.* 149, 532–540.
- Croxford, J.L., Pryce, G., Jackson, S.J., Ledent, C., Giovannoni, G., Pertwee, R.G., Yamamura, T., (...), Baker, D., 2008. Cannabinoid-mediated neuroprotection, not immunosuppression, may be more relevant to multiple sclerosis. *J. Neuroimmunol.* 193(1-2), 120-129.
- Da Porto, C., Decorti, D., Tubaro, F., 2012. Fatty acid composition and oxidation stability of hemp (*Cannabis sativa* L.) seed oil extracted by supercritical carbon dioxide. *Ind. Crops Prod.* 36, 401–404.
- Fekete, S., Oláh, E., Fekete, J., 2012. Fast liquid chromatography: The domination of core-shell and very fine particles. *J. Chromatogr. A* 1228, 57-71.

Fischedick, J.T., Hazekamp, A., Erkelens, T., Choi, T.H., Verpoorte, R., 2010. Metabolic fingerprinting of *Cannabis sativa* L., cannabinoids and terpenoids for chemotaxonomic and drug standardization purposes. *Phytochemistry* 71, 2058–2073.

Frassinetti, S., Moccia, E., Caltavuturo, L., Gabriele, M., Longo, V., Bellania, L., Giorgi, G., Giorgetta, G., 2018. Nutraceutical potential of hemp (*Cannabis sativa* L.) seeds and sprouts. *Food Chem.* 262, 56–66.

Ingrao, C., Lo Giudice, A., Bacenetti, J., Tricase, C., Dotelli, G., Fiala, M., Siracusa, V., Mbohwa, C., 2015. Energy and environmental assessment of industrial hemp for building applications: A review. *Renew. Sust. Energ. Rev.* 51, 29-42.

Korus, J., Witzcak, M., Ziobro, R., Juszczak, L., 2017. Hemp (*Cannabis sativa* subsp. *sativa*) flour and protein preparation as natural nutrients and structure forming agents in starch based gluten- free bread. *LWT - Food Sci. Technol.* 84, 143-150.

Kreuger, E., Prade, T., Escobar, F., Svensson, S.-E., Englund, J.-E., Björnsson, L., 2011. Anaerobic digestion of industrial hemp—Effect of harvest time on methane energy yield per hectare. *Biomass Bioenergy* 35(2), 893-900.

Lühr, C., Pecenka, R., Budde, J., Hoffmann, T., Gusovius, H.-J., 2018. Comparative investigations of fibreboards resulting from selected hemp varieties. *Ind. Crops Prod.* 118, 81-94.

Mikulcová, V., Kašpárková, V., Humpolíček, P., Bunková, L., 2017. Formulation, Characterization and Properties of Hemp Seed Oil and Its Emulsions. *Molecules* 22, 700.

Montserrat-de la Paz, S., Marín-Aguilar, F., García-Giménez, M.D., Fernández-Arche, M.A., 2014. Hemp (*Cannabis sativa* L.) Seed Oil: Analytical and Phytochemical Characterization of the Unsaponifiable Fraction. *J. Agric. Food Chem.* 62, 1105-1110.

Nalli, Y., Arora, P., Riyaz-UI-Hassan, S., Ali, A., 2018. Chemical investigation of *Cannabis sativa* leading to the discovery of a prenylspiroidinone with anti-microbial potential. *Tetrahedron Lett.* 59, 2470–2472.

Nissen, L., Zatta, A., Stefanini, I., Grandi, S., Sgorbati, B., Biavati, B., Monti, A., 2010. Characterization and antimicrobial activity of essential oils of industrial hemp varieties (*Cannabis sativa* L.). *Fitoterapia* 81, 413-419.

Oomaha, B.D., Bussonb, M., Godfrey, D.V., Drovera, J.C.G., 2002. Characteristics of hemp (*Cannabis sativa* L.) seed oil. *Food Chem.* 76, 33-43.

Sobolev, A.P., Segre, A., Lamanna, R., 2003. Proton high-field NMR study of tomato juice. *Magn. Res. Chem.* 41(4), 237-245.

Yu, L.L., Zhou, K.K., Parry, J., 2005. Antioxidant properties of cold-pressed black caraway, carrot, cranberry, and hemp seed oils. *Food Chemistry* 91, 723–729.

Zhou, Y., Wang, S., Lou, H., Fan, P., 2018. Chemical constituents of hemp (*Cannabis sativa* L.) seed with potential anti- neuroinflammatory activity. *Phytochem. Lett.*, 57-61.

Chapter 5: Olive Oils

5.1 Panel Test and Chemical Analyses of commercial Olive Oils

5.1.1 Introduction

EEC Regulation 2568/91 (Commission Regulation (EEC) No. 2568/91) and International Olive Council (IOC) (IOC/T.20/Doc. No. 15/Rev. 8/2015) have established both analytical and organoleptic criteria to define the quality grade of an olive oil. According to the results of chemical and sensory analyses, an olive oil can be classified as extra virgin olive oil (EVOO), virgin olive oil or lampante olive oil. Each category has a completely different commercial and nutritional value. Extra virgin olive oil (EVOO) is a natural fruit juice with peculiar nutritional, healthy (Frankel, 2011) and sensory (Angerosa, 2000) qualities as well as it represents a fundamental component of Mediterranean diet which is very rich in mono-unsaturated fatty acids (Salas, Harwood et Martinez-Force, 2013) and polyphenols (Commission Regulation (EU) No. 432/2012). On the contrary, lampante olive oils have a distinctly unpleasant smell, are not edible and are used for the production of refined olive oils. It is well known that selling virgin olive oils or lampante olive oils as EVOOs is a fraud. However, another important aspect to consider is that the downgrading of an EVOO to a lower category implies a big economic loss for the producers. So, it is fundamental that both the chemical analyses and the organoleptic evaluations used to define quality grade are “sufficiently” objective and reproducible.

Here, a pilot analysis of data supplied by International Certificated Body, relative to 16 olive oils produced in the Mediterranean area, was carried out to verify reproducibility and consistency of chemical analyses and organoleptic evaluations and therefore to highlight

possible problems relative to quality grade classification. ICB data, including chemical analyses and organoleptic evaluations, were produced by nine official IOC labs according to EEC Regulation 2568/91. The recent scandals involving Italian olive oils, such as the one revealed in the 'New York Times' (Camin et al., 2016), prompted us to include data from olive oils purchased not only in Italy, the largest consumer of EVOOs, but also in non-Mediterranean countries such as USA.

5.1.2 Material and Methods

Olive oils (16 samples) of 2014/2015 harvest year were purchased in Italy and Miami (USA) by an International Certificated Body, a recognized EU company that deals with services of certification. ICB also verified the preparation of samples carried out according to EN ISO 5555 reported in EEC Regulation 2568/91, shipped olive oils to laboratories and released a report on all the activity. Samples were collected and labelled with an alphanumeric code without any reference to the origin country. Brands and the packaging places of olive oils were made purposely anonymous to avoid damage from a possible negative or defamatory propaganda.

Chemical analyses and organoleptic evaluation were carried out by nine recognized IOC laboratories, selected from the lists of IOC-recognized laboratories (IOC/T.21/Doc. No. 13/Rev. 17/2014; IOC/T.28/Doc. No. 3/Rev. 17/2014), see Table 5.1, located in countries with a well-recognized tradition in the production of olive oils such as Italy (5 labs in Abruzzo, Lazio, Liguria, Sicily and Veneto regions), Spain (2 labs), and Greece (1 lab). A Slovenian lab was also included as a reference for the Eastern countries.

Chemical analyses included the determination of free acidity, peroxide index, UV spectrophotometric evaluation (K 232, K 270, ΔK), fatty acid ethyl esters (FAEE) and stigmadiens content. Stigmadiens content, a parameter closely related to the presence of refined oils rather than a quality marker, was also considered as genuineness index. All the

analyses were carried out according to the EEC Regulation 2568/91 (Annex II, III, IX, XVII, XX). For the determination of free acidity and peroxide index, the Slovenian lab used IOC method (ISO 660:2009 and ISO 3960:2010, respectively).

According to the official method (EEC Regulation 2568/91, Annex XII), in each IOC lab, organoleptic evaluations were carried out by a group of 8–12 professional tasters trained to recognize, describe and quantify basic taste and odour properties. Olive oils were described through positive (“fruity”, “bitter” and “pungent”) and negative (for instance “rancid”, “fusty”, “musty” and “winey”) attributes.

Quality grade classifications of olive oils purchased in Italy and in USA were determined by our laboratory according to EEC Regulation 2568/91.

Table 5.1. IOC laboratories chosen to carry out chemical analyses and organoleptic evaluation.

| IOC Labs | Scientific Director and Address of IOC laboratories |
|---------------------|--|
| Greece | Aliki Gali, Ministry for Development, Competitiveness, Infrastructure, Transport & Networks - General Secretariat of Consumer Affairs; Chemical Laboratories; Cannigos Square - 2010181 ATHENS |
| Slovenia | Milena Bucar Miklavcic, University of Primorska, Science and Research Centre of Koper, Garibaldijeva, 1 - 6000 KOPER (Laboratory for olive oil testing, Headquarters of laboratory: Zelena Ulica 8 - 6310 IZOLA) |
| Spain 1 | Fernando Martínez Román, Instituto de la Grasa, Consejo Superior de Investigaciones Científicas, Universidad Pablo de Olavide, edificio n°46. Carretera Utrera, Km 1 - 41013 SEVILLA |
| Spain 2 | Yolanda Avilés Mora, Laboratorio Agroalimentario de Córdoba, Dirección General de Industrias y Promoción Agroalimentaria, Consejería de Agricultura y Pesca - Junta de Andalucía, Avda. Menéndez Pidal s/n - 14004 CÓRDOBA |
| Abruzzo (IT) | Luciana Di Giacinto, CRA – OLI, Centro di Ricerca per l’Olivicoltura e l’Industria Olearia, Sede Scientífica di Pescara, Viale Petrucci, 75 - 65013 C. SANT'ANGELO (PE) |
| Lazio (IT) | Gianfranco De Felici, S.O. Laboratorio Chimico Regionale di Roma, Agenzia delle Dogane, Via M. Carucci, 71 - 00143 ROMA |
| Liguria (IT) | Cristina Borgogni, Direzione Regionale per la Liguria, Laboratorio Chimico di Genova - Agenzia delle Dogane, Via Rubattino n. 6 - 16126 GENOVA |
| Sicily (IT) | Rosalía Linda Pipia, Direzione Regionale per la Sicilia, Laboratorio e Servizi Chimici di Palermo - Agenzia delle Dogane, Via Francesco Crispi, n. 143 - 90133 PALERMO |
| Veneto (IT) | GianPaolo Fasoli, S.O. Laboratorio Chimico Regionale di Verona, Agenzia delle Dogane, Via Sommacampagna 61/a - 87137 VERONA |

5.1.3 Results and Discussion

Chemical analysis results regarding olive oils from Italy and USA are reported in Tables 5.2 and 5.3, respectively.

Quality grade classifications of olive oils purchased in Italy and in USA, reported in Tables 5.4 and 5.5, respectively, were determined according to EEC Regulation 2568/91 and will be discussed separately. Defects detected by panel test of olive oils purchased in Italy and Miami are reported in Tables 5.6 and Table 5.7, respectively, whereas positive attributes are reported in Table 5.8. Classification percentages of the olive oils purchased in Italy and in USA are reported in Tables 5.9 and Table 5.10, respectively.

Table 5.2. Chemical analyses results performed by IOC laboratories on 8 olive oils purchased in Italy.

| O _i 1 | Free Acidity (% Oleic Acid) | Peroxide Index (meq O ₂ /Kg) | K 232 | K 270 | ΔK | FAEE (mg/Kg) | Stigmadienes (mg/Kg) |
|------------------|-----------------------------|---|--------------------------|----------------------------|-----------------------------|-------------------------|----------------------|
| Greece | /* | / | / | / | / | / | / |
| Slovenia | 0.26 ± 0.03 ¹ | 9.8 ± 1.8 ² | 1.80 ± 0.04 ³ | 0.147 ± 0.009 ⁴ | -0.002 ± 0.001 ⁵ | 30.2 ± 4.2 ⁶ | 0.0491 ± 0.0280 |
| Spain 1 | / | / | / | / | / | / | / |
| Abruzzo (IT) | 0.23 ± 0.02 | 11.1 ± 0.1 | 1.79 ± 0.04 | 0.151 ± 0.040 | -0.001 ± 0.001 | 29 ± 1 | 0.04 ± 0.01 |
| Lazio (IT) | / | / | / | / | / | / | / |
| Liguria (IT) | 0.2 ± 0.1 | 9 ± 2 | 1.88 ± 0.16 | 0.20 ± 0.06 | 0.00 ± 0.01 | 32 ± 8 | 0.06 ± 0.01 |
| Sicily (IT) | 0.24 ± 0.05 | 11 ± 3 | 1.77 ± 0.05 | 0.14 ± 0.02 | 0.002 ± 0.006 | 28 ± 8 | 0.04 ± 0.02 |
| Veneto (IT) | 0.28 ± 0.06 | 10.0 ± 2.3 | 2.12 ± 0.39 | 0.16 ± 0.04 | 0.002 ± 0.002 | 28 | 0.04 |
| O _i 2 | Free Acidity (% Oleic Acid) | Peroxide Index (meq O ₂ /Kg) | K 232 | K 270 | ΔK | FAEE (mg/Kg) | Stigmadienes (mg/Kg) |
| Greece | / | / | / | / | / | / | / |
| Slovenia | 0.35 ± 0.30 | 12.8 ± 2.3 | 2.07 ± 0.04 | 0.176 ± 0.009 | 0.001 ± 0.001 | 36.8 ± 5.1 | 0.0376 ± 0.0088 |
| Spain 1 | / | / | / | / | / | / | / |
| Abruzzo (IT) | 0.34 ± 0.02 | 13.5 ± 0.1 | 1.891 ± 0.004 | 0.160 ± 0.004 | 0.0040 ± 0.0001 | 37 ± 1 | 0.03 ± 0.01 |
| Lazio (IT) | / | / | / | / | / | / | / |
| Liguria (IT) | 0.3 ± 0.1 | 13 ± 2 | 1.96 ± 0.17 | 0.19 ± 0.06 | 0.00 ± 0.01 | 38 ± 10 | 0.03 ± 0.01 |
| Sicily (IT) | 0.36 ± 0.05 | 13 ± 3 | 1.95 ± 0.05 | 0.21 ± 0.02 | 0.0000 ± 0.0006 | 30 ± 9 | 0.05 ± 0.02 |
| Veneto (IT) | 0.35 ± 0.06 | 13.0 ± 2.3 | 2.04 ± 0.39 | 0.17 ± 0.04 | 0.001 ± 0.002 | 33 | 0.02 |

| O _i 3 | Free Acidity (% Oleic Acid) | Peroxide Index (meq O ₂ /Kg) | K 232 | K 270 | ΔK | FAEE (mg/Kg) | Stigmadienes (mg/Kg) |
|------------------|--------------------------------|--|---------------|---------------|-----------------|-----------------|-------------------------|
| Greece | / | / | / | / | / | / | / |
| Slovenia | 0.24 ± 0.03 | 7.3 ± 1.3 | 1.78 ± 0.04 | 0.201 ± 0.009 | 0.004 ± 0.001 | 24.6 ± 3.4 | 0.0238 ± 0.0068 |
| Spain 1 | / | / | / | / | / | / | / |
| Abruzzo (IT) | 0.23 ± 0.02 | 9.4 ± 0.1 | 1.615 ± 0.004 | 0.168 ± 0.004 | 0.0090 ± 0.0001 | 25 ± 1 | 0.01 ± 0.01 |
| Lazio (IT) | / | / | / | / | / | / | / |
| Liguria (IT) | 0.2 ± 0.1 | 8 ± 2 | 1.74 ± 0.15 | 0.20 ± 0.06 | 0.00 ± 0.01 | 27 ± 7 | 0.01 ± 0.01 |
| Sicily (IT) | 0.23 ± 0.05 | 8 ± 3 | 1.60 ± 0.05 | 0.17 ± 0.02 | 0.004 ± 0.006 | 20 ± 6 | 0.05 ± 0.02 |
| Veneto (IT) | 0.24 ± 0.06 | 8.0 ± 2.3 | 1.82 ± 0.39 | 0.18 ± 0.04 | 0.004 ± 0.002 | 23.7 | 0.03 |
| O _i 4 | Free Acidity (% Oleic Acid) | Peroxide Index (meq O ₂ /Kg) | K 232 | K 270 | ΔK | FAEE (mg/Kg) | Stigmadienes (mg/Kg) |
| Greece | / | / | / | / | / | / | / |
| Slovenia | 0.28 ± 0.03 | 6.2 ± 1.1 | 1.79 ± 0.04 | 0.122 ± 0.009 | 0.000 ± 0.001 | 35.1 ± 4.9 | < 0.01 |
| Spain 1 | / | / | / | / | / | / | / |
| Abruzzo (IT) | 0.28 ± 0.02 | 7.9 ± 0.1 | 1.760 ± 0.004 | 0.117 ± 0.004 | 0.000 ± 0.001 | 35 ± 1 | 0.03 ± 0.01 |
| Lazio (IT) | / | / | / | / | / | / | / |
| Liguria (IT) | 0.3 ± 0.1 | 8 ± 2 | 1.84 ± 0.16 | 0.13 ± 0.04 | 0.00 ± 0.01 | 40 ± 12 | 0.01 ± 0.01 |
| Sicily (IT) | 0.27 ± 0.05 | 8 ± 3 | 1.78 ± 0.05 | 0.12 ± 0.02 | 0.004 ± 0.006 | 33 ± 9 | 0.05 ± 0.02 |
| Veneto (IT) | 0.26 ± 0.06 | 7.0 ± 2.3 | 1.98 ± 0.39 | 0.13 ± 0.04 | 0.001 ± 0.002 | 39.7 | 0.02 |
| O _i 5 | Free Acidity (% Oleic Acid) | Peroxide Index (meq O ₂ /Kg) | K 232 | K 270 | ΔK | FAEE (mg/Kg) | Stigmadienes (mg/Kg) |
| Greece | / | / | / | / | / | / | / |
| Slovenia | 0.39 ± 0.03 | 8.2 ± 1.5 | 1.86 ± 0.04 | 0.140 ± 0.009 | -0.002 ± 0.001 | 35.5 ± 5.0 | 0.0136 ± 0.0025 |
| Spain 1 | / | / | / | / | / | / | / |
| Abruzzo (IT) | 0.36 ± 0.02 | 9.1 ± 0.1 | 1.812 ± 0.004 | 0.138 ± 0.004 | -0.001 ± 0.001 | 36 ± 1 | 0.02 ± 0.01 |
| Lazio (IT) | / | / | / | / | / | / | / |
| Liguria (IT) | 0.4 ± 0.1 | 8 ± 2 | 1.96 ± 0.17 | 0.16 ± 0.05 | 0.00 ± 0.01 | 39 ± 10 | 0.01 ± 0.01 |
| Sicily (IT) | 0.36 ± 0.05 | 9 ± 3 | 1.69 ± 0.05 | 0.12 ± 0.02 | 0.001 ± 0.006 | 36 ± 10 | 0.04 ± 0.02 |
| Veneto (IT) | 0.38 ± 0.06 | 8.0 ± 2.3 | 1.96 ± 0.39 | 0.16 ± 0.04 | 0.002 ± 0.002 | 35 | 0.04 |
| O _i 6 | Free Acidity (% Oleic Acid) | Peroxide Index (meq O ₂ /Kg) | K 232 | K 270 | ΔK | FAEE (mg/Kg) | Stigmadienes (mg/Kg) |
| Greece | / | / | / | / | / | / | / |
| Slovenia | 0.19 ± 0.03 | 8.9 ± 1.6 | 2.21 ± 0.04 | 0.149 ± 0.009 | -0.001 ± 0.001 | 11.7 ± 1.6 | 0.0129 ± 0.0023 |
| Spain 1 | / | / | / | / | / | / | / |
| Abruzzo (IT) | 0.16 ± 0.02 | 10.2 ± 0.1 | 2.089 ± 0.004 | 0.136 ± 0.004 | -0.001 ± 0.001 | 14 ± 1 | 0.02 ± 0.01 |
| Lazio (IT) | / | / | / | / | / | / | / |
| Liguria | 0.2 ± 0.1 | 9 ± 2 | 2.16 ± 0.19 | 0.17 ± 0.06 | 0.00 ± 0.01 | 10 ± 3 | < 0.01 ± 0.01 |

| (IT) | | | | | | | |
|------------------|-----------------------------|---|---------------|---------------|----------------|--------------|----------------------|
| Sicily (IT) | 0.16 ± 0.05 | 11 ± 3 | 2.12 ± 0.05 | 0.16 ± 0.02 | 0.000 ± 0.006 | 10 ± 4 | 0.03 ± 0.02 |
| Veneto (IT) | 0.18 ± 0.06 | 9.0 ± 2.3 | 2.26 ± 0.39 | 0.16 ± 0.04 | 0.002 ± 0.002 | 11 | 0.02 |
| O _i 7 | Free Acidity (% Oleic Acid) | Peroxide Index (meq O ₂ /Kg) | K 232 | K 270 | ΔK | FAEE (mg/Kg) | Stigmadienes (mg/Kg) |
| Greece | / | / | / | / | / | / | / |
| Slovenia | 0.23 ± 0.03 | 7.9 ± 1.4 | 1.86 ± 0.04 | 0.126 ± 0.009 | -0.003 ± 0.001 | 24.4 ± 3.4 | 0.0176 ± 0.0032 |
| Spain 1 | / | / | / | / | / | / | / |
| Abruzzo (IT) | 0.23 ± 0.02 | 9.7 ± 1.0 | 1.807 ± 0.004 | 0.126 ± 0.004 | -0.003 ± 0.001 | 30 ± 1 | 0.02 ± 0.01 |
| Lazio (IT) | / | / | / | / | / | / | / |
| Liguria (IT) | 0.2 ± 0.1 | 8 ± 2 | 1.87 ± 0.16 | 0.15 ± 0.05 | 0.00 ± 0.01 | 32 ± 8 | 0.01 ± 0.01 |
| Sicily (IT) | 0.22 ± 0.05 | 8 ± 3 | 1.87 ± 0.05 | 0.15 ± 0.02 | 0.003 ± 0.006 | 20 ± 6 | 0.02 ± 0.02 |
| Veneto (IT) | 0.25 ± 0.06 | 9.0 ± 2.3 | 1.99 ± 0.39 | 0.14 ± 0.04 | 0.004 ± 0.002 | 22 | 0.04 |
| O _i 8 | Free Acidity (% Oleic Acid) | Peroxide Index (meq O ₂ /Kg) | K 232 | K 270 | ΔK | FAEE (mg/Kg) | Stigmadienes (mg/Kg) |
| Greece | / | / | / | / | / | / | / |
| Slovenia | 0.31 ± 0.03 | 11.6 ± 2.1 | 2.38 ± 0.04 | 0.152 ± 0.009 | -0.002 ± 0.001 | 29.0 ± 4.1 | 0.0161 ± 0.0030 |
| Spain 1 | / | / | / | / | / | / | / |
| Abruzzo (IT) | 0.32 ± 0.01 | 13.1 ± 0.1 | 2.049 ± 0.004 | 0.143 ± 0.004 | -0.002 ± 0.001 | 33 ± 1 | 0.03 ± 0.01 |
| Lazio (IT) | / | / | / | / | / | / | / |
| Liguria (IT) | 0.3 ± 0.1 | 11 ± 2 | 2.57 ± 0.22 | 0.18 ± 0.06 | 0.00 ± 0.01 | 31 ± 8 | 0.01 ± 0.01 |
| Sicily (IT) | 0.32 ± 0.05 | 13 ± 3 | 2.35 ± 0.05 | 0.15 ± 0.02 | 0.002 ± 0.006 | 25 ± 7 | 0.04 ± 0.02 |
| Veneto (IT) | 0.33 ± 0.06 | 13.0 ± 2.3 | 2.49 ± 0.39 | 0.16 ± 0.04 | 0.003 ± 0.002 | 27 | 0.04 |

/* = Analysis was not performed.

The limits of the parameters of quality and genuineness of an EVOO are (¹) ≤ 0.8, (²) ≤ 20, (³) ≤ 2.50, (⁴) ≤ 0.22, (⁵) ≤ 0.01, (⁶) ≤ 35 (for crop year 2014/2015).

The limits of the parameters of a virgin olive oil are 2 ≤ (¹) ≤ 0.8, (²) ≤ 20, (³) ≤ 2.60, (⁴) ≤ 0.25, (⁵) ≤ 0.01.

Table 5.3. Chemical analyses results performed by IOC laboratories on 8 olive oils purchased in USA (Miami).

| O _u 1 | Free Acidity (% Oleic Acid) | Peroxide Index (meq O ₂ /Kg) | K 232 | K 270 | ΔK | FAEE (mg/Kg) | Stigmadienes (mg/Kg) |
|------------------|-----------------------------|---|-------------|---------------|----------------|--------------|----------------------|
| Greece | /* | / | / | / | / | / | / |
| Slovenia | 0.41 ± 0.03 | 9.1 ± 1.6 | 2.17 ± 0.04 | 0.130 ± 0.009 | -0.002 ± 0.001 | 34.5 ± 4.8 | 0.0117 ± 0.0021 |
| Spain 1 | / | / | / | / | / | / | / |
| Spain 2 | 0.39 | 10.60 | 2.27 | 0.13 | < 0.01 | 38.80 | < 0.05 |
| Lazio (IT) | / | / | / | / | / | / | / |
| Liguria (IT) | 0.4 ± 0.1 | 10 ± 2 | 2.32 ± 0.20 | 0.14 ± 0.04 | 0.00 ± 0.01 | 35 ± 9 | < 0.01 ± 0.01 |
| Sicily (IT) | 0.40 ± 0.05 | 10 ± 3 | 2.04 ± 0.05 | 0.09 ± 0.02 | 0.002 ± 0.006 | 37 ± 10 | 0.01 ± 0.02 |
| Veneto | 0.40 ± 0.06 | 10.0 ± 2.3 | 2.45 ± 0.39 | 0.15 ± 0.04 | 0.003 ± 0.002 | 34 | 0.02 |

| (IT) | | | | | | | |
|------------------|--------------------------------|--|-------------|---------------|----------------|-----------------|-------------------------|
| O _u 2 | Free Acidity (% Oleic Acid) | Peroxide Index (meq O ₂ /Kg) | K 232 | K 270 | ΔK | FAEE (mg/Kg) | Stigmadienes (mg/Kg) |
| Greece | / | / | / | / | / | / | / |
| Slovenia | 0.27 ± 0.03 | 16.0 ± 2.9 | 2.79 ± 0.04 | 0.225 ± 0.009 | 0.004 ± 0.001 | < 15 | 0.089 ± 0.016 |
| Spain 1 | / | / | / | / | / | / | / |
| Spain 2 | / | / | / | / | / | / | / |
| Lazio (IT) | / | / | / | / | / | / | / |
| Liguria (IT) | 0.3 ± 0.1 | 18 ± 2 | 2.98 ± 0.26 | 0.23 ± 0.07 | 0.00 ± 0.01 | 22 ± 6 | 0.10 ± 0.02 |
| Sicily (IT) | 0.28 ± 0.05 | 20 ± 3 | 2.76 ± 0.05 | 0.24 ± 0.02 | 0.002 ± 0.006 | 22 ± 7 | 0.10 ± 0.03 |
| Veneto (IT) | 0.27 ± 0.06 | 17.8 ± 2.3 | 3.08 ± 0.39 | 0.24 ± 0.04 | 0.002 ± 0.002 | 15 | 0.06 |
| O _u 3 | Free Acidity (% Oleic Acid) | Peroxide Index (meq O ₂ /Kg) | K 232 | K 270 | ΔK | FAEE (mg/Kg) | Stigmadienes (mg/Kg) |
| Greece | / | / | / | / | / | / | / |
| Slovenia | 0.41 ± 0.03 | 12.0 ± 2.2 | 2.84 ± 0.04 | 0.266 ± 0.009 | 0.006 ± 0.001 | 18.6 ± 2.6 | 0.0392 ± 0.0071 |
| Spain 1 | / | / | / | / | / | / | / |
| Spain 2 | 0.41 | 16.90 | 2.71 | 0.28 | 0.01 | 27.60 | < 0.05 |
| Lazio (IT) | / | / | / | / | / | / | / |
| Liguria (IT) | 0.4 ± 0.1 | 14 ± 2 | 2.98 ± 0.26 | 0.28 ± 0.09 | 0.00 ± 0.01 | 25 ± 6 | 0.05 ± 0.01 |
| Sicily (IT) | 0.43 ± 0.05 | 16 ± 3 | 2.79 ± 0.05 | 0.29 ± 0.02 | 0.006 ± 0.006 | 28 ± 8 | 0.05 ± 0.02 |
| Veneto (IT) | 0.41 ± 0.06 | 14.6 ± 2.3 | 3.02 ± 0.39 | 0.30 ± 0.04 | 0.005 ± 0.002 | 28 | 0.06 |
| O _u 4 | Free Acidity (% Oleic Acid) | Peroxide Index (meq O ₂ /Kg) | K 232 | K 270 | ΔK | FAEE (mg/Kg) | Stigmadienes (mg/Kg) |
| Greece | / | / | / | / | / | / | / |
| Slovenia | 0.21 ± 0.03 | 7.9 ± 1.4 | 1.90 ± 0.04 | 0.140 ± 0.009 | -0.001 ± 0.001 | 39.0 ± 5.5 | 0.0162 ± 0.0029 |
| Spain 1 | / | / | / | / | / | / | / |
| Spain 2 | 0.21 | 8.80 | 2.05 | 0.14 | < 0.01 | 47.80 | < 0.05 |
| Lazio (IT) | / | / | / | / | / | / | / |
| Liguria (IT) | 0.2 ± 0.1 | 8 ± 2 | 2.00 ± 0.17 | 0.16 ± 0.05 | 0.00 ± 0.01 | 45 ± 11 | 0.01 ± 0.01 |
| Sicily (IT) | 0.21 ± 0.05 | 10 ± 3 | 1.85 ± 0.05 | 0.14 ± 0.02 | 0.007 ± 0.006 | 49 ± 13 | 0.02 ± 0.02 |
| Veneto (IT) | 0.21 ± 0.06 | 8.3 ± 2.3 | 2.12 ± 0.39 | 0.18 ± 0.04 | 0.002 ± 0.002 | 46 | 0.05 |
| O _u 5 | Free Acidity (% Oleic Acid) | Peroxide Index (meq O ₂ /Kg) | K 232 | K 270 | ΔK | FAEE (mg/Kg) | Stigmadienes (mg/Kg) |
| Greece | / | / | / | / | / | / | / |
| Slovenia | 0.21 ± 0.03 | 8.6 ± 1.6 | 1.92 ± 0.04 | 0.238 ± 0.009 | 0.007 ± 0.001 | 39.5 ± 5.5 | 0.0331 ± 0.0060 |
| Spain 1 | / | / | / | / | / | / | / |
| Spain 2 | 0.20 | 9.60 | 2.04 | 0.24 | 0.01 | 43.20 | < 0.05 |
| Lazio (IT) | / | / | / | / | / | / | / |
| Liguria (IT) | 0.3 ± 0.1 | 9 ± 2 | 2.16 ± 0.19 | 0.27 ± 0.08 | 0.01 ± 0.01 | 43 ± 11 | 0.03 ± 0.01 |

| | | | | | | | |
|------------------------|------------------------------------|--|--------------|---------------|-----------------|---------------------|-----------------------------|
| Sicily (IT) | 0.22 ± 0.05 | 10 ± 3 | 1.99 ± 0.05 | 0.26 ± 0.02 | 0.007 ± 0.006 | 48 ± 13 | 0.03 ± 0.02 |
| Veneto (IT) | 0.22 ± 0.06 | 8.7 ± 2.3 | 2.10 ± 0.39 | 0.25 ± 0.04 | 0.006 ± 0.002 | 38 | 0.03 |
| O_u 6 | Free Acidity (% Oleic Acid) | Peroxide Index (meq O₂/Kg) | K 232 | K 270 | ΔK | FAEE (mg/Kg) | Stigmadienes (mg/Kg) |
| Greece | / | / | / | / | / | / | / |
| Slovenia | 0.25 ± 0.03 | 9.9 ± 1.8 | 2.00 ± 0.04 | 0.129 ± 0.009 | -0.003 ± 0.001 | 29.7 ± 4.2 | 0.0084 ± 0.0015 |
| Spain 1 | / | / | / | / | / | / | / |
| Spain 2 | 0.23 | 13.20 | 2.04 | 0.13 | < 0.01 | 35.00 | < 0.05 |
| Lazio (IT) | / | / | / | / | / | / | / |
| Liguria (IT) | 0.30 ± 0.01 | 11 ± 2 | 2.03 ± 0.18 | 0.14 ± 0.05 | 0.00 ± 0.01 | 32 ± 8 | 0.01 ± 0.01 |
| Sicily (IT) | 0.39 ± 0.05 | 9 ± 3 | 1.93 ± 0.05 | 0.13 ± 0.02 | 0.003 ± 0.006 | 34 ± 9 | 0.01 ± 0.02 |
| Veneto (IT) | 0.24 ± 0.06 | 10.9 ± 2.3 | 2.14 ± 0.39 | 0.15 ± 0.04 | 0.004 ± 0.002 | 29 | 0.05 |
| O_u 7 | Free Acidity (% Oleic Acid) | Peroxide Index (meq O₂/Kg) | K 232 | K 270 | ΔK | FAEE (mg/Kg) | Stigmadienes (mg/Kg) |
| Greece | / | / | / | / | / | / | / |
| Slovenia | 0.27 ± 0.03 | 10.0 ± 1.8 | 1.95 ± 0.04 | 0.148 ± 0.009 | -0.001 ± 0.001 | 63.8 ± 8.9 | 0.0257 ± 0.0046 |
| Spain 1 | / | / | / | / | / | / | / |
| Spain 2 | 0.26 | 11.80 | 1.99 | 0.14 | < 0.01 | 67.40 | < 0.05 |
| Lazio (IT) | / | / | / | / | / | / | / |
| Liguria (IT) | 0.3 ± 0.1 | 10 ± 2 | 2.07 ± 0.18 | 0.14 ± 0.05 | 0.00 ± 0.01 | 65 ± 17 | 0.01 ± 0.01 |
| Sicily (IT) | 0.27 ± 0.05 | 12 ± 3 | 1.95 ± 0.05 | 0.15 ± 0.02 | 0.001 ± 0.006 | 72 ± 18 | 0.01 ± 0.02 |
| Veneto (IT) | 0.26 ± 0.06 | 10.7 ± 2.3 | 2.17 ± 0.39 | 0.16 ± 0.04 | 0.002 ± 0.002 | 60 | 0.02 |
| O_u 8 | Free Acidity (% Oleic Acid) | Peroxide Index (meq O₂/Kg) | K 232 | K 270 | ΔK | FAEE (mg/Kg) | Stigmadienes (mg/Kg) |
| Greece | / | / | / | / | / | / | / |
| Slovenia | 0.32 ± 0.03 | 8.0 ± 1.4 | 2.01 ± 0.04 | 0.145 ± 0.009 | - 0.002 ± 0.001 | 29.8 ± 4.2 | < 0.01 |
| Spain 1 | / | / | / | / | / | / | / |
| Spain 2 | 0.30 | 12.00 | 2.16 | 0.15 | < 0.01 | 33.20 | < 0.05 |
| Lazio (IT) | / | / | / | / | / | / | / |
| Liguria (IT) | 0.3 ± 0.1 | 9 ± 2 | 2.15 ± 0.19 | 0.15 ± 0.04 | 0.00 ± 0.01 | 29 ± 8 | 0.01 ± 0.01 |
| Sicily (IT) | 0.31 ± 0.05 | 8 ± 3 | 2.03 ± 0.05 | 0.16 ± 0.02 | 0.002 ± 0.006 | 32 ± 9 | 0.01 ± 0.02 |
| Veneto (IT) | 0.29 ± 0.06 | 10.1 ± 2.3 | 2.20 ± 0.39 | 0.16 ± 0.04 | 0.003 ± 0.002 | 28 | 0.04 |

/*= Analysis was not performed.

Table 5.4. Olive oils purchased in Italy: commercial categories as determined by IOC labs.

| Sample | Origin | | LAB - Greece | LAB - Slovenia | LAB - Spain 1 | LAB - Abruzzo (IT) | LAB - Lazio (IT) | LAB - Liguria (IT) | LAB - Sicily (IT) | LAB - Veneto (IT) |
|------------------|---|-------------------------|--------------|----------------|---------------|--------------------|------------------|--------------------|-------------------|-------------------|
| O _i 1 | U.E. (Greece/Italy) | Organoleptic Evaluation | VIRGIN | VIRGIN | VIRGIN | VIRGIN | VIRGIN | EXTRA | EXTRA | EXTRA |
| | | Chemical Analysis | - | EXTRA | - | EXTRA | - | EXTRA | EXTRA | EXTRA |
| O _i 2 | U.E. | Organoleptic Evaluation | LAMPANTE | VIRGIN | LAMPANTE | VIRGIN | VIRGIN | VIRGIN | EXTRA | VIRGIN |
| | | Chemical Analysis | - | EXTRA | - | VIRGIN | - | EXTRA | EXTRA | EXTRA |
| O _i 3 | U.E. | Organoleptic Evaluation | LAMPANTE | VIRGIN | LAMPANTE | VIRGIN | VIRGIN | VIRGIN | EXTRA | VIRGIN |
| | | Chemical Analysis | - | EXTRA | - | EXTRA | - | EXTRA | EXTRA | EXTRA |
| O _i 4 | U.E. | Organoleptic Evaluation | LAMPANTE | VIRGIN | VIRGIN | VIRGIN | VIRGIN | VIRGIN | EXTRA | VIRGIN |
| | | Chemical Analysis | - | EXTRA | - | EXTRA | - | EXTRA | EXTRA | VIRGIN |
| O _i 5 | U.E. | Organoleptic Evaluation | LAMPANTE | VIRGIN | VIRGIN | VIRGIN | VIRGIN | EXTRA | EXTRA | EXTRA |
| | | Chemical Analysis | - | EXTRA | - | EXTRA | - | EXTRA | EXTRA | EXTRA |
| O _i 6 | U.E. | Organoleptic Evaluation | VIRGIN | EXTRA | EXTRA | EXTRA | EXTRA | EXTRA | EXTRA | EXTRA |
| | | Chemical Analysis | - | EXTRA | - | EXTRA | - | EXTRA | EXTRA | EXTRA |
| O _i 7 | U.E. | Organoleptic Evaluation | VIRGIN | VIRGIN | VIRGIN | VIRGIN | VIRGIN | EXTRA | EXTRA | EXTRA |
| | | Chemical Analysis | - | EXTRA | - | EXTRA | - | EXTRA | EXTRA | EXTRA |
| O _i 8 | U.E. and not U.E. (Italy/Spain/Tunisia) | Organoleptic Evaluation | VIRGIN | VIRGIN | VIRGIN | VIRGIN | EXTRA | EXTRA | EXTRA | VIRGIN |
| | | Chemical Analysis | - | EXTRA | - | EXTRA | - | EXTRA | EXTRA | EXTRA |

“EXTRA” Extra Virgin Olive Oil; “VIRGIN” Virgin Olive Oil; “LAMPANTE” Lampante Olive Oil

Table 5.5. Olive oils purchased in USA (Miami): commercial categories determined by IOC labs.

| Sample | Origin | | LAB - Greece | LAB - Slovenia | LAB - Spain 1 | LAB - Spain 2 | LAB - Lazio (IT) | LAB - Liguria (IT) | LAB - Sicily (IT) | LAB - Veneto (IT) |
|------------------|---|-------------------------|--------------|----------------|---------------|---------------|------------------|--------------------|-------------------|-------------------|
| O _u 1 | Spain | Organoleptic Evaluation | LAMPANTE | LAMPANTE | VIRGIN | VIRGIN | VIRGIN | VIRGIN | EXTRA | VIRGIN |
| | | Chemical Analysis | - | EXTRA | - | VIRGIN | - | EXTRA | EXTRA | EXTRA |
| O _u 2 | Italy/Greece/Spain/Turkey/Tunisia/Morocco | Organoleptic Evaluation | LAMPANTE | VIRGIN | LAMPANTE | - | VIRGIN | VIRGIN | EXTRA | LAMPANTE |
| | | Chemical Analysis | - | LAMPANTE | - | - | - | LAMPANTE | LAMPANTE | LAMPANTE |
| O _u 3 | Tunisia/Spain | Organoleptic Evaluation | LAMPANTE | VIRGIN | LAMPANTE | LAMPANTE | VIRGIN | VIRGIN | EXTRA | LAMPANTE |
| | | Chemical Analysis | - | LAMPANTE | - | LAMPANTE | - | LAMPANTE | LAMPANTE | LAMPANTE |

| | | | | | | | | | | |
|------------------|---|----------------------------|--------------|--------------|--------------|--------------|------------|------------|------------|------------|
| O _u 4 | Italy/Greece/Spain/ Turkey/Tunisia/Mo rocco | Organoleptic Evaluation | VIRGI N | VIRGIN | VIRGIN | VIRGIN | VIRGI N | EXTR A | EXTRA | VIRGI N |
| | | Chemical Analysis | - | EXTRA | - | VIRGIN | - | EXTR A | VIRGI N | VIRGI N |
| O _u 5 | Spain | Organoleptic Evaluation | LAMP ANTE | VIRGIN | LAMP ANTE | VIRGIN | VIRGI N | VIRGI N | EXTRA | VIRGI N |
| | | Chemical Analysis | - | VIRGIN | | VIRGIN | - | EXTR A | VIRGI N | VIRGI N |
| O _u 6 | Italy/Spain/Greece/ Tunisia | Organoleptic Evaluation | EXTR A | VIRGIN | EXTRA | VIRGIN | VIRGI N | EXTR A | EXTRA | VIRGI N |
| | | Chemical Analysis | - | EXTRA | - | EXTRA | - | EXTR A | EXTRA | EXTRA |
| O _u 7 | Spain | Organoleptic Evaluation | LAMP ANTE | LAMP ANTE | LAMP ANTE | LAMP ANTE | VIRGI N | VIRGI N | VIRGI N | VIRGI N |
| | | Chemical Analysis | - | VIRGIN | - | VIRGIN | - | VIRGI N | VIRGI N | VIRGI N |
| O _u 8 | Spain/Morocco/Chi le/Greece | Organoleptic Evaluation | VIRGI N | VIRGIN | VIRGIN | VIRGIN | VIRGI N | VIRGI N | EXTRA | VIRGI N |
| | | Chemical Analysis | - | EXTRA | - | EXTRA | - | EXTR A | EXTRA | EXTRA |

“EXTRA” Extra Virgin Olive Oil; “VIRGIN” Virgin Olive Oil; “LAMPANTE” Lampante Olive Oil

Table 5.6. Defects, resulting by organoleptic evaluation performed by the eight IOC laboratories, of the eight olive oils purchased in Italy. The median values are reported for each defect. In certain cases, some laboratories provided only the predominant defect of an olive oil despite the detection of more defects. Labs of Spain 1 and Greece just supplied the median of the predominant defect without further details.

| Sample | LAB - Greece | LAB - Slovenia | LAB - Spain 1 | LAB - Abruzzo (IT) | LAB - Lazio (IT) | LAB - Liguria (IT) | LAB - Sicily (IT) | LAB - Veneto (IT) |
|------------------|-----------------|---|------------------|--------------------------|---------------------|-----------------------------|----------------------|-------------------------|
| O _i 1 | 3.1 | Rancid 1.5 | 1.7 | Rancid 2.2 | Musty 1.20 | 0.0 | 0.0 | 0.0 |
| O _i 2 | 4.2 | Rancid 1.8, Fusty 1.4 | 3.9 | Rancid 2.9 | Rancid 1.20 | Fusty 1.7, Rancid 1.2 | 0.0 | Fusty 1.4, Musty 0.9 |
| O _i 3 | 4.3 | Rancid 2.0, Fusty 1.5 | 4.6 | Rancid 3.0 | Musty 1.30 | Rancid 1.8, Musty 1.3 | 0.0 | Rancid 1.2 |
| O _i 4 | 3.9 | Fusty 2.2, Rancid 1.5, Musty 1.4 | 2.3 | Fusty 2.0 | Rancid 1.40 | Fusty 1.6, Rancid 1.1 | 0.0 | Fusty 2.0 |
| O _i 5 | 4 | Fusty 1.4, Rancid 1.3, Winey 1.0 | 1.6 | Fusty 2.1 | Winey 1.30 | 0.0 | 0.0 | 0.0 |
| O _i 6 | 2.2 | 0.0 | 0.0 | 0.0 | 0.00 | 0.0 | 0.0 | 0.0 |
| O _i 7 | 2.9 | Rancid 1.5 | 1.3 | Fusty 2.2 | Rancid 1.45 | 0.0 | 0.0 | 0.0 |
| O _i 8 | 2.6 | Rancid 1.2 | 2.0 | Fusty 2.1 | 0.00 | 0.0 | 0.0 | Rancid 1.0 |

Table 5.7. Defects, resulting by organoleptic evaluation performed by 8 IOC laboratories, of the eight olive oils purchased in USA (Miami). The median values are reported for each defect. In certain cases, some laboratories provided only the predominant defect of an olive oil despite the detection of more defects. Labs of Spain 2 and Greece just supplied the median of the predominant defect without further details. *Sample Ou 2 was not analyzed by Spain 2 lab.

| Sample | LAB - Greece | LAB - Slovenia | LAB - Spain 1 | LAB - Spain 2 | LAB - Lazio (IT) | LAB - Liguria (IT) | LAB - Sicily (IT) | LAB - Veneto (IT) |
|------------------|--------------|----------------------------------|---------------|-------------------|------------------|--------------------|-------------------|------------------------|
| O _u 1 | 4.3 | Rancid 3.7, Fusty 1.9 | Winey 3.1 | 3.0 | Fusty 2.20 | Fusty 1.7 | 0.0 | Fusty 1.6, Musty 1.5 |
| O _u 2 | 4.0 | Fusty 2.0, Rancid 1.9, Musty 1.4 | Rancid 4.4 | ---* [*] | Rancid 1.95 | Rancid 1.8 | 0.0 | Rancid 3.8, Fusty 0.6 |
| O _u 3 | 4.7 | Rancid 1.8, Musty 1.2 | Rancid 5.1 | 3.9 | Rancid 1.70 | Rancid 2.9 | 0.0 | Rancid 4.1 |
| O _u 4 | 3.1 | Rancid 1.4 | Winey 1.6 | 2.7 | Fusty 1.50 | 0.0 | 0.0 | Frozen 1.1 |
| O _u 5 | 5.2 | Fusty 1.6, Rancid 1.5 | Musty 4.2 | 3.3 | Rancid 1.90 | Rancid 1.9 | 0.0 | Rancid 1.9, Musty 0.8 |
| O _u 6 | 0.0 | Fusty 1.2 | 0.0 | 2.1 | Fusty 1.10 | 0.0 | 0.0 | Rancid 0.2 |
| O _u 7 | 5.6 | Fusty 3.7, Rancid 2.2, Winey 1.6 | Fusty 5.3 | 4.7 | Rancid 1.50 | Fusty 1.8 | Fusty 2.0 | Fusty 2.1, Rancid 2.0 |
| O _u 8 | 2.5 | Rancid 1.4 | Winey 1.6 | 3.2 | Rancid 1.40 | Musty 1.1 | 0.0 | Frozen 0.3, Rancid 0.2 |

Table 5.8. Positive attributes, resulting by organoleptic evaluation performed by 8 IOC laboratories, of the eight olive oils purchased in Italy and the eight olive oils purchased in USA (Miami). The median values are reported for each defect. Results of “Bitter” and “Pungent” attributes were not provided by all laboratories. *Sample Ou 2 was not analyzed by Spain 2 lab.

| O _i 1 | Fruity | Bitter | Pungent |
|------------------|--------|--------|---------|
| Greece | 1.5 | 2.8 | 3.2 |
| Slovenia | 3.4 | --- | --- |
| Spain 1 | 2.0 | --- | --- |
| Abruzzo (IT) | 2.0 | --- | --- |
| Lazio (IT) | > 0 | --- | --- |
| Liguria (IT) | 1.7 | 2.6 | 3.1 |
| Sicily (IT) | 3.8 | 3.7 | 4.3 |
| Veneto (IT) | 1.8 | 2.5 | 3.6 |

| O _u 1 | Fruity | Bitter | Pungent |
|------------------|--------|--------|---------|
| Greece | 0.0 | --- | --- |
| Slovenia | 2.1 | --- | --- |
| Spain 1 | 1.3 | --- | --- |
| Spain 2 | 2.1 | --- | --- |
| Lazio (IT) | > 0 | --- | --- |
| Liguria (IT) | 1.2 | 2.0 | 2.3 |
| Sicily (IT) | 4.2 | 2.3 | 3.0 |
| Veneto (IT) | 1.2 | 1.1 | 2.0 |

| O _i 2 | Fruity | Bitter | Pungent |
|------------------|--------|--------|---------|
| Greece | 0.0 | ----- | ----- |
| Slovenia | 3.0 | ----- | ----- |
| Spain 1 | 0.0 | ----- | ----- |
| Abruzzo (IT) | 1.8 | ----- | ----- |
| Lazio (IT) | > 0 | ----- | ----- |
| Liguria (IT) | 2.1 | 2.6 | 3.2 |
| Sicily (IT) | 3.6 | 3.4 | 3.7 |
| Veneto (IT) | 1.0 | 1.7 | 1.9 |
| O _i 3 | Fruity | Bitter | Pungent |
| Greece | 0.0 | ----- | ----- |
| Slovenia | 2.7 | ----- | ----- |
| Spain 1 | 0.0 | ----- | ----- |
| Abruzzo (IT) | 1.7 | ----- | ----- |
| Lazio (IT) | > 0 | ----- | ----- |
| Liguria (IT) | 2.1 | 2.1 | 2.7 |
| Sicily (IT) | 3.5 | 3.2 | 2.9 |
| Veneto (IT) | 1.0 | 1.3 | 2.0 |
| O _i 4 | Fruity | Bitter | Pungent |
| Greece | 0.0 | ----- | ----- |
| Slovenia | 2.6 | ----- | ----- |
| Spain 1 | 1.9 | ----- | ----- |
| Abruzzo (IT) | 1.8 | ----- | ----- |
| Lazio (IT) | > 0 | ----- | ----- |
| Liguria (IT) | 2.1 | 2.0 | 2.6 |
| Sicily (IT) | 3.3 | 3.0 | 3.2 |
| Veneto (IT) | 1.0 | 1.0 | 1.6 |
| O _i 5 | Fruity | Bitter | Pungent |
| Greece | 0.0 | ----- | ----- |
| Slovenia | 2.4 | ----- | ----- |
| Spain 1 | 1.9 | ----- | ----- |
| Abruzzo (IT) | 2.0 | ----- | ----- |
| Lazio (IT) | > 0 | ----- | ----- |
| Liguria (IT) | 1.8 | 2.5 | 3.6 |
| Sicily (IT) | 4.0 | 3.8 | 3.5 |
| Veneto (IT) | 2.0 | 3.0 | 3.4 |
| O _i 6 | Fruity | Bitter | Pungent |
| Greece | 2.5 | 2.4 | 3.1 |
| Slovenia | 2.8 | ----- | ----- |
| Spain 1 | 2.5 | ----- | ----- |
| Abruzzo (IT) | 3.0 | ----- | ----- |

| O _u 2 | Fruity | Bitter | Pungent |
|------------------|--------|--------|---------|
| Greece | 0.0 | ----- | ----- |
| Slovenia | 1.7 | ----- | ----- |
| Spain 1 | 0.0 | ----- | ----- |
| Spain 2 | -----* | ----- | ----- |
| Lazio (IT) | > 0 | ----- | ----- |
| Liguria (IT) | 1.8 | 2.2 | 2.4 |
| Sicily (IT) | 3.4 | 2.9 | 2.6 |
| Veneto (IT) | 0.8 | 0.9 | 1.6 |
| O _u 3 | Fruity | Bitter | Pungent |
| Greece | 0.0 | ----- | ----- |
| Slovenia | 1.8 | ----- | ----- |
| Spain 1 | 0.0 | ----- | ----- |
| Spain 2 | 0.0 | ----- | ----- |
| Lazio (IT) | > 0 | ----- | ----- |
| Liguria (IT) | 0.8 | 1.5 | 2.0 |
| Sicily (IT) | 3.4 | 2.6 | 2.6 |
| Veneto (IT) | 0.5 | 0.6 | 1.5 |
| O _u 4 | Fruity | Bitter | Pungent |
| Greece | 1.8 | ----- | ----- |
| Slovenia | 2.6 | ----- | ----- |
| Spain 1 | 2.2 | ----- | ----- |
| Spain 2 | 2.1 | ----- | ----- |
| Lazio (IT) | > 0 | ----- | ----- |
| Liguria (IT) | 1.9 | 2.7 | 2.8 |
| Sicily (IT) | 3.7 | 2.8 | 3.3 |
| Veneto (IT) | 1.5 | 1.7 | 3.0 |
| O _u 5 | Fruity | Bitter | Pungent |
| Greece | 0.0 | ----- | ----- |
| Slovenia | 1.9 | ----- | ----- |
| Spain 1 | 1.4 | ----- | ----- |
| Spain 2 | 1.6 | ----- | ----- |
| Lazio (IT) | > 0 | ----- | ----- |
| Liguria (IT) | 1.2 | 1.9 | 2.1 |
| Sicily (IT) | 3.8 | 3.1 | 2.7 |
| Veneto (IT) | 1.3 | 1.3 | 1.8 |
| O _u 6 | Fruity | Bitter | Pungent |
| Greece | 2.8 | ----- | ----- |
| Slovenia | 2.6 | ----- | ----- |
| Spain 1 | 2.5 | ----- | ----- |
| Spain 2 | 2.7 | ----- | ----- |

| | | | |
|------------------------|---------------|---------------|----------------|
| Lazio (IT) | > 0 | ---- | ---- |
| Liguria (IT) | 2.6 | 2.0 | 3.4 |
| Sicily (IT) | 3.6 | 3.8 | 3.3 |
| Veneto (IT) | 1.9 | 1.5 | 2.9 |
| O_i 7 | Fruity | Bitter | Pungent |
| Greece | 1.8 | 2.6 | 3.0 |
| Slovenia | 2.9 | ---- | ---- |
| Spain 1 | 2.2 | ---- | ---- |
| Abruzzo (IT) | 2 | ---- | ---- |
| Lazio (IT) | > 0 | ---- | ---- |
| Liguria (IT) | 2.4 | 2.8 | 3.7 |
| Sicily (IT) | 3.8 | 3.7 | 4.3 |
| Veneto (IT) | 2.0 | 2.5 | 3.5 |
| O_i 8 | Fruity | Bitter | Pungent |
| Greece | 2.1 | 2.7 | 3.0 |
| Slovenia | 3.2 | ---- | ---- |
| Spain 1 | 1.6 | ---- | ---- |
| Abruzzo (IT) | 2.3 | ---- | ---- |
| Lazio (IT) | > 0 | ---- | ---- |
| Liguria (IT) | 1.9 | 2.4 | 3.5 |
| Sicily (IT) | 3.2 | 3.2 | 2.6 |
| Veneto (IT) | 1.8 | 1.7 | 2.7 |

| | | | |
|------------------------|---------------|---------------|----------------|
| Lazio (IT) | > 0 | ---- | ---- |
| Liguria (IT) | 1.9 | 3.0 | 3.7 |
| Sicily (IT) | 4.3 | 3.8 | 3.4 |
| Veneto (IT) | 2.4 | 2.5 | 3.7 |
| O_u 7 | Fruity | Bitter | Pungent |
| Greece | 0.0 | ---- | ---- |
| Slovenia | 1.0 | ---- | ---- |
| Spain 1 | 0.0 | ---- | ---- |
| Spain 2 | 0.0 | ---- | ---- |
| Lazio (IT) | > 0 | ---- | ---- |
| Liguria (IT) | 2.0 | 2.5 | 2.9 |
| Sicily (IT) | 2.8 | 2.6 | 2.9 |
| Veneto (IT) | 1.0 | 1.2 | 2.0 |
| O_u 8 | Fruity | Bitter | Pungent |
| Greece | 2.6 | ---- | ---- |
| Slovenia | 3.3 | ---- | ---- |
| Spain 1 | 2.0 | ---- | ---- |
| Spain 2 | 2.1 | ---- | ---- |
| Lazio (IT) | > 0 | ---- | ---- |
| Liguria (IT) | 2.4 | 2.0 | 3.3 |
| Sicily (IT) | 3.4 | 3.1 | 3.4 |
| Veneto (IT) | 1.5 | 1.3 | 2.5 |

Table 5.9. Percentage of classification of the eight olive oils purchased in Italy using results obtained by Organoleptic Evaluation and Chemical Analysis performed on these olive oils by 8 IOC laboratories. * In brackets the percentages of classification according to the chemical analysis without the ethyl esters content are reported.

| Sample | Classification | Extra Virgin Olive Oil | Virgin Olive Oil | Lampante Olive Oil |
|------------------|-------------------|------------------------|------------------|--------------------|
| O _i 1 | Panel Test | 37.5% | 62.5% | - |
| | Chemical Analysis | 100% | - | - |
| O _i 2 | Panel Test | 12.5% | 62.5% | 25% |
| | Chemical Analysis | 80% (100%)* | 20% | - |
| O _i 3 | Panel Test | 12.5% | 62.5% | 25% |
| | Chemical Analysis | 100% | - | - |
| O _i 4 | Panel Test | 12.5% | 75% | 12,5% |
| | Chemical Analysis | 80% (100%)* | 20% | - |
| O _i 5 | Panel Test | 37.5% | 50% | 12.5% |

| | | | | |
|------------------------|--------------------------|--------------|--------------|----------|
| | Chemical Analysis | 100% | - | - |
| O_i 6 | Panel Test | 87.5% | 12.5% | - |
| | Chemical Analysis | 100% | - | - |
| O_i 7 | Panel Test | 37.5% | 62.5% | - |
| | Chemical Analysis | 100% | - | - |
| O_i 8 | Panel Test | 37.5% | 62.5% | - |
| | Chemical Analysis | 100% | - | - |

Table 5.10. Percentage Percentage of classification of the eight olive oils purchased in USA using results obtained by Panel Test and Chemical Analysis performed on these olive oils by 8 IOC laboratories. *In brackets the percentages of classification according to the chemical analysis with- out the ethyl esters content are reported.

| Sample | Classification | Extra Virgin Olive Oil | Virgin Olive Oil | Lampante Olive Oil |
|------------------------|--------------------------|-------------------------------|-------------------------|---------------------------|
| O_u 1 | Panel Test | 12.5% | 62.5% | 25% |
| | Chemical Analysis | 80% (100%)* | 20% | - |
| O_u 2 | Panel Test | 14% | 43% | 43% |
| | Chemical Analysis | | | 100% |
| O_u 3 | Panel Test | 12.5% | 37.5% | 50% |
| | Chemical Analysis | | | 100% |
| O_u 4 | Panel Test | 25% | 75% | - |
| | Chemical Analysis | 40% (100%)* | 60% | - |
| O_u 5 | Panel Test | 12.5% | 62.5% | 25% |
| | Chemical Analysis | 20% (40%)* | 80% (60%)* | |
| O_u 6 | Panel Test | 50% | 50% | - |
| | Chemical Analysis | 100% | - | - |
| O_u 7 | Panel Test | - | 50% | 50% |
| | Chemical Analysis | (100 %)* | 100% | - |
| O_u 8 | Panel Test | 12.5% | 87.5% | - |
| | Chemical Analysis | 100% | - | - |

Samples purchased in Italy. In the case of olive oils purchased in Italy, samples turned out to be EVOOs or virgin olive oils from the chemical point of view (Tables 5.2, 5.4 and Table 5.9). Five samples (Oi 1, Oi 3, Oi 6, Oi 7 and Oi 8) were judged as EVOOs whereas samples Oi 2, Oi 4 and Oi 5 turned out to be EVOOs or virgin olive oils according to the specific lab. In particular, sample Oi 2 turned out to be EVOO according to the chemical analysis results provided by Sicilian and Venetian labs and virgin olive oil for Abruzzo, Slovenian and Ligurian labs, whereas sample Oi 4 turned out to be EVOO according to Abruzzo and Sicilian labs and virgin olive oil for Slovenian, Ligurian and Venetian labs. Sample Oi 5 was classified virgin olive oil according to all the labs except the Venetian one. The parameter responsible for the declassing of Oi 2, Oi 4 and Oi 5 samples from EVOOs to not EVOOs was the content of FAEE. The importance of FAEE content to define the quality of an olive oil is well known (Gómez-Coca, Moreda et Pérez-Camino, 2012; Conte et al., 2014): fatty acid ethyl esters are the products of the trans-esterification reaction between fatty acids and ethanol produced by bacteria fermentation that occurs when olives are of poor quality. Because of this narrow relationship between olive oil quality and FAEE content, the threshold for FAEE content in EVOOs has been decreased along the time, from 40 mg/kg in 2013/2014 harvest year down to 35 mg/kg in 2014/2015. Although this limit has been further reduced to ≤ 30 mg/kg in 2015, it has been set again to 35 mg/kg (IOC/T.15/NC No. 3/Rev. 11/2016; Commission Delegated Regulation (EU) No. 2016/2095) on July 2016 by IOC and on September 2016 by EEC.

It is interesting to note, see Table 5.2, that the FAEE content was reported by different IOC labs with or without uncertainty. For instance, IOC lab located in Veneto (Italy) never provided the uncertainty related to FAEE measurement. Sample Oi 4 with a FAEE content of 39.7 mg/kg reported without any uncertainty has to be classified as virgin olive oil, whereas Oi 1 with a FAEE content of 28 mg/kg has to be classified as extra virgin olive oil. On the other hand, some labs reported a value higher than 35 mg/kg (the threshold value for

year 2014/2015) with the threshold value within the uncertainty, see for example the results of Slovenian lab reported for sample Oi 2 with a FAEE content of 36.8 ± 5.1 mg/kg. Finally, other labs reported a value lower than 35 mg/kg with the threshold within the uncertainty, see for example the results of Ligurian lab for sample Oi 1 with a FAEE content of 32 ± 8 mg/kg. How to use these data to classify olive oils? A strict interpretation of EEC Regulation 2568/91 that does not give any indication on the way to report the uncertainty of the results implies that any olive oil with a FAEE content value above the threshold has to be declassified from extra virgin olive oil to not extra virgin olive. Therefore, Oi 2 with a FAEE content of 36.8 ± 5.1 mg/kg has to be classified as not extra virgin olive oil, whereas Oi 1 with a FAEE content of 32 ± 8 mg/kg has to be classified as extra virgin olive oil. Whereas an analytical point of view to report a result with the uncertainty is a correct way, to consider the uncertainty for the olive oil classification can give rise to confusion. In fact, if the uncertainty is considered, these two olive oils should have the same grade, i.e. extra virgin olive oil. On the other hand, taking into account the upper limit of uncertainty, an olive oil with a value of 32 ± 8 mg/kg could be considered not extra virgin. Therefore, the way to report the FAEE content with the uncertainty can create confusion, when the olive oil commercial classification is required.

Organoleptic evaluation carried out from the different labs were extremely controversial. For instance, all the olive oils were judged as EVOOs according to the results of the Sicilian lab, whereas no sample was judged as EVOO according to the results of the Greek lab. These results clearly show that the same olive oil can be judged EVOO, virgin olive oil or lampante olive oil according to the the lab. This is the case of samples Oi 2, Oi 3, Oi 4, Oi 5, whereas samples Oi 1, Oi 6, Oi 7, Oi 8 were judged virgin olive oils or EVOOs. Only sample Oi 6 was judged EVOO according to the results of all the labs except the Greek one. It is important to note that this olive oil has a FAEE concentration <15 mg/kg well below the threshold of 35 mg/kg, whereas the other olive oils exhibit a FAEE content which is slightly less or higher than the threshold value. The strict connection between FAEE content

and the positive attributes by organoleptic evaluation of an olive oil has been previously reported (Gómez-Coca, Moreda et Pérez-Camino, 2012; Di Loreto et al., 2014).

Therefore, all the obtained results seem to suggest that only in the case of olive oils with extremely “good” chemical analyses, including a low FAEE content (neither borderline nor higher than the threshold value), the organoleptic evaluation can be reproducible.

Samples purchased in USA. Olive oils purchased in Miami (USA) were judged, see Tables 5.3 and 5.5 and Table 5.10, EVOOs (Ou 6 and Ou 8), virgin olive oils (Ou 4, Ou 5 and Ou 7) and lampante olive oils (Ou 2 and Ou 3) according to the chemical analysis results. The judgment given by the different labs for these five samples was univocal: samples Ou 2 and Ou 3 turned out to be lampante olive oils because of their high K 232 value (>2.60) whereas samples Ou 4 and Ou 7 were classified as virgin olive oil due to the high FAEE content (>35 mg/kg). Sample Ou 5 turned out to be virgin olive oil because of the high content of FAEE (>35 mg/kg) in the case of Ligurian and Venetian labs or for both K 270 value ($0.22 < K 270 < 0.25$) and FAEE content in the case of Slovenian, Sicilian and Spain 2 labs.

Finally, samples Ou 1 and Ou 4 were judged virgin olive oils or EVOOs according to the labs results: the critical point was again the FAEE content given without error or with a high error.

The results of organoleptic evaluation given by the different laboratories turned out to be in disagreement. For instance, all samples were judged virgin olive oils due to a median of defects >0 according to the Lazio lab results, whereas all samples, except one, were judged EVOOs according to the Sicilian lab results. Samples Ou 1, Ou 2, Ou 3 and Ou 5 turned out to be lampante olive oils, virgin olive oils or EVOOs according to the lab, whereas sample Ou 7 was judged lampante olive oil or virgin olive oil. Finally, samples Ou 4, Ou 6 and Ou 8 were judged virgin olive oils or EVOOs according to the labs.

Again, this disagreement of sensory evaluation can be related to some borderline

value in the chemical parameters. It is interesting to note that the only two samples, Ou 6 and Ou 8, judged EVOOs by the chemical analysis, with a slightly less FAEE content than the threshold value were classified as EVOOs or virgin olive oils by the organoleptic evaluation. A similar case is also represented by the sample Ou 1 which, through chemical analyses, was judged EVOO in three cases out of five with a borderline FAEE content, whereas, through organoleptic evaluation, it was classified as EVOO, virgin olive oil or even lampante olive oil.

5.1.4 Conclusions

The results reported here highlight some important aspects to be considered in the olive oil commercial classification.

First of all, the non-uniform way to report the FAEE content with or without uncertainty can create confusion in the quality grade classification, especially in case of borderline values of FAEE content. It is important to underline that the EEC Regulation 2568/91 does not give any indication on the way to report the uncertainty of the results.

Our data analysis underlines that it is crucial to find out what causes the variability of judgement in the organoleptic evaluation. Sensory panel test seems to work well in the case of extremely good olive oils, whereas in the case of common commercial EVOOs can give discordant results. A different sensory sensibility seems to be present in the different IOC panel labs, especially in case of EVOOs characterized by a FAEE content very close to the threshold. For a given olive oil, the question to be or not to be classified as EVOO becomes a question strictly linked to the lab.

In our opinion, organoleptic evaluation is extremely important for a global picture of the sensory properties of olive oil and it is particularly precious and not replaceable with other analysis to give add values to PDO or other peculiar EVOOs. On the other hand, this analysis seems to be not enough reproducible in the case of common commercial EVOOs probably due to different sensory sensibility in the different IOC panel labs and therefore it is not

198

suitable for a legally accepted official evaluation.

5.1.5 References

Angerosa F. Sensory quality of olive oils. In: Aparicio R, Harwood J, editors, 2000. Handbook of olive oil, analysis and properties. Gaithersburg: Aspen Publishers. 355–392.

Camin, F., Pavone, A., Bontempo, L., Wehrens, R., Paolini, M., Faberi, A., Marianella, R.M., Capitani, D., Vista, S., Mannina, L., 2016. The use of IRMS, ¹H NMR and chemical analysis to characterise Italian and imported Tunisian olive oils. *Food Chem.* 19, 98–105.

Conte, L., Mariani, C., Gallina Toschi, T., Tagliabue, S., 2014. Alchil esteri e composti correlati in oli d'oliva vergini: loro evoluzione nel tempo. *RISG* 91, 21–9.

Gómez-Coca, R.B., Moreda, W., Pérez-Camino, M.C., 2012. Fatty acid alkyl esters presence in olive oil versus organoleptic assessment. *Food Chem.* 135, 1205–9.

Frankel, E.N., 2011. Nutritional and biological properties of extra virgin olive oil. *J. Agric. Food Chem.* 59, 785–792.

International Olive Oil Council. Trade standard applying to olive oils and olive pomace oils. 2016. IOC/T.15/NC No. 3/Rev. 11.

International Olive Oil Council. List of chemical testing laboratories recognised by the International Olive Council for the period from 1.12.2014 to 30.11.2015. 2014. IOC/T.21/Doc. No. 13/Rev. 17.

International Olive Oil Council. List of laboratories undertaking the sensory analysis of virgin olive oils recognised by the International Olive Council for the period from 1.12.2014 to 30.11.2015. 2014. IOC/T.28/Doc. No. 3/Rev. 17.

International Olive Oil Council. Sensory analysis of olive oil, method for the organoleptic assessment of virgin olive oil. 2015. IOC/T.20/Doc. No. 15/Rev. 8. <http://www.internationaloliveoil.org/estaticos/view/224-testing-methods>.

Loreto, G., Giansante, L., Alfei, B., Giacinto, L., 2014. Alchil esteri ed altri indicatori per la tutela della qualità e della genuinità degli oli extra vergini italiani. *RISG* 91, 35–45.

Salas, J.J., Harwood, J.L., Martínez-Force, E. Lipid metabolism in olive: biosynthesis of triacylglycerols and aroma components. In: Aparicio, R., Harwood, J., Editors, 2013. Handbook of olive oil, analysis and properties. New York: Springer. 97–127.

The Commission of the European Communities. Commission Regulation (EEC) No. 2568/91 on the characteristics of olive oil and olive-residue oil and on the relevant methods of analysis. *Off. J. Eur. Union.* L248, 1–102.

The European Commission. Commission Regulation (EU) No. 432/2012 establishing a list of permitted health claims made on foods, other than those referring to the reduction of disease risk and to children's development and health. *Off. J. Eur. Union.* L136, 1–40.

The European Commission. Commission Delegated Regulation (EU) No. 2016/2095 of 26 September 2016 amending Regulation (EEC) No. 2568/91 on the characteristics of olive oil and olive-residue oil and on the relevant methods of analysis. Off. J. Eur. Union. L326, 1–6.

5.2 A Multi-Methodological Protocol to Characterize PDO Olive Oils

5.2.1 Introduction

Foodstuff authentication and geographical origin certification (Regulation (EU) No 510/2006; Regulation (EC) No. 1151/2012) is an actual issue and an important challenge faced by different analytical methodologies. Regarding olive oils, a mandatory labelling reporting the geographical origin is required by the EU Regulation 182/11 (Regulation (EU) No 182/2011; Likudis, 2016).

The olive growing area of the district of Latina, recognized as PDO “Colline Pontine” in 2009, extends behind the agro Pontino, developing parallel to the sea, through the mountain systems of Lepini, Ausoni and Aurunci Mounts. The “Colline Pontine” PDO area is one of the wider Italian olive growing areas characterized by the constant presence of the “Itrana” cultivar, which is used for olive oil and table olives production (Gaeta’s olive).

In the last years, the emergence of producers who have brought innovation to the traditional production process has allowed olive oil of the PDO “Colline Pontine” area to achieve excellence aims highlighted by both prestigious awards obtained and by consumer responses. This aspect is at the origin of the project “Quality olive growing and territory” in the PDO “Colline Pontine” area, developed under the program “Integrated Skills for Sustainability and Innovation of Food Made in Italy” promoted by the Italian Ministry of Finance.

Today both chemical and sensorial analyses represent the official methods to define the commercial value of olive oils, as established by EEC Regulation 2568/91 (Commission Regulation (EEC) No 2568/91).

An important analysis is the Panel test that develops a global picture of olive oil sensory properties. In this way, this analysis, not yet replaceable with other analyses, gives add values to peculiar extra virgin olive oils (EVOOs) by describing their special sensorial characteristics. On the other hand, as discussed in literature (Circi et al., 2017), in the case of

common commercial EVOOs this analysis can give discordant results, turning out to be dependent from panel laboratory.

In recent years many studies have been performed to characterize and classify according to the geographical origin olive oils using different “unconventional” techniques, such as Isotope Ratio Mass Spectrometry (IRMS) (Camin et al., 2010a; Camin et al., 2010b; Bontempo et al., 2009) and Nuclear Magnetic Resonance (NMR) (Mannina & Sobolev, 2011; D’Imperio et al., 2010; Mannina, Sobolev & Segre, 2003; Laincer et al., 2016; Bianchi et al., 2001; Del Coco et al., 2016; Di Vaio et al., 2013; Schievano et al., 2006; Rotondo et al., 2011) or their combination (Camin et al., 2016).

The H, O and C isotopic composition of plant materials as olive oils depends on many factors, including geographical conditions (altitude, latitude, distance from the sea, etc.) and climatic conditions (relative humidity, temperature, amount of precipitation) (Camin et al., 2010b; Bontempo et al., 2009; Angerosa et al., 1999; Aramendia et al., 2007).

As reported in literature (D’Imperio et al., 2007; Dugo et al., 2015), ¹H NMR spectroscopy enables the attainment of a good chemical characterization of an olive oil, giving information on major (triglycerides) and minor (aldehydes, terpenes, sterols) (Rotondo et al., 2017) compounds in a single experiment, with an experimental error which is exactly the same and extremely low for all compounds analysed.

Here, an analytical protocol is reported with the aim of promoting the diffusion of high quality olive growing in the “Colline Pontine” PDO area and to create a connection between research and industry. This protocol involves Panel Test along with IRMS and NMR spectroscopy.

5.2.2 Material and Methods

The basic characteristics of 62 olive oil samples produced in different areas of the district of Latina, Lazio (see Figure 5.1), are reported in Table 5.11. Olive oils were extracted from olive batches from known place, production years and variety.



Figure 5.1. Map of Lazio region (Italy): the area of Latina district is highlighted.

The sampling consists of 14 monovarietal olive oils (13 Itrana and 1 Carolea) of a first harvest year, 26 monovarietal and multivarietal olive oils (24 Itrana, 1 Carolea, and 1 Itrana, Frantoio) of a second harvest year and 22 monovarietal olive oils belonging to the cultivar Itrana of a third harvest year.

Table 5.11. Characteristics of olive oil samples.

| Code | Geographical origin | Cultivar | Harvesting year |
|------|---------------------|----------|-----------------|
| 1 | Priverno | Itrana | 2011-2012 |
| 2 | Sonnino | Itrana | 2011-2012 |
| 3 | Sonnino | Itrana | 2011-2012 |
| 4 | Terracina | Itrana | 2011-2012 |
| 5 | Lenola | Itrana | 2011-2012 |
| 6 | Gaeta | Itrana | 2011-2012 |
| 7 | SS Cosma e Damiano | Itrana | 2011-2012 |
| 8 | Cisterna di Latina | Itrana | 2011-2012 |
| 9 | Cisterna di Latina | Carolea | 2011-2012 |

| | | | |
|----|--------------------|------------------|-----------|
| 10 | Rocca Massima | Itrana | 2011-2012 |
| 11 | Sonnino | Itrana | 2011-2012 |
| 12 | Maenza | Itrana | 2011-2012 |
| 13 | Maenza | Itrana | 2011-2012 |
| 14 | Sermoneta | Itrana | 2011-2012 |
| 15 | Priverno | Itrana | 2012-2013 |
| 16 | Sonnino | Itrana | 2012-2013 |
| 17 | Sonnino | Itrana | 2012-2013 |
| 18 | Terracina | Itrana | 2012-2013 |
| 19 | Lenola | Itrana | 2012-2013 |
| 20 | Gaeta | Itrana | 2012-2013 |
| 21 | SS Cosma e Damiano | Itrana | 2012-2013 |
| 22 | Cisterna di Latina | Itrana | 2012-2013 |
| 23 | Rocca Massima | Itrana | 2012-2013 |
| 24 | Sonnino | Itrana | 2012-2013 |
| 25 | Maenza | Itrana | 2012-2013 |
| 26 | Maenza | Itrana | 2012-2013 |
| 27 | Sermoneta | Itrana | 2012-2013 |
| 28 | Cisterna di Latina | Carolea | 2012-2013 |
| 29 | Spigno S. | Itrana | 2012-2013 |
| 30 | Spigno S. | Itrana | 2012-2013 |
| 31 | Cisterna di Latina | Itrana | 2012-2013 |
| 32 | Terracina | Itrana | 2012-2013 |
| 33 | Fondi | Itrana | 2012-2013 |
| 34 | Aprilia | Itrana | 2012-2013 |
| 35 | Itri | Itrana | 2012-2013 |
| 36 | Sonnino | Itrana | 2012-2013 |
| 37 | Terracina | Itrana | 2012-2013 |
| 38 | Itri | Itrana | 2012-2013 |
| 39 | Aprilia | Itrana, Frantoio | 2012-2013 |
| 40 | Terracina | Itrana | 2012-2013 |
| 41 | Priverno | Itrana | 2013-2014 |
| 42 | Sonnino | Itrana | 2013-2014 |
| 43 | Sonnino | Itrana | 2013-2014 |
| 44 | Terracina | Itrana | 2013-2014 |

| | | | |
|----|--------------------|------------------|-----------|
| 45 | Lenola | Itrana | 2013-2014 |
| 46 | Gaeta | Itrana | 2013-2014 |
| 47 | SS Cosma e Damiano | Itrana | 2013-2014 |
| 48 | Rocca Massima | Itrana | 2013-2014 |
| 49 | Sonnino | Itrana | 2013-2014 |
| 50 | Maenza | Itrana | 2013-2014 |
| 51 | Minturno | Itrana | 2013-2014 |
| 52 | Sermoneta | Itrana | 2013-2014 |
| 53 | Castelforte | Itrana | 2013-2014 |
| 54 | Spigno S. | Itrana | 2013-2014 |
| 55 | Cisterna | Itrana | 2013-2014 |
| 56 | Terracina | Itrana | 2013-2014 |
| 57 | Lenola | Itrana | 2013-2014 |
| 58 | Aprilia | Itrana | 2013-2014 |
| 59 | Itri | Itrana | 2013-2014 |
| 60 | Sonnino | Itrana | 2013-2014 |
| 61 | Itri | Itrana, Frantoio | 2013-2014 |
| 62 | Formia | Itrana | 2013-2014 |

Sensory Analysis. Sensory analysis on 40 olive oil samples from the first and the second crop years was performed in the tasting room of “Camera di Commercio” of Latina by a fully trained analytical taste panel, made up of a panel head and 9 tasters, and recognized by the International Olive Council (IOC). The evaluation of the samples was carried out according to the official method described in the EC Regulation 2568/91 (Commission Regulation (EEC) No 2568/91) and the EC Regulation 640/08 (Commission Regulation (EC) No 640/2008). Samples were stored in 0.50 L bottles, having the same colour and shape and without any reference to the producer. Each taster smelled and tasted the oils in order to analyse positive and negative attributes. Each assessor rated the intensity of the sensory attributes using an unstructured scale of 10 cm, ranging from low to high intensity. Results were expressed as the median intensity of the sensory perceptions of the tasters.

In the case of olive oils coming from the district of Latina the attribute “tomato” was added to the positive attributes. In fact, “tomato” is a typical sensory attribute that characterized olive oils of the PDO “Colline Pontine” area.

Isotope Ratio Mass Spectrometry. The analysis of the ratios $^{13}\text{C}/^{12}\text{C}$, $^{18}\text{O}/^{16}\text{O}$ and $^2\text{H}/^1\text{H}$ of bulk olive oils was performed on the same forty samples submitted to the sensory analysis.

The ratio $^{13}\text{C}/^{12}\text{C}$ was measured using an Isotope Ratio Mass Spectrometer (DELTA V, Thermo Scientific, Langensfeld, Germany) following total combustion in an elemental analyzer (EA Flash 1112, Thermo Scientific). The ratios $^2\text{H}/^1\text{H}$ and $^{18}\text{O}/^{16}\text{O}$ were measured in one run using IRMS (Finnigan DELTA XP, Thermo Scientific) coupled with a Pyrolyser (Finnigan TC/EA, high temperature conversion elemental analyzer, Thermo Scientific), following the methods described elsewhere (Camin et al., 2017).

The values were expressed as following:

$$\delta\text{‰} = [(R_{\text{sample}} - R_{\text{standard}})/R_{\text{standard}}]$$

where R is the ratio between the heavier isotope and the lighter one.

The values were expressed in $\delta\text{‰}$ against international standards Vienna-Pee Dee Belemnite (V-PDB) for $\delta^{13}\text{C}$, Vienna–Standard Mean Ocean Water (V-SMOW) for $\delta^2\text{H}$ and $\delta^{18}\text{O}$. For the calculation of $\delta\text{‰}$, 2 olive oil working inhouse standards were calibrated against international reference materials: fuel oil NBS-22 (IAEA) and sugar IAEA-CH-6 (IAEA) for $^{13}\text{C}/^{12}\text{C}$, Benzoic Acid IAEA-601 (IAEA) for $^{18}\text{O}/^{16}\text{O}$, fuel oil NBS-22 (IAEA) for $^2\text{H}/^1\text{H}$, Icosanoic Acid Methyl Esters USGS70 and USGS71 for $^{13}\text{C}/^{12}\text{C}$ and $^2\text{H}/^1\text{H}$.

The standard deviation of repeatability (Sr) for oil was 0.1‰ for $\delta^{13}\text{C}$, 0.4‰ for $\delta^{18}\text{O}$ and 1‰ for $\delta^2\text{H}$.

NMR Measurements. All the NMR spectra were carried out in December to have fresh EVOO with the same shelf-life.

Olive oil samples (20 μL) were dissolved in CDCl_3 (700 μL) plus DMSO-d_6 (20 μL), directly in the 5 mm NMR tube, to solubilize all minor components. For NMR measurements we considered both the forty olive oil samples from the first and the second crop years and the twenty-two samples from the third harvesting year.

^1H NMR experiments were recorded at 300 K on a Bruker AVANCE 600 NMR spectrometer operating at the proton frequency of 600.13 MHz ($B_0 = 14.1$ T) and equipped with a Bruker multinuclear Z gradient 5 mm probe head. The ^1H spectra were acquired using the following conditions: number of scans 1024, $\pi/2$ pulse ~ 8 μs , time domain (TD) 64 K data points, relaxation delay plus acquisition time 3.5 s and spectral width 18.5 ppm. ^1H NMR spectra were obtained by the Fourier transformation of the Free Induction Decay, applying an exponential multiplication with a line-broadening factor of 0.3 Hz and a zero filling (size = 64 K) procedure. ^1H NMR spectra were manually phased. Chemical shifts were reported with respect to the residual CHCl_3 signal set at 7.26 ppm. The baseline was corrected using the Cubic Spline Baseline Correction routine in the Bruker Topspin software.

The intensity of several selected signals (hexanal and trans 2-hexenal, terpene 2 and terpene 1, *sn*-1,3 diglycerides, *sn*-1,2 diglycerides, squalene, unsaturated fatty chains, saturated fatty chains, 24-methylene cycloartanol, linolenic fatty chains, linoleic fatty chains, β -sitosterol), see Table 5.12, was measured using the semi-automatic peak picking routine of Bruker TOPSPIN software and normalized with respect to the resonance at 2.251 ppm, due to α -methylene protons of all acyl chains, normalized to 1000.

Statistical Analysis. NMR data were submitted to the STATISTICA software package for Windows. A statistical procedure based on the following points was performed:

- Analysis of variance (ANOVA). In this analysis the variables with the highest index of variability were selected according to their p level and F values. The p level represents a decreasing index of the reliability of a result and gives the probability of error involved in accepting a result as valid. A p level of 0.05 (5% probability of error) is usually treated as a borderline acceptable error level. The F value is the ratio between groups' variability to within-group variability: the larger this ratio, the larger the discrimination power of the corresponding variable.
- Principal component analysis (PCA). PCA was performed on the variables with the highest index of variability: the percentage of variance for each specific principal component was reported. PCA results are shown reporting the scores of the principal components and also as a plot of the variable loadings.

Table 5.12. Chemical shifts and assignment of the thirteen NMR variables selected for ANOVA analysis.

| | Assignment | NMR Resonances (ppm) |
|----|---|----------------------|
| 1 | Hexanal | 9.704 |
| 2 | Trans 2-hexenal | 9.454 |
| 3 | Terpene 2 | 4.885 |
| 4 | Terpene 1 | 4.541 |
| 5 | Methinic protons in β -glycerol moiety of sn-1,3 diglycerides | 3.988 |
| 6 | Methylene protons in α -glycerol moiety of sn-1,2 diglycerides | 3.636 |
| R | Reference peak due to methylenic protons bound to C2 normalized to 1000 | 2.251 |
| 7 | Squalene | 1.620 |
| 8 | Methylene protons of all unsaturated fatty chains | 1.244 |
| 9 | Methylene protons of palmitic and stearic fatty chains | 1.197 |
| 10 | 24-methylene cycloartanol | 0.978 |
| 11 | Methyl of linolenic fatty chains | 0.910 |
| 12 | Methyl of linoleic fatty chains | 0.843 |
| 13 | Methyl-18 of β -sitosterol | 0.623 |

5.2.3 Results and Discussion

In order to obtain a comprehensive characterization of olive oils from “Colline Pontine” PDO area 40 olive oils samples of two harvest years were analysed by means of a multidisciplinary protocol including Panel Test, IRMS, and ^1H NMR spectroscopy, see Table 5.11. The effect of the harvesting year was investigated in more details considering other 22 olive oils of a third crop year, see Table 5.11. These olive oils were analysed and included in the statistical analysis together with the previous 40 samples.

Sensory Analysis. 40 olive oil samples coming from different geographical areas of the district of Latina (Lazio) were assayed according to the official method reported in the EC Regulation 2568/91 (Commission Regulation (EEC) No 2568/91) and the EC Regulation 640/08 (Commission Regulation (EC) No 640/2008).

The sensorial analysis recognized 34 of 40 samples as extra virgin olive oils, see Table 5.13. On the other hand, 6 of 40 samples were defined as “defective” due to the detection of negative sensory attributes, namely fusty/muddy sediment (samples 8, 12, 25 and 37), musty/humid/earthy (sample 9), winey/vinegary/acid/sour (sample 33) and rancid (sample 37). Therefore, these 6 samples were classified as virgin olive oils. It is important to note that “tomato” is neither a positive attribute nor a negative attribute and therefore it does not affect the score value. This term is specific to evidence and appreciate a “nose-sensed” feature of olive oils.

Table 5.13. Sensory profiles of olive oils. The defective samples are reported in bold type.

| Code | Score | Fruity | Bitter | Pungent | Tomato | Fusty/ muddy sediment | Musty/ humid/ earthy | Winey/ vinegary/ acid/ sour | Metallic | Rancid | Defected |
|------|------------|------------|------------|------------|------------|-----------------------------|----------------------------|-----------------------------------|------------|------------|------------|
| 1 | 7.6 | 4.0 | 3.5 | 4.0 | 3.5 | 0.0 | 0.0 | 0.0 | 0.0 | 0.0 | 0.0 |
| 2 | 7.9 | 6.0 | 5.0 | 5.0 | 4.0 | 0.0 | 0.0 | 0.0 | 0.0 | 0.0 | 0.0 |
| 3 | 7.7 | 5.0 | 4.5 | 4.0 | 4.0 | 0.0 | 0.0 | 0.0 | 0.0 | 0.0 | 0.0 |
| 4 | 7.0 | 4.0 | 3.8 | 4.0 | 2.5 | 0.0 | 0.0 | 0.0 | 0.0 | 0.0 | 0.0 |
| 5 | 8.1 | 6.0 | 4.5 | 5.0 | 4.5 | 0.0 | 0.0 | 0.0 | 0.0 | 0.0 | 0.0 |
| 6 | 7.0 | 4.0 | 3.0 | 3.0 | 0.0 | 0.0 | 0.0 | 0.0 | 0.0 | 0.0 | 0.0 |
| 7 | 7.0 | 4.0 | 3.0 | 3.2 | 1.0 | 0.0 | 0.0 | 0.0 | 0.0 | 0.0 | 0.0 |
| 8 | 6.0 | 3.0 | 3.0 | 2.5 | 0.0 | 2.0 | 0.0 | 0.0 | 0.0 | 0.0 | 2.0 |
| 9 | 6.9 | 4.0 | 4.0 | 3.0 | 0.0 | 0.0 | 1.0 | 0.0 | 0.0 | 0.0 | 1.0 |
| 10 | 7.6 | 4.5 | 3.5 | 3.5 | 3.0 | 0.0 | 0.0 | 0.0 | 0.0 | 0.0 | 0.0 |
| 11 | 7.8 | 5.5 | 5.0 | 4.8 | 4.5 | 0.0 | 0.0 | 0.0 | 0.0 | 0.0 | 0.0 |
| 12 | 6.0 | 3.0 | 2.0 | 3.0 | 0.0 | 1.5 | 0.0 | 0.0 | 0.0 | 0.0 | 1.5 |
| 13 | 7.7 | 5.0 | 4.0 | 4.5 | 4.0 | 0.0 | 0.0 | 0.0 | 0.0 | 0.0 | 0.0 |
| 14 | 8.1 | 6.5 | 5.0 | 4.7 | 4.9 | 0.0 | 0.0 | 0.0 | 0.0 | 0.0 | 0.0 |
| 15 | 8.4 | 6.5 | 5.5 | 5.5 | 4.0 | 0.0 | 0.0 | 0.0 | 0.0 | 0.0 | 0.0 |
| 16 | 7.9 | 3.8 | 3.5 | 3.7 | 1.1 | 0.0 | 0.0 | 0.0 | 0.0 | 0.0 | 0.0 |
| 17 | 7.8 | 5.1 | 5.0 | 5.0 | 2.5 | 0.0 | 0.0 | 0.0 | 0.0 | 0.0 | 0.0 |
| 18 | 7.3 | 3.7 | 2.9 | 2.9 | 1.2 | 0.0 | 0.0 | 0.0 | 0.0 | 0.0 | 0.0 |
| 19 | 8.3 | 5.9 | 5.1 | 5.3 | 3.4 | 0.0 | 0.0 | 0.0 | 0.0 | 0.0 | 0.0 |
| 20 | 8.1 | 5.9 | 5.0 | 5.0 | 3.4 | 0.0 | 0.0 | 0.0 | 0.0 | 0.0 | 0.0 |
| 21 | 7.1 | 3.8 | 3.6 | 3.3 | 2.0 | 0.0 | 0.0 | 0.0 | 0.0 | 0.0 | 0.0 |
| 22 | 7.8 | 5.2 | 3.9 | 4.2 | 2.9 | 0.0 | 0.0 | 0.0 | 0.0 | 0.0 | 0.0 |
| 23 | 7.7 | 4.8 | 4.0 | 4.0 | 3.0 | 0.0 | 0.0 | 0.0 | 0.0 | 0.0 | 0.0 |
| 24 | 8.4 | 6.2 | 5.6 | 5.4 | 4.0 | 0.0 | 0.0 | 0.0 | 0.0 | 0.0 | 0.0 |
| 25 | 6.7 | 2.4 | 1.8 | 2.3 | 0.0 | 1.0 | 0.0 | 0.0 | 0.0 | 0.0 | 1.0 |
| 26 | 7.5 | 4.1 | 3.5 | 4.1 | 3.1 | 0.0 | 0.0 | 0.0 | 0.0 | 0.0 | 0.0 |
| 27 | 8.0 | 5.1 | 4.5 | 5.0 | 3.0 | 0.0 | 0.0 | 0.0 | 0.0 | 0.0 | 0.0 |
| 28 | 7.2 | 4.0 | 3.2 | 3.3 | 1.0 | 0.0 | 0.0 | 0.0 | 0.0 | 0.0 | 0.0 |
| 29 | 7.4 | 4.0 | 3.2 | 3.2 | 2.4 | 0.0 | 0.0 | 0.0 | 0.0 | 0.0 | 0.0 |
| 30 | 7.4 | 4.5 | 4.0 | 4.1 | 1.3 | 0.0 | 0.0 | 0.0 | 0.0 | 0.0 | 0.0 |
| 31 | 7.8 | 4.0 | 3.5 | 4.3 | 2.5 | 0.0 | 0.0 | 0.0 | 0.0 | 0.0 | 0.0 |
| 32 | 7.5 | 4.5 | 3.1 | 3.8 | 2.7 | 0.0 | 0.0 | 0.0 | 0.0 | 0.0 | 0.0 |
| 33 | 6.7 | 3.5 | 3.0 | 3.3 | 0.0 | 0.0 | 0.0 | 1.0 | 0.0 | 0.0 | 1.0 |
| 34 | 7.8 | 3.8 | 3.7 | 3.8 | 3.2 | 0.0 | 0.0 | 0.0 | 0.0 | 0.0 | 0.0 |
| 35 | 7.7 | 5.3 | 4.2 | 4.5 | 3.1 | 0.0 | 0.0 | 0.0 | 0.0 | 0.0 | 0.0 |
| 36 | 7.0 | 5.0 | 3.8 | 4.0 | 2.3 | 0.0 | 0.0 | 0.0 | 0.0 | 0.0 | 0.0 |
| 37 | 6.0 | 3.0 | 2.0 | 1.6 | 0.2 | 1.2 | 0.0 | 0.0 | 0.0 | 2.0 | 2.0 |
| 38 | 7.6 | 5.4 | 3.8 | 4.3 | 2.5 | 0.0 | 0.0 | 0.0 | 0.0 | 0.0 | 0.0 |
| 39 | 7.6 | 4.5 | 4.8 | 5.0 | 2.5 | 0.0 | 0.0 | 0.0 | 0.0 | 0.0 | 0.0 |
| 40 | 7.1 | 4.0 | 3.3 | 3.0 | 2.0 | 0.0 | 0.0 | 0.0 | 0.0 | 0.0 | 0.0 |

Isotope Ratio Mass Spectrometry. The results of stable isotope ratios of H, O and C carried out on 40 olive oil samples are reported in Table 5.14. As expected for samples produced in a narrow area, we did not find a large variability of the isotopic data, with $\delta^2\text{H}$ ranging from -152 to -135‰ , $\delta^{18}\text{O}$ from 22.0 to 26.3‰ and $\delta^{13}\text{C}$ from -31.9 to -28.1‰ . These values may be considered characteristic of the PDO “Colline Pontine” olive oils.

Table 5.14. $\delta^2\text{H}$, $\delta^{18}\text{O}$ and $\delta^{13}\text{C}$ of olive oils.

| | Mean | Sd | Min | Max |
|--|-------|-----|-------|-------|
| $\delta^2\text{H} \text{‰ vs V-SMOW}$ | -142 | 4 | -152 | -135 |
| $\delta^{18}\text{O} \text{‰ vs V-SMOW}$ | 24.0 | 1.1 | 22.0 | 26.3 |
| $\delta^{13}\text{C} \text{‰ vs V-PDB}$ | -30.2 | 1.0 | -31.9 | -28.1 |

Nuclear Magnetic Resonance Spectroscopy. Olive oils (62 samples) were submitted to the NMR analysis. The ^1H NMR spectrum of an olive oil is shown in Figure 5.2. In the 3.5–4.0 ppm spectral region, the signal due to *sn*-1,2 diglycerides and *sn*-1,3 diglycerides are observable, giving an index of the olive oil freshness (Mannina, Sobolev & Segre, 2003).

Freshly made olive oil from healthy olive fruits contains almost only *sn*-1,2 diglycerides whose content decreases during the storage, whereas the *sn*-1,3 diglycerides content increases (Spyros, Philippidis & Dais, 2004) due to the gradual isomerization of *sn*-1,2 diglycerides to *sn*-1,3 ones. Different factors, such as the extraction process, shelf-life, storage conditions, presence of macromolecules, metals are responsible for the *sn*-1,2/1,3 diglycerides ratio (Belitz, 2009; Perez-Camino, Modera et Cert, 2001). Therefore, this ratio is strongly related to the freshness of an olive oil (Mannina & Sobolev, 2011; Salvo et al., 2017). In fresh olive oils, this ratio is greater than 4, whereas a ratio < 4 indicates a low-quality olive oil (Mannina et al., 2012).

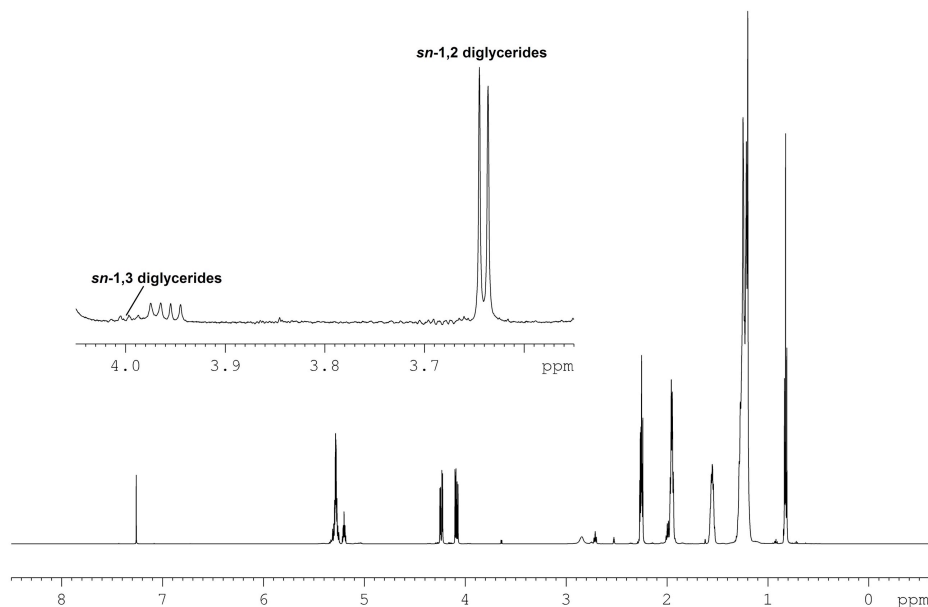


Figure 5.2. 600.13 MHz ¹H NMR spectrum of an olive oil. An expansion of the 3.5–4.0 ppm spectral region including *sn*-1,2 diglycerides and *sn*-1,3 diglycerides signals, is shown.

In our case, all olive oil samples possessed a *sn*-1,2/*sn*-1,3 diglycerides ratio greater than 4, suggesting a good quality product and a suitable storage process, see Table 5.15.

Statistical Analysis. In order to assess the harvesting year influence over the olive oil chemical composition, a statistical analysis was performed: 13 selected resonances (see Table 5.16) sensitive to the geographical origin (D’Imperio et al., 2007) were carefully measured and the normalized intensities were submitted to a suitable statistical analysis.

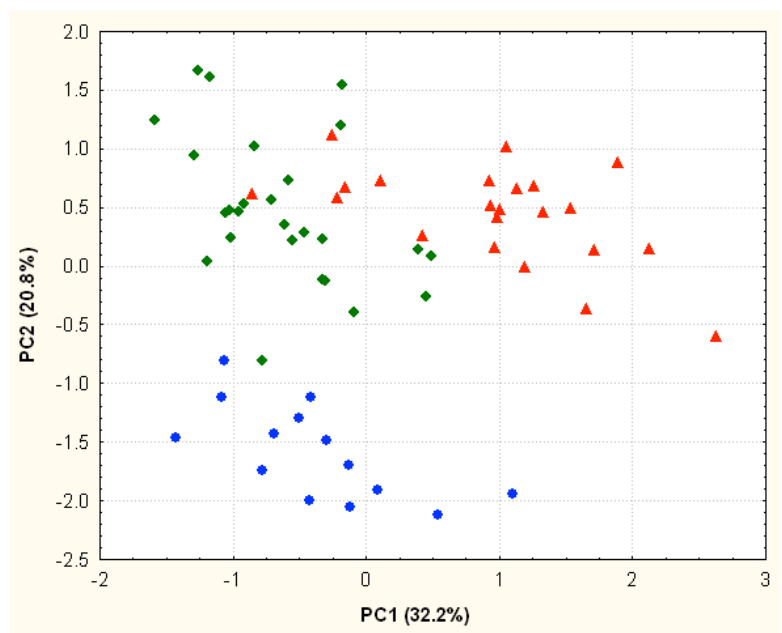
Table 5.15. The sn-1,2/sn-1,3 diglycerides ratio obtained from ¹H-NMR normalized signal intensities.

| Code | Ratio <i>sn1,2/sn1,3</i> | Code | Ratio <i>sn1,2/sn1,3</i> | Code | Ratio <i>sn1,2/sn1,3</i> | Code | Ratio <i>sn1,2/sn1,3</i> |
|------|-----------------------------|------|-----------------------------|------|-----------------------------|------|-----------------------------|
| 1 | 41.30 | 21 | 46.00 | 41 | 13.83 | 61 | 6.74 |
| 2 | 56.75 | 22 | 12.86 | 42 | 17.49 | 62 | 4.53 |
| 3 | 44.33 | 23 | 33.20 | 43 | 14.74 | | |
| 4 | 19.92 | 24 | 39.58 | 44 | 13.82 | | |
| 5 | 35.30 | 25 | 31.22 | 45 | 9.20 | | |
| 6 | 57.89 | 26 | 31.25 | 46 | 12.63 | | |
| 7 | 49.60 | 27 | 47.67 | 47 | 11.84 | | |
| 8 | 5.73 | 28 | 15.57 | 48 | 16.06 | | |
| 9 | 17.21 | 29 | 25.12 | 49 | 6.80 | | |
| 10 | 65.29 | 30 | 38.22 | 50 | 29.74 | | |
| 11 | 43.67 | 31 | 57.00 | 51 | 20.38 | | |
| 12 | 17.88 | 32 | 41.69 | 52 | 20.73 | | |
| 13 | 33.53 | 33 | 24.14 | 53 | 11.58 | | |
| 14 | 40.09 | 34 | 51.17 | 54 | 5.60 | | |
| 15 | 37.33 | 35 | 35.64 | 55 | 11.75 | | |
| 16 | 27.32 | 36 | 27.00 | 56 | 8.26 | | |
| 17 | 47.40 | 37 | 70.50 | 57 | 9.48 | | |
| 18 | 37.92 | 38 | 18.20 | 58 | 11.43 | | |
| 19 | 65.33 | 39 | 57.91 | 59 | 5.74 | | |
| 20 | 46.70 | 40 | 30.46 | 60 | 7.59 | | |

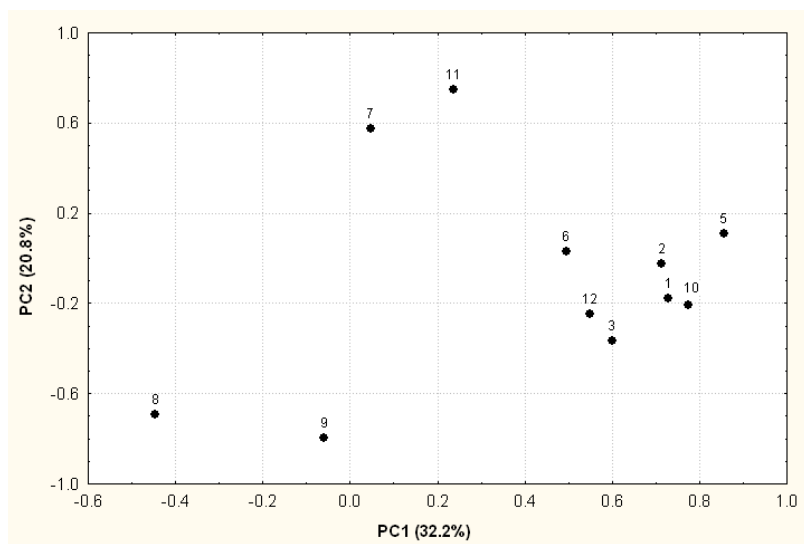
The ANOVA was performed on the intensity of the selected resonances to find the variables with the highest discriminating power. Except for “Terpene 1” (4) and “β-sitosterol” (13), the remaining eleven variables showed to be significant for the characterization of olive oil samples and they were submitted to the PCA analysis. Terpene 1 seems to represent a variable independent from the harvesting effect because its content was found to be, on average, constant in the three different harvest years.

The PCA map, labelled according to the three harvesting years, is shown in Figure 2a. The PC1, explaining 32.2% of the total variance, facilitates observation of a good separation between olive oil samples from the first two harvesting years and the third

harvesting year. The PC2, explaining 20.8% of the total variance, shows a discreet separation between olive oil samples from the first harvesting year and the other two ones.



(a)



(b)

Figure 2. (a) Score plot of PCA along the two main components performed on NMR data regarding 62 olive oil samples, produced during three harvesting years labelled as blue circles, green diamonds, red triangles according to the respective year time order. The eleven variables with the highest discrimination power selected by ANOVA were used for the PCA and labelled by the Arabic numbers 1–3 and 5–12 (explained in the text); these are displayed in the (b) analogous plot of loadings.

The most discriminant parameters correspond to saturated (9) and unsaturated (8) fatty acids, having a high value in samples of the first harvesting year, to linolenic acid (11) and squalene (7), having a high value in samples of the second and the third harvesting years, and to 24-methylene cycloartanol (10), sn-1,3 diglycerides (5) and the two aldehydes (1, 2), having a high value in samples of the third harvesting year (see the corresponding loadings shown in Figure 2b). The variability of all these compounds in the three harvests can be due to different factors such as the different climatic conditions.

5.2.4 Conclusions

The investigation carried out in the present work offers a reliable protocol that can play a significant role in the characterization and assessment quality of olive oils. This approach helped to describe olive oils of the “Colline Pontine” PDO area, which turned out to be characterized by specific sensory and chemical markers.

Therefore, the present findings suggest a positive contribution of this multidisciplinary analytical protocol for promoting the diffusion of high quality olive growing in the “Colline Pontine” PDO area. This methodology can give an important contribution in the PDO characterization and confirmation. This certification improves the value of the Mediterranean products and provides assurance that a product is of a high quality and has a defined origin.

5.2.5 References

- Angerosa, F., Breas, O., Contento, S., Guillou, C., Reniero, F., Sada, E., 1999. Application of Stable Isotope Ratio Analysis to the Characterization of the Geographical Origin of Olive Oils. *J. Agric. Food Chem.* 47, 1013–1017.
- Aramendia, M.A., Marinas, A., Marinas, J.M., Moreno, J.M., Moalem, M., Rallo, L., Urbano, F.J., 2007. Oxygen-18 measurement of Andalusian olive oils by continuous flow pyrolysis/isotope ratio mass spectrometry. *Rapid Commun. Mass Spectrom.* 21, 487–496.
- Bianchi, G., Giansante, L., Shaw, A., Kell, D.B., 2001. Chemometric criteria for the characterisation of Italian Protected Denomination of Origin (DOP) olive oils from their metabolic profiles. *Eur. J. Lipid Sci. Technol.* 103, 141–150.
- Belitz, H.D., Grosch, W., Schieberle, P., 2009. *Food Chemistry*. Springer: Berlin. ISBN 978-3-540-69934-7.
- Bontempo, L., Camin, F., Larcher, R., Nicolini, G., Perini, M., Rossmann, A., 2009. Coast and year effect on H, O and C stable isotope ratios of Tyrrhenian and Adriatic Italian olive oils. *Rapid Commun. Mass Spectrom.* 23, 1043–1048.
- Camin, F., Larcher, R., Perini, M., Bontempo, L., Bertoldi, D., Gagliano, G., Nicolini, G., Versini, G., 2010a. Characterisation of authentic Italian extra-virgin olive oils by stable isotope ratios of C, O and H and mineral composition. *Food Chem.* 118, 901–909.
- Camin, F., Larcher, R., Nicolini, G., Bontempo, L., Bertoldi, D., Perini, M., Schlicht, C., Schellenberg, A., Thomas, F., Heinrich, K., et al., 2010b. Isotopic and elemental data for tracing the origin of European olive oils. *J. Agric. Food Chem.* 58, 570–577.
- Camin, F., Pavone, A., Bontempo, L., Wehrens, R., Paolini, M., Faberi, A., Marianella, R.M., Capitani, D., Vista, S., Mannina, L., 2016. The use of IRMS, ¹H NMR and chemical analysis to characterise Italian and imported Tunisian olive oils. *Food Chem.* 196, 98–105.
- Circi, S., Capitani, D., Randazzo, A., Ingallina, C., Mannina, L., Sobolev, A.P., 2017. Panel test and chemical analyses of commercial olive oils: A comparative study. *Chem. Biol. Technol. Agric.* 4(18).
- Council of the European Union. Regulation (EU) No 510/2006 on the protection of geographical indications and designations of origin for agricultural products and foodstuffs. <https://eur-lex.europa.eu/legal-content/EN/TXT/?uri=celex:32006R0510>
- Del Coco, L., Mondelli, D., Mezzapesa, G.N., Miano, T., De Pascali, S.A., Girelli, C.R., Fanizzi, F.P., 2016. Protected Designation of Origin extra virgin olive oils assessment by nuclear magnetic resonance and multivariate statistical analysis: “Terra di Bari”, an Apulian (Southeast Italy) case study. *J. Am. Oil Chem. Soc.* 93, 373–381.
- D’Imperio, M., Mannina, L., Capitani, D., Bidet, O., Rossi, E., Bucarelli, F.M., Quaglia, G.B., Segre, A.L., 2007. NMR and statistical study of olive oils from Lazio: A geographical, ecological and agronomic characterization. *Food Chem.* 105, 1256–1267.

- D'Imperio, M., Gobbino, M., Picanza, A., Costanzo, S., Della Corte, A., Mannina, L., 2010. Influence of harvest method and period on olive oil composition: An NMR and statistical study. *J. Agric. Food Chem.* 58, 11043–11051.
- Di Vaio, C., Nocerino, S., Paduano, A., Sacchi, R., 2013. Influence of some environmental factors on drupe maturation and olive oil composition. *J. Sci. Food Agric.* 93, 1134–1139.
- Dugo, G., Rotondo, A., Mallamace, D., Cicero, N., Salvo, A., Rotondo, E., Corsaro, C., 2015. Enhanced detection of aldehydes in extra-virgin olive oil by means of band selective NMR spectroscopy. *Phys. A Stat. Mech. Appl.* 420, 258–264.
- Laincer, F., Iaccarino, N., Amato, J., Pagano, B., Pagano, A., Tenore, G., Tamendjari, A., Rovellini, P., Venturini, S., Bellan, G., et al., 2016. Characterization of monovarietal extra virgin olive oils from the province of Béjaïa (Algeria). *Food Res. Int.* 89, 1123–1133.
- Likudis, Z. Olive Oils with Protected Designation of Origin (PDO) and Protected Geographical Indication (PGI). In: Boskou, D., Editor, 2016. *Products from Olive Tree*. InTech: Munich, Germany. 175–190.
- Mannina, L., D'Imperio, M., Gobbino, M., D'Amico, I., Casini, A., Sobolev, A.P., 2012. Nuclear magnetic resonance study of flavoured olive oils. *Flavour Fragr. J.* 27, 250–259
- Mannina, L., Sobolev, A.P., Segre, A.L., 2003. Olive oil as seen by NMR and chemometrics. *Spectrosc. Eur.* 15, 6–14.
- Mannina, L., Sobolev, A.P., 2011. High resolution NMR characterization of olive oils in terms of quality, authenticity, and geographical origin. *Magn. Reson. Chem.* 49, S3–S11.
- Perez-Camino, M.C., Modera, W., Cert, A., 2001. Effects of olive oil fruit quality and oil storage practices on the diacylglycerols content of virgin olive oils. *J. Agric. Food Chem.* 49, 699–704.
- Rotondo, A., Salvo, A., Gallo, V., Rastrelli, L., Dugo, G., 2017. Quick unreferenced NMR quantification of Squalene in vegetable oils. *Eur. J. Lip. Sci. Technol.* 119.
- Rotondo, A., Salvo, A., Giuffrida, D., Dugo, G., Rotondo, E., 2011. NMR analysis of aldehydes in sicilian extra-virgin olive oils by DPFGE techniques. *AAPP Phys. Math. Nat. Sci.* 89(1).
- Salvo, A., Rotondo, A., La Torre, G.L., Cicero, N., Dugo, G., 2017. Determination of 1,2/1,3-Diglycerides in Sicilian extra-virgin olive oils by ¹H-NMR over a one-year storage period. *Nat. Prod. Res.* 31, 822–828.
- Schievano, E., Arosio, I., Lava, R., Simionato, V., Mammi, S., Consonni, R., 2006. Olio di oliva DOP del lago di Garda: Uno studio NMR e analisi statistica multivariata. *RISG* 83, 14–17.
- Spyros, A., Philippidis, A., Dais, P., 2004. Kinetics of Diglyceride Formation and Isomerization in Virgin Olive Oils by Employing ³¹P NMR Spectroscopy. Formulation of a Quantitative Measure to Assess Olive Oil Storage History. *J. Agric. Food Chem.* 52, 157–164.

The Commission of the European Communities. Commission Regulation (EEC) No 2568/91 of 11 July 1991 on the characteristics of olive oil and olive-residue oil and on the relevant methods of analysis. <https://eur-lex.europa.eu/eli/reg/1991/2568/2015-01-01>

The Commission of the European Communities. Commission Regulation (EC) No 640/2008 of 4 July 2008 amending Regulation (EEC) No 2568/91 on the characteristics of olive oil and olive-residue oil and on the relevant methods of analysis. <https://eur-lex.europa.eu/legal-content/EN/ALL/?uri=CELEX:32008R0640>.

The European Parliament and the Council of the European Union. Regulation (EU) No 182/2011 laying down the rules and general principles concerning mechanisms for control by Member States of the Commission's exercise of implementing powers. <https://eur-lex.europa.eu/legal-content/EN/ALL/?uri=CELEX:32011R0182>

The European Parliament and the Council of the European Union. Regulation (EC) No. 1151/2012 of the European Parliament and of the Council of 21 November 2012 on quality schemes for agricultural products and foodstuffs. <http://www.wipo.int/wipolex/en/details.jsp?id=13384>

Chapter 6: Foods with High Biological Value

6.1 Blueberries

6.1.1 Introduction

Blueberries are sweet, nutritious and wildly popular fruits. In the last decade their consumption has increased rapidly because many studies suggested that a large consume of blueberries can be associated with a reduced risk of obesity, diabetes and heart diseases (Martineau et al., 2006; Manganaris et al., 2014; Blanck et al., 2008; Stull et al., 2010; Basu et al., 2010). For the beneficial health benefits blueberries are considered a “functional food” (Cho et al., 2004; Gonzalez-Gallego et al., 2010).

Anthocyanins, the main antioxidant compounds in these fruits are also responsible for the typical colour, together with proanthocyanidins, phenolic acids and stilbenes are responsible for the high antioxidant capacity of blueberries which provides protection against a number of diseases maintaining healthy bones, lowering blood pressure, managing diabetes, warding off heart disease and preventing cancer (Joshiyura et al., 2001, Castrejon et al., 2008; Krikorian et al., 2010; Seeram, 2008).

The blueberry plant belongs to the Ericaceae family, genus *Vaccinium*, which includes about 130 species. From the agronomic point of view, it is noteworthy the *Vaccinium myrtillus* or blackberry, spontaneous in Europe with black, solitary or paired berries, covered with bloom and colored pulp, the *Vaccinium vitis idaea* or cranberry, evergreen and spontaneous in Europe, with white or pink flowers and with red berries, the *Vaccinium uliginosum* or blueberries, spontaneous in Europe, white-red flowers and with berries of black-bluish colour, and the *Vaccinium corymbosum* or American highbush blueberries,

spontaneous in North America, high 4.1 m, deciduous, with white or pink flowers with berries gathered in clusters, black-blue colour and very cold-resistant (up to -30°C) (Gough, 1991). The varieties of blueberry cultivated today are mainly those derived from the giant blueberry.

Taking into account the complexity of blueberry composition, both targeted and untargeted methodologies have been applied for their chemical characterization. Recently, targeted analytical techniques focused on phenolic components, such as Gas Liquid Chromatography (GLC) (Zadernoski et al., 2005), High-Performance Liquid Chromatography coupled with Mass Spectrometry (HPLC-MS) (Nocoue et al., 2007; Barnes et al., 2009; Bunea et al., 2013), High-Performance Liquid Chromatography with photodiode array detection (HPLC-DAD) (Yousef et al., 2013) and Capillary Electrophoresis (CE) (Ichiyanagi et al., 2000; Ichiyanagi et al., 2004) methods allowed to separate and identify different phenolic compounds.

NMR spectroscopic characterization of anthocyanins isolated from different plants is reported in several studies (Ichiyanagi et al., 2004; Yawadio, Tanimori & Morita, 2007; Saito et al., 2011; Jordheim, Giske & Andersen, 2007; Lee & Choung, 2011; Byamukama et al., 2011). The mixture of deuterated methanol and TFA has been found to be the best solvent system (in terms of spectral resolution) for NMR analysis of anthocyanins. The identification of sugar moiety in anthocyanins in the mixture with other more abundant sugar metabolites using NMR is quite complicated due to considerable overlapping of their ^1H NMR signals. Fortunately, a simple C_{18} SPE extraction of anthocyanins and other phenolic compounds allows one to overcome this problem (Wizgoski et al., 2010). The combination of SPE extraction with the use of methanol and TFA as a solvent seems to be the best approach to NMR-based anthocyanin characterization. Five out of the six principal anthocyanidins (cyanidin, delphinidin, malvidin, petunidin, and peonidin, see Figure 6.1) have been found in blueberry up to now (Yousef et al., 2013; Simeone et al., 2012).



Figure 6.1. The structure of anthocyanidins.

Water-soluble metabolites belonging to different classes such as sugars, amino acids, organic acids, and phenolic compounds, as well as metabolites soluble in organic solvent such as triglycerides, sterols, and fatty acids, were identified (Capitani et al., 2014).

The study of the foodstuffs metabolic profiling turned out to be an important tool to have information regarding food varieties, nutritional properties, processing and shelf life, and also to monitor fruit development to assess the proper harvesting time. The study of the metabolic profile of several fruits, such as kiwifruits (Capitani et al., 2010; Capitani et al., 2013a; Capitani et al., 2013c), peaches (Capitani et al., 2013b), mango (Gil et al., 2000), melon (Biais et al., 2009), water melon (Tarachiwin et al., 2008), and tea (Daglia et al., 2014) has allowed to obtain information on geographical origin, varieties, quality and adulteration (Mannina et al., 2012).

In this PhD work, we have extended the targeted and untargeted NMR methodologies to the study of four different blueberry varieties, named Spartan, Jewell, Misty and Camelia.

6.1.2 Material and Methods

Sampling. Blueberries of four varieties (Camelia, Jewel, Misty and Spartan), harvested in June in three successive harvest years (2014, 2015 and 2016), were hand-harvested in an experimental field located in Ciampino, Lazio district, Italy (CREA).

Sample preparation. Berries (100 g) were frozen in liquid nitrogen and finely powdered using mortar and a pestle. Every harvesting year, five replicates (2 g each sample) for each variety were sampled and subjected to extraction.

Bligh-Dyer extraction adapted for blueberries was performed according to literature (Capitani et al. 2014). Solvents (3mL of methanol/chloroform mixture 2:1 v/v, 1mL of chloroform and 1.2 mL of pure water) were added to samples kept at 4°C for 40 minutes and then centrifuged at 4500 rpm for 15 minutes at 4°C. The upper hydroalcoholic phase and the lower organic phase were carefully separated. The pellets were re-extracted using half of the solvent volumes and the same procedure reported above was followed. The fractions of the first and second extractions were pooled. Hydroalcoholic and organic fractions were dried under an N₂ flow at room temperature. The hydroalcoholic phase was additionally freeze dried. The dried phases were then stored at -20°C until the NMR analysis.

The organic fraction was dissolved in 0.7 mL of CDCl₃/CD₃OD mixture (2:1 v/v) in bis(trimethylsilyl)amine (HMDS) and then placed into a 5-mm NMR tube. Finally, the NMR tube was flame-sealed.

The hydroalcoholic phase was dissolved in 0.7 mL D₂O/phosphate buffer containing 3-(trimethylsilyl)-propionic-2,2,3,3-d₄ acid sodium salt (TSP, 2 mM) and 0.1 mM EDTA, transferred into a standard 5-mm NMR tube and subjected to NMR analysis.

SPE was performed on C₁₈ column to isolate phenolic compounds according to the literature procedure originally developed for black raspberry (Wizgoski et al., 2010). Briefly,

SPE columns were equilibrated with 25 mL of 0.1% TFA in double-distilled H₂O after column washing with 25 mL of 0.1% TFA in HPLC-grade methanol. Successively aliquots (4 mL) of the hydroalcoholic phase, acidified by adding 0.1% TFA (v/v), were loaded onto C₁₈ columns. Anthocyanins and other phenolic compounds were eluted with 25 mL of methanol acidified with TFA. Methanol was removed from the eluted materials under N₂ flow and then water was removed by lyophilisation. The dried extract was dissolved in 0.7 mL of CD₃OD and CF₃COOD (95:5 v/v) solution, transferred into a standard 5-mm NMR tube and then the tube was flame-sealed and stored at -20 °C until NMR experiments.

NMR experiments. The NMR spectra of aqueous and organic blueberry extracts were recorded at 27°C on a Bruker AVANCE 600 NMR spectrometer operating at the proton frequency of 600.13 MHz, equipped with a Bruker multinuclear z-gradient inverse probe head capable of producing gradients in the z-direction with a strength of 55 G/cm. ¹H spectra were referenced to methyl group signals of TSP (δ=0.00 ppm) in D₂O and to the residual CHD₂ signal of methanol (set to 3.31 ppm) in CD₃OD/CDCl₃ mixture.

¹H spectra of aqueous extracts were acquired by co-adding 256 transients with a recycle delay of 3s. The residual HDO signal was suppressed using a pre-saturation. The experiment was carried out by using a 45° pulse of 6.68 μs, 32K data points. ¹H spectra of organic extracts were obtained using the following parameters: 256 transients, 32K data points, recycle delay of 3 s and a 45° pulse of 5 μs. ¹H spectra of CD₃OD/CDCl₃ extracts were obtained using the following parameters: 128 transients, 64K data points, recycle delay of 3s and a 90° pulse of 9.60 μs. The ¹H spectral assignment has been previously reported (Capitani et al., 2014)

Quantitative and statistical analysis. In order to analyse the multivariate structure of the data, the Principal Component Analysis (PCA) was applied to the integrals of ¹H

selected resonances: 25 (Table 6.1), 9 (Table 6.2) and 13 (Table 6.3) metabolites, in hydroalcoholic, organic and SPE extracts respectively, were integrated and the values of their integrals were submitted to the PCA. Integrals were normalized respect to the internal standard (TSP) in the hydroalcoholic extracts and to the sum, fixed at 100, of Non-Esterified Fatty Acids (FA) and Esterified Fatty Acids (EFA) in the organic extracts whereas integrals of anthocyanins were normalized with respect to the sum of the thirteen anthocyanins. The statistical analysis of NMR data was performed using an R-based chemometric software developed by the Group of Chemometrics of the Italian Chemical Society. ANOVA was also carried out to confirm some metabolites as markers of specific cultivars.

Table 6.1. The compounds (25), and relative signals (ppm), selected for PCA in hydroalcoholic extracts.

| ppm | Compounds |
|-------|------------------------------|
| 0.875 | Quercitina-3-Ramnoside (Q3R) |
| 0.939 | Unknown 1 (U1) |
| 0.983 | Unknown 2 (U2) |
| 0.998 | Val |
| 1.029 | Ile |
| 1.501 | Ala |
| 1.905 | Quinic Acid (QA) |
| 2.319 | GABA |
| 2.369 | Glu |
| 2.405 | Malic Acid (MA) |
| 2.488 | Gln |
| 2.575 | Citric Acid (CA) |
| 2.84 | Asp |
| 2.898 | Asn |
| 3.214 | Choline |
| 3.279 | β -Glucose |
| 3.31 | Myo-Inositol (MI) |
| 4.052 | Fructose |
| 4.49 | Unknown 3 (U3) |
| 4.518 | Unknown 4 (U4) |
| 5.117 | Unknown 5 (U5) |
| 5.276 | α -Glucose |
| 5.358 | Chlorogenic Acid (CGA) |
| 5.521 | Unknown 6 (U6) |
| 6.456 | Shikimic Acid (SHA) |

Table 6.2. The compounds (9), and relative signals (ppm), selected for PCA in organic extracts.

| ppm | Compounds |
|-------|-------------------------------------|
| 0.526 | Unknown Sterol (St1) |
| 0.675 | β -Sitosterol (bSito) |
| 2.262 | Non-Esterified Fatty Acids (FA) |
| 2.354 | Esterified Fatty Acids (EFA) |
| 2.754 | Di-Unsaturated Fatty Acids (C18:2) |
| 2.794 | Tri-Unsaturated Fatty Acids (C18:3) |
| 3.224 | Phosphatidylcholine (PC) |
| 4.152 | Triglycerides (TG) |
| 4.887 | Digalactosyldiacylglycerol (DGAL) |

Table 6.3. The thirteen compounds, and relative signals (ppm), selected for PCA in SPE extracts.

| ppm | Compounds |
|-------|------------------------------------|
| 8.894 | Unknown 1 (Ant1) |
| 8.917 | Unknown 2 (Ant2) |
| 8.937 | Unknown 3 (Ant3) |
| 8.945 | Unknown 4 (Ant4) |
| 8.958 | Unknown 5 (Ant5) |
| 8.971 | Delphinidina-3-Glucoside (D3GLC) |
| 8.982 | Delphinidina-3-Galactoside (D3GAL) |
| 9.000 | Unknown 6 (Ant6) |
| 9.014 | Petunidina-3-Glucoside (P3GLC) |
| 9.024 | Unknown 7 (Ant7) |
| 9.032 | Unknown 8 (Ant8) |
| 9.049 | Malvidin-3-Glucoside (M3GLC) |
| 9.063 | Malvidin-3-Galactoside (M3GAL) |

6.1.3 Results and Discussion

The ^1H spectra of hydroalcoholic blueberry extracts in D_2O /phosphate buffer (pH = 7.2) is shown in Figure 6.2. The ^1H spectra are dominated by the strong signals of sugars, in the 3.0–5.5 ppm spectral range, whereas, to observe other metabolites, some vertical expansions of the spectrum are necessary.

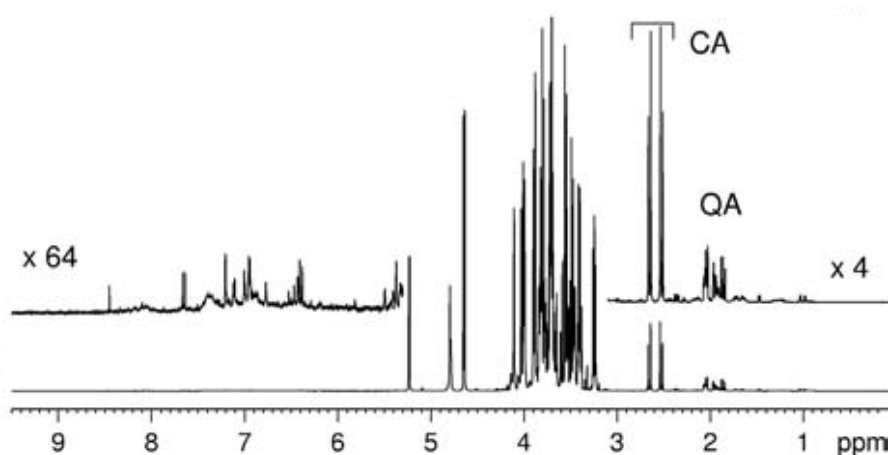


Figure 6.2. 600.13 MHz ^1H NMR spectrum of a blueberry extract at 27°C in D_2O /phosphate buffer. Vertical expansions show citric acid (CA) and quinic acid (QA) resonances.

An exhaustive assignment of both hydroalcoholic and organic blueberries extracts has been previously reported (Capitani et al., 2014).

As previously reported (Capitani et al., 2014), the 8.9–9.1 ppm spectral region of blueberry SPE extract shows the presence of at least 13 anthocyanins (Figure 6.3). It is noteworthy that in this region only the singlet signals attributed to H-4 proton of anthocyanidins are present and the spectrum can be read as a chromatogram, each signal indicating a specific compound. Five anthocyanins were identified as malvidin-3-glucoside, malvidin-3-galactoside, delphinidin-3-glucoside, delphinidin-3-galactoside, and petunidin-3-glucoside. Although cyanidin glycosides are reported among the major components of anthocyanin fraction in blueberry (Yousef et al., 2013), they constitute only a small part of anthocyanin fraction in the four investigated cultivar.

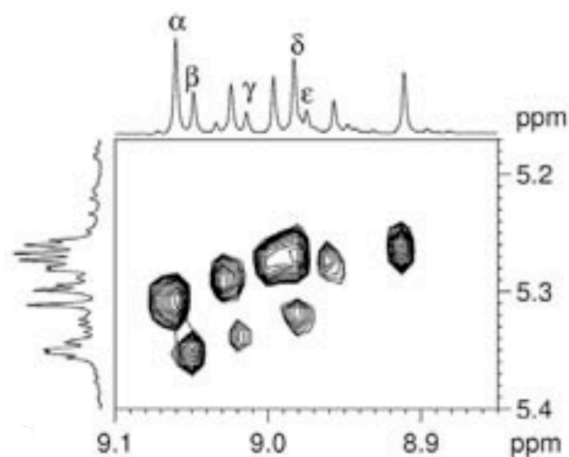


Figure 6.3. Expansion of ^1H - ^1H ROESY map of a Camelia blueberry SPE extract. The expansion of 8.85–9.10 ppm spectral region of H-4 proton of anthocyanidin moieties of Camelia blueberry is also reported as horizontal projection. α = malvidin-3-galactoside, β = malvidin-3-glucoside, γ = petunidin-3-glucoside, δ = delphinidin-3-galactoside, and ϵ = delphinidin-3-glucoside.

Other phenolic compounds namely 3-O- α -L-rhamnopyranosyl quercetin (Q3R) and chlorogenic acid (CGA), that represents one of the most abundant phenolic acids present in blueberries (Yousef et al., 2013), were also identified (Capitani et al., 2014).

The integrals of 25 metabolites in hydroalcoholic extracts were submitted to PCA. First, a PC1 versus PC2 plot (Figure 6.4) was constructed and PC1, accounting for 26.5% of the variability within the data, allowed to discriminate sample according to a harvesting year; in particular, samples from the first harvest year (2014), represented by the circles in the left side of the score plot, resulted well separated by the other ones (2015 and 2016). Samples belonging to Camelia and Misty cultivar resulted very different and are well separated whereas samples belonging to Jewel and Spartan ones are more similar. In order to obtain a different spatial disposition of samples, a PC2 versus PC3 diagram was also reported. Figure 6.5 shows the PCA score and loading plots considering the second and the third principal components as variables. These two PCs account for 38.8% of the variability within the data, PC2 providing for 23.0% and PC3 for 15.8%. In the score plot samples belonging to the same cultivar resulted in being clustered together independently by the harvest year. As already evidenced by the previous score plot, Camelia and Misty samples result very different and are

well grouped also in this plot whereas Jewel and Spartan samples, more similar to each other, occupied the same 2D space in the plot. PC3 maximizes the separation of samples belonging to the Camelia cultivar (on the left at the bottom of the score plot) according to the harvesting year, whereas PC2 maximizes the separation of samples belonging to the Misty cultivar (on the right at the bottom of score plot) according to the harvest year. Spartan and Jewel varieties are placed together at the top of the score plot. Looking at the loading plot we can have an idea for the metabolites responsible for the samples clustering. For instance, it is clear that Camelia samples have a higher content of Q3R and U1 with respect to other cultivar whereas Misty samples have a higher content of CGA. On the other side, Jewel and Spartan samples result more concentrated in U3.

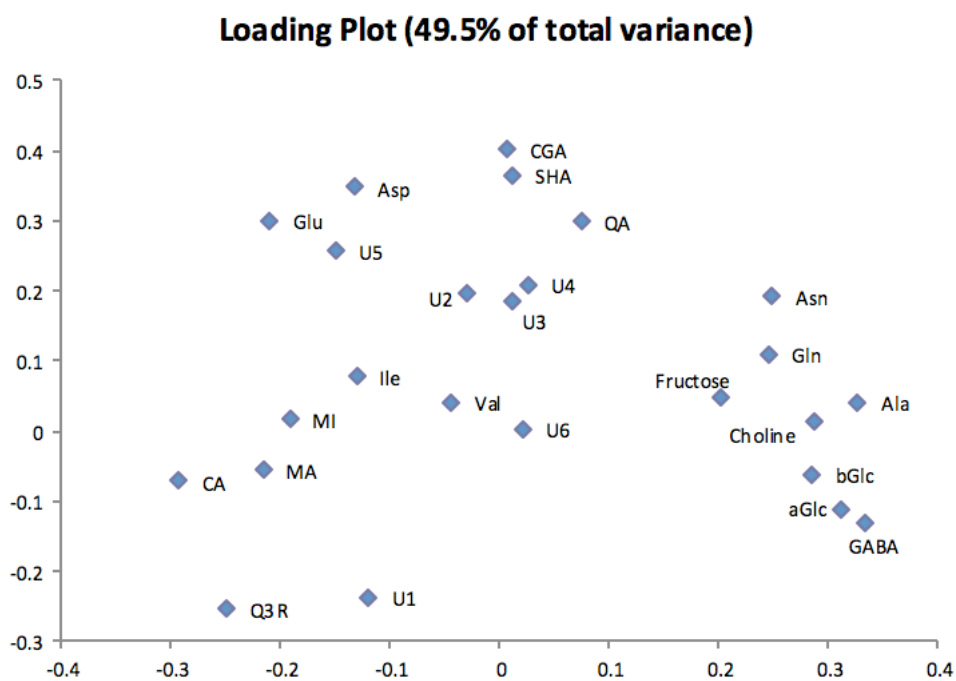
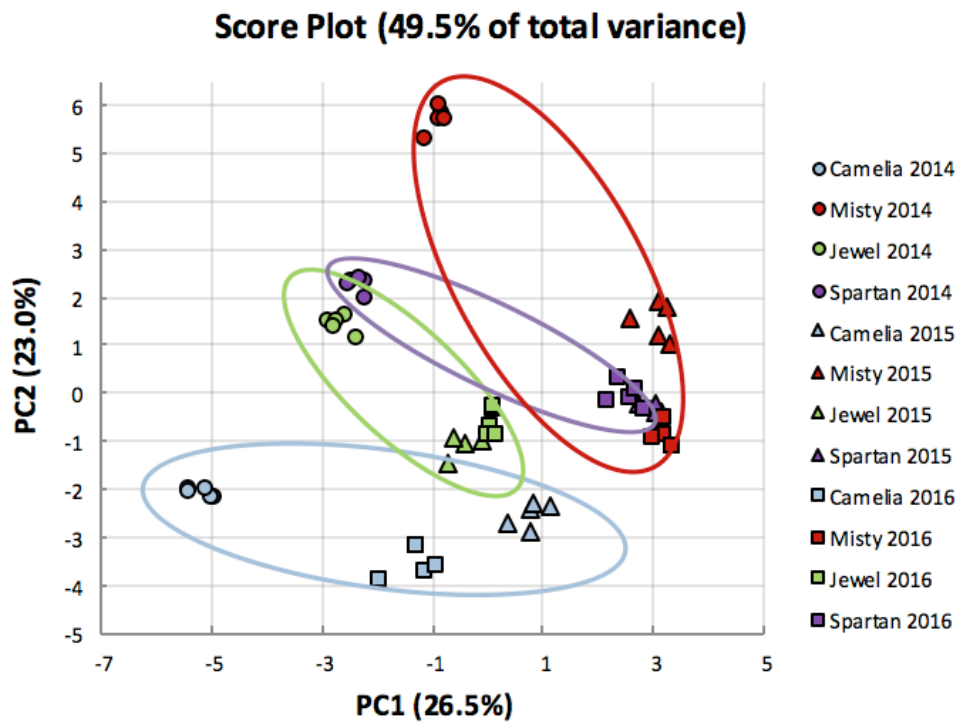


Figure 6.4. PCA Score and Loading Plots applied to the twenty-five compounds selected in the hydroalcoholic extracts (PC1 versus PC2).

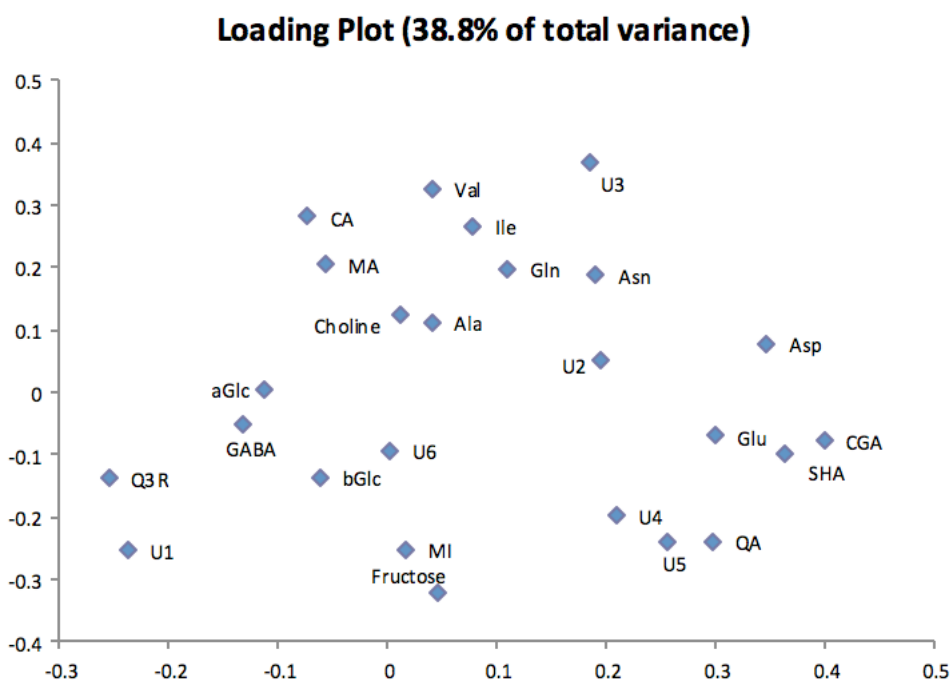
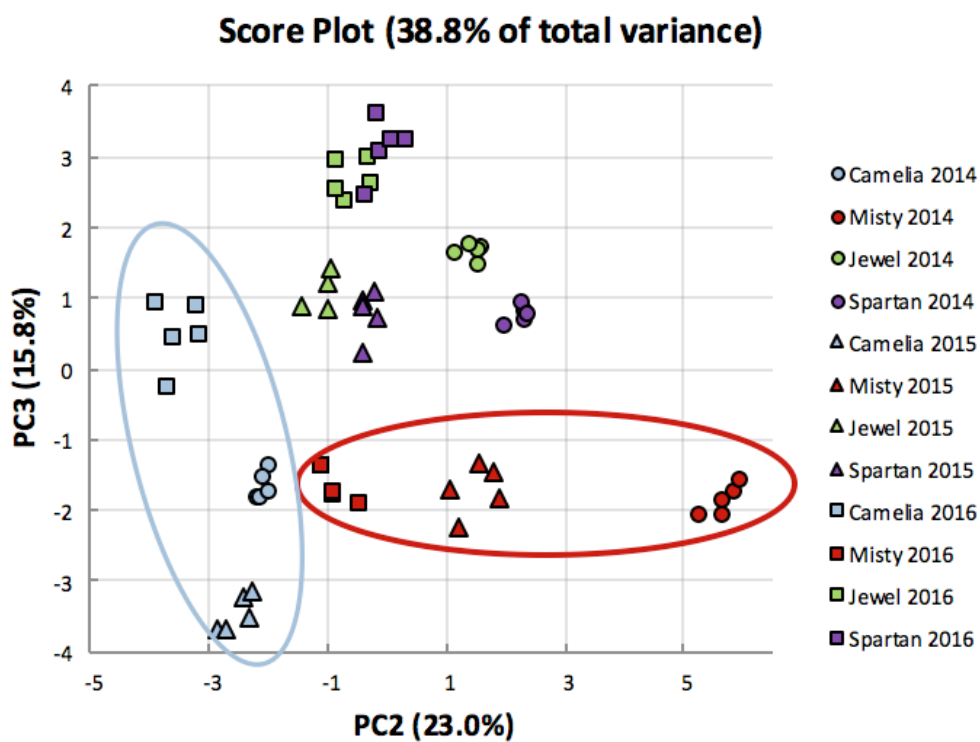


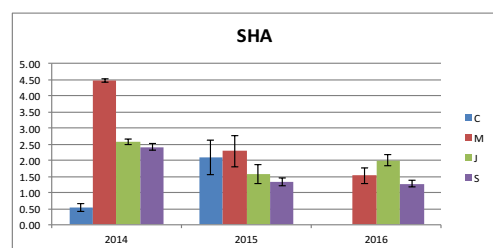
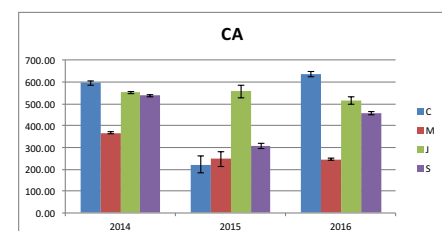
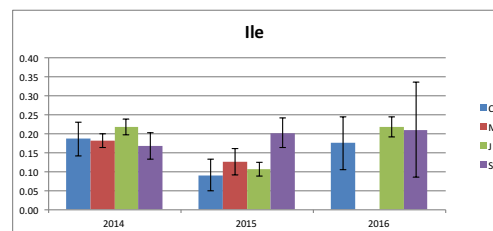
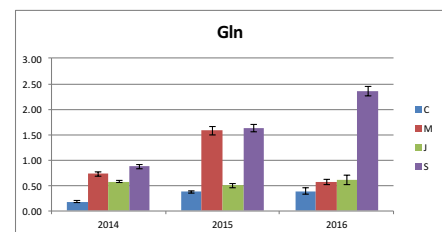
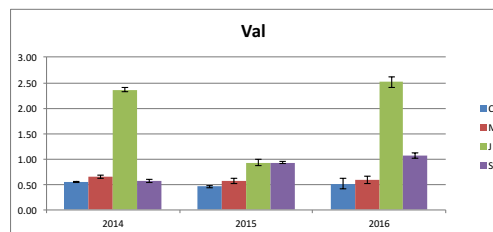
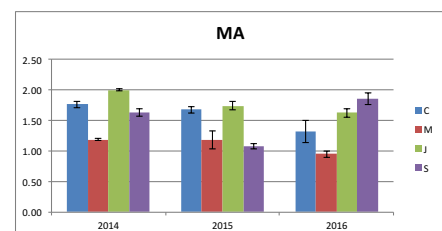
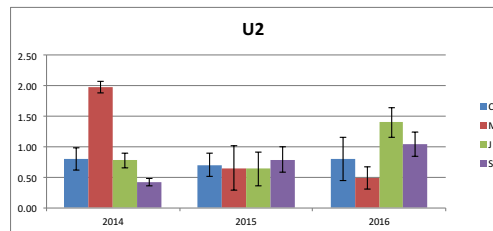
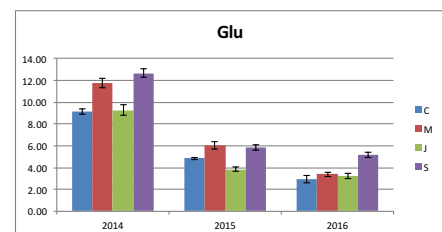
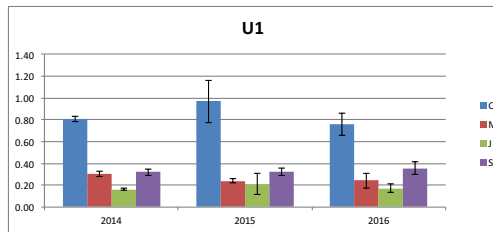
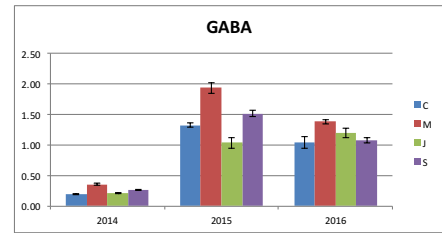
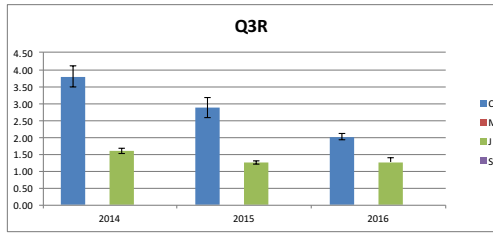
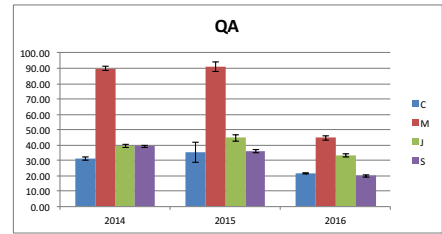
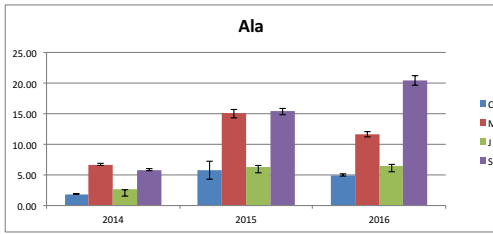
Figure 6.5. PCA Score and Loading Plots applied to the twenty-five compounds selected in the hydroalcoholic extracts (PC2 versus PC3).

In Figure 6.6 histograms are reported in order to visualize how the concentration of each metabolite changes according both to the cultivar and to the harvest year. Histograms allow us to validate our interpretation based on loading plot. Effectively, some metabolites resulted more concentrated in a particular variety with respect to the other ones independently by the harvest year: for instance, samples belonging to Misty cultivar always presents a higher content of CGA and QA in each harvesting year with respect to the other cultivar. According to the ANOVA results, these two metabolites can be considered as markers of the Misty cultivar. Looking at the CGA and QA histograms it can also be revealed a season effect: their concentrations change according to the harvesting year although there is a constant pattern of relative concentrations among cultivar.

Some metabolites were detected only in some cultivars. For instance, Q3R was identified in Camelia and Jewel varieties only and, for this reason, can be considered as a marker of these two cultivar, whereas U3 was not identified in Camelia and can be considered a marker of this variety. ANOVA confirmed these evidences.

U1 is particularly concentrated in Camelia samples independently by harvesting years. ANOVA also confirmed U1 as a marker of Camelia cultivar.

Most of metabolites increased or decreased their concentrations according to harvesting years since a season effect often interacted with the genotype of the blueberries. There were also some cases in which it was not true. For instance, GLN concentrations in Jewel samples were not affected by the season effect and remained constant over the years.



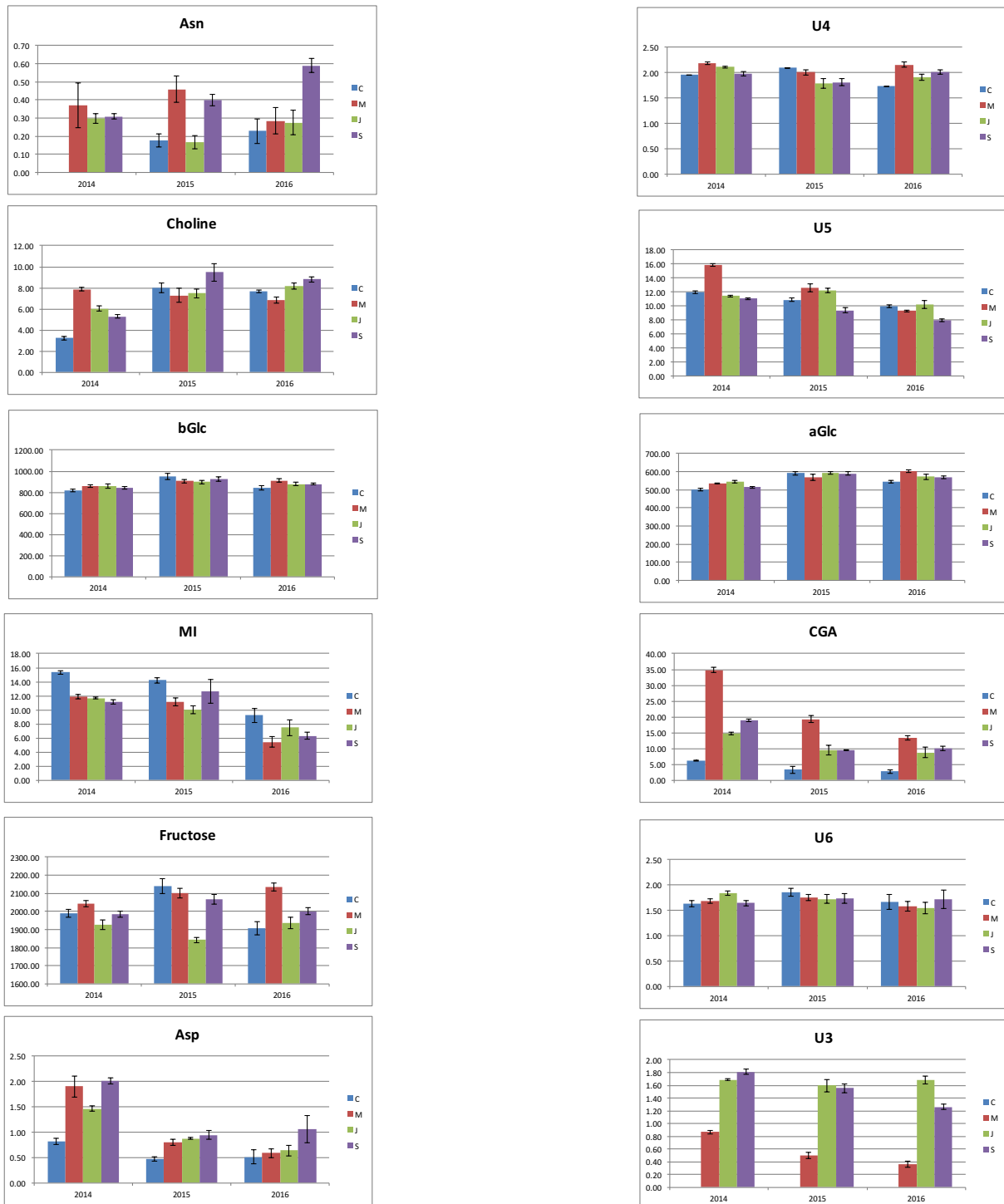


Figure 6.6. Histograms comparing the quantities of metabolites present in the four varieties of blueberries hydroalcoholic extracts during three consecutive harvesting years. Data shown are expressed as molecular abundance.

The integrals of 9 metabolites measured in organic extracts were also submitted to PCA. First, a PC1 versus PC2 plot (not shown) has been constructed but it resulted not informative in order to describe samples. PC1 accounted for 48.3% of the variability within the data.

In order to obtain a different spatial disposition of samples, a PC2 versus PC3 diagram was also built. Figure 6.7 shows the PCA score and loading plots considering the second and the third principal components as variables. These two PCs account for 40.8% of the variability within the data, PC2 providing for 32.4% and PC3 for 8.4%. PCA score plot shows that samples belonging to different cultivars but harvested in a specific year are clustered in three different areas of the plot. Samples harvested in 2014, in 2015 and in 2016 are at the top, at the right and at the left, respectively, of the score plot. Despite of these results, histograms of fat-soluble metabolites, reported in Figure 6.8, do not show significant differences according to the harvesting year.

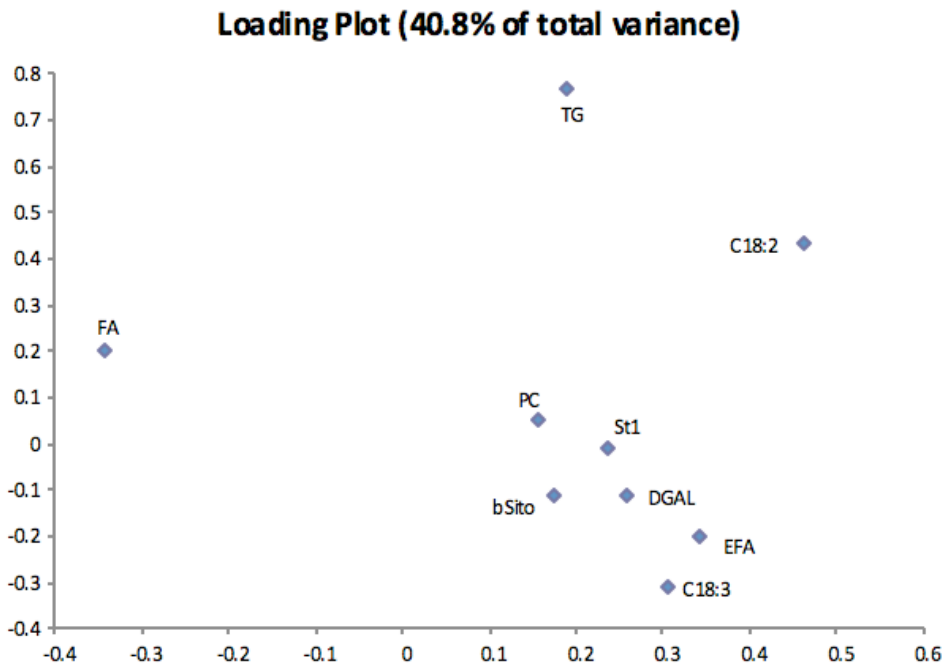
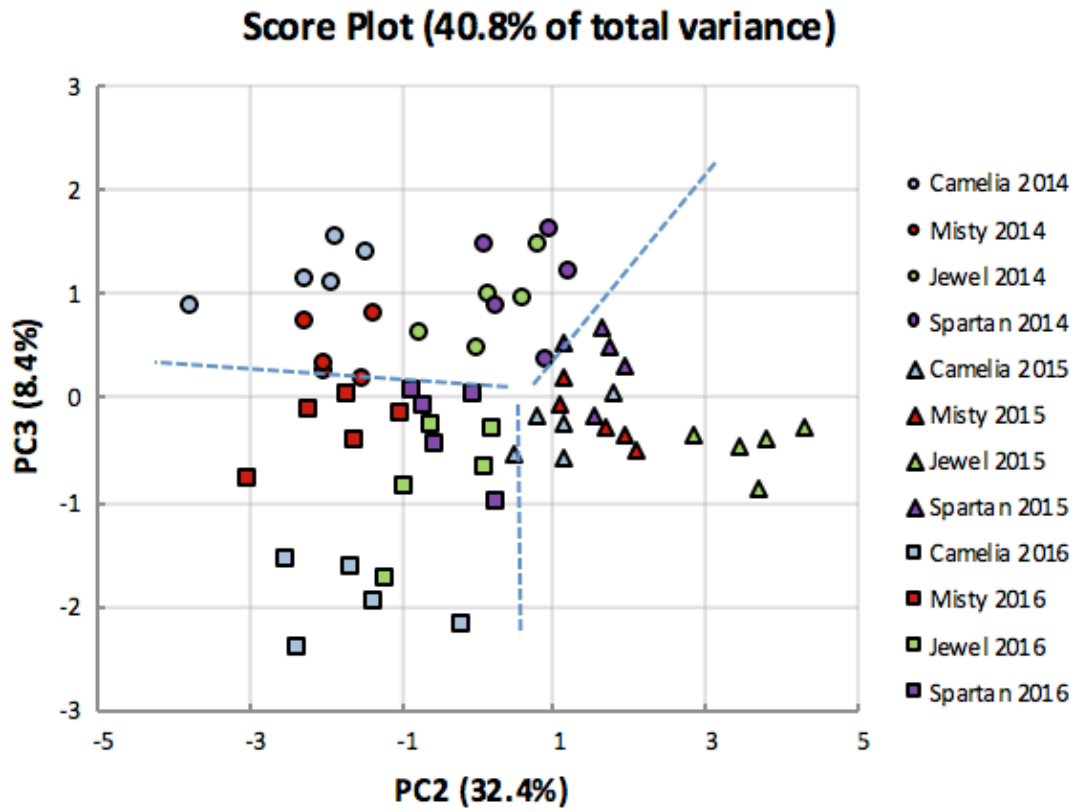


Figure 6.7. PCA Score and Loading Plots applied to the nine compounds selected in the organic extracts (PC2 versus PC3).

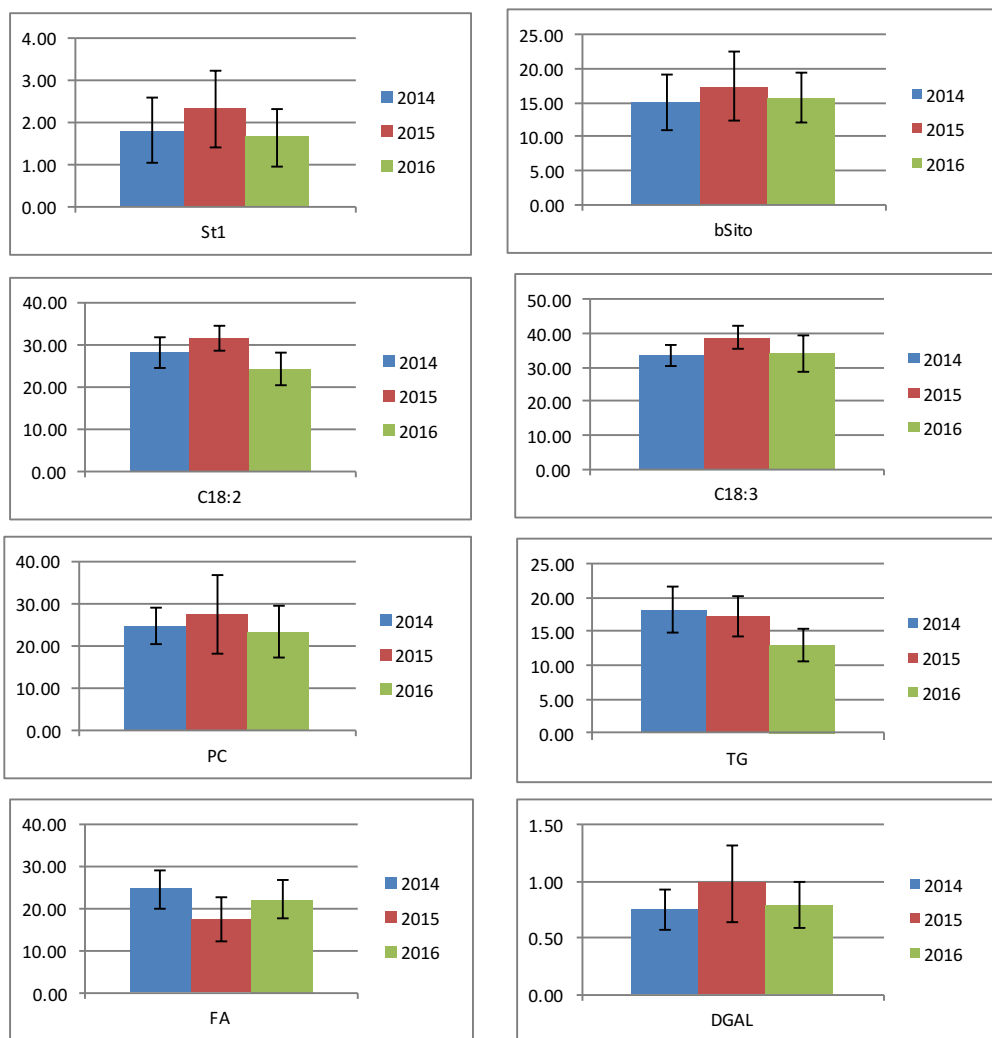


Figure 6.8. Histograms comparing the mean quantities of metabolites present in the four varieties of blueberries organic extracts according to the three consecutive harvesting years. Data shown are expressed in %.

The integrals of 13 anthocyanins (5 assigned and 8 unknown) in SPE extracts were also submitted to PCA. Figure 6.9 shows the PCA score and loading plot considering the first and the second principal components as variables. These two PCs account for 70.4% of the variability within the data, PC1 providing for 46.8% and PC2 for 23.6%. The score plot shows that PC1 maximizes the separation of samples belonging to Camelia and Misty cultivar (on the left of the score plot) by the samples belonging to Spartan and Jewel cultivar (on the right of the score plot). Instead, PC2 maximizes the separation of samples of each cultivar according to the harvest year. Looking at the loading plot we can have an idea for the metabolites responsible for the samples clustering. For instance, samples belonging to Camelia and Misty cultivar are characterized by a higher content of M3GAL and Ant6 whereas samples belonging to Jewel and Spartan cultivar have a higher content of D3GLC and P3GLC. Moreover, Jewel cultivar is rich in M3GLC over harvesting years with respect the other cultivar. In Figure 6.10 and Figure 6.11 histograms confirming these evidences are reported. These histograms allow to visualize how the concentration of each metabolite changes according both to the cultivar and to the harvesting year.

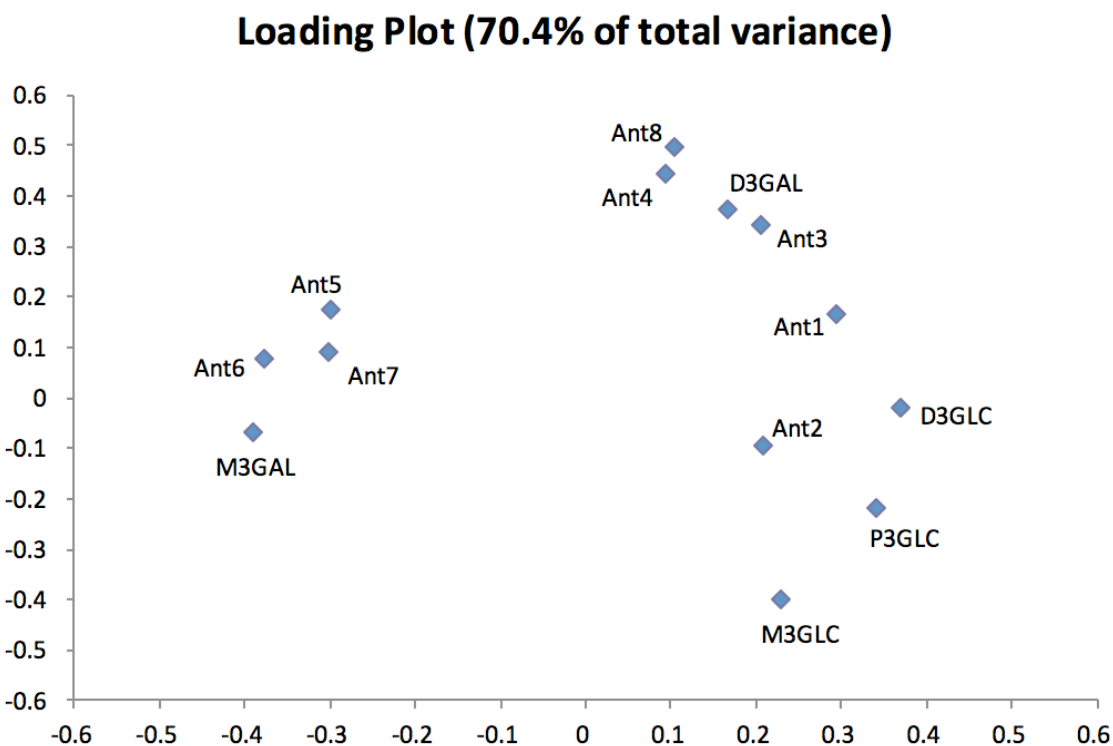
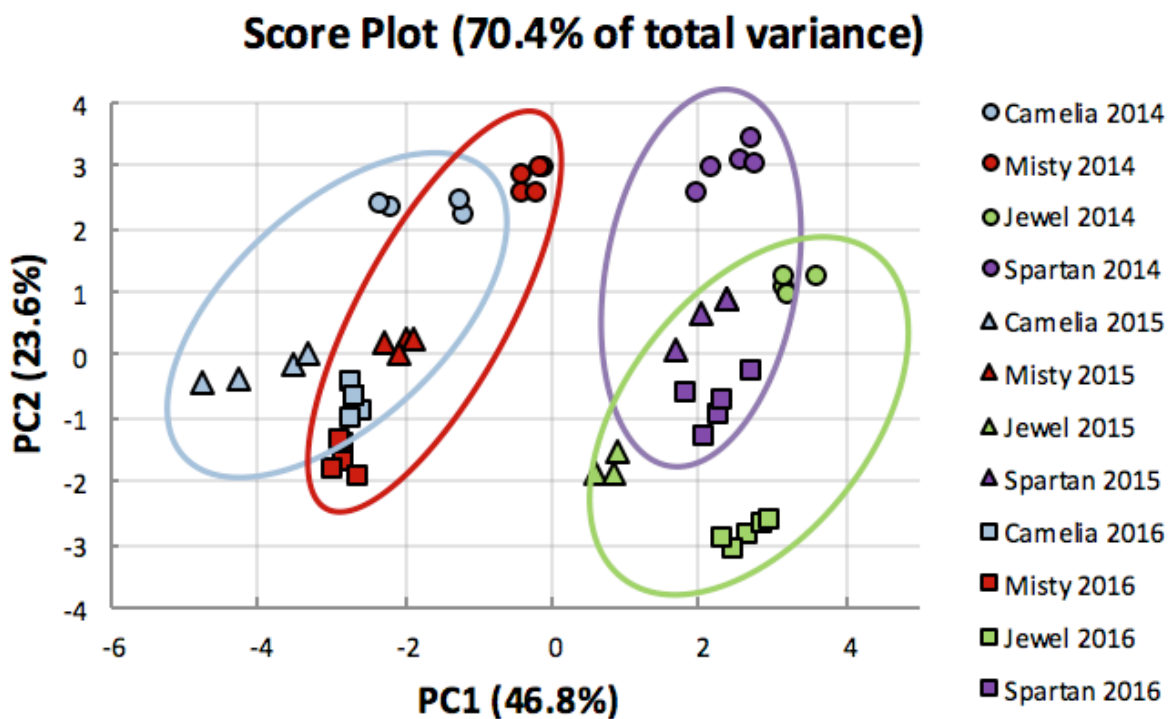


Figure 6.9. PCA Scores and Loadings Plot applied to the anthocyanins integrals (PC1 versus PC2).

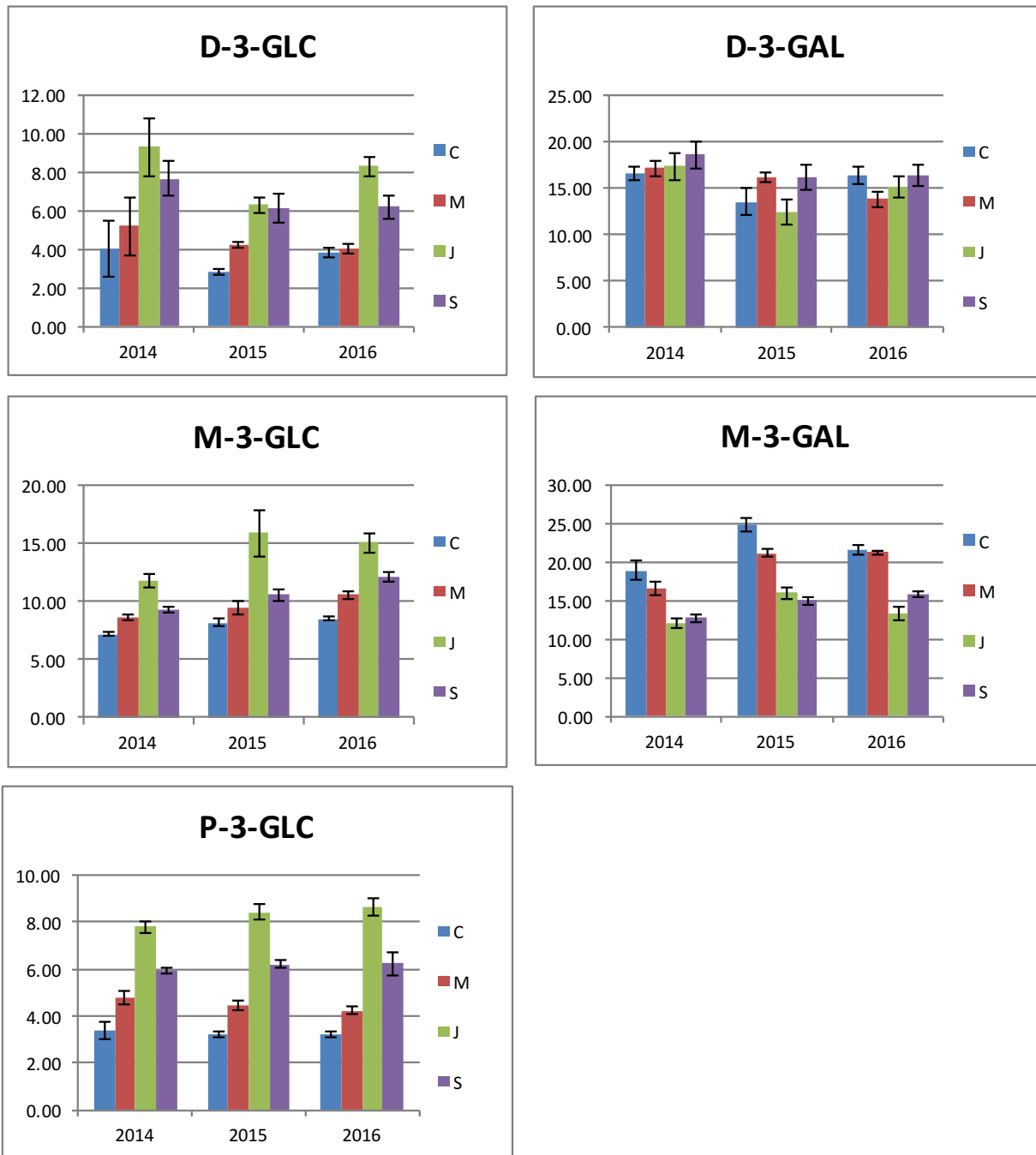


Figure 6.10. Histograms comparing the quantities of the five known anthocyanins present in the four varieties of blueberries SPE extracts during three consecutive harvest years. Data shown are expressed in %.

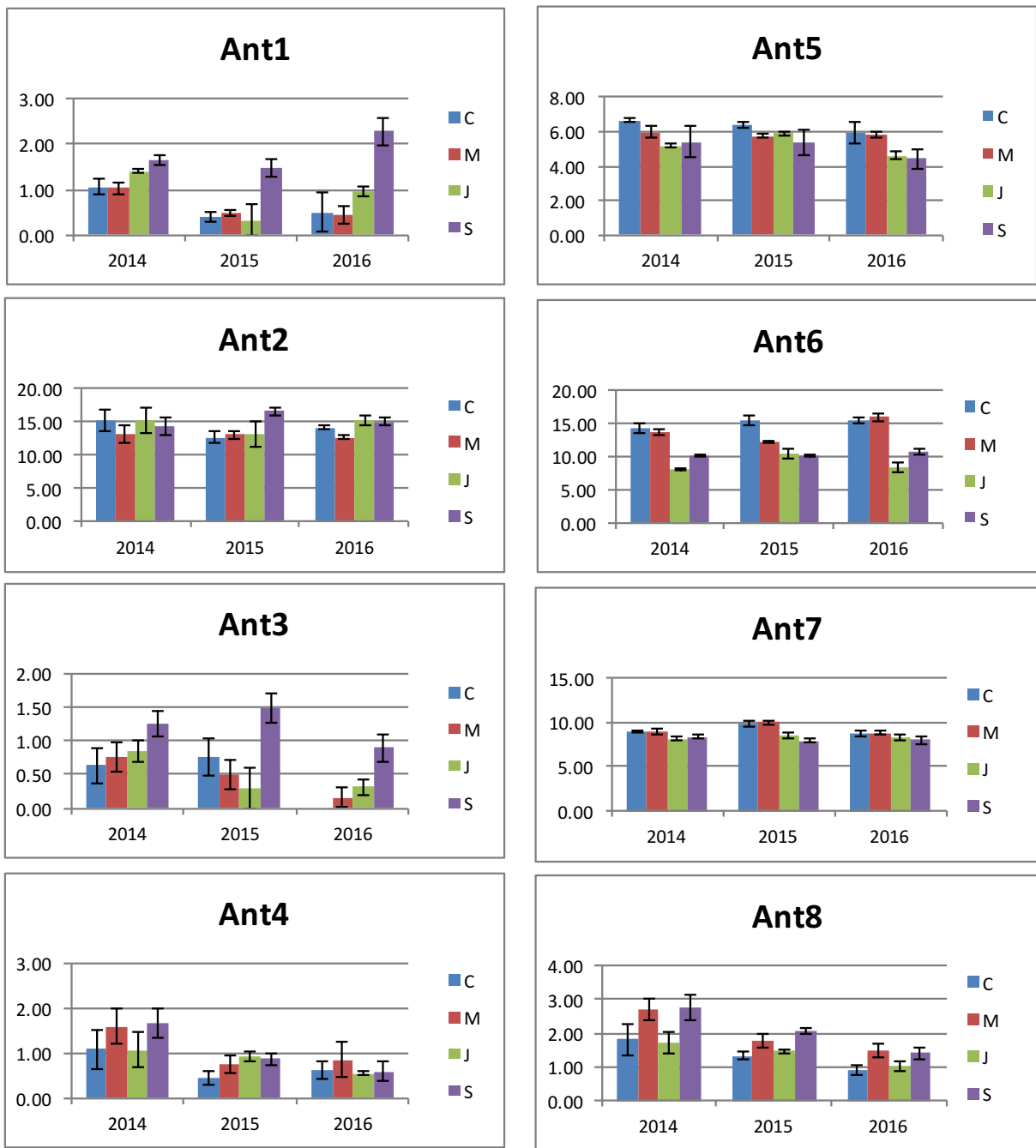


Figure 6.11. Histograms comparing the quantities of the eight unknown anthocyanins present in the four varieties of blueberries SPE extracts during three consecutive harvest years. Data shown are expressed in %.

6.1.4 References

- Barnes, J.S., Nguyen H.P., Shen, S., Schug, K.A., 2009. *J. Chromatogr. A* 1216, 4728-4735.
- Basu, A., Du, M., Leyva, M.J., Sanchez, K., Betts, N.M., Wu, M., Aston, C.E., Lyons, T.J., 2010. *J. Nutr.* 140, 1582-1587.
- Biais, B., Allwood, J.W., Deborde C., Xu, Y., Maucourt, M., Beauvoit, B., Dunn, W.B., Jacob, D., Goodacre, R., Rolin, D., Moing, A., 2009. *Anal Chem.* 81, 2884-2894.
- Blanck, H.M., Gillespie, C., Kimmons, J.E., Seymour, J.D., Serdula, M.K., 2008. *Prev. Chron. Dis.* 5, 1-10.
- Braun, S., Kalinowski, H.O., Berger, S., 1998. Wiley-VCH: Weinheim, Germany.
- Bunea, A., Rugina, D., Sconta, Z., Pop, R.M., Pinte, A., Socaciu, S., Tabaran, F., Grootaert, C., Stuijjs, K., Van-Camp, 2013. *J. Phytochemistry*, 436-444.
- Byamukama, R., Ogweng, G., Jordheim, M., Andersen, O.M., Kiremire, B.T., 2011. *Afr. J. Pure Appl. Chem.*, 5, 356-360.
- Capitani, D., Mannina, L., Proietti, N., Sobolev, A.P., Tomassini, A., Miccheli, A., Di Cocco, M., Capuani, G., De Salvador, R., Delfini, M., 2013a. *J. Agric. Food Chem.* 61, 1727-1740
- Capitani, D., Sobolev, Tomassini, A., Sciubba, F., De Salvador, R., Mannina, L., Delfini, M., 2013b. *J. Agric. Food Chem.* 61, 1718-1726
- Capitani, D., Proietti, N., Sobolev, A.P., Antiochia, R., Delfini, M., Sciubba, F., Miccheli, A., De Salvador, F.R., Mannina, L., 2013c. *Spectroscopy Europe* 25, 6-12.
- Capitani, D., Mannina, L., Proietti, N., Sobolev, A.P., Tomassini, A., Miccheli, A., Di Cocco, M., Capuani, G., De Salvador, R., Delfini, M., 2010. *Talanta* 82, 1826-1838
- Capitani, D., Sobolev, A.P., Delfini, M., Vista, S., Antiochia, R., Proietti, N., Bubici, S., Ferrante, G., Carradori, S., De Salvador, F.R., Mannina, L., 2014. *Electrophoresis* 35, 1615-1626.
- Castrejón A.D.R., Eichholz I., Rohn S., Kroh L.W., Huyskens-Keil S., 2008. *Food Chem.* 109(3), 564-572.
- Cho M.J., Howard L.R., Prior R.L., Clark J.R., 2004. *J. Sci. Food Agric.* 84(13), 1771-1782.
- Daglia, M., Antiochia, R., Sobolev, A.P., Mannina, L., 2014. *Food Res. Int.* 63, 275-289.
- Eriksson, L., Johansson, L., Ketteneh-wold, L., Trygg, J., Wikstrom, C., Wold, S., 2006. *Umetrics AB: Umea, Sweden.* 40-44.
- Gil, A.M., Duarte I.F., Delgadillo, I., Colquhoun, I.J., Casascelli, F., Humpfer, E., Spraul, M., 2000. *J. Agric. Food Chem.* 48, 1524-1536.

Gonzalez-Gallego, J., Garcia-Mediavilla M.V., Sanchez-Campos, S., Tunon M.J., 2010. *British J. Nutrition* 104, S15-S27.

Gough R.E., 1991. The Haworth Press Food Products Press: New York, USA. 1–4.

Ichiyanagi, T., Kashiwada, Y., Ikeshiro, Y., Hatano, Y., Shida, Y., Horie, M., Matsugo, S., Konishi, T., 2004. *Chem. Pharm. Bull.* 52, 226-229.

Ichiyanagi, T., Tateyama, C., Oikawa, K., Konishi, T., 2000. *Biol. Pharm. Bull.* 23, 492-497.

Ichiyanagi, T., Kashiwada, Y., Ikeshiro, Y., Hatano, Y., Shida, Y., Horie, M., Matsugo, S., Konishi, T., 2004. *Chem. Pharm. Bull.* 52, 226–229.

Johnson, C.S.Jr., 1999. *Progr. Nucl. Magn. Reson. Spectrosc.* 34, 203–256.

Jordheim, M., Giske, N.H., Andersen, O.M., 2007. *Biochem. Syst. Ecol.* 35, 153–159.

Joshipura K.J., Hu F.B., Manson J.E., Stampfer M.J., Rimm E.B., Speizer F.E., Colditz G., Ascherio A., Rosner B., Spiegelman D., et al., 2001. *Ann. Intern. Med.* 134(12), 1106–1114.

Krikorian R., Shidler M.D., Nash T.A., Kalt W., Vinqvist-Tymchuk M.R., Shukitt-Hale B., Joseph J.A., 2010. *J. Agric. Food Chem.* 58(7), 3996–4000.

Lee, J.H., Choung, M.G., 2011. *Food Chem.* 127, 1686-1693.

Manganaris, G.A., Goulas, V., Vicente, A.R., Terry, L.A., 2014. *J. Sci. Food Agric.* 94, 825-833.

Mannina, L., Cristinzio, M., Sobolev, A.P., Ragni, P., Segre, A.L., 2004. *J. Agric. Food Chem.* 52, 7988–7996.

Mannina, L., Sobolev, A., Viel, S., 2012. *Prog. Nucl. Magn. Reson. Spectrosc.* 66, 1-39.

Martineau, L.C., Couture, A., Spoor, D., Benhaddou-Andaloussi, A., Harris, C., Meddah, B., Leduc, C., Burt, A., Vuong, T., Mai Le, P., Prentki, M., Bennet, S.A., Arnason, J.T., Haddad, P.S., 2006. *Phytomedicine* 13, 612-623.

Nicoue, E.E., Savard, S., Belkacemi, K., 2007. *J. Agric. Food Chem.* 55, 5626-5635

Saito, T., Honma, D., Tagashira, M., Kanda, T., Nesumi, A., Maeda-Yamamoto, M., 2011. *J. Agric. Food Chem.* 59, 4779–4782.

Seeram, N.P., 2008. *J. Agric. Food Chem.* 56, 630-635.

Simeone, A.M., Nota P., Ceccarelli, D., Del Toro, A., Piazza, M.G., De Salvador, F.R., Caboni, E., Krupa, T., 2012. *Acta Horticulturae* 926, 713–716.

Sobolev, A.P., Brosio, E., Gianferri, R., Segre, A.L., 2005. *Magn. Reson. Chem.* 43, 625-638.

Stull, A.J., Cash, K.C., Johnson, W.D., Champagne, C.M., Cefalu, W., 2010. *J. Nutr.* 140, 1764-1768.

Tarachwin, L., Masako, O., Fukusaki, E., 2008. *J. Agric. Food Chem.* 56, 5827-5835.

Wizgoski, F.J., Paudel, L., Rinaldi, P.L., Reese, R.N., Ozgen, M., Tulio, A.Z., Miller, A.R., Scheerens, J.C., Hardy, J.K., 2010. *J. Agric. Food Chem.* 58, 3407-3414.

Yawadio, R., Tanimori, S., Morita, N., 2007. *Food Chem.* 101, 1616–1625.

Yousef, G.G., Brown, A.F., Funakoshi, Y., Mbeunkui, F., Grace, M.H., Ballington, J.R., Loraine, A., Lila, M.A., 2013. *J. Agric. Food Chem.* 61, 4806-4815.

Wizgoski, F.J., Paudel, L., Rinaldi, P.L., Reese, R.N., Ozgen, M., Tulio, A.Z., Miller, A.R., Scherens, J.C., Hardy, J.K., 2010. *J. Agric. Food Chem.* 58, 3407-3414.

Zadernoski, R., Naczek, M., Nesterowicz, J., 2005. *J. Agric. Food Chem.* 53, 2118-2124.

6.2 Teas

6.2.1 Introduction

Tea chemical composition has been extensively studied leading to the identification of many bioactive compounds responsible for tea protective activities especially against chronic diseases (Yarmolinsky, Gon & Edwards, 2015; Rahmani et al., 2015). These bioactive compounds can be divided into polyphenolic components and non-polyphenolic components. Green tea leaves are particularly rich in polyphenols (up to 30% of the dry weight), mainly flavan-3-ols, with EGCG being the most represented (9-13%) (Zhu et al., 2013). In oolong and black teas, polyphenol concentration is lower and depends on the degree of fermentation. In fact, during the oxidation process flavan-3-ols undergo oxidation and polymerisation reactions, catalysed by polyphenol oxidase and peroxidase, leading to the formation of TFs and TRs, the most representative compounds of oolong and black teas, respectively (Drynan et al., 2010). The chemical structure of the major TFs are known. Differently, chemical structure of TRs is still under investigation, due to their high molecular weight and complexity (Del Rio et al., 2004). Other flavonoids occurring in tea leaves are flavonol glycosides, such as quercetin, kaempferol and myricetin mono-, di- and triglycosides linked to pentose (xylose or arabinose) or hexose (glucose, galactose, rhamnose). Acylated and methylated flavonols and p-coumaroyl derivatives have been also detected by means of sophisticated hyphenated techniques (Ku et al., 2010). Non-flavonoid polyphenols such as benzoic acids (i.e. gallic acid and galloylquinic acid) and hydroxycinnamic acid derivatives (i.e. caffeoylquinic acid and p-coumaroylquinic acid) are also present in tea leaves.

Among non-polyphenolic components, xanthines and proteic and non-proteic amino acids are the most representative categories. Tea beverage contains caffeine and in lower amount theobromine and theophylline (Zulli et al., 2016). Theanine, the most abundant amino acid occurring in tea (37% of the whole amino acid content) and GABA, responsible for tea

umami taste, are important healthy tea compounds (Di Lorenzo et al., 2016; Daglia et al., 2017).

The growing demand for tea characterized by high concentrations of healthy compounds led in these years to the development of different approaches to study tea beverages. Gotti et al. studied the differentiation of green tea samples by the analysis of catechin via CD-MEKC (Gotti et al., 2009), meanwhile Meng et al. used proton NMR spectroscopy and Near-infrared spectroscopy for the geographic origin discrimination of Oolong tea (Meng et al., 2017). In the same year, a comparative study of the volatile components in Dianhong teas from the fresh leaves of four tea cultivars using chromatography-mass spectrometry, multivariate data analysis and descriptive sensory analysis was performed (Wang et al., 2017). Many more examples can be found in literature.

In the present study, an untargeted NMR-based approach to study tea beverages with differing degree of fermentation (green and oolong teas), harvesting season (autumn and spring) and production process (GABA teas) has been carried out.

6.2.2 Material and Methods

Tea samples were purchased from an Italian specialist tea shop (La Teiera Eclettica, Milan, Italy). Selected teas differ for the fermentation degree (green and oolong teas) and for the productive process (GABA teas and non-GABA teas) (Table 6.4).

Tea infusions preparation for NMR analysis required a fine homogenization of dried tea leaves to obtain a better recovery of soluble minor metabolites with respect to conventional infusions. Dried leaves of each tea sample were finely ground to obtain a homogeneous matrix.

Table 6.4. List of selected teas, their abbreviation, the degree of fermentation, the origin, the infusion conditions, as suggested by the supplier and the dry residue obtained after freeze-drying.

| N. | Tea sample | Abbreviation* | Degree of fermentation | Country of Origin | Infusion parameters | Dry residue (mg/mL) |
|----|------------------|---------------|----------------------------|--------------------------------------|---------------------|---------------------|
| 1 | Lung Ching | GT1 | green | China | 85°C 3 min | 12.3 |
| 2 | Gunpowder | GT2 | green | Zhejiang Province (China) | 85°C 3 min | 10.5 |
| 3 | Mao Feng | GT3 | green | Anhui Province (China) | 85°C 4 min | 17.0 |
| 4 | Jade Snow | GT4 | green | Guangxi region (China) | 80°C 4 min | 11.1 |
| 5 | Kabusecha | GT5 | Green | Japanese shaded tea (shaded 10 days) | 70°C 2 min | 13.7 |
| 6 | Sencha | GT6 | Green | Japanese unshaded tea | 80°C 2 min | 12.7 |
| 7 | Gyokuro Kyushu | GT7 | Green | Japanese shaded tea (shaded 20 days) | 75°C 2 min | 13.9 |
| 8 | GABA green | GGT1 | Green | Japan | 80°C 2 min | 11.2 |
| 9 | Dong Ding | OTA1 | low degree of fermentation | Taiwan | 85°C 4 min | 7.9 |
| 10 | Anxi Ti Kuan Yin | OTA2 | low degree of fermentation | Fujian region (China) | 85°C 4 min | 8.2 |
| 11 | Si Ji Chun | OTA3 | low degree of fermentation | Taiwan | 85°C 4 min | 8.0 |
| 12 | Wenshan Baozhong | OTA4 | low degree of fermentation | Taiwan | 85°C 4 min | 8.5 |
| 13 | Dong Ding | OTS1 | low degree of fermentation | Taiwan | 85°C 4 min | 7.1 |
| 14 | Si Ji Chun | OTS3 | low degree of fermentation | Taiwan | 85°C 4 min | 6.6 |
| 15 | Wenshan Baozhong | OTS4 | low degree of fermentation | Taiwan | 85°C 4 min | 11.7 |
| 16 | GABA oolong | GOT1 | low degree of fermentation | Taiwan | 80°C 2 min | 7.2 |
| 17 | GABA oolong | GOT2 | low degree of fermentation | Taiwan | 80°C 2 min | 3.6 |
| 18 | GABA | GOT3 | low degree of | Taiwan | 80°C | 4.2 |

| | | | | | | |
|----|-------------|------|----------------------------|--------|---------------|-----|
| | oolong | | fermentation | | 2 min | |
| 19 | GABA oolong | GOT4 | low degree of fermentation | Taiwan | 80°C 2 min | 2.2 |

* GT= Green Tea, GGT= GABA Green Tea, OTA= oolong, GOT= GABA oolong tea

Deuterated water (1 mL) was added to 50 mg of each ground tea sample in a 1.5 mL Eppendorf tube. The mixture was introduced in a water bath at 85 °C for 4 min followed by cooling to room temperature and filtering through cotton wool. The limpid solution (400 µL), D₂O phosphate buffer (300 µL, 400 mM, pH 7.00 with a small quantity of EDTA and 1mM of TSP as an internal standard) were mixed and transferred in a 5 mm NMR tube.

The NMR spectra were recorded at 27 °C on a Bruker AVANCE 600 spectrometer operating at the proton frequency of 600.13 MHz and equipped with a Bruker multinuclear z-gradient inverse probe head. The ¹H spectra of tea samples were acquired by co-adding 400 transients with a recycle delay of 7.1 s, using a 90° pulse of 13 µs and 32 K data points. The water signal was suppressed using a solvent presaturation during the relaxation delay. Data processing was carried out with Bruker TOPSPIN 3.5 software. An exponential function with line broadening factor as 0.3 Hz was applied, the spectra were manually phased and polynomial baseline correction was applied. All selected NMR peaks were integrated manually with the same integral limits for a given peak in all spectra. The integrals of the selected resonances were normalized by setting the integral of TSP resonance at 0.00 ppm to 100. NMR data were submitted to Statistica software package for Windows and a Principal Component Analysis (PCA) was carried out.

6.2.3 Results and Discussion

The ^1H spectra of the four types of teas, see Figure 6.11, were assigned according to the literature (Marchese et al., 2014) and show the presence of theanine at 1.118 ppm, threonine/lactate (THR/LAT) at 1.348 ppm, alanine (ALA) at 1.498 ppm, (quinic acid) QA at 1.888 ppm, GABA at 2.314 ppm, ECG at 5.057 ppm, 2-O-arabinopyranosyl-myoinositol (ARBMI) at 5.207 ppm, α -glucose at 5.255 ppm, sucrose at 5.427 ppm, GCG/GC at 6.563 ppm, EGCG at 6.597 ppm, EGC at 6.631 ppm, GA at 7.037 ppm, caffeine at 7.709 ppm. The levels of these metabolites turned out to be different in the investigated samples and can contribute to clusterize samples according to their commercial denomination.

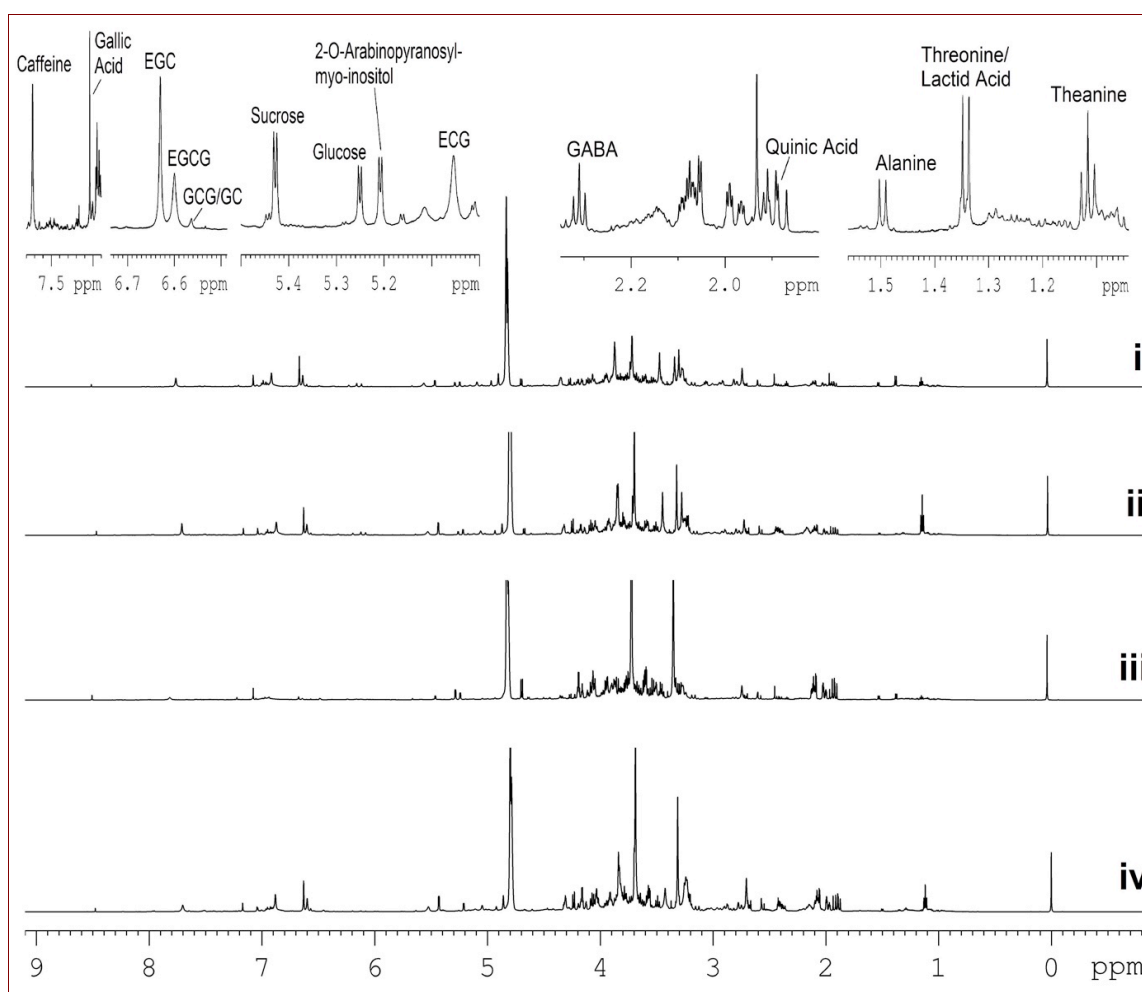


Figure 6.11 (A) ^1H spectra of the four types of teas. i = GABA Green tea GGT1; ii = Green tea GT2; iii = GABA Oolong tea GOT3; iv = Oolong tea OTA1. The fourteen ^1H NMR signals selected for the statistical analysis are indicated at the top.

Therefore, an explorative analysis of entire dataset was undertaken using PCA to highlight dissimilarities and similarities. Figure 6.12 showed a PCA sample biplot (PC2 versus PC1) with the first two PCs accounted for the 56.2 % of the variability within the data. PC1 provided the discrimination between GABA and non-GABA teas, whereas PC2 was mostly responsible for the discrimination between oolong and green teas. Loadings reported on biplot, see Figure 6.12, clearly shows the variables responsible for GABA and non-GABA teas separation. It is worth noting that the levels of GABA, GLUCOSE, ALA, THR/LAT and QA (loadings lying on the left side of PC1 axis) are higher in all GABA teas, whereas the other non GABA teas (oolong and green teas) have a higher content of CAFFEINE, THEANINE, EGC, EGCG and GCG/GC and SUCROSE (loadings lying on the right side of PC1 axis). Therefore, all the fine homogenated dried GABA teas leaves result to have very low concentrations of green tea characteristic polyphenolic compounds.

Independently from the production season (autumn or spring), oolong teas show a higher level of SUCROSE in comparison with green teas, whereas green teas show a very high level of CAFFEINE, ARBMI, and THEANINE that have a great stimulating power. It is worth noting that the sample GT7 with a low content of ARBMI, THEANINE and CAFFEINE results to be similar to oolong teas.

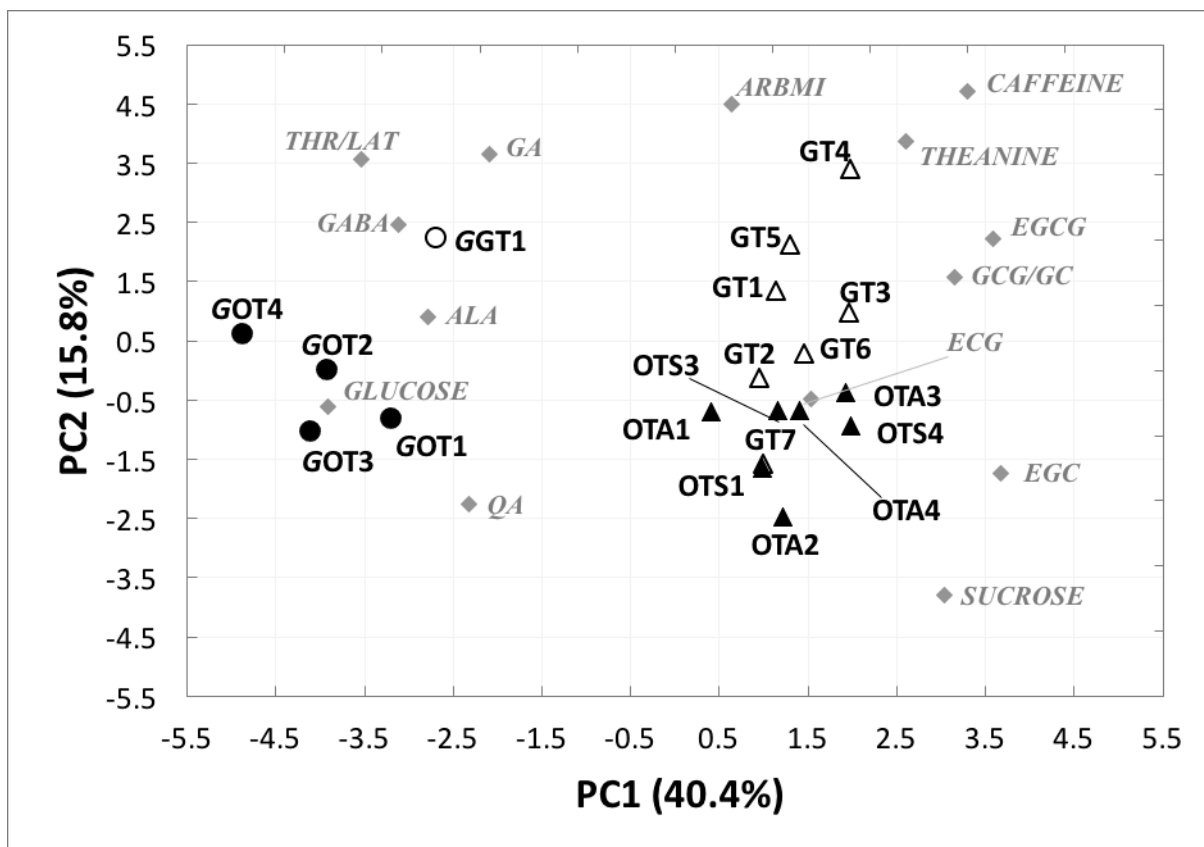


Figure 6.12. Biplot (scores and loadings) diagram of PCA. 19 tea samples, representing the scores, are marked in black with different symbols according to the different types of tea (unfilled triangle = green teas; unfilled circle = GABA green tea; filled triangle = oolong teas; filled circle = GABA oolong teas). The loadings of the fourteen variables selected for PCA are marked in grey rhombs.

6.2.4 References

- Daglia, M., Di Lorenzo, A., Nabavi, S.F., Sureda, A., Khanjani, S., Moghaddam, A.H., Braidly, N., Nabavi, S.M., 2017. *Nutrients* 9.
- Del Rio, D., Stewart, A. J., Mullen, W., Burns, J., Lean, M. E., Brighenti, F., Crozier, A., 2004. *J. Agric. Food Chem.* 52, 2807–2815.
- Di Lorenzo, A., Nabavi, S.F., Sureda, A., Moghaddam, A.H., Khanjani, S., Arcidiaco, P., Nabavi, S.M., Daglia, M., 2016. *Mol. Nutr. Food Res.* 60, 566-579.
- Drynan, J.W., Clifford M.N., Obuchowicz, J., Kuhnert, N., 2010. *Nat. Prod. Rep.* 27, 417–462.
- Gotti, R., Furlanetto, S., Lanteri, S., Olmo, S., Ragaini, A., Cavrini, V., 2009. *Electrophoresis* 30, 2922-2930.
- Ku, K.M., Kim, J., Park, H.J., Liu, K.H., Lee, C.H., 2010. *J. Agric. Food Chem.* 58, 345-352.
- Marchese, A., Coppo, E., Sobolev, A.P., Rossi, D., Mannina, L., Daglia, M., 2014. *Food Res. Intern.* 63, 182–191.
- Meng, W., Xu, X., Cheng, K.K., Xu, J., Shen, G., Wu, Z., Dong, J., 2017. *Food Anal. Methods* 10, 3508-3522.
- Rahmani, A.H., Al Shabrmi, F.M., Allemailem, K.S., Aly, S.M., Khan, M.A., 2015. *Biomed. Res. Int.*
- Yarmolinsky, J., Gon, G., Edwards, P. 2015. *Nutr. Rev.* 73, 236-246.
- Wang, C., Zhang, C., Kong, Y., Peng, X., Li, C., Liu, S., Du, L., Xiao, D., Xu, Y., 2017. *Food Res. Int.* 100, 267-275.
- Zhu, H.B., Li, B.M., Liu, C., Chen, R.Y., 2013. *Zhongguo Zhong Yao Za Zhi.* 38, 1386-1389.
- Zulli, A., Smith, R.M., Kubatka, P., Novak, J., Uehara, Y., Loftus, H., Qaradakh, T., Pohanka, M., Kobylak, N., Zagatina, A., Klimas, J., Hayes, A., La Rocca, G., Soucek, M., Kruzliak, P., 2016. *Eur. J. Nutr.* 55, 1331-1343.

Chapter 7: Baobab

7.1 Introduction

Adansonia digitata L. is a species of tree belonging to the Bombacaceae family, commonly known as baobab. It is widely distributed throughout sub-Saharan Africa and Western Madagascar and has many uses, including as an ingredient in food and beverages and in traditional medicine (Diop et al., 2006; Gebauer, El-Siddig & Ebert, 2002). While in African tradition all parts of the baobab tree (fruits, seeds, flowers, roots and bark) are used as food, only the fruit pulp is consumed in Europe, where it has been authorized as a novel food since 2008 (Sugandha & Shashi, 2017), whereas in the United States of America the fruit pulp was approved as a food ingredient in 2009 (FDA, 2009). Over the last decade, the baobab tree has attracted significant attention due to the nutritional properties of its fruits, leaves and seeds and the beneficial effects of extracts from all of its parts on human health (Chadare et al., 2008; Rahul et al., 2015).

As far as the chemical composition of fresh baobab fruit is concerned, the literature is mainly focused on certain specific compounds. The ascorbic acid content has been found to be at least 3 times higher than that of other typical food sources of vitamin C (i.e. orange, kiwifruit, red fruits) (Vertuani et al., 2002). Furthermore, it has been reported that baobab fruit pulp is also rich in vitamins B1, B2, and B6 (Diop et al., 2006) and in mineral salts (i.e. P, Mg, Ca, K, Na and Fe) (Glew et al., 1997). Baobab fruit pulp can contain as much as 56% pectin (Nour, Magboul & Kheiri, 1980) and is rich in essential and nonessential fatty acids (i.e. linoleic acid, linolenic acid, oleic acid) (Glew et al., 1997). In 2017, Li et al. (2017) isolated and identified some polyphenolic compounds from dried baobab fruit pulp (i.e. four

hydroxycinnamic acid glycosides, six iridoid glycosides, and three phenylethanoid glycosides).

Baobab leaves are traditionally used as a food in Africa, whereas they are not yet authorized as a novel food in Europe. Baobab leaves have been reported to be rich in palmitic acid, oleic acid and linoleic acid, and are an excellent source of Ca, K, Mg and Fe. Their vitamin content is also remarkable, being rich in Vitamins C, B1, B2, B3, and β -carotene, for young leaves. Baobab leaves contain mucilage (9–12%), which explains their traditional use as thickening agent in South-African culture. Phenolic acids (gallic and ellagic acids), hydroxycinnamic acids (chlorogenic and caffeic acid), flavonols (rutin, quercitrin, quercetin, kaempferol), flavan-3-ols (catechin, epicatechin), and a flavone (luteolin) were identified in fresh baobab leaves through reverse-phase high-performance liquid chromatography with diode-array detection (RP-HPLC-DAD) method (Irondi et al., 2017).

However, despite the growing importance of baobab fruit and leaves due to their nutritional and biological properties, data on the primary and especially the secondary metabolites are extremely sparse in literature and little is known about the concentration of nutrients and bioactive components to date.

To obtain a comprehensive picture of the composition of these foods, the most common analytical tools are nuclear magnetic resonance (NMR) and mass spectrometry (MS) based metabolomic approaches, allowing for “high-throughput” spectroscopic/structural information on a wide range of compounds with high analytical precision (Sobolev et al., 2015). Metabolomics is a technology-driven approach advanced by recent developments in analytical tools, software, and statistical data analysis.

Here, I report the identification and quantification of primary and secondary metabolites occurring in extracts obtained from baobab fruit pulp and dried leaf samples using untargeted NMR spectroscopy. The choice of dried samples instead of fresh samples was made in view of the most common forms of baobab consumption worldwide, both in the

countries of origin and in importing countries.

7.2 Material and Methods

In order to perform a more representative sampling, 5 samples of fresh baobab fruit pulp, baobab also known as *Adansonia digitata* var. *congolensis* (accepted name: *Adansonia digitata* L.), were collected, dried and mixed together, and 20 samples of dried leaves were collected and milled together. These samples were collected during the harvest season of January–February 2016, in a local market in Ngaoundéré, Cameroon, and transported by airplane in plastic bags inside a box to laboratories in Italy, where they were stored in vacuum plastic bags away from sunlight in a cool room.

Powdered baobab fruit pulp and dried leaves were submitted to extraction according to a modified Bligh–Dyer methodology (Bligh & Dyer, 1959). A mixture of methanol/chloroform (2:1 v/v) was used to extract the greatest number of metabolites. The mixture (3 mL) was added to the sample (0.5 g) and agitated, followed by the addition of 1 mL of chloroform and 1.2 mL of Millipore grade water and the emulsion was stored at 4 °C for 40 min after stirring. The sample was then centrifuged (800g for 15 min at 4 °C). The upper (hydroalcoholic) and lower (organic) phases were carefully separated. The pellets were re-extracted using half of the solvent volumes (in the same conditions described above) and the separated fractions were pooled. Both fractions were dried under a nitrogen flow at room temperature until the solvent was completely evaporated. The dried phases were stored at –20 °C pending NMR analysis.

NMR spectra were recorded at 27°C on a Bruker AVANCE 600 spectrometer operating at a proton frequency of 600.13MHz and equipped with a Bruker multinuclear z-gradient 5 mm probe head.

The dried hydroalcoholic phase of each sample was solubilized in 0.7 mL 400 mM phosphate buffer/deuterium oxide (D₂O), containing a 1 mM solution of (trimethylsilyl)-

propionic-2,2,3,3-d₄ acid sodium salt (TSP) as an internal standard, and then transferred into a 5 mm NMR tube. The dried organic fraction of each sample was dissolved in 0.7 mL of a deuterated chloroform/deuterated methanol (CDCl₃/CD₃OD) mixture (2:1 v/v) and then placed into a 5 mm NMR tube. In order to avoid solvent evaporation, tubes were flame-sealed.

¹H NMR spectra of hydroalcoholic and organic extracts were referenced against the methyl group signal of TSP ($\delta = 0.00$ ppm) in D₂O, and the residual deuterated methyl group (CHD₂) signal of methanol (set to 3.31 ppm) in a CD₃OD/CDCl₃ mixture, respectively. ¹H spectra of hydroalcoholic extracts were acquired using 256 transients and a recycle delay of 5 s. The residual deuterated water group (HDO) signal was suppressed using a pre-saturation pulse sequence. The experiment was carried out using a 45° pulse of 6.68 μ s, and 32 K data points. ¹H spectra of extracts in CD₃OD/CDCl₃ were acquired using 512 transients, a recycle delay of 5 s and a 90° pulse of 10 μ s, with 32 K data points. Two-dimensional (2D) NMR experiments, namely ¹H-¹H Total Correlation Spectroscopy (TOCSY), ¹H-¹³C Heteronuclear Single Quantum Coherence (HSQC) and ¹H-¹³C Heteronuclear Multiple-Bond Correlation (HMBC), were carried out under the same experimental conditions as previously reported (Capitani et al., 2013; Mannina et al., 2004).

The mixing time for the ¹H-¹H TOCSY experiment was 80ms, ¹H-¹³C HSQC experiments were performed using a coupling constant ¹J_{C-H} of 150 Hz, and the ¹H-¹³C HMBC experiments were performed using a delay of 80 ms for the evolution of long-range couplings (Braun, Kalinowski & Berger, 1998).

Pulsed field gradient spin echo (PGSE) experiments (Stilbs, 2010) were carried out with a pulsed field gradient unit, producing a magnetic field gradient in the z-direction with a strength of 55.25 G/cm. The sinusoidal gradient pulse was given a duration δ of 2.6 ms, with an intensity which was incremented in 32 steps, from 2% up to 95% of the maximum gradient strength, with a diffusion time Δ of 100 ms.

Signal area integration was used for quantitative analysis. Note that the quantitative analysis was performed on those metabolites not affected by overlapping peaks or on deconvoluted peaks, using the program DIM2015 (Massiot et al., 2002). For water-soluble metabolites, the integrals of selected ^1H resonances were measured with respect to the integral of the TSP signal normalized to 1000 and used as an internal standard.

In the case of $\text{CDCl}_3/\text{CD}_3\text{OD}$ spectra, the integrals were labelled by numbers (I_1 - I_{10}) for calculation. First, integrals were normalized with respect to the integral of $\alpha\text{-CH}_2$ groups for all fatty acid chains, I_4 (esterified fatty acids, $\alpha\text{-CH}_2$, 2.35 ppm) + I_3 (free fatty acids, $\alpha\text{-CH}_2$, 2.29 ppm) set to 100%. Then, the total content (% mol) of fatty acids of four different types (saturated fatty acids (SFA), monounsaturated fatty acids (MUFA), linoleic fatty acid, and linolenic fatty acid) was calculated according to Eqs. (1)–(4).

Lipid fractions (fatty acids, β -sitosterol, and squalene) were calculated according to Eqs. (5)–(7).

Distribution of esterified fatty acids in pulp among phosphatidylethanolamine (PE), phosphatidylcholine (PC), monoacylglycerol (MAG) and other lipids was calculated according to Eqs. (8)–(11).

$$\text{Linoleic} = I_5; (I_5, \text{CH}_2, 2.78 \text{ ppm}) \quad (1)$$

$$\text{Linolenic} = I_6/2; (I_6, 2\text{CH}_2, 2.82 \text{ ppm}) \quad (2)$$

$$\text{MUFA} = I_7 - 2I_5 - I_6 \cdot 6/4; (I_7, \text{all unsaturated fatty acids, CH=CH, 5.36 ppm}) \quad (3)$$

$$\text{SFA} = 100 - \text{MUFA} - \text{Linoleic} - \text{Linolenic}; \quad (4)$$

$$\text{Fatty acids} = \frac{I_3 I_4}{I_3 + I_4 + \frac{I_2}{3} + I_1 \frac{2}{3}}; (I_1, \beta\text{-Sitosterol, CH}_3, 0.70 \text{ ppm}; I_2, \text{squalene, } 2\text{CH}_3, 1.68 \text{ ppm})$$

(5)

$$\beta\text{-Sitosterol} = \frac{I_{1\frac{2}{3}}}{I_3 + I_4 + \frac{I_2}{3} + I_{1\frac{2}{3}}}; \quad (6)$$

$$\text{Squalene} = \frac{I_{2\frac{1}{3}}}{I_3 + I_4 + \frac{I_2}{3} + I_{1\frac{2}{3}}}; \quad (7)$$

$$\text{PE} = 2 \cdot I_9 / I_4; \quad (I_9, \text{phosphatidylethanolamine, CH}_2, 3.22 \text{ ppm}) \quad (8)$$

$$\text{PC} = 4 \cdot I_{10} / 9 \cdot I_4; \quad (I_{10}, \text{phosphatidylcholine, N(CH}_3)_3, 3.26 \text{ ppm}) \quad (9)$$

$$\text{MAG} = 2 \cdot I_8 / I_4; \quad (I_8, \text{monoacylglycerol, CH, 3.62 ppm}) \quad (10)$$

$$\text{Other lipids} = 1 - \text{PE} - \text{PC} - \text{MAG} \quad (11)$$

The pulsed field gradient NMR experiment allows the measurement of the translational diffusion of molecules. In this experiment, NMR signal intensity is attenuated depending on the diffusion time Δ and the selected gradient parameters (i.e. the gradient strength g and the gradient length δ). To obtain the self-diffusion coefficient, the intensity change of the NMR signal can be fit to the following Eq. (12):

$$\ln\left(\frac{I}{I_0}\right) = -D(2\pi)^2 \gamma^2 g^2 \delta^2 \left(\Delta - \frac{\delta}{3}\right) \quad (12)$$

where I is the observed intensity, I_0 the reference intensity, γ the ^1H gyromagnetic ratio (4257 Hz/Gauss), Δ the diffusion time, and D is the self-diffusion coefficient.

7.3 Results and Discussion

The assignment of ^1H spectra of hydroalcoholic extracts of fruits and leaves solubilized in D_2O phosphate buffer was executed by 1D and 2D NMR experiments and literature data (Duarte et al., 2005) on vegetable food matrices (Table 7.1). As an example, Figure 7.1A reports the ^1H spectrum of an aqueous extract of baobab pulp, the spectral ranges 5.5–10 and 0–2 ppm have been vertically magnified, and are reported in inserts.

Table 1. Metabolites identified in the 600MHz ^1H NMR spectrum of aqueous extracts of baobab pulp and leaves.

| | <i>Sample^a</i> | <i>type</i> | ^1H | <i>multiplicity</i> | ^{13}C |
|------------------------------------|---------------------------|--------------------------------------|--------------|---------------------|-----------------|
| <i>Carbohydrates</i> | | | | | |
| α -Glucose (α -GLC) | FP, L | CH-1 | 5.25 | d [3.8] | 93.1 |
| | | CH-2 | 3.55 | dd [9.8;3.8] | 72.3 |
| | | CH-3 | 3.72 | | 73.8 |
| | | CH-4 | 3.43 | | 70.6 |
| | | CH-5 | 3.84 | | 72.6 |
| | | CH ₂ -6,6' | 3.85;3.78 | | 61.7 |
| β -Glucose (β -GLC) | FP, L | CH-1 | 4.66 | d [7.9] | 97.2 |
| | | CH-2 | 3.27 | dd [9.3;8.0] | 75.3 |
| | | CH-3 | 3.50 | t [9.1] | 76.8 |
| | | CH-4 | 3.43 | | 70.6 |
| | | CH-5 | 3.48 | | 76.9 |
| | | CH ₂ -6,6' | 3.91;3.74 | | 61.8 |
| β -D-Fructofuranose | FP, L | CH-1,1' | 3.60;3.57 | | 63.7 |
| | | CH-2 | | | 102.4 |
| | | CH-3 | 4.13 | | 76.5 |
| | | CH-4 | 4.13 | | 75.4 |
| | | CH-5 | 3.83 | | 81.7 |
| | | CH ₂ -6,6' | 3.81;3.68 | | 63.5 |
| α -D-Fructofuranose | FP, L | CH-3 | 4.13 | | 83.0 |
| | | CH-5 | 4.07 | | 82.4 |
| β -D-Fructopyranose (FRU) | FP ^b , L | CH-1,1' | 3.57; 3.72 | | 64.8 |
| | | CH-3 | 3.82 | | 68.7 |
| | | CH-4 | 3.90 | | 70.6 |
| | | CH-5 | 4.01 | | 70.2 |
| | | CH ₂ -6,6' | 3.72;4.03 | | 64.4 |
| Sucrose (SUCR) | FP, L | CH-1 (Glc) | 5.42 | d [3.8] | 93.2 |
| | | CH-2 | 3.56 | | 72.5 |
| | | CH-3 | 3.77 | | 73.6 |
| | | CH-4 | 3.49 | | 70.6 |
| | | CH-5 | 3.85 | | 73.5 |
| | | CH ₂ -6 | 3.83 | | 60.9 |
| | | CH ₂ -1' (Fru) | 3.70 | | 62.1 |
| | | C-2' | | | 104.7 |
| | | CH-3' | 4.23 | | 77.4 |
| | | CH-4' | 4.05 | | 75.0 |
| | | CH-5' | 3.90 | | 82.3 |
| | | CH ₂ -6' | 3.81 | | 63.4 |
| | | α -Galactose (α -GAL) | L | CH-1 | 5.29 |
| CH-2 | 3.83 | | | | |
| CH-3 | 3.88 | | | | |

| | | | | | | |
|--|-------|------------------------|-------------------------------------|----------|----------|------|
| | | CH-4 | 4.01 | | | |
| β -Galactose (β -GAL) | L | CH-1 | 4.61 | d [8.0] | | |
| | | CH-2 | 3.51 | | | |
| | | CH-3 | 3.67 | | | |
| | | CH-4 | 3.96 | | | |
| β -Galacturonic acid (β -GALU) | FP | CH-1 | 4.59 | d [7.9] | | |
| | | CH-2 | 3.51 | | | |
| | | CH-3 | 3.71 | | | |
| | | CH-4 | 4.22 | | | |
| β -Galacturonic acid (pectic, reducing end) ^c | FP | CH-1 | 4.63 | | | |
| | | CH-2 | 3.52 | | | |
| | | CH-3 | 3.78 | | | |
| | | CH-4 | 4.40 | | | |
| α -Galacturonic acid (α -GALU) | FP | CH-1 | 5.31 | d [3.9] | | |
| | | CH-2 | 3.84 | | | |
| | | CH-3 | 3.92 | | | |
| | | CH-4 | 4.28 | | | |
| | | CH-5 | 4.41 | | | |
| α -Galacturonic acid (pectic, reducing end) | FP | CH-1 | 5.34 | | | |
| | | CH-2 | 3.86 | | | |
| | | CH-3 | 4.00 | | | |
| | | CH-4 | 4.31 | | | |
| α -Galacturonic acid (pectic, non reducing)/ α -rhamnose | FP | | 5.11 [4.02, 4.14, 4.29, 3.75, 3.94] | | | |
| | | | | | | |
| <i>Myo</i> -inositol (MI) | FP, L | CH-1 | 4.08 | | | |
| | | CH-2,5 | 3.55 | | | |
| | | CH-3,6 | 3.63 | | | |
| | | CH-4 | 3.30 | t [9.38] | | |
| <i>Organic acids</i> | FP, L | α, γ -CH | 2.53 | | d [15.0] | 46.4 |
| | | α', γ' -CH | 2.67 | | d [15.0] | 46.4 |
| Formic acid (FOA) | FP, L | HCOOC | 8.46 | | | |
| Quinic acid (QA) | L | CH ₂ -1,1' | 1.88 2.08 | | 41.8 | |
| | | CH-2 | 4.31 | | 68.1 | |
| | | CH-3 | 3.56 | | 76.2 | |
| | | CH-4 | 4.16 | | 71.5 | |

| | | | | | |
|------------------------|-------|---------------------------------|-----------|------------------|-------|
| | | CH ₂ -5,5' | 1.99 2.06 | | 38.6 |
| Malic acid (MA) | FP, L | α -CH | 4.30 | dd [9.9, 3.2] | 71.4 |
| | | β -CH | 2.68 | dd [3.2, 5.4] | 43.6 |
| | | β' -CH | 2.38 | dd [9.9, 5.4] | 43.6 |
| Succinic acid (SA) | FP, L | α,β -CH ₂ | 2.41 | s | 35.2 |
| Acetic acid | L | CH ₃ | 1.94 | s | 24.6 |
| Fumaric acid (FUA) | L | CH=CH | 6.54 | s | |
| D-threo-isocitric acid | FP | CH-3 | 4.00 | | |
| | | CH ₂ -1,1' | 2.51 2.44 | | |
| | | CH-2 | 2.98 | | |
| Shikimic acid | L | CH ₂ -7 | 2.20 2.77 | | |
| | | CH-6 | 4.00 | | |
| | | CH-5 | 3.73 | | |
| | | CH-4 | 4.42 | | |
| | | CH-3 | 6.45 | | 134.4 |
| Ascorbic acid (AA) | FP | CH-5 | 4.55 | d[2.0] | 79.6 |
| | | CH-1' | 4.04 | | 64.5 |
| | | CH ₂ -2' | 3.75 | | |
| Lactic acid | FP, L | CH ₃ | 1.34 | d | 21.3 |
| | | α -CH | 4.13 | | |
| Gallic acid (GA) | FP | CH-1 | 7.1 | s | 115.7 |
| <i>Amino acids</i> | | | | | |
| Alanine (ALA) | FP, L | α -CH | 3.79 | | 51.5 |
| | | β -CH ₃ | 1.49 | d [7.3] | 17.4 |
| Asparagine (ASN) | L | α -CH | 4.02 | | 52.5 |
| | | β -CH | 2.91 | dd [16.9;7.2] | 35.6 |
| | | β' -CH | 2.95 | dd [16.9;4.4] | 35.6 |
| Aspartate (ASP) | L | α -CH | 3.92 | | |
| | | β -CH | 2.74 | | |
| | | β' -CH | 2.83 | dd [3.9;17.4] | |
| Glutamate (GLU) | L | α -CH | 3.78 | | |
| | | β -CH | 2.13 | | |
| | | β' -CH | 2.09 | | |
| | | γ -CH ₂ | 2.35 | | |

| | | | | | |
|----------------------------------|-------|----------------------------|------|---------|-------|
| Glutamine (GLN) | L | α -CH | 3.78 | | 55.1 |
| | | β -CH ₂ | 2.15 | m | 27.3 |
| | | γ -CH | 2.47 | m | 31.9 |
| Isoleucine (ILE) | L | α -CH | 3.63 | | |
| | | β -CH | 1.98 | | |
| | | γ -CH | 1.27 | | |
| | | γ' -CH | 1.48 | | |
| | | γ -CH ₃ | 1.02 | | |
| | | δ -CH ₃ | 0.95 | | |
| Leucine (LEU) | L | α -CH | 3.75 | d | |
| | | β -CH ₂ | 1.73 | | |
| | | δ -CH ₃ | 0.97 | | |
| | | δ' -CH ₃ | 0.95 | | |
| γ -Aminobutyrate (GABA) | FP, L | α -CH ₂ | 2.30 | t [7.4] | 35.5 |
| | | β -CH ₂ | 1.92 | | 24.5 |
| | | γ -CH ₂ | 3.02 | t [7.5] | 40.4 |
| Proline (PRO) | L | α -CH | 4.15 | | 62.3 |
| | | β -CH | 2.36 | | |
| | | β' -CH | 2.07 | | |
| | | γ -CH ₂ | 2.02 | | |
| | | δ -CH | 3.42 | | |
| | | δ' -CH | 3.35 | | |
| Phenylalanine (PHE) | L | CH-2,6, ring | 7.34 | | 130.5 |
| | | CH-3,5, ring | 7.44 | | 130.2 |
| | | CH-4, ring | 7.39 | | 128.8 |
| Threonine (THR) | FP, L | α -CH | 3.62 | | 61.5 |
| | | β -CH | 4.27 | | |
| | | γ -CH ₃ | 1.35 | | |
| Tryptophan (TRP) | L | CH-4 | 7.73 | | |
| | | CH-7 | 7.54 | | |
| | | CH-6 | 7.27 | | |
| | | CH-5 | 7.20 | | |
| Valine (VAL) | L | α -CH | 3.63 | | 61.4 |
| | | β -CH | 2.28 | d [2.6] | |
| | | γ -CH ₃ | 1.01 | d [7.0] | |
| | | γ' -CH ₃ | 1.05 | d [7.0] | 18.9 |
| <i>Miscellaneous metabolites</i> | | | | | |
| Choline | FP, L | N-CH ₃ | 3.19 | s | 55.0 |
| | | N-CH ₂ | 3.52 | | 68.6 |

| | | | | |
|--------------|-------|---------------------|------------|---------------------|
| | | CH ₂ -OH | 4.07 | 56.6 |
| Ethanolamine | FP, L | N-CH ₂ | 3.15 | |
| | | OH-CH ₂ | 3.83 | |
| Trigonelline | FP, L | CH-1 | 9.12 | s |
| | | CH-3,5 | 8.83, 8.79 | d [8.0], d [6.0] |
| | | CH-4 | 8.08 | dd [6.0, 8.0] |
| Uridine | FP, L | CH-5 ring | 7.87 | d [8.0] |
| | | CH-6 ring | 5.91 | d [8.0] |
| | | Rib CH-1 | 5.93 | d [4.7] |
| | | CH-2 | 4.37 | |
| | | CH-3 | 4.24 | |
| | | CH-4 | 4.16 | |
| Adenosine | FP | CH-1 ring | 8.32 | s |
| | | CH-2 ring | 8.23 | s |
| | | Rib CH-3 | 6.07 | d [6.0] |
| | | CH-4 | 4.78 | |
| | | CH-5 | 4.43 | |
| | | CH-6 | 4.29 | |

^a FP, fruit pulp; L, leaves; ^b Traces; ^c Tentative assignment

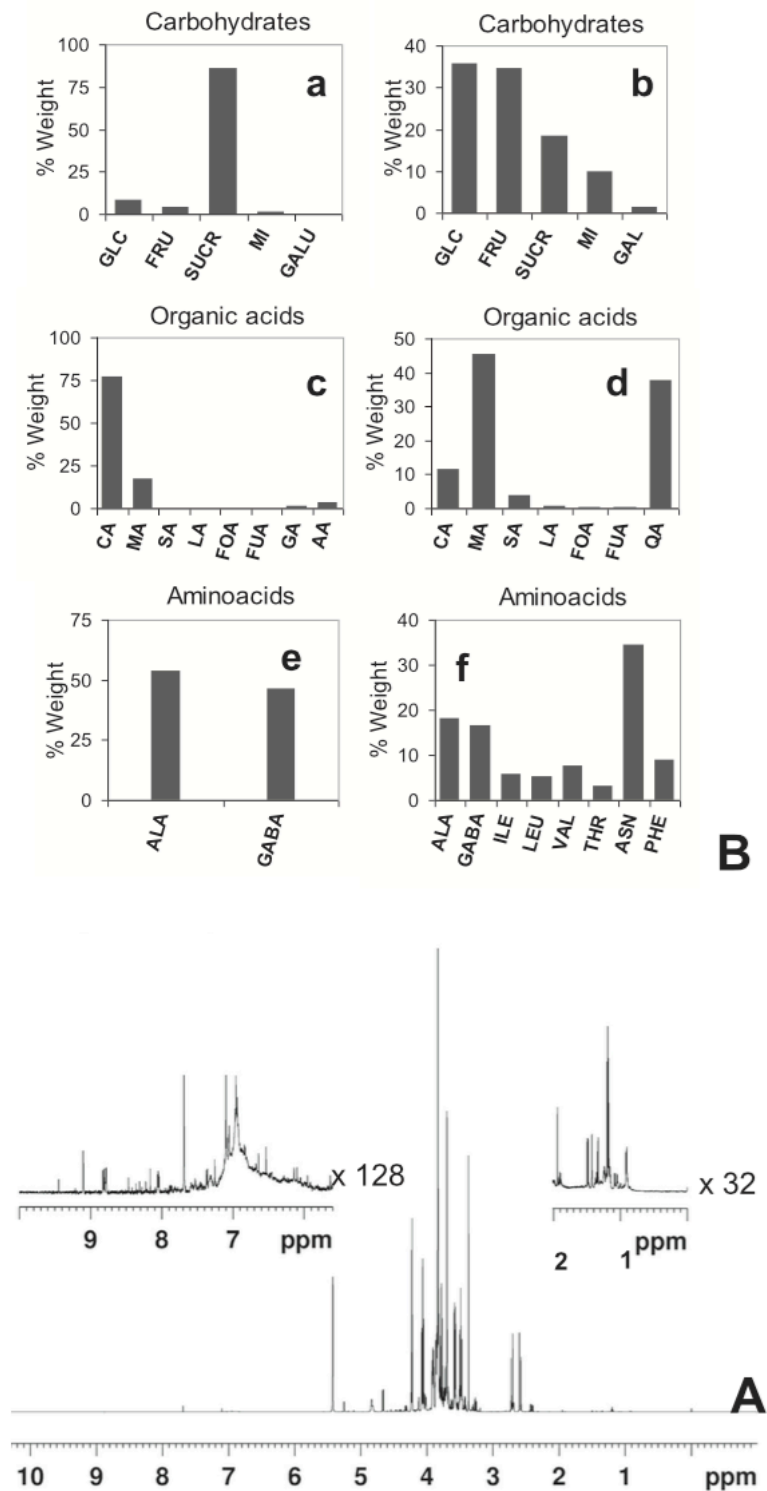


Figure 7.1. A) Regions of the 600.13 MHz ^1H NMR spectrum of an aqueous extract of baobab pulp. B) Histograms resulting from the quantitative NMR spectroscopic analysis of some metabolites present in aqueous extracts of baobab: sugars and derivatives in fruit pulp (a) and leaves (b), organic acids in fruit pulp (c) and leaves (d), and amino acids in fruit pulp (e) and leaves (f).

Analysis of the baobab fruit pulp extract. In the 3.2–5.5 ppm range, the ^1H NMR spectra of pulp extracts are dominated by the characteristic signals of glucose and fructose isomers, and sucrose (Figure 7.1A and Table 7.1). The ^1H spectrum also showed characteristic signals of myo-inositol.

The ^1H signals of α and β -galacturonic acid, and α -galacturonic acid pectic reducing end, and possibly α -galacturonic acid (pectic, non-reducing)/ α -rhamnose, and β -galacturonic acid pectic reducing end (tentative assignment) were identified from literature data (Duarte et al., 2005).

For the concentrations of sugars and their derivatives, as indicated by the histograms reported in Figure 7.1B, sucrose accounts for about 86% of the total amount of sugars in baobab pulp extract, with glucose in both its α and β isomers representing about 8%, whereas β -fructopyranose and myo-inositol are about 4% and 2%, respectively. Galacturonic acid represents less than 1% of the total amount of sugars and derivatives.

NMR signals of citric acid (CA), malic acid (MA), succinic acid (SA), D-threo-isocitric acid, lactic acid (LA), and ascorbic acid (AA), were identified in the 1.8–4.6 ppm region. Formic acid (FOA), fumaric acid (FUA), and gallic acid (GA) were identified in the low field region, along with a signal at 6.45 ppm belonging to shikimic acid.

Histograms reported in Figure 7.1B indicate that citric acid is present in high amounts in the baobab pulp extracts, about 77.3%, followed by malic acid (17.6%), ascorbic acid (3.2%), and gallic acid (1.3%), the other acids present are at amounts below 0.34%.

Minor signals belonging to amino acids were observed (i.e. alanine, γ -aminobutyrate, and threonine) in the high field NMR spectral region between 0.50 and 3.60 ppm.

Histograms reported in Figure 7.1B indicate that alanine and γ -aminobutyrate are present in baobab pulp extracts at similar levels, about 54 and 46%, respectively.

NMR signals of choline, ethanolamine, trigonelline, uridine and adenosine were identified by means of their diagnostic signals (Table 7.1).

Analysis of the baobab aqueous leaf extract. Like pulp extract outlined above, leaf extract also contains glucose, fructose and sucrose as again confirmed through the ^1H spectrum. NMR analysis also revealed the presence of the signals belonging to α and β -galactose and myo-inositol.

The histograms reported in Figure 7.1B compiled from the quantitative NMR spectroscopic analysis indicate that sucrose accounts for about 18% of the total amount of detected sugars in leaves, whereas glucose represents about 35% in both α and β isomers, and β -fructopyranose accounts for 34.5%. The amount of myo-inositol was found to be higher in leaves than in pulp, at about 10%, with both α and β galactose isomers accounting for 1.5% of the total amount of sugars detected in leaves.

Malic, citric, succinic, lactic, fumaric and formic acids, all detected in pulp, were also identified in leaf extracts, along with acetic acid, quinic acid, and shikimic acid. As reported in the histogram of Figure 7.1B, malic acid (45.3%) was the most abundant acid, followed by quinic acid (37.9%), citric acid (11.6%), and succinic acid (3.8%), other acids, namely lactic, formic, and fumaric were present in amounts of about 1.3%.

Alanine, γ -aminobutyrate, and threonine, previously identified in pulp, were also detected in leaf extracts. The ^1H spectrum of leaf extract also showed signals from asparagine, aspartate, glutamate, glutamine, isoleucine, leucine, proline, and valine. Moreover, in the low field region of the ^1H spectrum (Figure 7.1A), signals from aromatic rings of phenylalanine and tryptophan were detected. Asparagine is the most abundant amino acid (about 34.4%) in baobab leaf extracts, followed by alanine (18%), γ -aminobutyrate (16.6%), phenylalanine (9%), valine (7.7%), isoleucine and leucine in very similar amounts, 5.8 and 5.2% respectively, and threonine (3.2%).

Choline, ethanolamine, trigonelline, and uridine, which were identified in pulp, were also identified in the ^1H spectrum of leaf extracts.

Analysis of the baobab pulp and leaf organic extracts. ^1H NMR spectral regions of an organic extract of baobab pulp are shown in Figure 7.2 with the assignment of some selected resonances ($\text{I}_1\text{-I}_{10}$) which were used for quantitative analysis (Table 7.2).

Table 7.2. Metabolites identified in the 600MHz ^1H NMR spectrum of organic extracts of baobab pulp and leaves.

| <i>Compounds</i> | <i>Type</i> | ^1H (ppm) | <i>Multiplicity (J Hz)</i> | ^{13}C (ppm) |
|--------------------------------|------------------------|--------------------|----------------------------|-----------------------|
| Saturated fatty chains | COO | | | 175.0 |
| | CH ₂ -2 | 2.35 | t (7.8) | 34.5 |
| | CH ₂ -3 | 1.63 | | 25.2 |
| | CH ₂ (n3) | 1.32 | | 29.5 |
| | CH ₂ (n2) | 1.27 | | 32.2 |
| | CH ₂ (n1) | 1.31 | | 22.9 |
| | CH ₃ | 0.88 | t (6.9) | 14.2 |
| Oleic acid | COO-1 | | | 175.0 |
| | CH ₂ -2 | 2.35 | | 34.5 |
| | CH ₂ -3 | 1.63 | | 25.3 |
| | CH ₂ -4,7 | 1.34 | | 30.5 |
| | | 1.32 | | 29.5 |
| | CH ₂ -8 | 2.03 | | 27.5 |
| | CH=CH-9,10 | 5.35 | | 130.3 |
| | CH ₂ -11 | 2.06 | | 27.5 |
| | CH ₂ -12,15 | 1.34 | | 30.5 |
| | | 1.32 | | 29.5 |
| | CH ₂ -16 | 1.28 | | 32.2 |
| | CH ₂ -17 | 1.30 | | 23.0 |
| CH ₃ -18 | 0.88 | t (7.0) | 14.3 | |
| Linolenic fatty chain C18:3 | COO- | | | 175.6 |
| | 1(sn1,3) | | | |
| | CH ₂ -2 | 2.33 | | 34.5 |
| | CH ₂ -3 | 1.63 | | 25.2 |
| | CH ₂ -4 | 1.33 | | 29.50 |
| | CH ₂ -5,7 | 1.34 | | 30.4 |
| | CH ₂ -8 | 2.07 | | 27.4 |
| | CH-9 | 5.35 | | 130.5 |
| | CH-10 | 5.35 | | 128.5 |
| | CH ₂ -11 | 2.81 | | 25.9 |
| | CH-12,13 | 5.35 | | 128.5 |
| | CH ₂ -14 | 2.81 | t (6.1) | 25.9 |
| | CH-15 | 5.32 | | 127.5 |
| | CH-16 | 5.39 | | 132.2 |
| | CH ₂ -17 | 2.09 | | 20.9 |
| | CH ₃ -18 | 0.98 | t (7.5) | 14.4 |

| | | | | |
|----------------------------------|-----------------------|---------------|----------------------------------|-------|
| Free fatty acids (FFA) | | | | |
| | CH ₂ -2 | 2.29 | | 34.5 |
| | CH ₂ -3 | 1.62 | | 25.2 |
| | CH ₂ | 1.32 | | 24.6 |
| Monoacylglycerol (MAG) | | | | |
| | CH ₂ -sn1 | 3.56, 3.62 | dd (6.2, 11.4) dd (4.6, 11.4) | 63.6 |
| | CH-sn2 | 3.87 | | 70.3 |
| | CH ₂ -sn3 | 4.10, 4.15 | dd (6.2, 11.4) dd (4.9, 11.4) | 65.6 |
| | COO | | | 174.9 |
| Diacylglycerol (DAG) | | | | |
| | CH ₂ -sn1 | 4.19, 4.33 | | 62.5 |
| | CH sn2 | 5.09 | | 72.6 |
| | CH ₂ sn3 | 3.69 | | 61.0 |
| Triacylglycerol (TAG) | | | | |
| | CH ₂ sn1,3 | 4.18, 4.34 | dd (6, 11.9) dd (4, 12) | 62.5 |
| | CH sn2 | 5.27 | m | 70.1 |
| Linoleic fatty chain C18:2 | | | | |
| | COO-1 | | | 175.6 |
| | CH ₂ -2 | 2.33 | | 34.4 |
| | CH ₂ -3 | 1.63 | | 25.3 |
| | CH ₂ -4,7 | 1.32 | | 29.5 |
| | CH ₂ -8 | 2.06 | | 27.6 |
| | CH-9 | 5.36 | | 130.3 |
| | CH-10 | 5.36 | | 128.5 |
| | CH ₂ -11 | 2.78 | | 25.9 |
| Galactosyldiacylglycerols (DGDG) | | | | |
| | CH-sn2 | 5.27 | | 70.6 |
| | CH ₂ -sn1 | 3.72, 3.96 | | 68.2 |
| | CH ₂ -sn3 | 4.24, 4.39 | | 63.1 |
| | CH-1' | 4.23 | | 104.2 |
| | CH-2' | 3.54 | | 71.5 |
| | CH-3' | 3.51 | | 73.6 |
| | CH-4' | 3.91 | | 68.7 |
| | CH-5' | ----- | | |
| | CH2-6' | ----- | | |
| | CH-1'' | 4.91 | d (3.8) | 99.6 |
| | CH-2'' | 3.81 | | 69.3 |
| | CH-3'' | 3.75 | | 70.5 |
| | CH-4'' | 3.96 | | 70.2 |

| | | | |
|-------------------------------|---------------------------------------|-----------|-------|
| Phosphatidylcholine (PC) | CH-5'' | 3.75 | 70.5 |
| | CH ₂ -6'' | 3.76, | 62.2 |
| | | 3.86 | |
| | (CH ₃) ₃ N | 3.26 | 54.5 |
| | CH ₂ OP | 4.45 | 60.9 |
| | CH ₂ N | 3.77 | 66.2 |
| | CH ₂ sn3 | 4.17 | 63.4 |
| | CH ₂ sn1 | 4.38, | 62.4 |
| | | 4.22 | |
| | | CH sn2 | 5.27 |
| Phosphatidylethanolamine (PE) | CH ₂ OP | 4.24 | 63.4 |
| | CH ₂ N | 3.22 | 40.3 |
| β-Sitosterol | CH ₂ -1 | 1.08, | 37.6 |
| | | 1.87 | |
| | CH ₂ -2 | ---, 1.81 | 31.4 |
| | CH-3 | 3.47 | 71.6 |
| | CH ₂ -4 | 2.25 | 42.1 |
| | CH-6 | 5.35 | 121.8 |
| | CH ₂ -7 | 1.59, | 32.9 |
| | | 2.06 | |
| | CH-8 | 1.55 | 32.8 |
| | CH-9 | 0.94 | 50.6 |
| | CH ₂ -11 | 1.51 | 21.5 |
| | CH ₂ -12 | 1.19, | 40.2 |
| | | 2.05 | |
| | CH-14 | 1.02 | 57.2 |
| | CH ₂ -15 | 1.08, | 24.6 |
| | | 1.59 | |
| | CH ₂ -16 | 1.30, | 28.5 |
| | | 1.87 | |
| | CH-17 | 1.13 | 56.5 |
| | CH ₃ -18 (I ₁) | 0.70 | 12.1 |
| | CH ₃ -19 | 1.02 | 19.5 |
| | CH-20 | 1.38 | 36.5 |
| | CH ₃ -21 | 0.94 | 19.0 |
| | CH ₂ -22 | 1.04, | 34.4 |
| | | 1.34 | |
| | CH ₂ -23 | 1.11 | 26.2 |
| | CH-24 | 0.94 | 46.3 |
| | CH-25 | 1.64 | 28.9 |
| | CH ₃ -26 | 0.86 | 20.7 |
| CH ₃ -27 | 0.85 | 19.9 | |
| CH ₂ -28 | 1.30 | 23.0 | |
| CH ₃ -29 | 0.86 | 12.1 | |
| Squalene | CH-1 | 5.12 | 124.7 |
| | CH-2/CH-3 | 5.14 | 124.7 |
| | CH ₂ -4 | 2.07 | 26.8 |
| | CH ₂ -5 | 2.06 | 27.6 |

| | | | |
|---|---------------------|------|-------|
| | CH ₂ -6 | 2.03 | 28.4 |
| | CH ₂ -7 | 1.99 | 40.0 |
| | CH ₃ -8 | 1.61 | 17.8 |
| | CH ₃ -9 | 1.61 | 16.1 |
| | CH ₃ -10 | 1.68 | 25.8 |
| | C-11 | | 131.6 |
| | C-12/C-13 | | 135.2 |
| Isoprenoid compound (Only in leaves) | CH-17 | 5.14 | 125.3 |
| | CH ₃ -16 | 1.69 | 23.5 |
| | CH ₂ -14 | 2.06 | 32.4 |
| | CH ₂ -18 | 2.08 | 26.8 |
| | C-15 | | 135.5 |

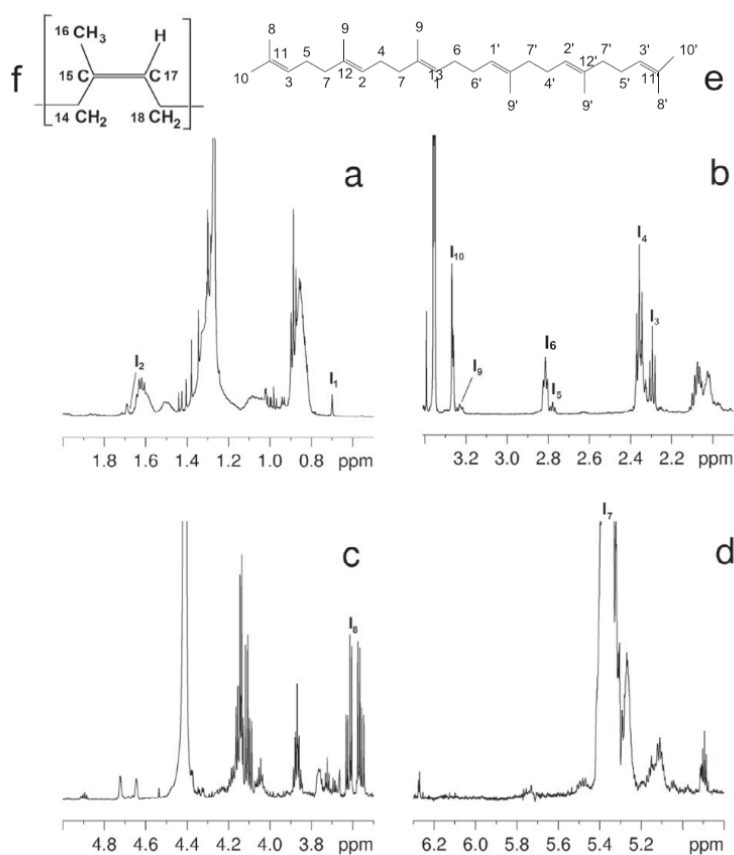


Figure 7.2. Regions of the 600.13 MHz ¹H NMR spectrum of a baobab pulp organic extract, signals used for the quantitative analysis have been labelled with I₁–I₁₀. (a) 0.5–2.0 ppm region, (b) 1.9–3.4 ppm region, (c) 3.5–5.0 ppm region, (d) 4.8–6.3 ppm region. (e) Sketch of squalene structure with nuclei labelling. (f) Sketch of the repetitive unit of the isoprenoid compound partially assigned, with the labelling. I₁, CH₃-18 β-sitosterol; I₂, 2CH₃ squalene; I₃, α-CH₂ free fatty acids; I₄, α-CH₂ esterified fatty acids; I₅, CH₂ linoleic fatty chain; I₆, 2CH₂ linolenic fatty chain; I₇, CH=CH all unsaturated fatty acids; I₈, CH MAG; I₉, CH₂ PE; I₁₀, N(CH₃)₃ PC.

The resonance at 0.70 ppm was ascribed to the CH₃-18 of β -sitosterol (I₁).

Phosphatidylcholine (PC) and phosphatidylethanolamine (PE) were the main diacylglycerophospholipids present in the baobab lipid fraction. The characteristic ¹H signals of these lipids belong to their head groups, specifically the singlet at 3.27 ppm of N(CH₃)₃ of PC (I₁₀) and the multiplet at 3.22 ppm of CH₂N of PE (I₉).

The peak at 2.29 ppm was assigned to the α -CH₂ of esterified fatty acids (I₃), the peak at 2.78 was assigned to CH₂-11 of linoleic fatty acids (I₅), and the peak at 2.82 ppm was assigned to CH₂-11 and CH₂-14 of linolenic fatty chain (I₆). The peak centred at 5.36 ppm was due to CH=CH protons of all unsaturated fatty acids (I₇).

The peak at 3.62 ppm was due to one of the two protons of monoacylglycerols (I₈). It was not possible to perform a quantitative analysis on di- and triacylglycerols due to the overlap of multiple strong peaks.

The resonance of the very weak peak at 1.68 ppm was assigned to two methyl protons of squalene (I₂). All resonances of squalene were assigned (Table 7.2) according to the labelling of the resonances reported in Figure 7.2e.

Peaks at frequencies very similar to those of squalene appeared in the ¹H spectrum of baobab leaf organic extracts. Figure 7.3 compares selected ranges of frequencies of the ¹H spectra of pulp and leaf organic extracts. An intense peak appeared at 1.69 ppm, whereas peaks centred at 5.15, 2.08 and 2.06 ppm were stronger in leaves than in the pulp extract. The TOCSY map revealed the presence of a spin system at 1.69, 2.06, 2.08, and 5.14 ppm. The HSQC map allowed the assignment of the corresponding carbon resonances at 25.5, 32.4, 26.8, and 125.3 ppm. The HMBC revealed long-range correlations between 5.14 ppm and 23.5 and 32.4 ppm, 1.69 ppm and 32.4, 125.3, and 135.5 ppm, 2.06 ppm and 26.8 ppm, 2.07 ppm and 32.4 ppm.

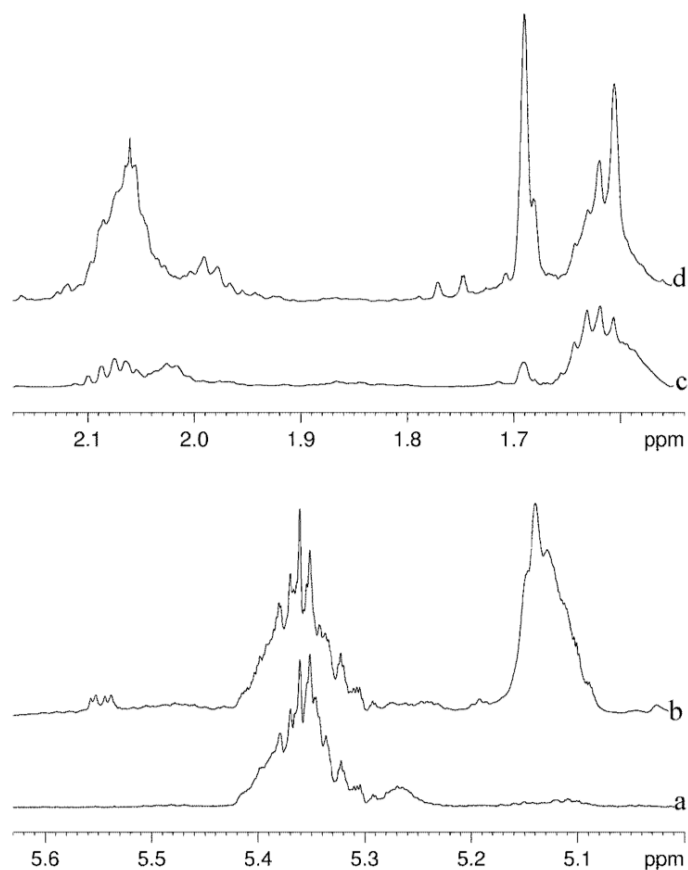


Figure 7.3. Comparison between two spectral ranges of the ¹H NMR spectrum of baobab pulp (bottom) and leaf (top) organic extracts. Intense peaks ascribed to the isoprenoid compound are evident in the spectrum of leaf extracts.

These data and data from literature (Maidunny & Dulngali, 1985) allowed partial assignment of the unknown compound, see Table 7.2. Whereas the assignment of the repetitive unit of squalene perfectly matches that of 1,4-polyisoprene in trans conformation, the assignment of the repetitive unit of cis 1,4-polyisoprene matches that of the unknown compound which, for this reason, was labelled as an “isoprenoid” compound (Table 7.2 and Figure 7.2f). This compound is probably an 1,4-polyisoprene oligomer with its chain in cis conformation, in fact the chemical structure of this isoprenoid compound closely resembles that of natural rubber, based on cis-1,4-polyisoprene chains. To identify other possible differences between squalene and the isoprenoid compound, the self-diffusion coefficients were calculated by fitting the collected NMR data to Eq. (12).

The self-diffusion coefficient of squalene was calculated as 3.79×10^{-10} m²/s, with a coefficient of determination R^2 of 0.999, whereas the self-diffusion coefficient of the isoprenoid compound worked out to be 4.62×10^{-10} m²/s, with a coefficient of determination R^2 of 0.998. As the self-diffusion coefficient is strictly related to translational molecular mobility, and thus to the molecular weight, these data indicate that the molecular weight of the isoprenoid compound should be slightly lower than that of squalene. The molar composition of baobab pulp and leaf organic extracts is reported in Table 7.3. With regards to their fatty acids, the amount of free FA in leaves was found to be about twice that of pulp, whereas the amount of esterified FA, and monounsaturated fatty acids (MUFA), was found to be higher in pulp than in leaves. The amount of linoleic acid in leaves was about twice that of pulp. The amount of linolenic acid and saturated acids in pulp was comparable with that found in leaves. In both cases the lipid fraction was mainly comprised of fatty acids, which account for about 90%. The amount of β -sitosterol was comparable in pulp and leaves, whereas the amount of squalene was much higher in leaves than in pulp. Table 1S reports the distribution of esterified FA in pulp. Specifically, MAG was identified as the predominant component in the distribution of esterified FA in baobab pulp (39.7%), followed by other lipids (33.6%), PC (17.5%), and PE (9.2%).

Table 7.3. Composition of baobab pulp and leaves organic extracts, and distribution of esterified fatty acids in pulp.

| | % mol | |
|--|-------|--------|
| | Pulp | Leaves |
| Fatty acids (FA) | | |
| Free FA | 21.2 | 48.3 |
| Esterified FA | 78.8 | 51.7 |
| Linoleic | 3.2 | 7.3 |
| Linolenic | 12.7 | 13.1 |
| Monounsaturated | 16.5 | 4.9 |
| Saturated | 67.6 | 74.7 |
| Lipid fractions | | |
| Fatty acids | 92.4 | 90.5 |
| β -Sitosterol | 7.4 | 5.3 |
| Squalene | 0.1 | 4.2 |
| Distribution of esterified FA in pulp | | |
| PE | 9.2 | |
| PC | 17.5 | |
| MAG | 39.7 | |
| Other lipids | 33.6 | |

7.4 Conclusions

The data pertaining to primary metabolites confirms that powdered fruit pulp and dried leaves are rich in carbohydrates, amino acids, and lipids. These results, showing the high nutritional value of baobab fruit pulp and leaves, support the use of fruit pulp in importing countries as well as their sub-Saharan countries of origin, and suggest that leaves could be considered for evaluation as an authorized novel food in Europe and other Western Countries.

In addition, as far as lipids are concerned, baobab fruit pulp and leaves were found to be especially rich in omega-3 essential fatty acids and β -sitosterol, which may be useful in the food industry for preparation of functional foods assisting in the maintenance of normal blood cholesterol levels. In addition, the relatively high squalene content present in organic leaf extract could be useful in the cosmetics industry, especially in barrier products, protecting the skin from free radicals generated by exposure to solar UV radiation and maintaining moisture by lubricating the skin surface.

In conclusion, the deeper understanding of the chemical composition of baobab provided by this investigation could enhance the value of baobab products and their industrial applications, both in the countries of origin and importing countries.

7.5 References

- Bligh, E.G., Dyer, W.J., 1959. A rapid method of total lipid extraction and purification. *Canadian J. Biochem. Phys.* 37, 911–917.
- Braun, S., Kalinowski, H.-O., Berger, S., 1998. 150 and more basic NMR experiments (2nd ed.). Weinheim: Wiley-VCH.
- Capitani, D., Sobolev, A.P., Tomassini, A., Sciubba, F., De Salvador, F.R., Mannina, L., Delfini, M., 2013. Peach Fruit: Metabolic comparative analysis of two varieties with different resistances to insect attacks by NMR spectroscopy. *J. Agric. Food Chem.* 61, 1718–1726.
- Chadare, F.J., Linnemann, A.R., Hounhouigan, J.D., Nout, M.J.R., Van Boekel, M.A.J.S., 2008. Baobab food products: A review on their composition and nutritional value. *Crit. Rev. Food Sci. Nutr.* 49, 254–274.
- Diop, A.G., Sakho, M., Domier, M., Cisse, M., Reynes, M., 2006. The African baobab (*Adansonia digitata* L.): Key features and uses. *Fruits* 61, 55–69.
- Duarte, I.F., Goodfellow, B.J., Gill, A.M., Delgadillo, I., 2005. Characterization of mango juice by high-resolution NMR, Hyphenated NMR, and diffusion-ordered spectroscopy. *Spectrosc. Lett.* 38, 319–342.
- Gebauer, J., El-Siddig, K., Ebert, G., 2002. Baobab (*Adansonia digitata* L.): A review on a multipurpose tree with a promising future in the Sudan. *Gartenbauwissenschaft* 67, 155–160.
- Glew, R.H., Vanderjagt, D.J., Lockett, C., Grivetti, L.E., Smith, G.C., Pastuszyn, A., Millson, M., 1997. Amino acid, fatty acid, and mineral composition of 24 indigenous plants of Burkina Faso. *J. Food Compos. Anal.* 10, 205–217.
- Ironi, E.A., Akintunde, J.K., Agboola, S.O., Boligon, A.A., & Athayde, M.L., 2017. Blanching influences the phenolics composition, antioxidant activity, and inhibitory effect of *Adansonia digitata* leaves extract on α -amylase, α -glucosidase, and aldose reductase. *Food Sci. Nutr.* 5, 233–242.
- Li, X.N., Sun, J., Shi, H., Yu, L.L., Ridge, C.D., Mazzola, E.P., ... Chen, P., 2017. Profiling hydroxycinnamic acid glycosides, iridoid glycosides, and phenylethanoid glycosides in baobab fruit pulp (*Adansonia digitata*). *Food Res. Int.* 99, 755–761.
- Maidunny, Z.A.B., Dulngali, S.B., 1985. Cis-trans isomerization of natural rubber by treatment with sulphur dioxide. I. Sequence distribution of isomeric structures. *J. Rubber Res. Inst. Malaysia* 33, 48–53.
- Massiot, D., Fayon, F., Capron, M., King, I., Le Calvé, S., Alonso, B., ... Hoatson, G., 2002. Modelling one- and two-dimensional solid state NMR spectra. *Magn. Reson. Chem.* 40, 70–76.
- Mannina, L., Cristinzio, M., Sobolev, A.P., Ragni, P., Segre, A.L., 2004. High-field NMR study of truffles (*Tuber aestivum vittadini*). *J. Agric. Food Chem.* 52, 7988–7996.
- Nour, A.A., Magboul, B.I., Kheiri, N.H., 1980. Chemical composition of baobab fruit

(*Adansonia digitata* L.). *Trop. Sci.* 22, 383–388.

Rahul, J., Jain, M.K., Singh, S.P., Kamal, R.K., Anuradha, L., Naz, A., ... Mrityunjay, S.K., 2015. *Adansonia digitata* L. (baobab): A review of traditional information and taxonomic description. *Asian Pac. J. Trop. Biomed.* 5, 79–84.

Sobolev, A.P., Mannina, L., Proietti, N., Carradori, S., Daglia, M., Giusti, A.M., ... Capitani, D., 2015. Untargeted NMR-based methodology in the study of fruit metabolites. *Molecules* 20, 4088–4108.

Stilbs, P., 2010. Diffusion studied using NMR Spectroscopy. In: J. Lindon, G. E. Tranter, D. Koppenaal (Eds.). *Encyclopedia of spectroscopy and spectrometry*. Elsevier. 423–428.

Sugandha, S., Shashi, R., 2017. Spectroscopic determination of total phenol, flavonoid content and anti-oxidant activity in different parts of *Adansonia digitata* L.: An important medicinal tree. *Eur. J. Pharm. Med. Res.* 4, 549–552.

Vertuani, S., Braccioli, E., Buzzoni, V., Manfredini, S., 2002. Antioxidant capacity of *Adansonia Digitata* fruit pulp and leaves. *Acta Phytother.* 2, 2–7.

Chapter 8: NMR metabolomic approach to investigate the stool metabolome of cirrhotic patients

8.1 Introduction

Metabolomics, one of the “omics” sciences, is concerned with the identification, quantification, and characterization of the complete set of low molecular weight metabolites, called metabolome, present in a biological specimen (Wishart et al., 2013). Metabolome is a dynamic and evolving entity that can be regarded as the downstream end product of the interaction between genome, transcriptome, and proteome, influenced by the environment, diet, drugs, diseases, lifestyle, and age (Slupsky et al., 2007). Nuclear magnetic resonance (NMR)-based metabolomics has been applied in many research fields such as food chemistry (Mannina, Sobolev et Viel, 2012), biological chemistry (Pelantová et al., 2015), and medicine (Assfalg et al., 2008; Bernini et al., 2009; Ghini et al., 2005). Considering the complexity and multiplicity of human pathologies, only few applications of NMR metabolomic approach have been reported so far especially in the areas of biomedical research focused on nutritional studies (Jones, Park et Ziegler, 2012), diagnosis of diseases (Bertini et al., 2008; Priori et al., 2013), identification of biomarkers, and definition of pathological status (Tenori et al., 2015; Bernini et al., 2011). One major application of metabolomics is the analysis of biological matrices, such as human urine, serum, and saliva, which are easily obtained and readily used for disease diagnosis and in clinical trials for the monitoring of drug therapy. With respect to a classical analytical approach focused on target diagnostic parameters, every application of metabolomics is untargeted, showing a comprehensive picture of metabolome with a high

possibility to meet with the unexpected or even unknown metabolic changes, and new markers of pathology can be discovered as a result of the metabolomic analysis.

The pioneering work of Li (Li et al., 2008) introduced the term ‘functional metagenomics’, intended as a multivariate statistical tool to discover functional relationships among bacterial species and metabolites derived from bacteria/host co-metabolism: very few studies have attempted such an integrated approach in clinical research (Yip & Chan, 2015; Nagao-Kitamoto et al., 2016; Chassard et al., 2012). In liver cirrhosis, a pathological condition in which the liver is unable to function normally, the combination of metagenomics and metabolomics would give insights into the yet unknown role of bacterial species involved in bacterial translocation (translocation of enteric bacteria or their products into the systemic circulation) and liver functionality, especially when considering portal blood as the main route for the gut-liver axis (Schierwagen et al., 2018; Giannelli et al., 2014; Macnaughtan & Jalan, 2015). The influence of the gut microbiota on host health is a concept progressively accepted, but the connection between gut microbiota bacterial translocation and liver cirrhosis remains to be investigated.

Although the underlying mechanisms require further investigation, there is an increasing body of evidence that the functional output of the gut microbiota, in particular bacterial metabolites like short chain fatty acids (SCFA) and amino acids, are important modulators of host physiology (Sridharan et al., 2014). For example, the SCFA receptor GPR43 has been reported to link the metabolic activity of the gut microbiota with host energy homeostasis (Kimura et al., 2014; Kimura et al., 2013).

Furthermore, studies in germ free and conventionalized mice reveal that gut bacteria alter the distribution of free amino acids in the gastrointestinal tract (Macfarlane et al., 1988). This may suggest that the gut microbiota affects the bioavailability of amino acids to the host. Interestingly, amino acids can also serve as precursors for the synthesis of SCFA by bacteria

_____ Chapter 8: NMR metabolomic approach to investigate the stool metabolome of cirrhotic patients (Tomé et al., 2013), suggesting an interplay between microbial activity and host amino acid and SCFA homeostasis.

Here, we adopt an NMR metabolomic analytical approach to investigate the stool metabolome in patients affected by liver cirrhosis and to compare it with that of healthy subjects. Studying such an unconventional matrix like human faeces allow us to investigate metabolites produced in gut environment, including those related to the gut microbiota metabolism. In particular, a possible alteration of stool metabolome in terms of amino acids and SCFA can be revealed.

8.2 Material and Methods

Twenty-one patients with liver cirrhosis (aged 62.1 ± 11.4 years, sex ratio M/F 14/7) hospitalized at the Department of Gastroenterology, University Hospital Policlinico Umberto I, were included in the study. The diagnosis of cirrhosis was proven through liver biopsy or based on clinical, biochemical and ultrasonographic signs. The exclusion criteria were as follows: diagnosis of infection (based on fever, leukocytosis, elevated C Reactive protein (CRP), erythrocytation rate (ESR), procalcitonin, clinical symptoms, and positive microbiological cultures when present), use of systemic antibiotics in the last 3 months, variceal bleeding within the last 4 weeks, or alcohol or illicit drug intake within the last 3 months. Lactulose or rifaximin therapy was not considered cause for exclusion. No patient took other drugs that could potentially affect the microbiota (such as metformin). Patients with any type of immunodeficiency (HIV, immunosuppression) or with a diagnosis of hepatocellular carcinoma without Milano criteria were also excluded. All the patients were followed throughout the time of hospitalization. Seven healthy age-matched individuals (aged 59.6 ± 2.1 years, sex ratio M/F 4/3) were recruited among their neighbours to serve as controls. Among this group, individuals who were taking, or had taken in the last 3 months, medications that could potentially modify the gut microbiota (antibiotics, probiotics) were

excluded. The origin of cirrhosis, past and current complications of the disease, and laboratory findings (hemogram, serum electrolyte levels, renal and liver function tests, inflammatory parameters) were collected. The severity of liver disease was evaluated by the Child-Turcotte-Pugh (CTP) and model for end stage liver disease (MELD) scores. The chronic use of beta-blockers, lactulose, proton pump inhibitors (PPI) and other drugs with the potential to influence the gut microbiota was recorded. The patients included in the study and the healthy controls gave a fresh stool sample that was promptly stored at $-80\text{ }^{\circ}\text{C}$.

Faecal metabolites were extracted as described elsewhere (Lamichhane et al., 2015). The aliquots of about 20 mg thawed stool material were mixed with 1 mL phosphate buffer saline (1.9 mM Na_2HPO_4 , 8.1 mM NaH_2PO_4 , 150 mM NaCl, pH 7.4) in deuterated water containing 2.0 mM sodium 3-trimethylsilyl-propionate- d_4 (TMSP-2,2,3,3- d_4) as chemical shift reference. The mixtures were homogenized and the faecal slurry was then centrifuged at 18000 rpm for 15 min at $4\text{ }^{\circ}\text{C}$. Supernatants were collected and centrifugation was repeated. Finally, 550 μL of the resulting faecal extracts were transferred to a 5 mm NMR tube.

Stool samples from the controls and the cirrhotic patients were investigated using NMR spectroscopy to solve the spectra of complex mixtures and to recognize and quantify each component without chemical separation (Mannina et al., 2004). Briefly, NMR spectra of faecal samples were recorded at $27\text{ }^{\circ}\text{C}$ on a Bruker AVANCE 600 spectrometer operating at a proton frequency of 600.13 MHz and equipped with a Bruker multinuclear z-gradient inverse probe head capable of producing gradients in the z-directions with a strength of 55 G/cm. The ^1H spectra were referenced to the methyl group signals of TSP ($\delta = 0.00\text{ ppm}$) and were acquired by co-adding 64 transients with a recycle delay of 7 s. The residual HDO signal was suppressed using a presaturation. The experiment was carried out by using a 90° pulse of 11.75 μs and 32 K data points. Spectra were transformed with 0.5 Hz line broadening and zero filling, size 65 K, manually phased, calibrated on the methyl group signals of TSP ($\delta = 0.00\text{ ppm}$), and baseline corrected using the TOPSPIN v1.3 software. The spectra were

282

_____ Chapter 8: NMR metabolomic approach to investigate the stool metabolome of cirrhotic patients prepared for statistical analysis by dividing the entire spectrum into small regions (0.02 ppm width), called “buckets”. Regions containing only background noise, water resonance, and the extreme regions of spectra were excluded from the buckets. The total integral (as the sum of all 418 buckets) for each spectrum was normalized to 1000.

Moreover, 2D NMR experiments, namely, ^1H - ^1H total correlation spectroscopy (TOCSY), and ^1H - ^{13}C heteronuclear single quantum coherence (HSQC) were performed using the same experimental conditions previously reported (Mannina et al., 2004). The mixing time for ^1H - ^1H TOCSY was 80 ms. The HSQC experiments were performed using a coupling constant $^1J_{\text{C-H}}$ of 150 Hz. A diffusion ordered spectroscopy (DOSY) experiment was performed using a bipolar LED sequence with a sine-shaped gradient of different intensities. The gradient strength was incremented in 32 steps from 2 to 95% of the maximum gradient strength (55 G/cm). The following experimental settings were used: diffusion time (Δ), 100 ms; gradient duration ($\delta/2$), 1.1 ms, longitudinal eddy current delay, 25 ms, and gradient pulse recovery time, 100 μs . After Fourier transformation and baseline correction, the diffusion dimension was processed by means of the Bruker TOPSPIN software (version 1.3).

A matrix of normalized and corrected NMR peak areas was generated for subsequent multivariate statistical analyses. Afterwards, our data set was submitted to the Principal Component Analysis (PCA) to provide useful information regarding the stool metabolome in cirrhotic patients.

8.3 Results and Discussion

A typical ^1H NMR spectrum of faecal extracts obtained from patients affected by liver cirrhosis is shown in Figure 8.1. Since the ^1H NMR spectrum of a stool sample can be considered as its metabolic fingerprint, a wide range of metabolites has been observed. Taking into account literature data (Le Gall et al., 2011; Jansson et al., 2009; Marchesi et al., 2007), we detected several metabolites belonging to different chemical classes of compounds. The ^1H NMR spectra contained resonances from SCFAs (predominantly acetate, propionate, butyrate), branched-chain fatty acids (BCFAs; valerate, iso-valerate, iso-butyrate), biogenic amines (trimethylamine and dimethylamine), organic acids (succinate, fumarate, lactate), carbohydrates (glucose, galactose), branched-chain amino acids (BCAAs; leucine, isoleucine, valine), tyrosine, phenylalanine, and others.

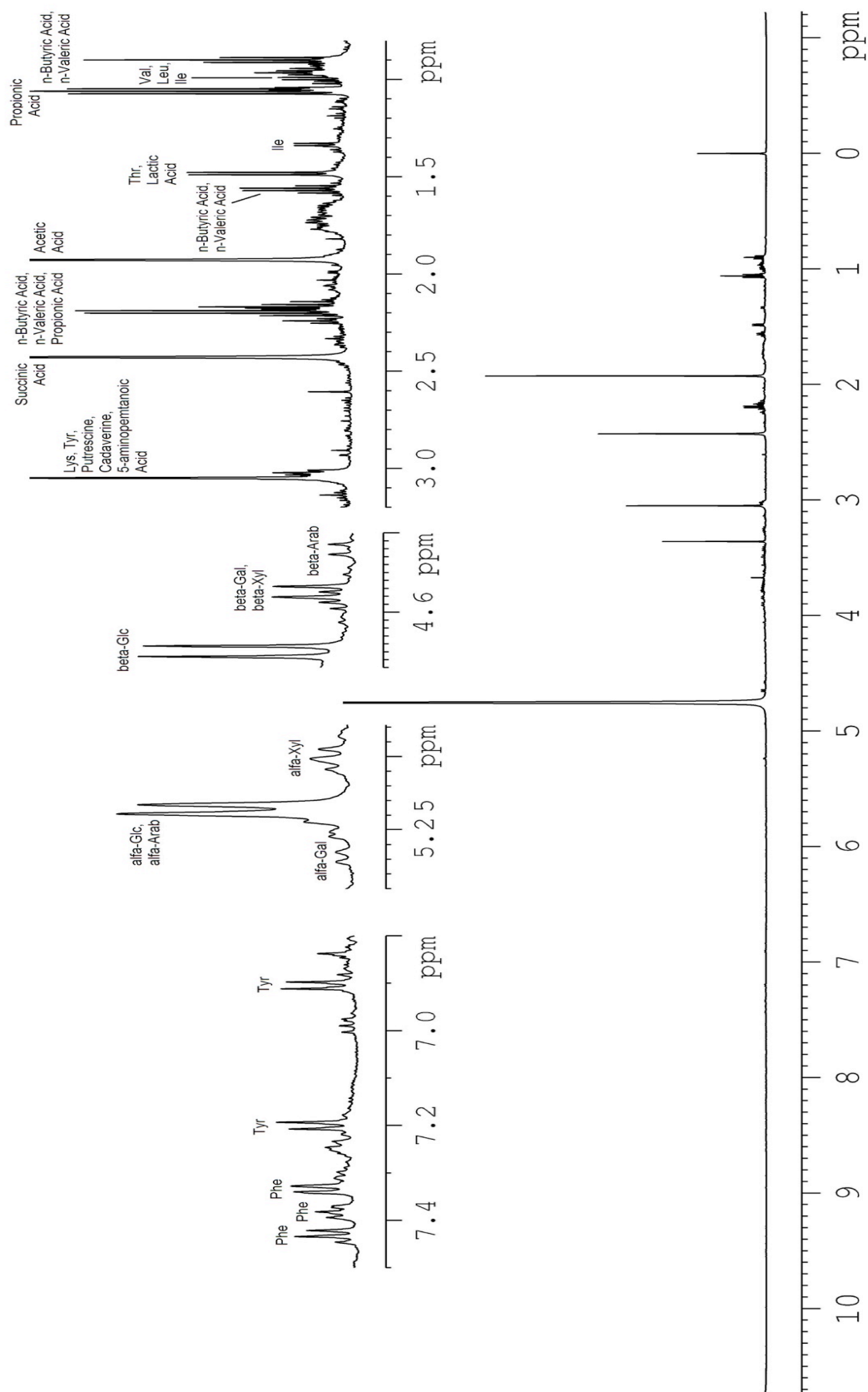


Figure 8.1. ¹H NMR spectrum of a stool sample in 550 mM phosphate/D₂O buffer with 2 mM TSP. Assignment is represented above in an expanded scale.

PCA was carried out on the mean-centred normalized ^1H NMR spectra acquired from the faecal extracts to generate an overview of the variations between the control volunteers and the patients with liver cirrhosis in order to detect possible analogies and differences between samples. The best separation of samples from healthy control subjects and patients with liver cirrhosis was observed along the PC1 direction of the “PC3 vs PC1” scores plot (Figure 8.2). Control samples are grouped along the direction of the PC3. These two PCs accounted for the 35.7% of the variability within the data, whereas the second principal component (PC2), with a variability of 12.7%, resulted to be not informative. PC1 provided mostly the discrimination between samples belonging to healthy and patients’ groups. Variables with the highest contribution to PC1 are responsible for the separation and can be selected using the plot of loadings. These variables were the branched chain amino acids (valine, leucine and isoleucine), with loadings lying on the left side of PC1 axis, and two organic acids (butyrate and valerate) with loadings lying on the right side of PC1 axis. It is interesting that 5 out of 21 cirrhotic patients’ samples have a metabolic profile more similar to the controls.

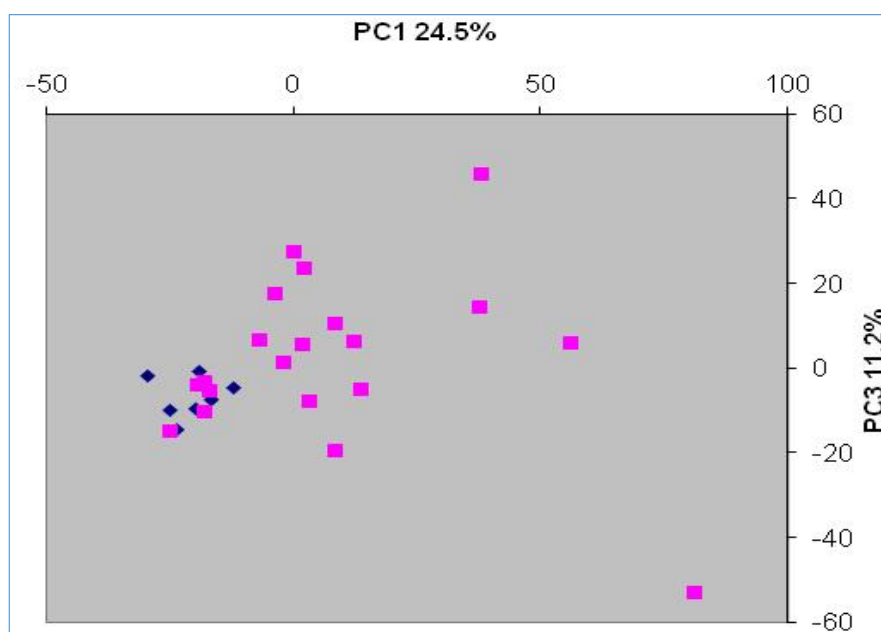


Figure 8.2. PCA score plot performed on 28 stool samples. Blue diamonds represent the control samples whereas pink squares represent the patients affected by hepatic cirrhosis.

To sum up, samples of cirrhotic patients resulted to have a higher content of branched chain amino acids with respect to control subjects (Figure 8.3). On the contrary a lower level of short chain fatty acids (butyric and valeric acids) was observed in cirrhosis patients. An altered faecal content of BCAA and some organic acids with respect to that of healthy subjects suggests a dysbiotic status of the gut environment in the patients affected with liver cirrhosis. In fact, the large intestinal microbiota metabolizes BCAAs and other amino acids (Dai, Wu and Zhu, 2011) resulting in the generation of a complex mixture of metabolic end products including among others ammonia, SCFA, and branched-chain fatty acids (BCFA; valerate, isobutyrate, and isovalerate). If an altered level of these metabolites in stool samples is present, an alteration of the bacterial populations in the human gut can be clearly diagnosed.

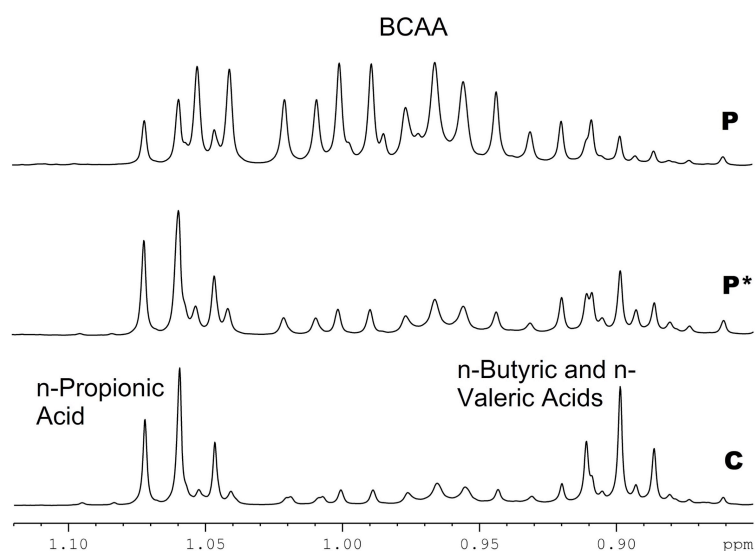


Figure 8.3. An expansion of the 0.85-1.10 ppm ^1H spectral region, including BCAA and SCFA signals, is shown for patients (P and P*) and healthy subjects (C).

In general, most of human diseases, like liver cirrhosis, have a multi-factorial etiology and a complex physiopathology. Among the factors responsible for the etiology of a disease, in recent decades a tremendous amount of evidence has strongly suggested also a

crucial role of the human microbiota in human health and disease (Ley et al., 2006; Gill et al., 2006; Cash et al., 2006; Hooper et al., 2003; Schaubert et al., 2003; Bouskra et al., 2008; Rakoff-Nahoum & Medzhitov, 2008; Macpherson & Harris, 2004; Sekirov et al., 2010; Sartor, 2008; Liu et al., 2004; Scanlan et al., 2008; Verhulst et al., 2008; Finegold et al., 2002; Wen et al., 2008) via several mechanisms.

In a biological sample altered by a pathological condition there will be an alteration of several metabolic products. The metabolic fingerprint composed by the superimposition of all the visible signals of the low molecular weight endogenous metabolites takes into account all those variations even if few metabolites are (slightly) significant. The fingerprint can be, therefore, a useful tool, like in the present case, to discriminate with good accuracy between healthy subjects and patients. This innovative approach of course needs to be validated on larger cohorts before being translated in the clinical routine. These results may allow for the development of novel approaches to the optimization of therapy and of robust, standardized protocols for biofluids of interest, critical to allow for safe comparisons among different patient groups and diseases. Moreover, the opportunity given by NMR to detect early metabolic perturbations even before the appearance of disease symptoms can provide new possibilities for early diagnosis, prevention therapies, and precision medicine approach to design an effective treatment protocol.

8.4 References

- Assfalg, M., Bertini, I., Colangiuli, D., Luchinat, C., Schäfer, H., Schütz, B., et al., 2008. Evidence of different metabolic phenotypes in humans. *Proc. Natl. Acad. Sci.* 105, 1420–1424.
- Bernini, P., Bertini, I., Luchinat, C., Nepi, S., Saccenti, E., Schäfer, H., et al., 2009. Individual human phenotypes in metabolic space and time. *J. Proteome Res.* 8, 4264–4271.
- Bernini, P., Bertini, I., Luchinat, C., Tenori, L., Tognaccini, A., 2011. The cardiovascular risk of healthy individuals studied by NMR metabonomics of plasma samples. *J. Proteome Res.* 10, 4983–4992.
- Bertini, I., Calabrò, A., De Carli, V., Luchinat, C., Nepi, S., Porfirio, B., et al., 2008. The metabonomic signature of celiac disease. *J. Proteome Res.* 8, 170–177.
- Bouskra, D., Brézillon, C., Bérard, M., Werts, C., Varona, R., Boneca, I.G., et al., 2008. Lymphoid tissue genesis induced by commensals through NOD1 regulates intestinal homeostasis. *Nature* 456(7221), 507-510.
- Cash, H.L., Whitham, C.V., Behrendt, C.L., Hooper, L.V., 2006. Symbiotic bacteria direct expression of an intestinal bactericidal lectin. *Science* 313(5790), 1126-1130.
- Chassard, C., et al., 2012. Functional dysbiosis within the gut microbiota of patients with constipated-irritable bowel syndrome. *Aliment. Pharmacol. Ther.* 35, 828–838.
- Dai, Z.L., Wu, G., Zhu, W.Y., 2011. Amino acid metabolism in intestinal bacteria: Links between gut ecology and host health. *Front. Biosci.* 16, 1768–1786.
- Finegold, S.M., Molitoris, D., Song, Y., Liu, C., Vaisanen, M.L., Bolte, E., et al., 2002. Gastrointestinal microflora studies in late-onset autism. *Clin. Infect. Dis.* 35, S6-S16.
- Ghini, V., Saccenti, E., Tenori, L., Assfalg, M., Luchinat, C., 2015. Allostasis and resilience of the human individual metabolic phenotype. *J. Proteome Res.* 14(7), 2951-2962.
- Giannelli, V., et al., 2014. Microbiota and the gut-liver axis: bacterial translocation, inflammation and infection in cirrhosis. *World J. Gastroenterol.* 20, 16795–16810.
- Gill, S.R., Pop, M., Deboy, R.T., Eckburg, P.B., Turnbaugh, P.J., Samuel, B.S., et al., 2006. Metagenomic analysis of the human distal gut microbiome. *Science* 312(5778), 1355-1359.
- Hooper, L.V., Stappenbeck, T.S., Hong, C.V., Gordon, J.I., 2003. Angiogenins: a new class of microbicidal proteins involved in innate immunity. *Nat. Immunol.* 4(3), 269-273.
- Jansson, J., Willing, B., Lucio, M., et al., 2009. Metabolomics reveals metabolic biomarkers of Crohn's disease. *PLoS One* 4(7).
- Jones, D.P., Park, Y., Ziegler, T.R., 2012. Nutritional metabolomics: progress in addressing complexity in diet and health. *Annu. Rev. Nutr.* 32, 183–202.

-
- Kimura, I., Inoue, D., Hirano, K., Tsujimoto, G., 2014. The SCFA Receptor GPR43 and Energy Metabolism. *Front. Endocrinol.* 5, 85.
- Kimura, I., Ozawa, K., Inoue, D., Imamura, T., Kimura, K., Maeda, T., Terasawa, K., Kashihara, D., Hirano, K., Taeko, T., et al., 2013. The gut microbiota suppresses insulin-mediated fat accumulation via the short-chain fatty acid receptor GPR43. *Nat. Commun.* 4, 1829.
- Lamichhane, S., Yde, C.C., Schmedes, M.S., Jensen, H.M., Meier, S., Bertram, H.C., 2015. Strategy for nuclear-magnetic-resonance-based Metabolomics of human feces. *Anal. Chem.* 87(12), 5930–5937.
- Le Gall, G., Noor, S.O., Ridgway, K., et al., 2011. Metabolomics of faecal extracts detects altered metabolic activity of gut microbiota in ulcerative colitis and irritable bowel syndrome. *J. Proteome Res.* 10(9), 4208–4218.
- Ley, R.E., Turnbaugh, P.J., Klein, S., Gordon, J.I., 2006. Microbial ecology: human gut microbes associated with obesity. *Nature* 444(7122), 1022-1023.
- Li, M., et al., 2008. Symbiotic gut microbes modulate human metabolic phenotypes. *Proc. Natl. Acad. Sci. USA* 105, 2117–2122.
- Liu, Q., Duan, Z., Ha, D., Bengmark, S., Kurtovic, J., Riordan, S.M., 2004. Synbiotic modulation of gut flora: effect on minimal hepatic encephalopathy in patients with cirrhosis. *Hepatology* 39(5), 1441-1449.
- Macfarlane, G.T., Allison, C., Gibson, S.A.W., Cummings, J.H., 1988. Contribution of the microflora to proteolysis in the human large intestine. *J. Appl. Bacteriol.* 64, 37–46.
- Macnaughtan, J., Jalan, R., 2015. Clinical and pathophysiological consequences of alterations in the microbiome in cirrhosis. *Am. J. Gastroenterol.* 110, 1399–1410.
- Macpherson, A.J., Harris, N.L., 2004. Interactions between commensal intestinal bacteria and the immune system. *Nat. Rev. Immunol.*, 4(6), 478-485.
- Marchesi, J.R., Holmes, E., Khan, F., et al., 2007. Rapid and noninvasive metabonomic characterization of inflammatory bowel disease. *J. Proteome Res.* 6(2), 546–551.
- Mannina, L., Sobolev, A.P., & Viel, S., 2012. Liquid state 1H high field NMR in food analysis. *Prog. Nucl. Magn. Reson. Spectrosc.* 66, 1-39.
- Mannina, L., et al., 2004. High-Field Nuclear Magnetic Resonance (NMR) Study of Truffles (*Tuber aestivum vittadini*). *J. Agric. Food Chem.* 52, 7988–7996.
- Nagao-Kitamoto, H., et al., 2016. Functional Characterization of Inflammatory Bowel Disease–Associated Gut Dysbiosis in Gnotobiotic Mice. *Cellular and Molecular Gastroenterology and Hepatology* 2, 468–481.
- Pelantová, H., Bártová, S., Anýž, J., Holubová, M., Železná, B., Maletínská, L., et al., 2015. Metabolomic profiling of urinary changes in mice with monosodium glutamate-induced obesity. *Anal. Bioanal. Chem.* 408, 567–78.

Priori, R., Scrivo, R., Brandt, J., Valerio, M., Casadei, L., Valesini, G., et al., 2013. Metabolomics in rheumatic diseases: the potential of an emerging methodology for improved patient diagnosis, prognosis, and treatment efficacy. *Autoimmun Rev.* 12, 1022–1030.

Rakoff-Nahoum, S., Medzhitov, R., 2008. Innate immune recognition of the indigenous microbial flora. *Mucosal Immunol.* 1, S10-S14.

Sartor, R.B., 2008. Microbial influences in inflammatory bowel diseases. *Gastroenterology* 134 (2), 577-594.

Scanlan, P.D., Shanahan, F., Clune, Y., Collins, J.K., O’Sullivan, G.C., O’Riordan, M., et al., 2008. Culture-independent analysis of the gut microbiota in colorectal cancer and polyposis. *Environ. Microbiol.* 10(3), 789-798.

Schauber, J., Svanholm, C., Termén, S., Iffland, K., Menzel, T., Scheppach, W., et al., 2003. Expression of the cathelicidin LL-37 is modulated by short chain fatty acids in colonocytes: relevance of signalling pathways. *Gut* 52(5), 735-741.

Schierwagen, R., et al., 2018. Circulating microbiome in blood of different circulatory compartments. *Gut*.

Slupsky, C.M., Rankin, K.N., Wagner, J., Fu, H., Chang, D., Weljie, A.M., et al., 2007. Investigations of the effects of gender, diurnal variation, and age in human urinary metabolomic profiles. *Anal Chem.* 79, 6995–7004.

Sekirov, I., Russell, S.L., Antunes, L.C., Finlay, B.B., 2010. Gut microbiota in health and disease. *Physiol. Rev.* 90(3), 859-904.

Sridharan, G.V., Choi, K., Klemashevich, C., Wu, C., Prabakaran, D., Pan, L.B., Steinmeyer, S., Mueller, C., Yousofshahi, M., Alaniz, R.C., et al., 2014. Prediction and quantification of bioactive microbiota metabolites in the mouse gut. *Nat. Commun.* 5, 5492.

Tenori, L., Oakman, C., Morris, P.G., Gralka, E., Turner, N., Cappadona, S., et al., 2015. Serum metabolomic profiles evaluated after surgery may identify patients with oestrogen receptor negative early breast cancer at increased risk of disease recurrence. Results from a retrospective study. *Mol. Oncol.* 9, 128–139.

Tomé, D., Gotteland, M., Pierre Henri, B., Andriamihaja, M., Sanz, Y., Blachier, F., Davila, A.M., 2013. Reprint of “Intestinal luminal nitrogen metabolism: Role of the gut microbiota and consequences for the host”. *Pharmacol. Res.* 69, 114–126.

Verhulst, S.L., Vael, C., Beunckens, C., Nelen, V., Goossens, H., Desager, K., 2008. A longitudinal analysis on the association between antibiotic use, intestinal microflora, and wheezing during the first year of life. *J. Asthma* 45(9), 828-832.

Yip, L.Y. & Chan, E.C.Y., 2015. Investigation of Host–Gut Microbiota Modulation of Therapeutic Outcome. *Drug Metab. Dispos.* 43, 1619–1631.

Wen, L., Ley, R.E., Volchkov, P.Y., Stranges, P.B., Avanesyan, L., Stonebraker, A.C., et al., 2008. Innate immunity and intestinal microbiota in the development of Type 1 diabetes.

Nature 455(7216), 1109-1113. Wishart, D.S., Jewison, T., Guo, A.C., Wilson, M., Knox, C., Liu, Y., et al., 2013. HMDB 3.0-the Human Metabolome Database in 2013. Nucleic Acids Res. 41, D801-807.

ACKNOWLEDGMENTS

First and foremost I want to thank my tutor Prof. Luisa Mannina and my co-tutor Anatoly P. Sobolev. It has been an honor to be their Ph.D. student. They have introduced me to the complex world of “Nuclear Magnetic Resonance” since I was a graduate student. I appreciate all their contributions of time, ideas, and advices to make my Ph.D. experience productive and stimulating.

I would also like to express my sincere thanks to all the other members of the Laboratorio di Risonanza Magnetica “Annalaura Segre” (Istituto di Metodologie Chimiche, CNR, Montelibretti), Dr. Donatella Capitani e Dr. Noemi Proietti, for all their support and the good working atmosphere.

I want to thank also all the PhD students, the graduating students and the professors with whom I have interacted in these 3 years because they have helped me to grow up and to be the person I am today.

Finally, I wish to thank my family and friends for their infinite love, encouragement and support that made all of the above possible.